AD-A130 695 EVALUATION OF THE VARIABLE RELUCTANCE TRANSDUCER/CARRIER AMPLIFIER METHOD..(U) AIR FORCE WRIGHT AERONAUTICAL LABS WRIGHT-PATTERSON AFB OH 1/3

UNCLASSIFIED D L MCCORMICK FEB 83 AFWAL-TR-82-2100 F/G 14/2 NL

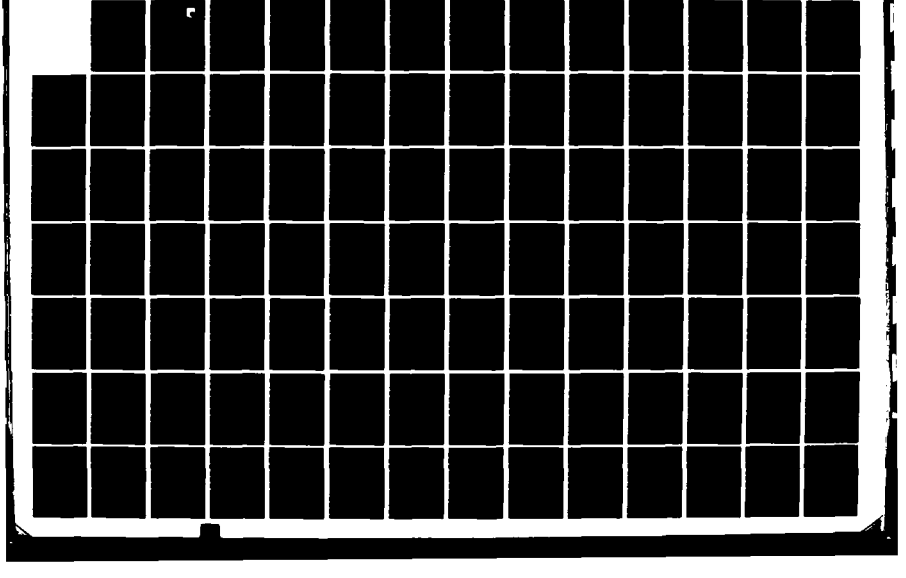

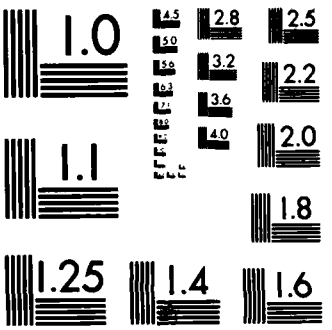

MICROCOPY RESOLUTION TEST CHART
NATIONAL BUREAU OF STANDARDS-1963-A

AFWAL-TR-82-2100

(12)

AD A130695

EVALUATION OF THE VARIABLE RELUCTANCE TRANSDUCER/ CARRIER AMPLIFIER METHOD OF MEASURING LOW PNEUMATIC PRESSURES IN AERODYNAMIC AND PROPULSION TESTING

D. L. McCormick
Components Branch
Turbine Engine Division

February 1983
Final Report for Period January 1975 through June 1981

Approved for public release; distribution unlimited

AERO PROPULSION LABORATORY
AIR FORCE WRIGHT AERONAUTICAL LABORATORIES
AIR FORCE SYSTEMS COMMAND
WRIGHT-PATTERSON AIR FORCE BASE, OHIO 45433

NOTICE

When Government drawings, specifications, or other data are used for any purpose other than in connection with a definitely related Government procurement operation, the United States Government thereby incurs no responsibility nor any obligation whatsoever; and the fact that the government may have formulated, furnished, or in any way supplied the said drawings, specifications, or other data, is not to be regarded by implication or otherwise as in any manner licensing the holder or any other person or corporation, or conveying any rights or permission to manufacture use, or sell any patented invention that may in any way be related thereto.

This report has been reviewed by the Office of Public Affairs (ASD/PA) and is releasable to the National Technical Information Service (NTIS). At NTIS, it will be available to the general public, including foreign nations.

This technical report has been reviewed and is approved for publication.

Donald L. McCormick

DONALD L. McCORMICK
Project Engineer

Lester L. Small

LESTER L. SMALL, Tech Area Manager
Controls Technology

FOR THE COMMANDER

Robert W. Baker

ROBERT W. BAKER, Major, USAF
Deputy Director
Turbine Engine Division

"If your address has changed, if you wish to be removed from our mailing list, or if the addressee is no longer employed by your organization please notify AFWAL/POTC, *W-PAFB, OH 45433 to help us maintain a current mailing list".*

Copies of this report should not be returned unless return is required by security considerations, contractual obligations, or notice on a specific document.

UNCLASSIFIED

SECURITY CLASSIFICATION OF THIS PAGE (When Data Entered)

REPORT DOCUMENTATION PAGE		READ INSTRUCTIONS BEFORE COMPLETING FORM
1. REPORT NUMBER AFWAL-TR-82-2100	2. GOVT ACCESSION NO.	3. RECIPIENT'S CATALOG NUMBER
4. TITLE (and Subtitle) EVALUATION OF THE VARIABLE RELUCTANCE TRANSDUCER/ CARRIER AMPLIFIER METHOD OF MEASURING LOW PNEUMATIC PRESSURES IN AERODYNAMIC AND PROPULSION TESTING		5. TYPE OF REPORT & PERIOD COVERED Final Report 1 Jan 75 - 1 Jun 81 6. PERFORMING ORG. REPORT NUMBER
7. AUTHOR(s) Donald L. McCormick		8. CONTRACT OR GRANT NUMBER(s)
9. PERFORMING ORGANIZATION NAME AND ADDRESS Aero Propulsion Laboratory AF Wright Aeronautical Laboratories, AFSC Wright-Patterson Air Force Base, Ohio 45433		10. PROGRAM ELEMENT, PROJECT, TASK AREA & WORK UNIT NUMBERS 3066 13 18
11. CONTROLLING OFFICE NAME AND ADDRESS		12. REPORT DATE February 1983 13. NUMBER OF PAGES 219
14. MONITORING AGENCY NAME & ADDRESS(if different from Controlling Office)		15. SECURITY CLASS. (of this report) Unclassified 15a. DECLASSIFICATION/DOWNGRADING SCHEDULE

16. DISTRIBUTION STATEMENT (of this Report)

Approved for public release; distribution unlimited

17. DISTRIBUTION STATEMENT (of the abstract entered in Block 20, if different from Report)

18. SUPPLEMENTARY NOTES

19. KEY WORDS (Continue on reverse side if necessary and identify by block number)

Pressure Transducers	Variable Reluctance Pressure Transducers
Wind Tunnel Pressure Measurements	Wind Tunnel Instrumentation
Pressure Instrumentation	Flight Test Instrumentation
Carrier Amplifiers	Sensor, Pressure

20. ABSTRACT (Continue on reverse side if necessary and identify by block number)

A complete evaluation is presented of the Variable Reluctance Transducer/ Carrier Amplifier combination as a possible solution to many low-pressure measurement problems in experimental aerodynamics and turbine engine testing. Characteristic steady-state precision and accuracy of the method are bracketed. The quantitative evaluation is based mainly on empirical data, and theory is only used to show the simplicity of the principles of transduction and analog

DD FORM 1 JAN 73 1473 EDITION OF 1 NOV 65 IS OBSOLETE

UNCLASSIFIED

SECURITY CLASSIFICATION OF THIS PAGE (When Data Entered)

20. ABSTRACT (Cont'd)

signal processing involved. Effects of elective and sometimes arbitrary choices on the part of equipment designers upon system performance, reliability, and operational effectiveness are discussed.

FOREWORD

The work which is the subject of this report was performed as part of R&D Work Unit 30661318, "Compressor/Turbine Instrumentation and Transient Analysis Equipment." The objective of this task was to study and develop practical measurement and data analysis techniques of value in research testing of turbine engines. The study of the pressure measurement equipment described herein was prompted by the requirements and test activities of other in-house R&D programs, such as compressor aerodynamics studies performed on Work Unit 30660418 and engine controls studies on Work Unit 30660340. This report covers all work performed from 1973 through 1980, and constitutes the final item required for completion of Work Unit 30661318. The principal investigator was D. L. McCormick.

TABLE OF CONTENTS

TABLE OF CONTENTS (Cont'd)

ILLUSTRATIONS

ILLUSTRATIONS (Cont'd)

ILLUSTRATIONS (Cont'd)

ILLUSTRATIONS (Cont'd)

ILLUSTRATIONS (Cont'd)

LIST OF TABLES

LIST OF TABLES (Concluded)

SECTION I

WHY USE A VARIABLE RELUCTANCE PRESSURE TRANSDUCER?

Various methods are used in the design and application of pressure transducers to extend the useful range sensitivity, which is the number of units of electrical output per unit of pressure input. The typical limitations of the transducers themselves are most evident in low velocity gas dynamics testing requiring either pipe flow or free stream measurements where the process energy available to actuate the transducers is extremely low.

The application of pneumatic/electrical transducers to free stream flow measurement which is of most concern in aerodynamics research testing usually involves the following:

- Many dedicated channels

- Limited space for transducers and pneumatics

- High precision measurement of low pressures achieved by the following:

    - Optimum selection of range sensitivities of transducers

    - Frequent remote actuation of zero and span check pneumatics

- Moderate to severe temperature and acceleration environment and electrical disturbances.

The mechanical test assembly, transducer, and electrical system are almost always crucial parts of the test program and represent a very large capital investment. In almost all cases, the characteristics and limitations of the basic pressure transducer govern the design

configuration and test performance. The principle interest in the variable reluctance transducer/carrier amplifier is as an alternate to miniature strain gage types and DC signal conditioners where the greater range sensitivity of the variable reluctance (VR) type would give improved data precision, especially in the steady state and low frequency regime. The instrumentation for measuring fluctuating pressures and the upper frequency limit of interest are peculiar to each experiment and the overall continuum from zero frequency to the maximum is sometimes covered by separate parallel transducer channels.

The most common transducer design approaches to optimizing range sensitivity are "brute force", either in cost, size, or complexity, and involve a wide variety of mechanical and electrical techniques. Carrying such approaches to the extremes needed to achieve adequate range sensitivity often results in one or more of the following handicaps:

- Very large pressure integrating surface areas with attendant slow response

- Very high gain electronic equipment

- Complicated, delicate lever systems or other mechanisms

- Complex modulation schemes and circuitry

- Difficult or costly fabrication processes, often proprietary and often not available from second sources.

Only the variable reluctance (VR) transducer is free of the need for these burdensome approaches and their attendant limitations. However, the usefulness of VR transducers is generally questioned

because of widespread unfamiliarity and misconceptions about the equipment and the operational techniques needed to apply them to test measurements. The many signal phase and amplitude relationships existing in a transducer and carrier amplifier combination are seldom controlled sufficiently to permit definition of useable system accuracy, linearity, and repeatability or to maximize measurement precision (self-consistency), particularly in a real test environment.

The quadrature and harmonics in the output of VR transducers are other sources of practical difficulty. They not only cause confusion in balancing and adjusting the carrier signal conditioner, but also undergo uncontrolled and untraceable changes with physical load and environment. The necessity for, or expedient of, ignoring these changes degrades the useful accuracy and precision of this method of pressure measurement. As a result, the strain gage transducer, used with a precision D.C. signal conditioner, has become dominant in pressure data system applications. It is commonly held that the intrinsic precision of the VR transducer/carrier signal conditioner combination is of the order of two percent of full-scale at best. Commonly available signal conditioners and read-out devices for VR pressure transducers are often designed as if this limitation is inescapable.

Even if this serious apparent limitation on precision could not be overcome, the VR transducer still possesses several unique advantages in some applications. Because of its inherent high range sensitivity, it can easily be constructed in ranges as low as $\pm$0.01 PSID full-scale. The transducers may be extremely small, rugged, inexpensive, stable, have infinite resolution, and can withstand very high temperatures. They have relatively high frequency response and are repairable in the field. They are electrically, mechanically, and pneumatically symmetrical in construction, contributing to stability. The simplicity of the mechanical structure of the VR transducer makes it relatively insensitive to thermal shocks, although it has never been put to a

serious test in this regard because of the massive body designs traditionally used. The replacement of the center plate can also serve as a modification of span sensitivity as well as a repair procedure, and can be accomplished in the field with only an allen wrench (Reference 1). This would simplify inventory logistics. The basic design may easily be modified to support the center plate during pressure overloads, thereby preventing damage. The enclosed volume of a typical VR transducer is less than that of the bellows or aneroid types by a factor of ten or more.

A carrier system is inherently free from normal and common mode pick-up of extraneous electrical signals (noise) in the cabling from the transducer to the conditioner, and is totally free from the effects of thermo EMFs which would appear as measurement errors in low level DC transducer circuits. The carrier technique is an integral part of the internal design of precision DC data amplifiers used in large numbers in high performance analog and digital data acquisition systems. Unlike direct systems, no form of low frequency electrical pick-up will affect the processed signal because the carrier amplifier and associated circuits pass and respond only to signals which appear as the product of the carrier and the pressure analog (Section III). Common mode pick-up is eliminated in the input transformer and the AC gain circuitry, both of which are conventional in design and construction. For these reasons, the carrier amplifier and VR transducer pressure measurement system can be used in extreme environments for recording data from superconductivity experiments, nuclear blasts, arc discharge wind tunnels, and other applications involving extremely high steady state and changing magnetic fields, particularly when very long lines (2-3 miles) between transducer and signal conditioner are required. This does not mean that the magnetic material in the transducers is totally immune from the effects of strong magnetic fields, nuclear radiation or high temperature. The construction lends itself to insulating and shielding the coils from the case if desired for further system noise reduction and safety reasons.

Other instrumentation system applications make use of carrier amplifiers because of their unique circuit isolation capability. Circuit and component isolation from power lines, from ground, and other system components afford safety and noise reduction benefits. A biomedical application is described in Reference 2. Reference 3 describes an induction carrier system which provides a contactless rotary coupling between a sensor on a rotating device and the stationary data read-out equipment.

The combination of a VR pressure transducer and carrier signal conditioner has several practical limitations. They are:

- Maximum pressure response frequency is limited by center plate resonant frequency. (The enclosed volume is usually very small.)

- Upper data frequencies when using commonly available carrier signal conditioners are limited to those considerably less than the carrier center-frequency, which in turn must be kept low enough to avoid line capacitance and transducer eddy current problems.

- The casual, empirical approach to system configuration and circuit design often taken by transducer and signal conditioner manufacturers.

- Channel rigging and adjustment difficulties due to the many signal phase and amplitude relationships and the effects of transducer harmonics. These are not readily overcome by the average instrumentation systems technician without special background and supervision.

- Channel checking is not practical. Any electrical circuit change in the signal conditioner input to check electrical calibration must simulate the exact phase, amplitude and harmonic output of the transducer under pressure load. Therefore, a simple channel check with an inductive transducer may be misleading except as a test for gross

circuit malfunction. An end-to-end calibration of physical input ("measurand") versus electrical output is necessary to assure valid data.

The above remarks apply specifically to data channels using a carrier amplifier and the VR transducer of the type shown in Figure 1, which predominates in the market. This transducer design is referred to in Reference 4 as the "classical" type of VR pressure transducer. Pressures to be measured are applied to either or both sides of the center plate (CP) causing complementary changes in the air gaps, and therefore, in the inductance of each coil. The most common method of obtaining an electrical output is shown conceptually.

Pressure transducers using an aneroid or bourdon tube moving a linear variable differential transformer (LVDT) or moving armature differ significantly from the VR transducer with respect to the magnetic circuit and the effects of mutual inductance and eddy currents. They are also significantly less energy efficient than the classical VR type. Adjustments normally provided on carrier signal conditioners are usually adequate to accommodate all types. A detailed discussion of the principles and performance of VR accelerometers is contained in Reference 5, and an analysis of the external armature and "E-Core" transducer element used therein is given in Reference 6.

The inherent advantages of the classical VR pressure transducer are evidently the result of concentrating both the pneumatic process energy and circuit electrical energy in the same small volume at the airgaps, and of the natural symmetry of the mechanical, pneumatic, magnetic, and electrical systems. Unlike capacitance transducers of similar geometry, they are not sensitive to the dielectric constant of the pneumatic medium, which may be affected by moisture, chemical composition, or radioactivity. Capacitance transducers require special design of connecting cables due to capacitive and conductive effects on the low level circuit. These do not seriously affect the operation of a

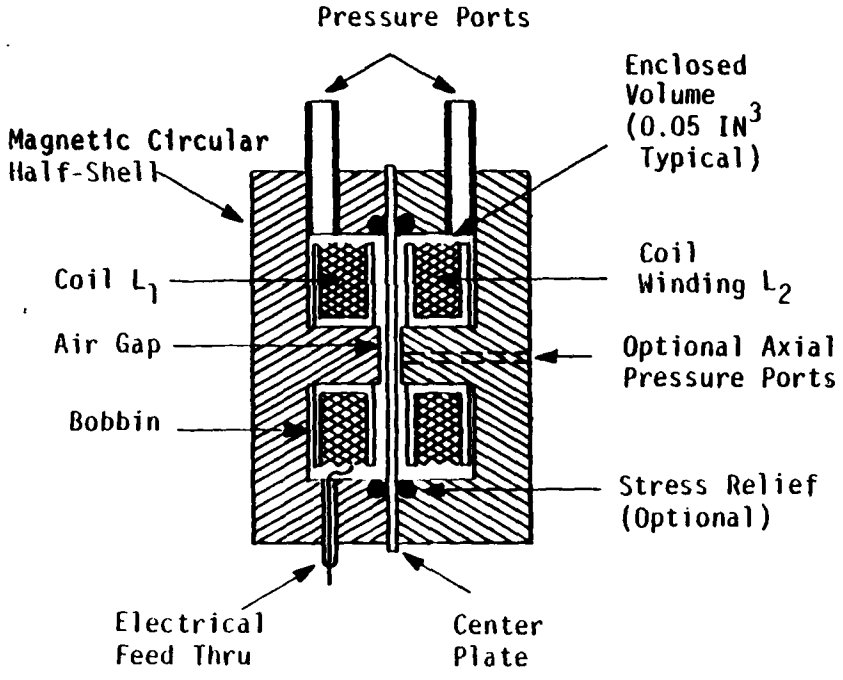

CENTERPLATE RESONANT FREQUENCIES (TYPICAL): 500-15000 HERTZ

RANGE SENSITIVITIES:
0 to ± 0.02 PSI FULL SCALE TO
0 to ± 5000 PSI FULL SCALE

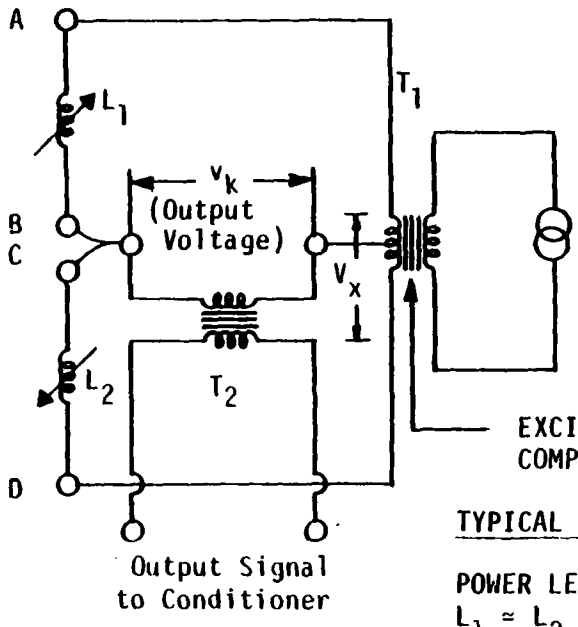

CARRIER OSCILLATOR - POWER AMPLIFIER

FREQUENCY 1-20 KHz (TYP.)

EXCITATION AND BRIDGE COMPLETION TRANSFORMER

TYPICAL PARAMETERS

POWER LEVEL ~ 0.1 VA
$L_1 \approx L_2 = 20$ MILLIHENRIES
ΔL AT FULL LOAD ≈ 2 MH
$V_x = 5$ VOLTS RMS

$$\frac{V_k}{V_x} = \frac{\Delta L}{2L} = 50 \text{ MILLIVOLTS PER VOLT}$$

Figure 1. Operating Principle and Typical Circuitry - Variable Reluctance Pressure Transducer

properly designed VR transducer input network. Work done in developing capacitance transducers is relevant to this study because:

- The merits of both capacitance and VR transducers should be compared to assure that further in-depth study of the VR type is warranted.

- Mechanical design and construction problems, especially those concerning stress and deflection of the center plate, are similar and may have similar solutions.

- Alternating current (AC) electrical circuit techniques developed for capacitance transducers may also be of value for use with VR transducers.

It is evident from its construction that the VR transducer is by nature a differential pressure transducer, although a wide range of absolute types are commercially available. The basic design is well suited to measurement of low or medium range pressure differentials at high line pressures such as are encountered in venturi and orifice plate pipe flow measurements ("DP Cells"). Their ruggedness, repairability, and electrical noise immunity may prove invaluable in such applications.

The "classical" VR transducer which is the subject of this report is described in a patent application submitted to the US Patent Office by James Clark on March 21, 1947, and titled "Electromagnetic Pressure Sensitive Device." The patent, number 2,581,359, was issued on January 8, 1952. James Clark was in the employ of the United States Government at the time of application and rights to manufacture and use the device were assigned to the Government.

A comprehensive bibliography on the subject of capacitive, reluctive, and other "diaphragm" type pressure transducers appears in NASA Contractor Report NASA CR-135282, "Development Of A High Temperature Pressure Transducer," by R. L. Egger of Boeing Aerospace Company, and is dated October 1977.

SECTION II

SIMPLIFIED TRANSDUCTION PRINCIPLE OF THE VARIABLE RELUCTANCE PRESSURE TRANSDUCER

A mechanically ideal, electrically linear pressure transducer of the self-generating type will have an electrical output voltage $v_o = n \cdot p_k$ where p_k is the applied pressure and n is the sensitivity constant or voltage calibration in volts per unit of pressure (Figure 2a).

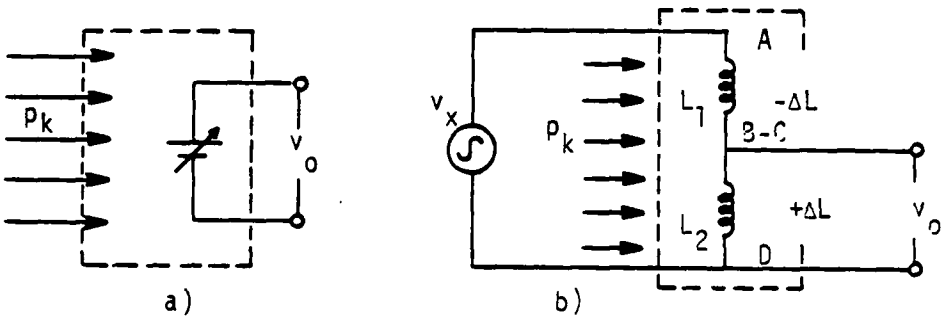

$$v_x = V_x \cos \omega_c t$$

Figure 2. Basic Transduction Circuit Equivalent

In the case of the VR transducer in Figure 2b, which is assumed to be magnetically, mechanically, and electrically ideal, the electrical output cannot be obtained directly since it is a passive network. A source of AC "excitation," $v_x = V_x \cos \omega_c t$, of radian frequency ω_c, is required. The electrical output may then be obtained by a simple application of Ohm's law. The sign convention chosen to indicate an increase in voltage from point (B - C) to D with applied pressure is purely arbitrary. At zero applied pressure, the inductances L_1 and L_2 are both equal to L, and the current in the circuit i_o is $i_o = \frac{v_x}{2j\omega_c L}$. The output voltage v_o is given by

$$v_o = V_{(B-C)-D} = i_o j\omega_c L = \frac{v_x}{2}$$

At an applied pressure p_k the complementary inductance changes will be $|\Delta L|$. The current in the circuit is now i_k.

$$i_k = \frac{V_x}{j\omega_c[(L+\Delta L)+(L-\Delta L)]} = \frac{V_x}{2j\omega_c L}$$

as before. The output voltage is v_k.

$$v_k = i_k j\omega_c(L+\Delta L) = \frac{V_x}{2}\left(1+\frac{\Delta L}{L}\right) = \frac{V_x}{2}(1+np_k)$$

Thus, the factor $n = \frac{\Delta L}{L} \div p_k$ is developed which relates electrical inductance change to applied pressure. In some cases in physical testing, p_k may contain a steady state component, P_s, and a fluctuating component of frequency, ω_f, having a peak amplitude, P_f. The pressure data then has the form $p(t) = (P_s + P_f \cos \omega_f t)$. The transducer circuit output in this case will be

$$v_o(t) = v_{(BC)-D} = \frac{V_x}{2} + \frac{nV_x}{2}(P_s + P_f \cos \omega_f t)$$

$$= \frac{V_x \cos \omega_c t}{2}(1 + nP_s + nP_f \cos \omega_f t)$$

Note that ω_c and ω_f are unrelated. The first term is a fixed electrical circuit residual unrelated to pressure which may be avoided by taking the output signal from a point (B-C) to a point $\frac{V_x}{2}$ volts above point D as shown in Figure 3. Although this circuit has the appearance of a "bridge" circuit used in electrical metrology, it is not

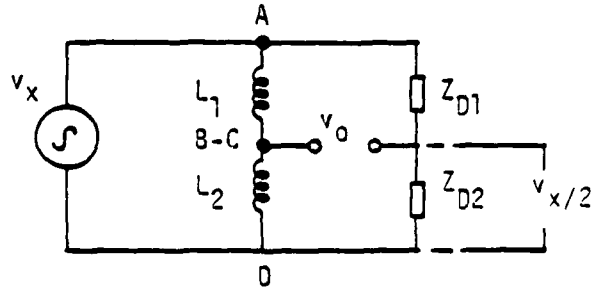

Figure 3. Basic Electrical Circuit

strictly so, since it is required to develop the useful output in an unbalanced condition. The same result may be accomplished by means of a center tapped supply transformer, T_1, in Figure 1. The output is then

$$v_o = \frac{nV_x \cos \omega_c t}{2} (P_s + P_f \cos \omega_f t) = \eta_1 (P_s + P_f \cos \omega_f t)$$

(Instantaneous Volts)

This form is comparable to the basic form $v_k = \eta p_k$, but the voltage calibration factor η_1 contains the term $\cos \omega_c t$. It is the only signal fully analogous to applied pressure and only this expression contains all the pressure information available from the transducer. The unavoidable presence of the $\cos \omega_c t$ term makes it difficult to interpret the electrical output in terms of the original physical input. The factor, η_1, for a VR transducer has a useful meaning only when the effects of signal processing are quantified, as will be discussed in Section VIII.

There are several ways of processing such a signal to increase its usefulness in a data system, all having distinct disadvantages. The choice of signal processing will depend on the method of data recording and processing used. An elementary signal processor for a VR transducer, however, consists of no more than a source of voltage $v_x = V_x \cos \omega_c t$, called the "excitation" or "carrier" voltage supply, and if needed, an AC amplifier capable of passing the frequency, ω_c, and any product functions of the form $\cos \omega_f t \cdot \cos \omega_c t$. All other elements of commonly used carrier signal conditioners are traditional rather than functional.

SECTION III

AC AMPLIFIER DESIGN PRACTICES AID PERFORMANCE CHARACTERISTICS

AC amplifiers are often used to increase the output signal of a VR transducer. Typical amplitude and phase output/input relationships of an AC coupled amplifier are shown in Figure 4. Such amplifiers are used wherever power, voltage, or

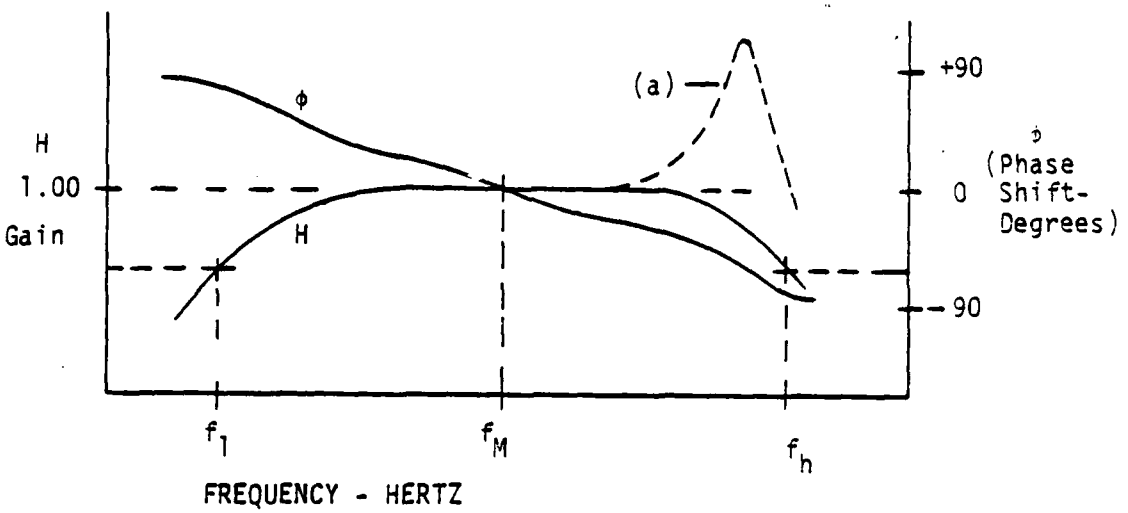

Figure 4. Typical AC Amplifier Characteristics

current gain, H, is needed within a given range of frequencies from f_l to f_h, not including zero frequency (DC). The complex form for the gain which combines both phase ϕ and amplitude H_2 is n_2, so that $n_2 = H_2 \angle\phi$. Typical applications for AC amplifiers are sound and vibration measurements with microphones, velocity pick-ups, or accelerometers, and in wired and radio communications. In sound recording and reproduction,

amplifiers having a ratio of f_h to f_l of 10,000 (12 octaves) at high power output levels are common at competitive consumer prices. The loss of gain at frequencies below f_l occurs in capacitance coupled amplifiers due to the rise in series reactance of coupling capacitors (lead networks). In transformer-coupled amplifiers, a similar loss will occur due to shunt inductive reactance which would add to the loss from series capacitors. At high frequencies, the decrease in gain in both types is due to shunt circuit capacities and series inductive reactance (lag networks) in components and wiring. Unless properly designed, a high frequency resonance of the type shown at (a) accompanied by a large overall phase shift may occur in amplifiers using inductors or transformers, and a lowering of f_l may occur as a result of leakage reactance and eddy current losses in these iron core components. (Reference 7, Chapter XVIII, and Reference 8, Chapter 11.)

In audio and communications work, it is customary to specify f_l and f_h as those frequencies at which the relative gain must be within 41 percent ($\pm$ 3db) of the gain at mid-frequencies. In instrumentation work, a gain variation or uncertainty of more than 0.1 percent is sometimes excessive. The design effort and construction cost for AC amplifiers results from the need in a particular application for; a) high gain, b) high parameter stability, c) low noise, d) high power output, e) high power efficiency, f) uniform output or gain over a wide range of frequencies, or any combination of those qualities. Unlike DC amplifiers, considerable variations in circuit DC operating points, gain and phase shift within stages may be tolerated while maintaining overall AC performance, particularly AC gain stability. This capability is used to advantage in the design of precision DC amplifiers by using a chopper and AC amplifier to stabilize or regulate forward gain or feedback in the overall DC signal path. (Reference 9.)

AC amplifiers for use with VR or other AC transducers normally need only meet modest bandwidth and gain requirements, and the necessary gain and phase stability is easily achieved. The DC power supply voltage regulation requirements are much less stringent than for DC amplifiers.

The bandwidth requirements for the circuitry in the signal path in a carrier signal conditioner are directly dependent on the frequency content of the physical data. Where the carrier center frequency, ω_c, is much greater than the highest signal frequency, (ω_f), tuned amplifiers may be used to advantage, as is done in AM radio receivers. The 400 kilohertz carrier amplifier reported upon in Reference 10 was a narrow band-pass tuned amplifier.

The gain of any amplifier used in signal conditioners for pressure transducers is selected to provide a convenient scaling of the processed output signal with respect to the pressure input magnitude. The overall system scale factor depends on the transducer calibration factor, n_1, and on the processing principles and circuitry used to develop the output signal. The voltage gain of the signal electronics is often made adjustable for operating convenience. The overall input-output relationship is also affected by design choices of input and output transformer ratios and calibration (gain trim) potentiometer settings. To simplify all subsequent discussion, all such factors will be combined to give a single gain factor, n_2. Where n_2 is not mentioned, it will be assumed to be a scalar quantity equal to unity and ϕ will be assumed to be zero; that is, $H_2/\underline{0^o} = 1$.

SECTION IV

SIGNAL PROCESSING TECHNIQUES

In the following discussion of signal processing techniques, the following assumptions are held:

- The selection of a VR transducer has been made after a determination that its response time and that of the connecting tubulation is low enough to provide the desired measurement accuracy.(1)

- A processed output signal is required which is both a true analog of physical input ("measurand") within the desired accuracy and has a voltage or current level suitable for subsequent processing along with other data signals.

- The nature of the processor block, shown conceptually in Figure 5 as having a transfer function, η_3, is that which is to be determined.

- Since only the performance of the pressure transducer and signal conditioner sub-system is being considered, a worst-case situation will be imposed on these elements by assuming zero tubulation lag.

In Figure 5, a generalized pressure input signal in the frequency domain is assumed. It has a steady state component, P_s, and a fluctuating component, P_f, of frequency ω_f, which is the highest data frequency of interest. A comparison of the processing of the electrical signal from an ideal DC transducer and from an ideal AC transducer is illustrated in this figure. The AC signal conditioner case, (b), differs from both the DC data channel (a) and the amplitude modulated (AM) radio transmitter broadcasting a sound signal (c) in that the

---

1. Data on lag time of a hypothetical typical tubulation system is presented in Appendix B.

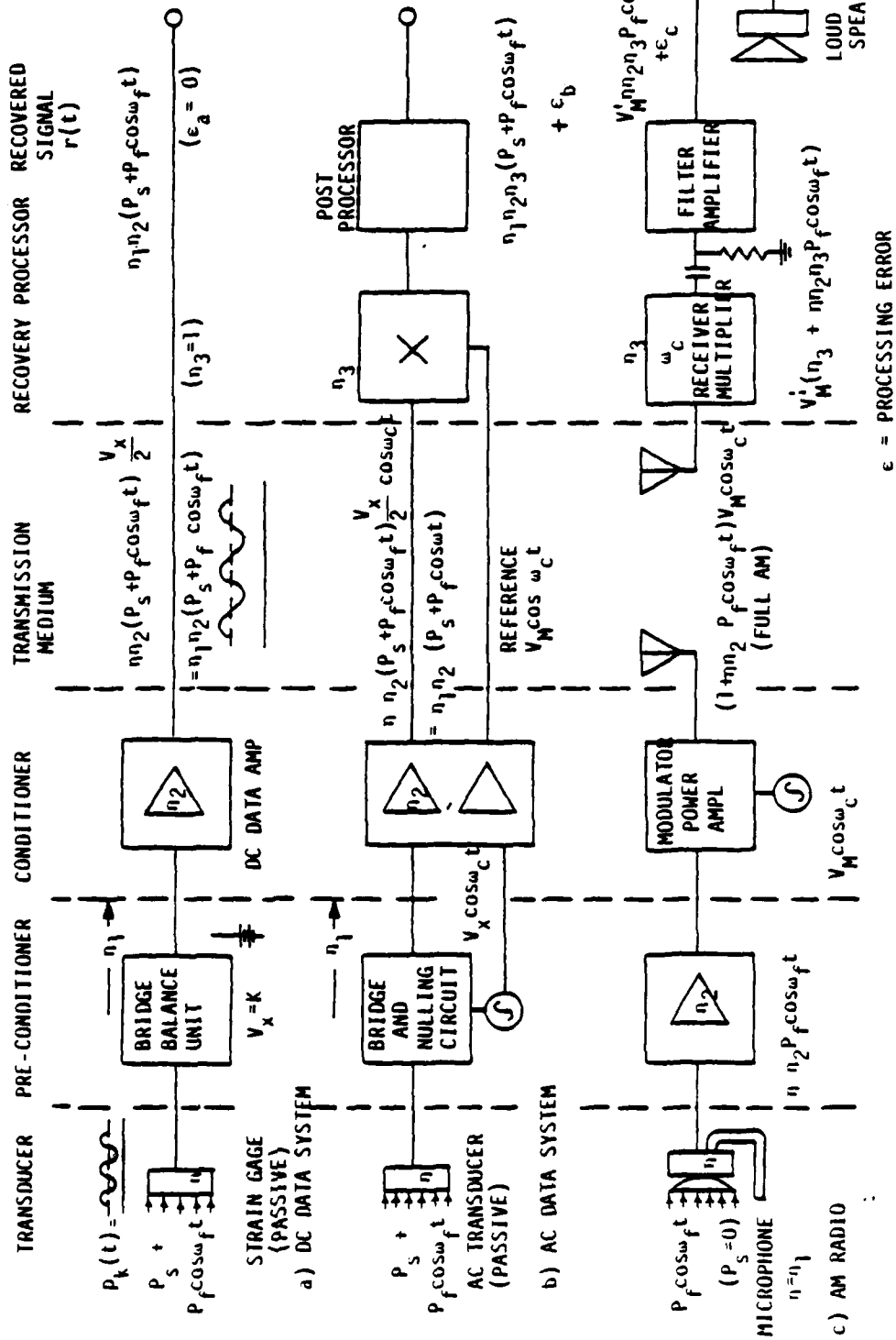

Figure 5. Elementary Signal Transmission Systems

signal available from an AC powered transducer is not a true analog of pressure.(2) It also differs from the wireless transmission case in that there is no signal information rate versus bandwidth trade-off necessary, since signals are relatively large and effects of external interference are less. A second wire for the voltage $V_M \cos\omega_c t$ is provided to maintain phase coherence. No frequency translation takes place in case (a).

A steady-state component in the data signal in either case (a) or (b) in Figure 5 can arise from four sources:

a. A steady-state component, P_s, in the pressure, which is defined in Appendix A;

b. An electrical or structural asymmetry in the transducer;

c. An intentional or unintentional residual signal due to the transducer network (signal pre-conditioner) used, or to the adjustments made on this circuit; or, in case (b) only,

d. The intentional addition of a "carrier" voltage, $V_M \cos\omega_c t$ to the data sidebar for the purpose of creating a true AM signal, thereby simplifying the de-modulation processor circuitry. AM signals such as the illustration in Figure 5 (c) contain a large carrier component by definition.

The input circuit and adjustment procedures must facilitate a careful accounting of the phase and amplitude of all sources of steady-state signal components to assure that no adverse effects on steady-state precision of the pressure data occur.

---

2. It is common practice to refer to the effects of the VR transducer on the excitation power, V_x, as modulation. This is not strictly true. The creation of a signal of the form $\cos\omega_c t$ arises solely and unavoidably from the mechanical and electrical nature of the transducer and not as a result of circuits or devices employed specifically to multiply two electrical signals, such as all electrical "modulator" circuits used in communications equipment, or electromechanical or electro-optical "choppers" used in instrumentation equipment.

Pressure input functions likely to be encountered arise from a variety of test situations, some of which are illustrated in Figure 6. The generalized frequency domain signal of the form $C(P_s + P_f \cos \omega_f t)$ might be generated in the example shown as Case 4. Although the form of this signal is common in analog electronic equipment technology, such an idealized periodic function is rarely encountered in the form of a pressure in real life test situations. The unusual, specialized aerodynamic study test programs described in References 11 and 12 are available as examples of this exceptional case, however. The generation of variable frequency pressure "signals" of known amplitudes for direct calibration of pressure data channels is an interesting technical problem. It has been the subject of much specialized study and experimental work, most notably that reported upon by the National Bureau of Standards and NASA. These methods are applicable to systems using transducers having well-known, standardized characteristics such as strain gage and piezoelectric types. The procedures for making such response calibrations, often called "dynamic" calibrations, are listed in Reference 13 and discussed in more detail in Section XI. They would be applicable to VR transducer/carrier amplifier pressure data channels only after the complete steady state signal generating and processing mechanism has been fully described. Response tests on pneumatic systems are usually performed in the time domain using pressure ramps or steps.

A quasi steady state pressure-time function such as is illustrated in Figure 6, Case I, is typical of those likely to be encountered as a practical test problem. The rise time (ramp rate) normally depends on the physical constants of the plant process, test facility or test article. Choosing some reasonable values of ramp rate and dwell time gives the time function shown in Figure 7. The frequency content of a single occurrence of this time function, $p(t)$, is given by the Fourier transform of the function.[3]

---

3. A closing technique for analyzing functions which do not return to the origin is described in Reference 5.

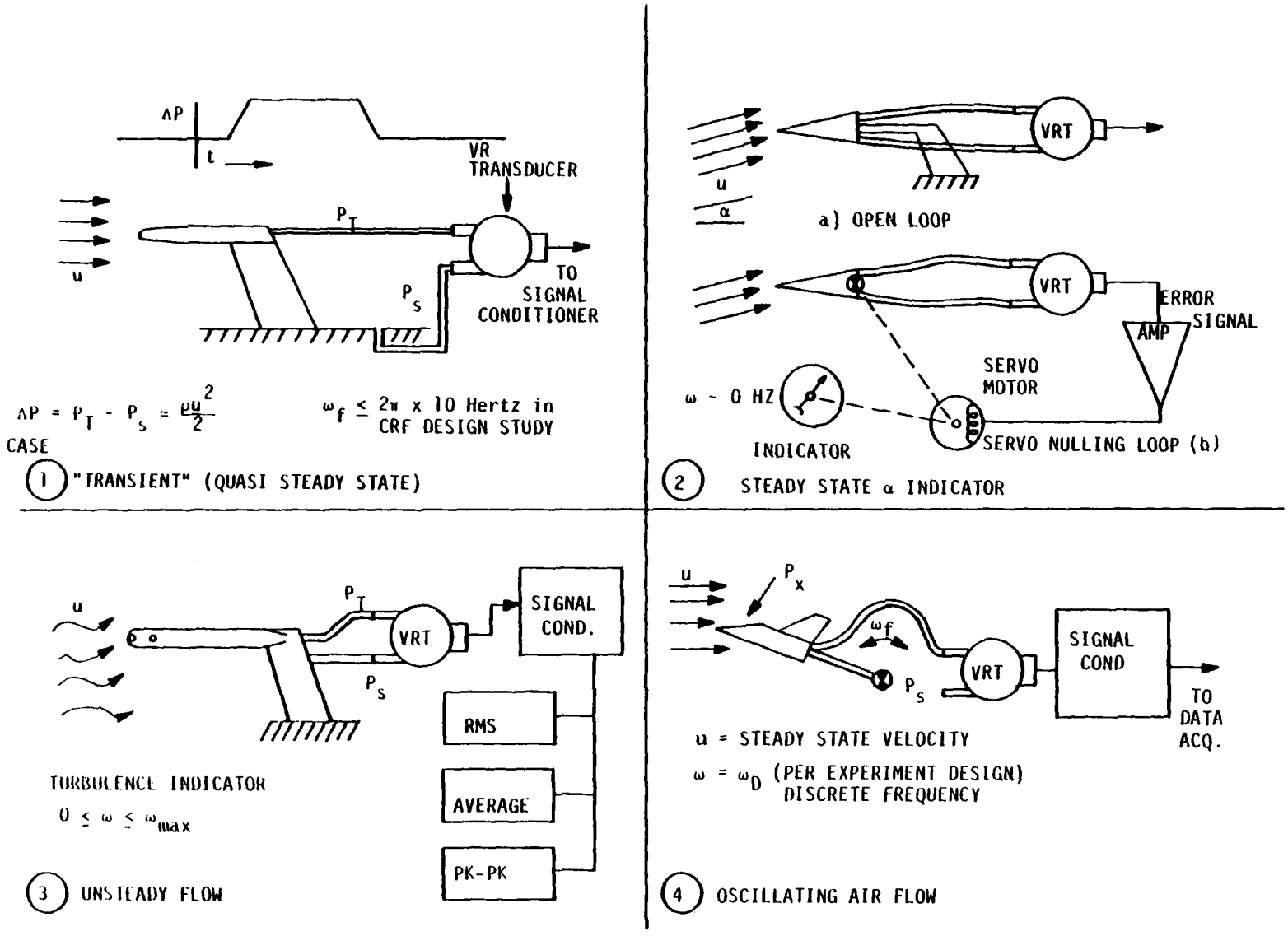

Figure 6. Low Velocity Free Stream Measurement Applications - VR Transducer

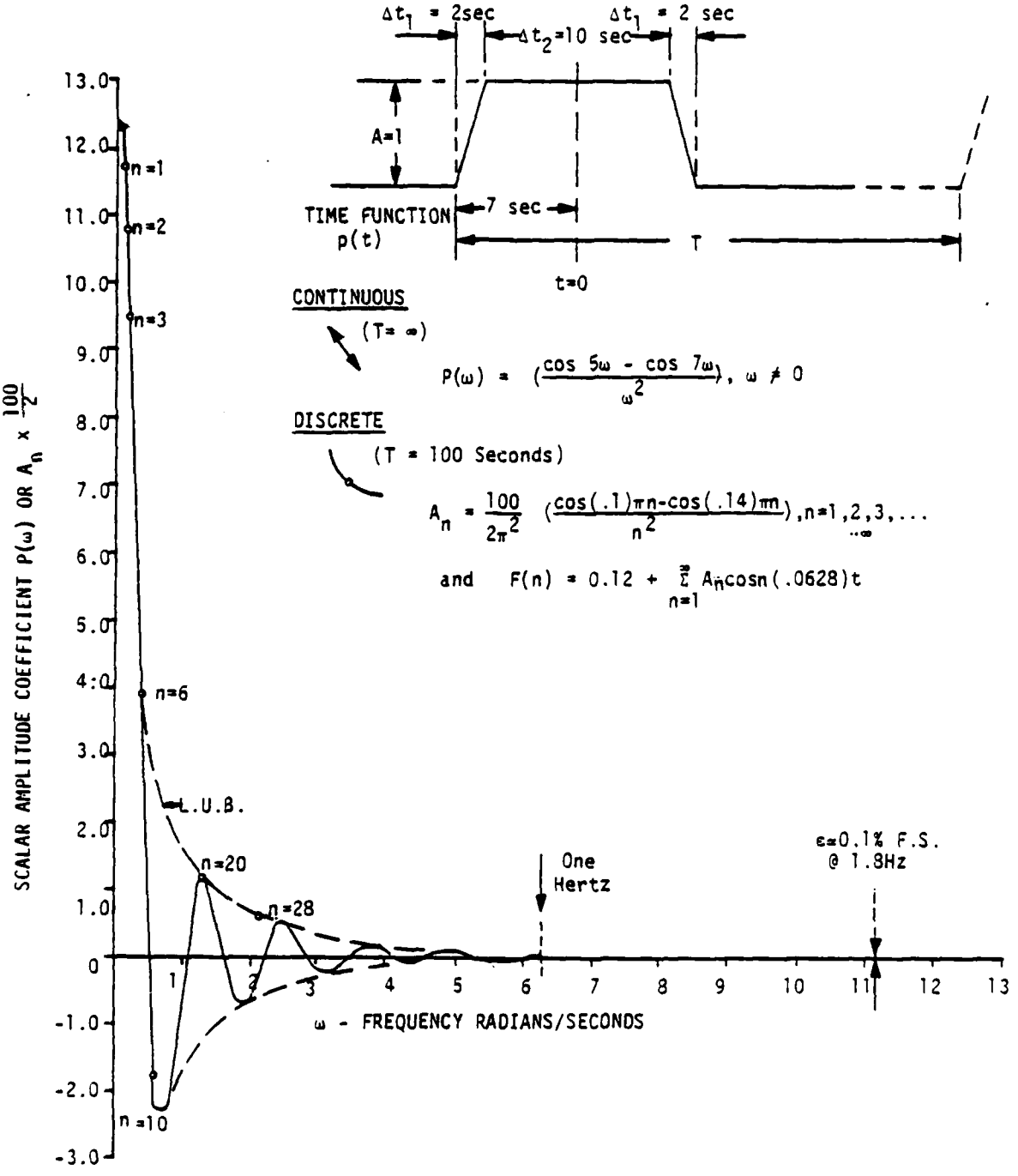

Figure 7. Frequency Spectrum-Facility Induced Pressure Transient

By its definition, the Fourier transform of this function is:

$$F[p(t)] = P(\omega)$$

$$P(\omega) = \int_{t=-7}^{t=-5} (\frac{7+t}{2})\exp(-j\omega t)dt + \int_{t=-5}^{t=+5} 1\cdot\exp(-j\omega t)dt + \int_{t=+5}^{t=+7} (\frac{7-t}{2})\exp(-j\omega t)dt$$

$$= \frac{-1}{j^2\omega^2}\left[\tfrac{1}{2}(\exp(5j\omega)+\exp(-5j\omega)) - \tfrac{1}{2}(\exp(7j\omega)+\exp(-7j\omega))\right]$$

Using the Euler identities and noting that $j^2=-1$, the result, in trigonometric functions, is

$$P(\omega) = (\frac{\cos 5\omega - \cos 7\omega}{\omega^2}) \quad , \omega \neq 0$$

In Figure 7, the amplitude coefficients for the series form for the periodic case in which this same time function repeats every 100 seconds are also plotted for comparison. After normalizing amplitudes, the values for both cases lie within the same "envelope"; that is, they have the same least upper bound and greatest lower bound. This spectrum contains little energy above several Hertz. Even assuming the sharp-cornered pressure function is physically possible and further assuming there is no frequency discrimination in the pneumatic system, the amplitude of this hypothetical pressure "signal" applied to the VR transducer center plate at about 1.8 Hertz will be less than 0.1 percent of the limit value as ω approaches zero. This limit value is for all practical purposes the "DC" component amplitude. The electrical output from the VR transducer in response to this pressure signal will be

$$\eta_1 p(t) = \frac{nV_x}{2}p(t)\cos\omega_c t = p(t)\frac{nV_x}{2}\cdot\tfrac{1}{2}[\exp(j\omega_c t)+\exp(-j\omega_c t)]$$

The frequency spectrum of the corresponding product function can be obtained directly as before.

$$P(\omega,\omega_c) = \frac{nV_x}{4}\left[\frac{\cos 5(\omega+\omega_c)-\cos 7(\omega+\omega_c)}{(\omega+\omega_c)^2} + \frac{\cos 5(\omega-\omega_c)-\cos 7(\omega-\omega_c)}{(\omega-\omega_c)^2}\right]$$

Using the discrete form describing the case where the event recurs every 100 seconds, p(t) is given by the series

$$p(t) = \frac{A_o}{2} + \sum_{n=1}^{n=\infty} \tfrac{1}{2}\left(\frac{10}{\pi n}\right)^2 [\cos(.10)\pi n - \cos(.14)\pi n]\cos\, n(.0628)t$$

$$= 0.12 + .2343\cos(.0628)t + .2173\cos(.1256)t + .1909\cos(.1884)t + \ldots.$$

The product function, $p(t)\cos\omega_c t$, may be found by multiplying each term of the series for p(t) by $\cos\omega_c t$ and reducing the compound terms by means of these trigonometric identities.

$$\sin u \cdot \cos v = \tfrac{1}{2}\sin(u+v) + \tfrac{1}{2}\sin(u-v)$$

$$\cos u \cdot \cos v = \tfrac{1}{2}\cos(u+v) + \tfrac{1}{2}\cos(u-v)$$

$$\sin u \cdot \sin v = \tfrac{1}{2}\cos(u-v) - \tfrac{1}{2}\cos(u+v)$$

$$\sin(-u) = -\sin(u)$$

For example, the first few terms are

$$p(t)\cos\omega_c t = .12\cos\omega_c t + .2343\cos(.0628)t \cdot \cos\omega_c t + .2173\cos(.1256)t \cdot \cos\omega_c t + .1909\cos(.1884)t \cdot \cos\omega_c t + \ldots\ldots$$

$$= .12\cos\omega_c t + \frac{.2343}{2}[\cos(\omega_c - .0628)t + \cos(\omega_c + .0628)t] + \frac{.2173}{2}[\cos(\omega_c - .1256)t + \cos(\omega_c + .1256)t] + \frac{.1909}{2}[\cos(\omega_c - .1884)t + \cos(\omega_c + .1884)t] + \ldots.$$

Therefore, at $\omega = \omega_c$ and $\omega = -\omega_c$, maxima of two electrical signals of magnitude $\frac{nV}{4}x$ times the original pressure input of unit amplitude will appear at the output of the transducer, as shown in Figure 8, while there will be no electrical output at or near $\omega = 0$, the location of the

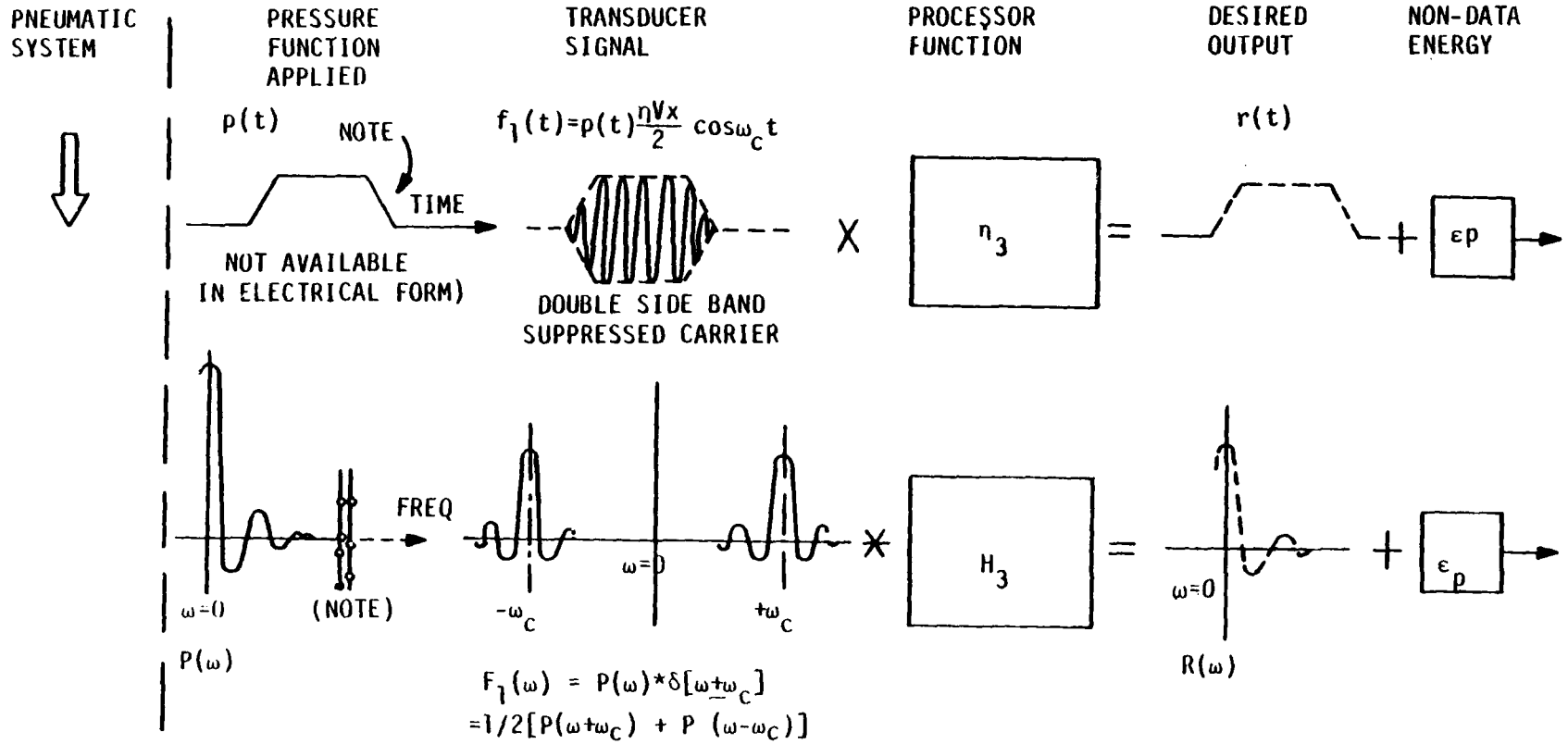

NOTE: BAND LIMITING EFFECTS OF PNEUMATIC LAG TIME NOT SHOWN.
IN DISCUSSION, LAG TIME IS ASSUMED ZERO FOR WORST CASE ANALYSIS.
SHARP CORNERS ON p(t) ARE ALSO A WORST CASE ASSUMPTION AND ARE IMPOSSIBLE IN PRACTICE.

Figure 8. Information System for Processing Compressor Transient Pressure Signal-Variable Reluctance Pressure Transducer

pressure function. This is true of all AC excited passive transducers (VR, capacitive, LVDT, and strain gage). The original identity of the signal will be irreversibly altered when $\omega=\omega_c$ because product terms of the form ω_c^2, $\omega_c.2\omega_c$, and so on, will be formed. That part of the signal energy will be transformed into a $\omega=0$, or "DC", component. A similar identity change will occur when $\omega>\omega_c$. This is called frequency folding and is the same as the aliasing problem in sampled data systems. Choosing ω_c to be several times as large as the highest frequency in the pressure signal is not done simply to avoid complications in data processing, however. In the design and construction of VR pressure transducers, the internal pneumatic volume, center plate resonant frequency and magnetic properties combine to impose a practical upper limit on useful response to the pneumatic input. However, this method of determining the effective maximum frequency present in the pressure data will indicate the high frequency response required of the transducer and signal conditioner.

Figure 8 illustrates the process of artificially creating an electrical output signal, r, which is an approximate analog of the original pressure input, p, making use of the natural band-limiting characteristics of the VR transducer pneumatic and mechanical system to justify discarding the higher frequency products. Some ways of implementing this process are illustrated in Figure 9. Multiplying the periodic function, $f_1(t)$, by another, $f_2(t)$, of the same frequency, ω_c, will result in terms, $\cos^2 \omega_c t$, which have a useful data frequency component; that is, one centered about $\omega = 0$. This is also true of the process illustrated in Figure 9-b, where $f_1(t)$ is subjected to a nonlinear element. The output/input characteristic of a nonlinear element is a power series of the form $a + bx + cx^2 + dx^3 + \ldots$. (Reference 14, Page 161) Small signal operation of semiconductor and vacuum tube diodes approximates this characteristic. The signal might be sampled synchronously at non-zero points, as shown in Figure 9-a(4). The most simple operation from a formal mathematics standpoint would be multiplying the signal function, $f_1(t)$, by another cosine function, $f_2(t) = \cos \omega_c t$, giving $f_1(t).f_2(t) = \frac{1+\cos 2\omega_c t}{2}$. Discarding the double frequency term by means of a filter will yield the desired analog

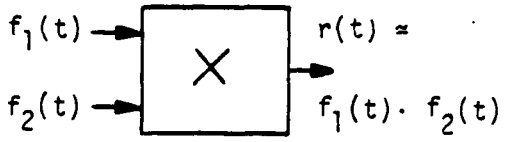

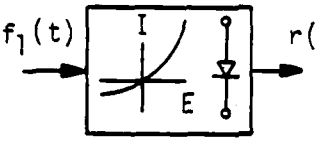

$r(t)=a+bf_1(t) + c[f_1(t)]^2 + d[f_1(t)]^3 + e[f_1(t)]^4+...$

A | MULTIPLIERS

B | NON-LINEAR ELEMENT

1) SQUARE WAVE

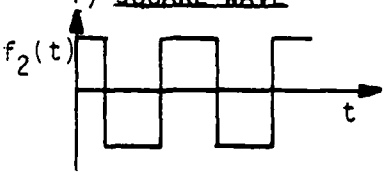

$$f_2(t)= \frac{4}{\pi} [\cos \omega_c t - 1/3 \cos 3\omega_c t + 1/5 \cos 5\omega_c t - \ldots]$$

$$= \frac{-4}{\pi} \sum_{m=1}^{\infty} \frac{(-1)^m}{[2m-1]} \cos(2m-1)\omega_c t$$

2) TRIANGULAR WAVE

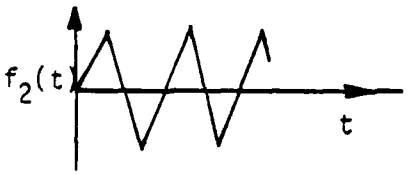

$$f_2(t) = \frac{8}{\pi^2} [\sin \omega_c t - 1/3^2 \sin 3\omega_c t + 1/5^2 \sin 5\omega_c t - \ldots]$$

$$= \frac{-8}{\pi^2} \sum_{m=1}^{\infty} \frac{(-1)^m}{[2m-1]^2} \sin (2m-1)\omega_c t$$

3) GENERAL CASE

$$f_2(t) = \Gamma_0 + \Gamma_1 \cos \omega_c t + \Gamma_2 \cos 2\omega_c t + \Gamma_3 \cos 3\omega_c t + \Gamma_4 \cos 4\omega_c t + \ldots$$
$$+ \Gamma_1' \sin \omega_c t + \Gamma_2' \sin 2\omega_c t + \Gamma_3' \sin 3\omega_c t + \Gamma_4' \sin 4\omega_c t + \ldots$$

4) SYNCHRONOUS SAMPLING

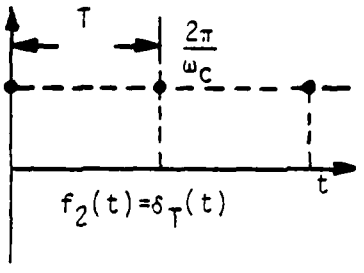

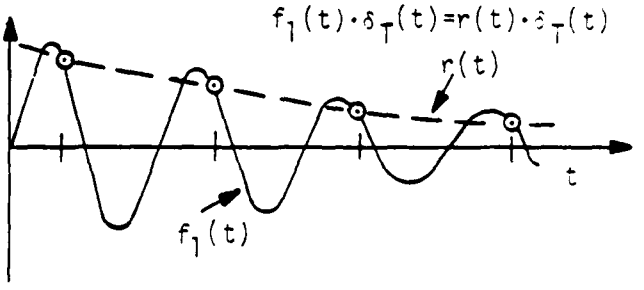

Figure 9. Signal Processing Principles

approximation of p(t). The underlying principle is referred to in communications systems as frequency translation or amplitude modulation. The process may be defined concisely in the frequency domain in terms of Fourier transforms.

$$F[f_1(t)\cdot f_2(t)] = F[f_1(t)\cos\omega_c t] = \tfrac{1}{2}[F_1(\omega+\omega_c) + F_1(\omega-\omega_c)]$$

The function F_1 is the frequency domain transform of the time function $f_1(t)$. The case of a square wave (a zero centered gate function) for $f_2(t)$ is of particular interest because of the availability of the simple circuit shown in Figure 10. It has been widely used because it does not require costly precision linear components to provide the same result as a precision analog multiplier circuit. This circuit, used in communications equipment, is called a diode ring or phase sensitive modulator (or demodulator). Highly reliable, high performance carrier signal conditioners use this circuit, or minor variations such as are described in Reference 15. The voltage function, n_2V_s, in Figure 10 is the instantaneous value of the signal, such as one generated by a VR pressure transducer in response to a steady state pressure input, after amplification by the factor n_2. As in normal practice, the reference voltage, V_R, corresponding to $f_2(t)$, and the signal voltage, n_2V_s, have been adjusted so that their zero crossings coincide. The semiconductor diodes are assumed to be perfect switches, a condition which is closely approximated when the amplitude of V_R is very large. This amplitude condition is also required to prevent the output signal from reversing polarity when the transducer output signal, V_s, becomes very large. The use of relatively large values of V_R also will overcome (swamp) the fixed forward voltage drop in semiconductors, which is about 0.25 volts for germanium and 0.6 volts for silicon. Although the only electrical process occurring is that of the addition of sinusoidal currents, the switch action of the diodes creates a net effect of multiplying the signal n_2V_s, by the square wave of frequency, ω_c , having an amplitude of $\pm$ 2 units, assuming the arbitrary constants shown.

A practical circuit so constructed would also contain large currents in the direct path through the transformers, T_3 and T_4, and

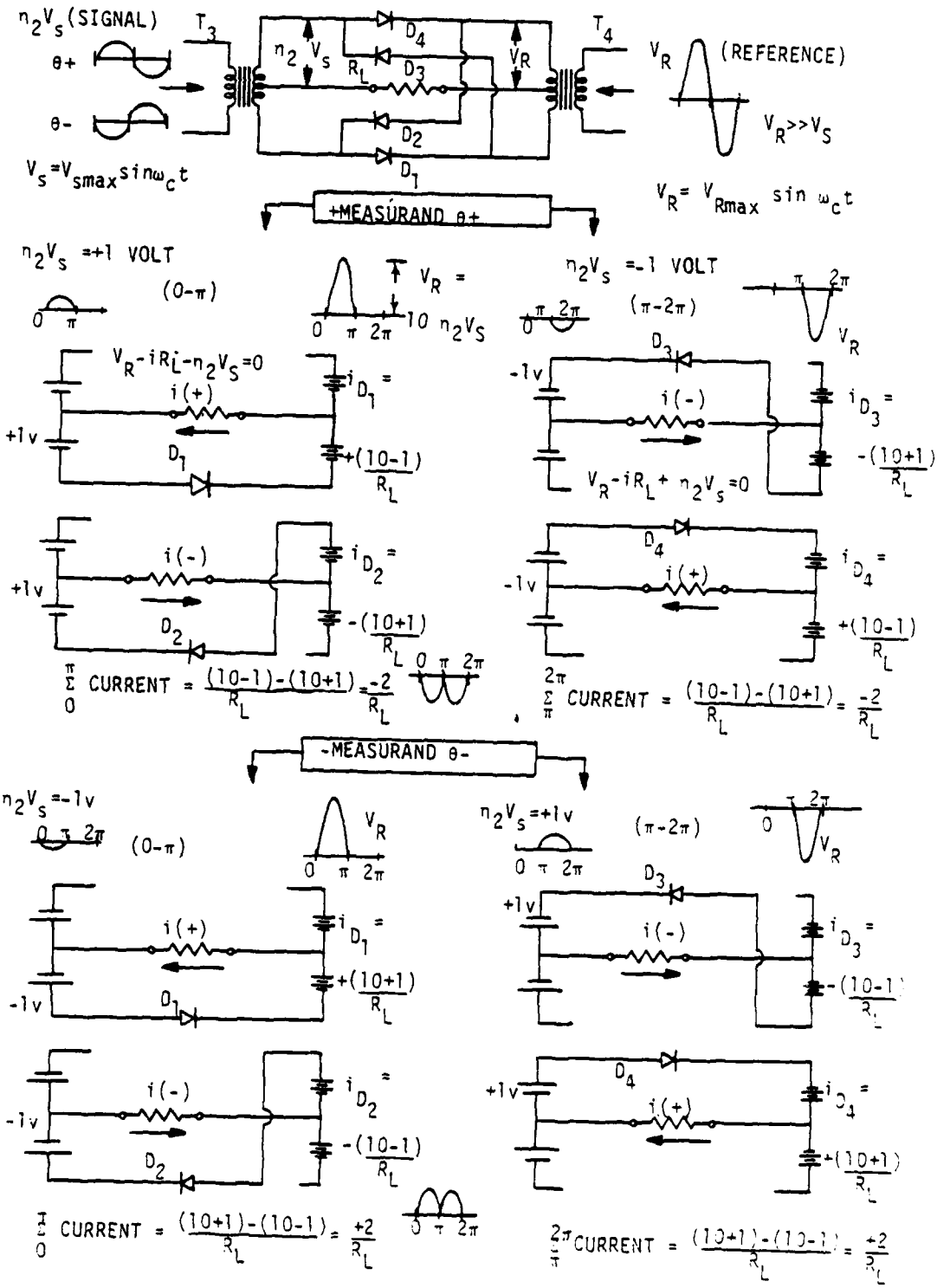

Figure 10. Current Ring Modulator (De-modulator)

either pair of diodes. They have not been shown graphically to simplify the exposition. These currents average to zero over the period 0-2π in the load R_L, and therefore, the assumption of a value of V_R exactly ten times that of $n_2 V_{s(max)}$ is not critical to the argument. These currents are of concern only as they affect diode and transformer operation. In practice, a current limiting resistor is placed in series with each diode. The power losses thus caused are easily supplied by increasing the power gain of the AC electronics driving the transformers. If this is done, however, the circuit will become more sensitive to random temperature induced changes in the volt-ampere characteristics and junction capacitance effects in the diodes. Since the output is the small difference of two large currents, these changes can seriously limit circuit performance. For this reason, the Schottky barrier or majority carrier diode, References 16 and 17, is well suited to this application because of the absence of effects on forward voltage drop, reverse current leakage, and charge storage caused by minority (slow) carrier activity. These effects, present in junction diodes and bipolar transistors, are temperature dependent and highly variable with time and from unit to unit. This same freedom from minority carrier activity is also possessed by field-effect transistors, which are often used in complementary pairs in a three-terminal function multiplier demodulator circuit (Reference 18). The effective output impedance of this circuit is equal to the value of each current limiting resistance. A bi-polar transistor circuit also used in commercially manufactured equipment is described in Reference 17, Section 17-16. Such circuits perform the same mathematical operation as that of Figure 10.

A feature of the transformer-driven ring modulator circuit which has great practical value is its ability to isolate (insulate completely) the two output terminals from all other system connections, eliminating or simplifying all electrical noise and system safety problems. The electrical noise immunity of a "carrier" data channel is due both to the circuit configuration and to the frequency spectra involved. Undesirable electrical disturbances not related to transducer input, commonly referred to as "noise," usually originate in utility power systems and

are introduced into the input of a signal conditioner, adding to the transducer output by two means. Normal mode signals appear as a voltage across the two input terminals of the signal conditioner in addition to the data signal from the transducer. Common mode signals appear as voltages between both input terminals and circuit common or electrical ground, ultimately developing within the signal conditioner circuitry as a normal mode signal, with a similar undesirable result. For a complete treatment of this subject, see References 19 and 20.

A "carrier" data channel of the type shown in Figure 5(b) is much less susceptible to normal mode "noise" than the DC system of Figure 5(a) for three reasons: 1) Spectrum Separation: The fundamental and dominant harmonics of commonly used utility power system frequencies of 25, 50, 60, and 400 hertz normally lie outside the pass band of the signal circuitry designed to pass ω_c (Figure 4). "Noise" signals of these frequencies picked up in cables and components will be greatly reduced in amplitude. Thermo-emfs and other low frequency spurious signals are completely removed. 2) Connecting Cable Circuit: A natural characteristic of VR transducers is the manufacturability of medium impedance (100 to 1000 ohms) devices. This means that neither magnetic nor electrostatic field pickup will be significant using ordinary cable and connectors, even if the line lengths are great (up to 3 miles). This is a designed-in feature of telephone lines (600 ohms) and of extremely low-level microphone circuits (200 ohms) used in sound recording and broadcasting. A dominant characteristic of these systems is that power system frequencies and their harmonics do lie within the pass band of the equipment and would be very evident and objectionable were it not for the effectiveness of this circuit technique. 3) Useful signal levels from most AC transducers are usually much higher than other types, such as strain gages.

These advantages are inherent in the VR transducer/carrier amplifier method, and accrue even when least-effort equipment designs are used.

Common mode noise reduction capabilities of this method may be enhanced by using low cost transformers to isolate all input terminals of the signal conditioner from utility ground, and also to isolate the output of the signal conditioner from grounds in both the transducer lines and the electronics power supplies. All outputs in a multi-channel system may be isolated from each other as well as from instrument system and utility grounds, so any kind of down-channel data acquisition or signal monitoring device can be connected without creating ground loops. The use of frequency translation to create a convenient signal shifted downward to the original spectrum location of the pressure input (called "baseband" in communications work) will at the same time translate the small amount of "noise" not removed by the amplifier upward to $\omega = \pm \omega_c$, where it can easily be removed with other non-data products.

The functional block in Figure 5(b) labeled "Post Processor," is in reality a low-pass filter. Its function can be viewed in a number of ways, all of which are pertinent and accurate. It may be described as:

a) An interpolator which fills in missing values of periodically interrupted data,

b) A separator of spectrum components,

c) An eliminator of objectionable "hash" or "ripple" in the reconstructed data signal,

d) A corrector of errors produced in the frequency translation process, as illustrated in Figure 8.

This filter will obviously restrict the throughput frequency response of the transducer-signal conditioner channel. The best that can be achieved is an effective compromise of "smoothing" the signal and preserving the high frequency data. This requires a careful trade-off and sometimes results in very elaborate filter designs. Filter

requirements are dictated by the characteristics of the readout or data acquisition devices which must be accommodated as down-channel destinations of the signal. These are listed in Table 1. Since the design of the anti-aliasing filters in sampled data systems is very critical, they may serve to alleviate the signal conditioner output filter problem.

The design of output filters is dictated by the amplitudes and frequencies of the frequency translation by-products, such as the term $1/2nn_2p(t)\cdot V_M\cos 2\omega_c t$ resulting from the use of a cosine function for the multiplier, $f_2(t)$. When $f_2(t)$ is one of the periodic waves of the kind shown in Figure 9 and when the pressure signal p is a constant, P_s, the overall output/input relationship can be determined by multiplying the signal $(nn_2P_s\cos\omega_c t.\frac{x}{2})$ term-by-term by the series form of $f_2(t)$. To be general, it is assumed that the zero crossings of $f_1(t)$ and $f_2(t)$ do not coincide, in which case a definite time reference must be adopted. This is done by using the two-phase (orthogonal component) form for $f_1(t)$ and $f_2(t)$. Then, $f_2(t)$ will be

$$f_2(t) = \Gamma_1\cos\omega_c t + \Gamma_3\cos 3\omega_c t + \Gamma_5\cos 5\omega_c t + \Gamma_7\cos 7\omega_c t + \ldots. +$$

$$\Gamma'_1\sin\omega_c t + \Gamma'_3\sin 3\omega_c t + \Gamma'_5\sin 5\omega_c t + \Gamma'_7\sin\omega_c t + \ldots. +$$

In this case, the product will be

$$f_1(t)\cdot f_2(t) = \frac{nn_2V_xP_s}{2}\left[\Gamma_1 + \frac{\Gamma_1+\Gamma_3}{2}\cos 2\omega_c t + \frac{\Gamma_3+\Gamma_5}{2}\cos 4\omega_c t + \frac{\Gamma_5+\Gamma_7}{2}\cos 6\omega_c t + \ldots.\right.$$

$$\left. + \frac{\Gamma'_1+\Gamma'_3}{2}\sin 2\omega_c t + \frac{\Gamma'_3+\Gamma'_5}{2}\sin 4\omega_c t + \frac{\Gamma'_5+\Gamma'_7}{2}\sin 6\omega_c t + \ldots.\right]$$

The "phase angle" Θ between the signal f_1 and the fundamental component of f_2 is given by

$$\cos\Theta = \frac{\Gamma_1}{[\Gamma_1^2+(\Gamma'_1)^2]^{\frac{1}{2}}}$$

In practice, circuit adjustments are provided to produce the condition $\cos\Theta=1$ for optimum operation of circuits such as in Figure 10. A discussion of such signal phasor adjustments in equipment is presented in Section VIII.

TABLE 1

REQUIREMENTS FOR OUTPUT FILTERING -
FREQUENCY TRANSLATING SIGNAL CONDITIONERS

READOUT DEVICE	DEVICE FREQ. RESPONSE	FILTER REQUIREMENT
Analog Panel Meter	<1.0 Hz	(None Required)
Digital Panel Meter	<5.0 Hz	Probably <10 Hz
DC Servo Motor	<100 Hz	Compensation Network
Oscillograph Galvo	Band Limiting	Varies(1)
Analog Tape	Band Limiting	Severe -Requires Study
Oscilloscope	Wide Band	Severe(2)
Digital Data Acq Sys.	Band Limiting	Use Anti-Aliasing Filter (See Text)

(1) Ballistic characteristics of galvanometer assist in filtering.
(2) When used as a data display, not for circuit diagnostics.

The output of the multiplier (modulator) when the pressure "transient" of Figure 7 is applied to the transducer is defined by the result of term-by-term multiplication of the product signal, $\eta_1 p(t)\cos\omega_c t$, in its series form in the time domain with the series form of the function $f_2(t)$. Reduction to first power sine and cosine terms is accomplished by the use of the trigonometric identities as before. The complete expression for the processed or "recovered" signal r(t) is

$$r(t) = \eta_1\eta_2\eta_3 p(t) = \frac{n\eta_2\eta_3 V_x}{2} p(t)\cos\omega_c t$$

$$= \frac{n\eta_2 V_x}{2}\left[0.12+\sum_{n=1}^{\infty} A_n \cos\, n(.0628)t\right]\cos\omega_c t \cdot \sum_{m=1}^{\infty}(\Gamma_m \cos\, m\omega_c t + \Gamma_m' \sin\, m\omega_c t)$$

The m-term series is therefore the desired operator η_3 in this example. The pressure signal amplitude coefficients, A_n, are calculated as shown in Figure 7. When $f_2(t)$ is a square wave of frequency, ω_c, and is adjusted so that the zero crossings coincide with those of the cosine $\omega_c t$ term, the quadrature terms, $\Gamma_m' \sin\, m\,\omega_c t$, become zero and the expression is simplified. The form of r(t) then becomes as shown in Table 2, in which several typical computations are also displayed.

Even in this specific case, a large number of product terms is generated. Fortunately, those which contribute to the reconstruction of a signal which is a recognizable analog of the original pressure function are relatively easy to identify, since they will not contain sine or cosine functions of frequency ω_c or its integral multiples.

The foregoing principles apply to all the commonly used "demodulator" circuits and form the basis for a large number of signal conditioner designs. This equipment may be designed for a wide variety of specific applications and known by a variety of names, some of which are either misleading or not definitive. Such equipment may be termed carrier amplifiers, carrier indicators, transducer demodulators, carrier

TABLE 2

TOTAL SYSTEM OUTPUT -- FREQUENCY TRANSLATED
VARIABLE RELUCTANCE PRESSURE TRANSDUCER SIGNAL
r(t) = OUTPUT (VOLTS) =

$$\underbrace{\frac{nn_2\ V_x}{2}}_{\text{ELECTRICAL SCALING}} \left\{ \underbrace{[0.12 + \sum_{n=1}^{\infty} A_n \cos n\,(0.628)t]}_{\text{APPLIED PRESSURE "TRANSIENT" (FIG 7)}} \cdot \underbrace{\cos \omega_c t}_{\text{"CARRIER" FUNCTION}} \cdot \underbrace{[\frac{-4}{\pi} \sum_{m=1}^{\infty} \frac{(-1)^m}{(2m-1)} \cos(2m-1)\omega_c t]}_{\text{(DE) MODULATOR FUNCTION } n_3 \text{ FIGURE 10)}} \right\}$$

$\frac{\text{VOLTS}}{(k)P_A}$ (KILO)PASCAL ——— DIMENSIONLESS ———

$$A_n = \frac{100}{2\pi^2} \left(\frac{\cos(.1)\pi n - \cos(.14)\pi n}{n^2}\right)$$

TYPICAL TERMS:

n=1, m=1

$$\left\{ \underbrace{\frac{.24}{\pi} + \frac{.47}{\pi} \cos\,(.063)\ t}_{\text{"DATA" TERM}} + \frac{.24}{\pi} \cos 2\omega_c t + \frac{.234}{\pi} [\cos(2\omega_c + .063)t + \cos(2\omega_c - .063)t] \right\}$$

n=2, m=1

$$\left\{ \underbrace{\frac{.435}{\pi} \cos(.126)t}_{\text{"DATA" TERM}} + \frac{.217}{\pi} [\cos(2\omega_c + .126)t + \cos(2\omega_c - .126)t] \right\}$$

n=2, m=3

$$\left\{ \frac{.24}{5\pi} (\cos 6\omega_c t + \cos 4\omega_c t) + \frac{.217}{5\pi} [\cos(6\omega_c + .126)t + \cos(6\omega_c - .126)t + \cos(4\omega_c + .126)t + \cos(4\omega_c - .126)t] \right\}$$

n=1, m=4

$$\left\{ \frac{-.24}{7\pi} (\cos 8\omega_c t + \cos 6\omega_c t) + \frac{.234}{7\pi} [\cos(8\omega_c t + .063)t + \cos(8\omega_c - .063)t + \cos(6\omega_c + .063)t + \cos(6\omega_c - .063)t] \right\}$$

demodulators, strain indicators[4], strain amplifiers, LVDT indicators, and others. All such devices belong to a general class which can be definitively termed "frequency translating signal conditioners" (FTSC). The output of such signal conditioners will be termed "frequency translated output" (FTO), often erroneously termed "DC" output. The expression for the instantaneous value of this output will be designated as $r(t)$ when resulting from generalized nonstationary pressures, and by r_k when due to a steady state pressure input, P_k, applied to the transducer.

The requirements for output filters, as outlined in Table 1, arise only out of the desirability of eliminating for convenience those frequency translation by-products in the FTO which do not contribute to an understanding of the input pressure. Filtering required for modifying system response to real but irrelevant pressure information or other physical stimuli is not considered part of the fundamental signal processing operation, although most manufacturers make no distinction between these two functions when describing their equipment.

In summary, the output of a VR transducer and FTSC contains many components which might wrongly be suspect as uncontrollable sources of imprecision. These are a result of the complexity of the electrical signal from the transducer and input circuit and the large number of non-data processing by-products. These "errors" are mathematically similar to the errors from truncation of the series form of the pressure input function caused by tubulation lag. In both cases, the scaling

---

[4]The "carrier amplifier-demodulator" method of signal processing is often used in equipment packaged for strain measurements in preference to a DC system because of the extremely small signals available from single- and two- active arm strain gage "bridges." The high noise immunity of the carrier method is unique in that thermo emfs in leads and connections as well as AC pickup do not cause errors in the measurement.

error within, and only within, the band-limited region of data frequencies of interest is easily compensated for by adjusting the scale factor (gain) n_2. However, the pneumatic system lag time errors theoretically never become zero no matter how long an equalization time is allowed. The existence of the same type of mathematical upper frequency limitation imposed by the pneumatics and by this type of signal processing operation can be confusing if viewed superficially. It sometimes leads to a "chicken-egg" application dilemma which can be simplified by the approach illustrated in Figure 7. The most important practical result of this analysis is that if high frequency data is of concern, the carrier frequency, ω_c, must be made as high as possible.

SECTION V

MECHANICAL DESIGN CONSIDERATIONS

In Reference 10, the author states, about his own VR transducer design: "Tests using a carrier frequency of 20 KC/S showed that the change of loss resistance in the solid cores contributed more to the output signal than did the change of inductance. The instrument consequently displayed a large zero shift with temperature." This problem, and also the difficulty of fabrication, was given as the reason for the author's abandonment of the VR transducer and pursuit of a capacitance design. The analysis of this "core loss resistance" problem, not further explained in this reference, requires consideration of the mechanical and magnetic features of the design.

The magnetic processes in VR transducers occur as shown in Figure 11. The pressure input differential, $P_2 - P_1$, applied to the center plate through the openings in each case half appears in the magnetic circuit as a complementary change in the air gap lengths, ℓ_1 and ℓ_2, at each pole piece. The pressure-deflection relationship is essentially linear, due to the choice of center plate suspension. The classical VR transducer uses the clamped flat plate suspension shown in Figure 12 as case (a). Although not specifically stated in commonly available engineering references, the stress, deflection, and resonance behavior of circular plates rigidly supported at the edge appears to fall into four distinct classes. These are:

a) Thick plate, with deflections limited to the smallest possible values, much less than the thickness;

b) Thin plate, with design values of deflection no greater than half the thickness;

c) Thin plate prestressed by means of radial tension; and

d) Very thin membrane or diaphragm with radial tension, designed to undergo deflections during normal conditions which are greater than half the thickness.

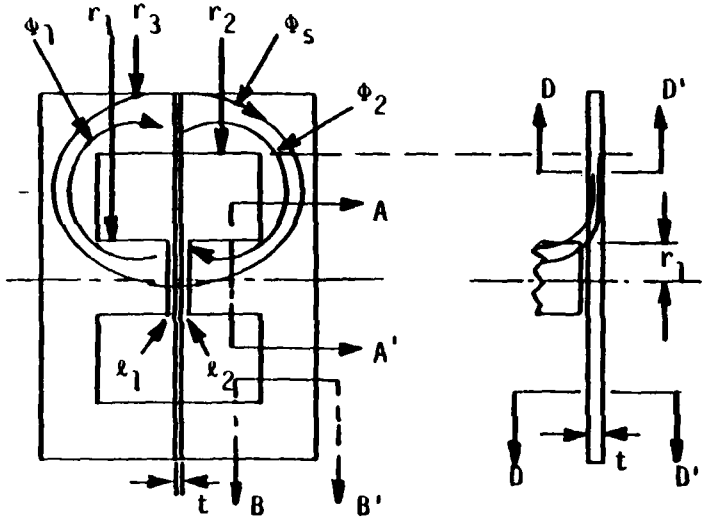

TRANSDUCER ASSEMBLY

CENTER PLATE

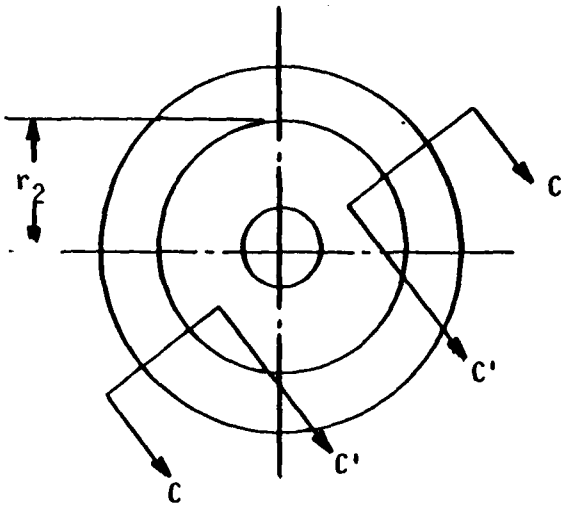

CASE-HALF

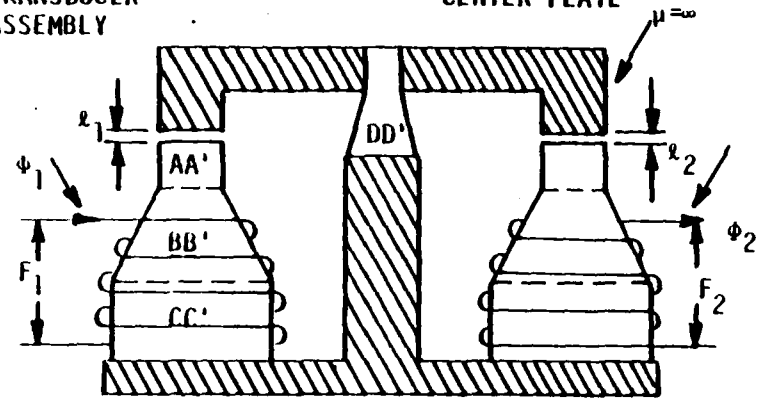

MAGNETIC FLUX PATHS -- 2-DIMENSIONAL GEOMETRIC TRANSFORMATION

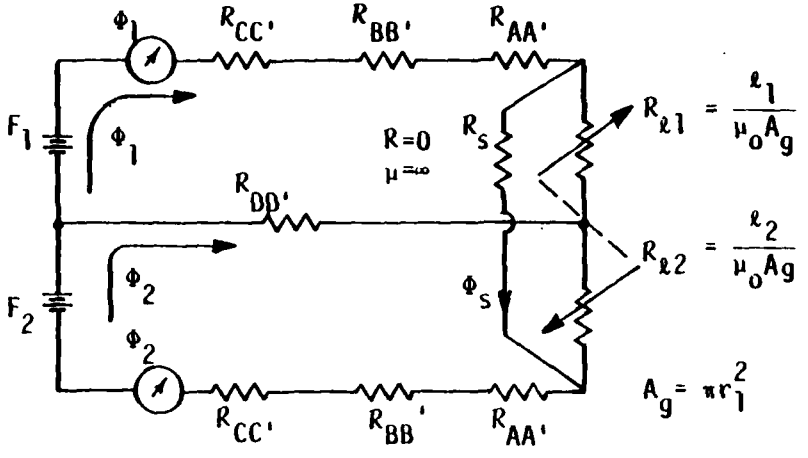

MAGNETIC EQUIVALENT CIRCUIT (NEGLECTING EDDY CURRENTS)

Figure 11. Variable Reluctance Transducer Magnetic Circuit

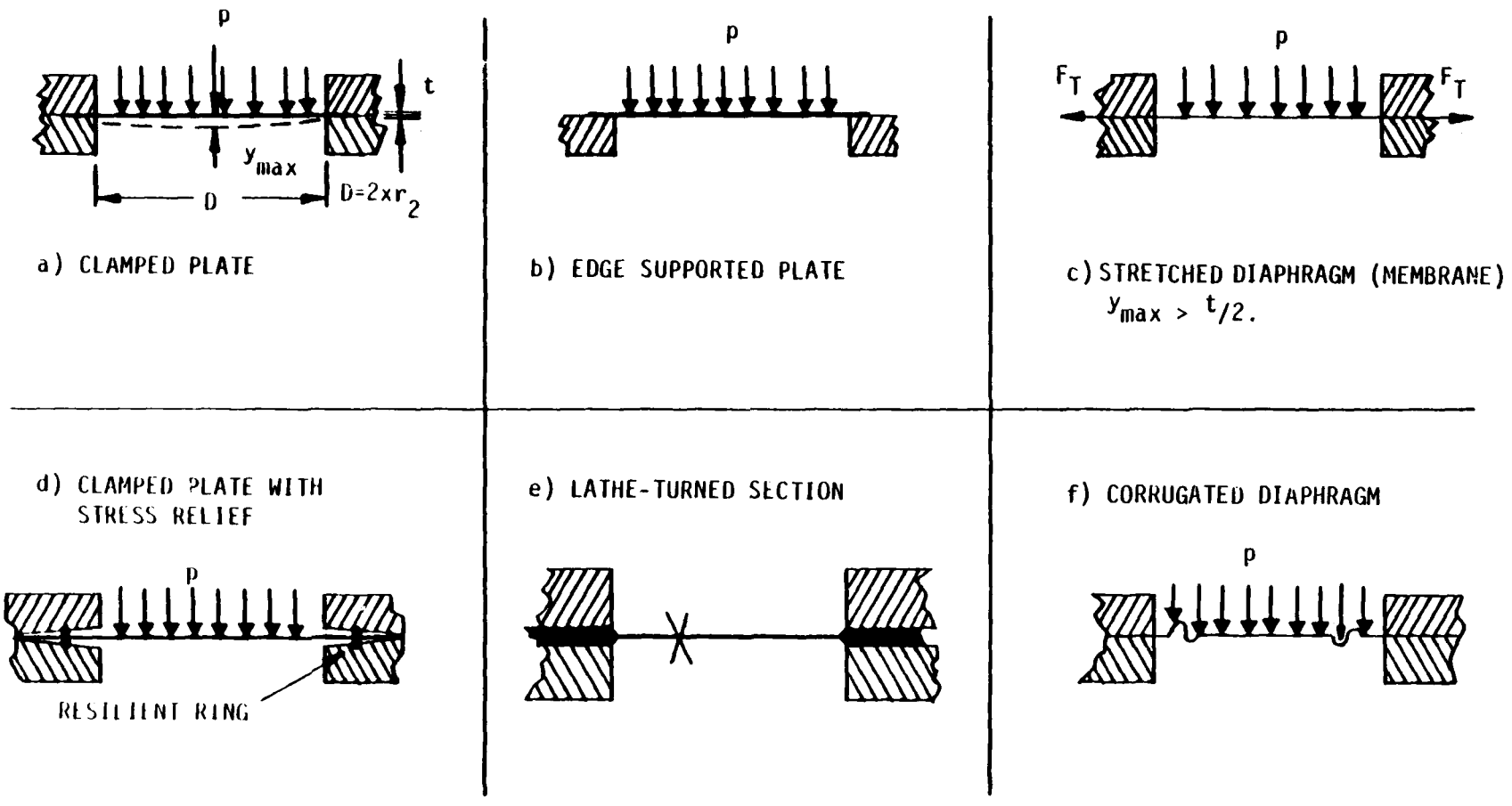

Figure 12. Types of Pressure Element Suspensions

An expression for resonant frequency found in Reference 21 for the thick plate does not contain Poisson's ratio, either as a variable or an assumed constant. This suggests that it is intended to apply to the case where shear at the clamped edge is dominant and bending stress is negligible. It is obviously intended for design of thick, rigid structural systems rather than members which have as their main function to undergo deflection. The existence of several different expressions for resonant frequency for the various ranges of deflection magnitude also suggests that a given CP suspension can exhibit resonances at frequencies which are affected significantly by both steady-state and fluctuating pressure load magnitude. For the thin plate used in VR transducers, Reference 21 gives the maximum deflection (y_{max}), which occurs at the center, resulting from a uniformly applied load, p, per unit area.

$$y_{max} = \frac{3pr_2^4}{16\ Et^3}(1-\gamma^2)$$

This reference gives the constants and variables in engineering units as follows:

p = applied pressure - pounds per square inch

r_2 = free radius of the CP - inches

E = Young's modulus - pounds per square inch

= 29 X 10^6 PSI for steel alloy

t = thickness of CP - inches

γ = Poisson s ratio

= 0.29 for steel alloy

This formula is valid where $y \leq t/2$. Thus, the deflection is linear with pressure in this range. The maximum stress, s_{max}, in the plate due to pressure load, p, occurs in the radial direction and is given by

$$s_{max} = \frac{3}{4} \frac{p r_2^2}{t^2}$$

In the case where the load, p, is large enough to cause $y > t/2$, the radial tension in the plate becomes large enough to restrain the deflection at the center and the linear relationship no longer holds. This deflection can be found by solution of the implicit relationship

$$\frac{p r_2^4}{E t^4} = \frac{16}{3(1-\gamma^2)} \left(\frac{y}{t}\right) + \frac{6}{7} \left(\frac{y}{t}\right)^3$$

The first circular mode resonant frequency of this suspension is given in Reference 22 in cgs units. Converted to engineering units the expression given becomes

$$f_{01} = 0.471 \frac{t}{r_2^2} \left[\frac{gE}{(1-\gamma^2)\rho}\right]^{\frac{1}{2}}$$

where ρ = density of center plate material - pounds per cubic inch

g = gravitational acceleration - 386.4 in. per second squared.

The center plate suspension shown in Figure 12(d), not normally used by transducer manufacturers, modifies the stress and deflection characteristics by relieving the sharply defined point of inflection of the surface. The edge supported plate of Figure 12(b), having an inflection point at $r_2 = \infty$, has stress, deflection, and resonant frequency formulas similar to case (a), but with different constant coefficients. Reference 21 gives the maximum (center) deflection as

$$y_{max} = \frac{3 p r_2^4}{16 E t^3} (\gamma^2 - 6\gamma + 5) \text{ where } y \leq \frac{t}{2}$$

The maximum stress in the plate is given as

$$s_{max} = \frac{3pr_2^2}{8t^2}(3+\gamma)$$

For the nonlinear case, when $y > t/2$, the center deflection is given by

$$\frac{pr_2^4}{Et^4} = \frac{64}{63(1-\gamma^2)}\left(\frac{y}{t}\right) + 0.376\left(\frac{y}{t}\right)^3$$

The first circular mode resonant frequency is given in Reference 22 as

$$f_{01} = 0.235\,\frac{t}{r_2^2}\left[\frac{gE}{(1-\gamma^2)\rho}\right]^{\frac{1}{2}}$$

It is reasonable to assume that the stress and deflection characteristics of the plate suspension with stress relief, case (d), will differ from those of case (a) and (b) only by the constants, and these constants will lie between those for cases (a) and (b), provided a suitable adjustment to the value of effective free radius r_2 is made. This modification will improve the calibration repeatability by reducing high stress concentrations near the clamping edge and will facilitate making a leak-proof seal. Resonant frequencies and damping characteristics may be affected greatly.

Several VR transducers were found to have a lathe-turned CP with a compound cross section such as shown in Figure 12 (e). This method of CP fabrication was employed by the author of Reference 10 for both his VR transducer and his capacitance transducer.

The acceleration sensitivity of a VR transducer is wholly due to the deflection of the distributed mass of the free portion of the CP in the same manner as if it were responding to a pressure load. As stated in Reference 10, the equivalent pressure due to an acceleration of 1 "g" is d·t where d is the weight of the CP material.

The stretched membrane, Figure 12(c) is employed in transducers where both high deflection sensitivities at low pressure loads and high resonant frequencies are required. This thin membrane is properly

called a diaphragm and is used in pressure microphones.[1] The thin diaphragm would present an undesirably high magnetic reluctance path for the circuit flux in a VR transducer. The VR pressure transducer described in Reference 23 uses the thin plate with a moderate amount of radial tension to raise the resonant frequency, reduce the effects of local stress nonuniformities, and improve calibration linearity and mechanical hysteresis. The improved linearity of this type suspension at large deflections is due to the presence of a constant component of radial tension which is very large compared to the load induced component. In practice, it is difficult to maintain this tension constant due to structural response to environmental changes and assembly and installation forces.

The thin corrugated pressure element, Figure 12(f), used to provide high values of linear deflection, would present an undesirably high reluctance magnetic return path. The transducer described in Reference 24 uses this type diaphragm made of beryllium copper, with an attached iron center disk facing each pole piece to provide a good magnetic return path. The spring-mass characteristic of this design would give an exceedingly low mechanical resonant frequency and a high sensitivity to axial acceleration. The linearity and hysteresis characteristics would be considerably better than the edge clamped plates and the overall mechanical performance would be much more predictable.

A hypothetical model classical VR transducer is shown in Figure 13. If a maximum deflection of $\frac{t}{2}$ = .005 inches is assumed, the nominal full scale pressure would be about 24 PSID. The center plate deflection and natural frequency characteristics are calculated but the choices of air gap length and the effects of the large variation in cross-sectional area along the flux path and determination of electrical performance require consideration of magnetic circuit principles.

---

1. Steady state (barometric) pressure differentials across the microphone diaphragm are eliminated by a low response pressure vent on the reverse side.

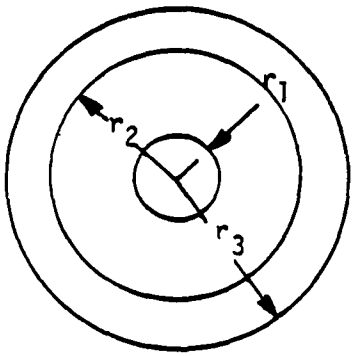

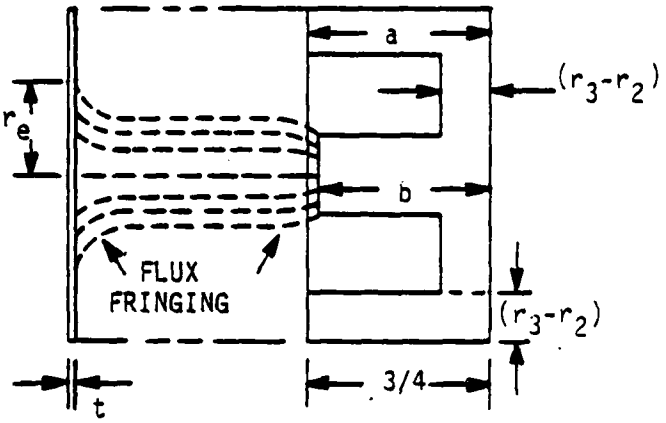

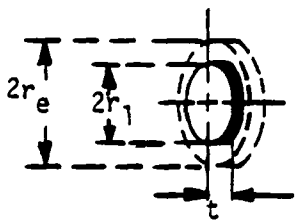

ACTIVE ANNULUS OF
CENTER PLATE

ASSUME

r_3 = 3/4" r_2 = 7/16" r_1 = 5/32" t = 0.01"

ℓ_g = (a-b) = 0.025"

FOR MAGNETIC STAINLESS STEEL:

$\rho = 0.2817 \frac{lb}{in^3}$ $E = 29 \times 10^6 \frac{lb}{in^2}$

$\gamma = 0.29$

MINIMUM AREA IN FLUX PATH = $2\pi r_1 \times t = 0.009$ in^2 (ANNULUS)

MAXIMUM AREA IN FLUX PATH = $(r_3^2 - r_2^2)\pi = 1.17$ in^2

NEGLECTING FRINGING, THE FLUX DENSITY WILL VARY ALONG THE FLUX PATH BY A FACTOR OF 120 TO 1

$y_{max} = t/2$ WHEN ΔP APPLIED = 24 PSI

$f_{01} = \frac{t}{r_2^2}(9.8 \times 10^4) = 5120$ HERTZ

TOTAL VOLUME OF METAL (PER HALF) = 1.09 in^3
WEIGHT (PER HALF) = 5 OUNCES

Figure 13. Mechanical Profile - Hypothetical Variable Reluctance Pressure Transducer

SECTION VI

MAGNETIC CIRCUIT DESIGN CONSIDERATIONS

The mechanical displacement of the center plate as a result of applied differential pressure causes complementary changes in the length, ℓ_g, of each air gap. The magnetic reluctance, R, of each gap is given by

$$R = \frac{\ell_g}{\mu_o A_g}$$

where A_g is the area of the pole piece, section AA' in Figure 11, adjacent to the gap, and μ_o is the magnetic permeability of air. This change in reluctance causes a change in the output function, Φ, which is the flux which flows due to the applied magnetomotive force (MMF), F. The resultant flux is given by

$$\Phi = \frac{F}{R}$$

This is the magnetic equivalent of Ohm's Law for electrical circuits. The electrical analogy in Figure 11 relates steady state AC conditions in the real transducer to instantaneous or DC magnitudes of the electrical analogs. The reluctances of the various elements in the series path add as in the case of resistances. The electrical input to the inductor is applied as an electrical current, i, in a coil of N turns, comprising a magnetomotive force per unit length, H. This causes a flux of density, B, in the magnetic path. The electrical output is an opposing voltage, or counter emf, numerically equal to $N \frac{d\Phi}{dt}$, in the winding of the inductor which cannot be measured directly in practice. In the case of a transformer, the output is an output voltage across a separate pair of terminals which may be measured directly. Assuming a fixed magnetic circuit geometry with known values of A, ℓ, μ, and N, the the instantaneous values of current, i, and voltage, e, in an electrical circuit containing the inductor can be obtained in terms of the reluctance, R, the independent variable.

The basic magnetomotive force or electrical input relationship is

$$Ni = \frac{F}{4\pi} = \frac{H\ell}{4\pi}$$

The resultant total flux (Φ) in a medium with a permeability μ is found from the resultant flux density

B (flux density) = μH

$\Phi = B \times A$ where A is the area of the magnetic medium normal to the flux path. Then the current, i, as a function of R, becomes

$$i = \frac{B\ell}{4\pi N\mu} = \frac{\Phi\ell}{4\pi N\mu A} = \frac{\Phi R}{4\pi N}$$

The voltage, e, across the coil is

$$e = N \frac{d\Phi}{dt}$$

This voltage in terms of input current can be found by differentiating the expression for i.

$$i = \frac{\Phi R}{4\pi N} \text{ and } \frac{di}{dt} = \frac{R}{4\pi N} \frac{d\Phi}{dt}$$

Therefore,

$$e = \frac{4\pi N^2}{R} \cdot \frac{di}{dt}$$

These expressions reveal some practical guidelines for dealing with electro-magnetic components. These are:

- The excitation of an electro-magnetic circuit occurs as a result of the establishment of a current in the coil. The result of applying a voltage to an inductor is not fundamental or definitive. In fact, applying a voltage of any magnitude to an ideal inductor will result in a current which is indeterminate.

- The electrical inductance of a given design is inversely proportional to the total reluctance of the magnetic circuit, directly proportional to the permeability, μ, and directly proportional to the square of the number of turns, N.

- An ideal inductor (such as an ideal VR transducer) draws no real power from its excitation source. When the applied current is sinusoidal, having a frequency, $\omega_c = 2\pi f_c$, the instantaneous current is the function

$$i = I_{max} \sin\omega_c t$$

$$\frac{di}{dt} = \omega_c I_{max} \cos\omega_c t$$

The following expressions relate electrical quantities to magnetic variables.

$$\frac{d\Phi}{dt} = \frac{4\pi N}{R} \omega_c I_{max} \cos\omega_c t$$

Then the instantaneous power is w(t).

$$w(t) = e \cdot i = \frac{4\pi N^2}{R} I^2_{max} \sin\omega_c t \cdot \cos\omega_c t$$

$$= \frac{2\pi N^2}{R} \omega_c I^2_{max} \sin 2\omega_c t$$

Over a period of $n\pi$ radians, the power will average to zero, assuming an electrically and magnetically ideal circuit.

The permeability, μ, of the magnetic material in the flux path is a natural characteristic. It is determined by making measurements of resultant flux density, B, due to applied MMF-per-unit-length, H, of the magnetic circuit on samples of the material under test conditions which minimize the effects of geometry and eddy currents. A typical B-H curve for a magnetic material commonly referred to as "iron" or "steel" is shown in Figure 14(a). When an AC MMF is applied, the material will be operated cyclically through a loop as shown. The shape as well as the size of the loop will depend on the magnitude of the applied AC MMF. The hysteresis process requires some power input. The power loss is proportional to the product of the area within the B-H curve and the total volume of magnetic material in the flux path. While it is of concern in the design of electrical power system components, the hysteresis power loss has little direct effect on the performance of VR transducers, except to set a practical lower limit on the excitation

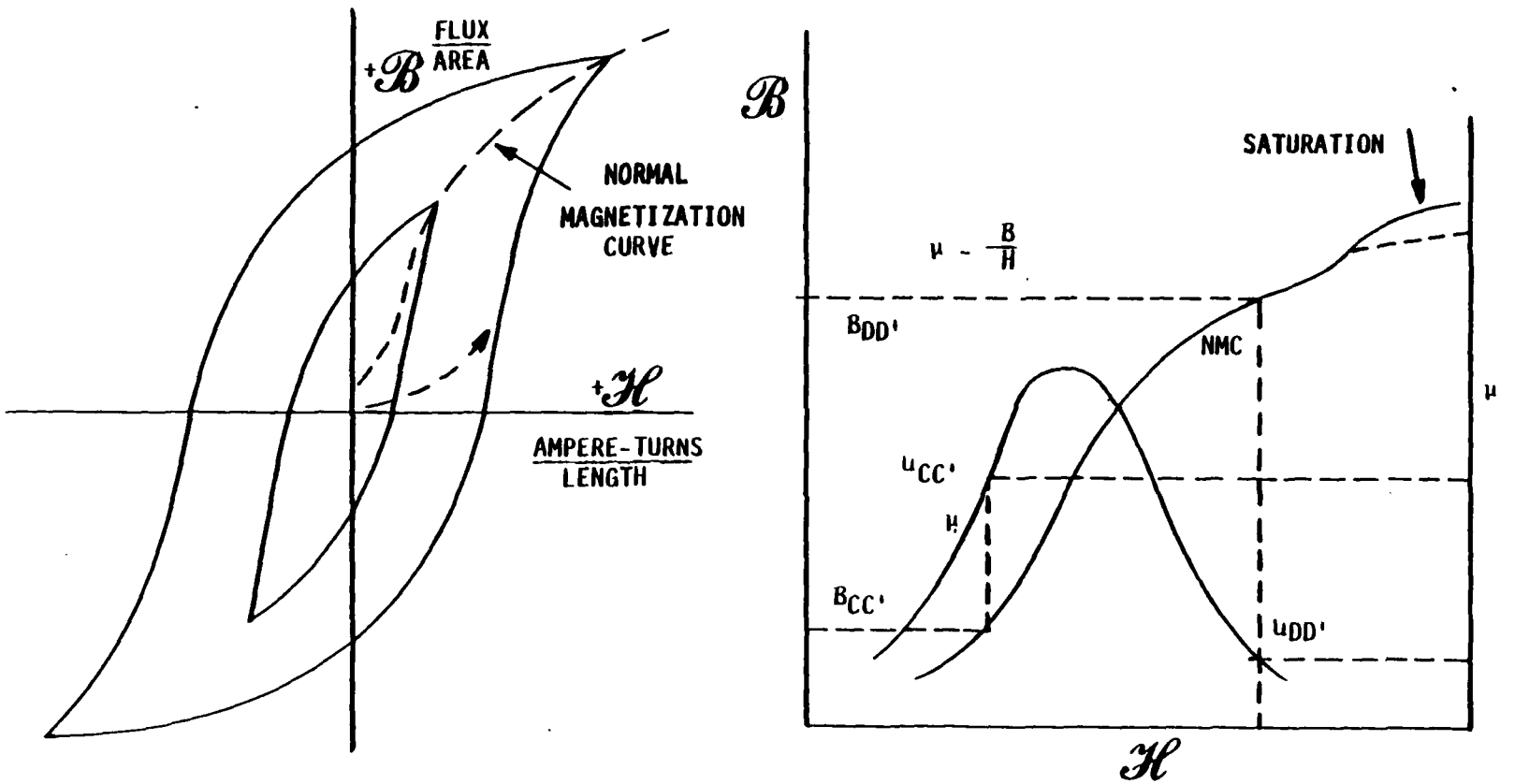

a) INSTANTANEOUS MAGNETIZATION CURVE

b) STEADY STATE AC (CYCLICAL) DESIGN PARAMETERS

Figure 14. Typical Characteristics of Electrical Steel

frequency at which a given transducer can be operated at a given voltage. For this reason, operation of AC electromagnetic components is often based on "Volts-Per-Cycle" ratings.

A series of loops corresponding to a series of increasing values of AC MMF is the basis for a single-valued *B-H* relationship useful in the design of AC magnetic devices. This curve is called the normal magnetization curve (NMC). It is the locus of the tips of the loops corresponding to all values of applied cyclical MMF. Working values of permeability, μ_s, at a given level of *H* may be obtained by taking the slope of this curve, as shown in Figure 14(b). Selected magnetic materials used in linear electrical devices such as power and audio transformers exhibit μ_s values from 500 to 20,000 relative to μ_o, the permeability of free space.[1,2] Published (handbook) data of this kind are not directly applicable to the design of VR transducers, but materials such as magnetic stainless steel and others chosen mainly for structural properties exhibit similar magnetic properties. The same principles govern their behavior in an electromagnetic circuit. Since the total flux, Φ, must be constant along each closed path, Φ_1 and Φ_2, and since the cross sectional areas of the transducer elements vary greatly along the path, the flux density *B* varies accordingly at any set level of applied field intensity, *H*. The effective μ_s for each path element will be different, and in the case of sections AA' and DD' in Figure 11, it will vary continuously as the radius changes. Practical designs of VR transducers may have a maximum to minimum area ratio of 100 to one or more along the flux path. The location of operating points $B_{CC'}$ and $B_{DD'}$ in Figure 14(b) is established by the MMF input, which is set by the input current in the coils. The values of μ_s are then determined by transfer from the corresponding values of *H* on the NMC. When a reasonable value of flux density exists in the transducer

1. It can be seen that this "linearity" is only an approximation and applies over a limited range of operation on the *B-H* curve.

2. The value of μ_o is $4\pi \times 10^{-7}$ Henry per Meter.

case, Section CC', the relatively thin center plate could be in saturation, where the slope of the NMC is nearly horizontal if the MMF polarities are arranged to cause the two fluxes to add in the CP. If one coil connection is reversed, this material will operate in the equally nonlinear portion of the NMC around zero. Thus, the CP may be the greatest contributor to magnetic (and therefore electrical) nonlinearity which causes harmonics to be generated. This effect may become more prominent as the thickness of the CP is decreased. To take into account the "fringing" of some of the flux at the air gap edges, some adjustment can be made in the effective value of r_1

The operating flux density in the larger cross sectional areas AA', BB', and CC' can be set to any value over a wide range and still maintain a permeability of at least a thousand times that of air. These reluctances can be considered zero, reducing the magnetic circuit variables to only the air gaps and the CP. The electrical analog of Figure 11 may be simplified to that shown in Figure 15A. The basic form of the sensitivity function, η_1, of the mechanically ideal VR transducer and input network can be obtained from this analog. With zero pressure (differential) applied to the transducer, the flux magnitude will be given by

$$\Phi_1 = \Phi_2 = \frac{F_1}{R_{\ell 1} + R_{DD'}} = \frac{F_2}{R_{\ell 2} + R_{DD'}}$$

With a pressure load applied, R_{ℓ_1} will be replaced by $(R_{\ell_1} + \Delta R_{\ell_1})$ and R_{ℓ_2} will be replaced by $(R_{\ell_2}+\Delta R_{\ell_2})$, where ΔR_{ℓ_1} and ΔR_{ℓ_2} are small compared to R_{ℓ_1} and R_{ℓ_2}. Then the expression for the flux in path ϕ, becomes Φ_1'.

$$\Phi_1' = \frac{F}{R_{\ell 1} + \Delta R_{\ell 1} + R_{DD'}} = \frac{F}{R_{T_1} + \Delta R_{\ell}}$$

The unchanging components are R_{ℓ_1} and $R_{DD'}$, which are combined as R_T. Similarly, since $\Delta R_{\ell_2} = -\Delta R_{\ell_1}$ and $R_{\ell_2} = R_{\ell_1}$, the other resultant flux becomes Φ_2'.

$$\Phi_2' = \frac{F}{R_{T_1} - \Delta R_{\ell 1}}$$

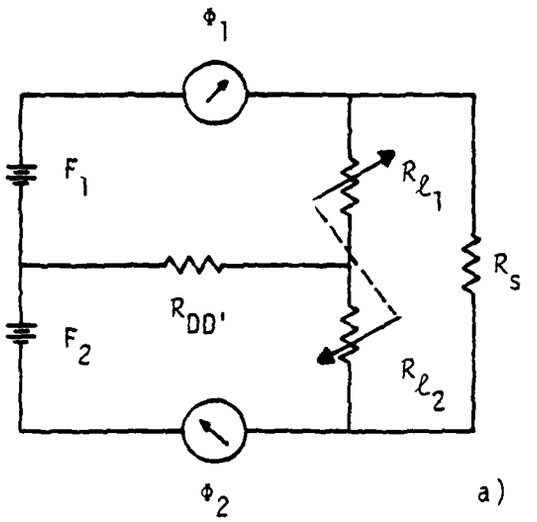

$$\Delta\Phi = \Phi - \Phi' = \frac{F_1}{R_{T_1}}\left(\frac{\Delta R_{\ell_1}}{R_{T_1} + \Delta R_{\ell_1}}\right)$$

a) SIMPLIFIED CIRCUIT

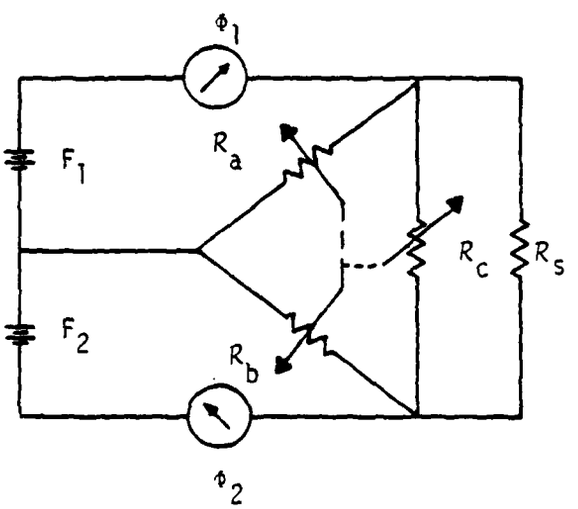

$$R_a = \frac{R_{\ell_1} \cdot R_{\ell_2} + R_{\ell_1} \cdot R_{DD'} + R_{\ell_2} \cdot R_{DD'}}{R_{\ell_2}}$$

$$R_b = \frac{R_{\ell_1} \cdot R_{\ell_2} + R_{\ell_1} \cdot R_{DD'} + R_{\ell_2} \cdot R_{DD'}}{R_{\ell_1}}$$

$$R_c = \frac{R_{\ell_1} \cdot R_{\ell_2} + R_{\ell_1} \cdot R_{DD'} + R_{\ell_2} \cdot R_{DD'}}{R_{DD'}}$$

b) AFTER Y-Δ TRANSFORMATION

Figure 15. Simplified Analog of Magnetic Circuit-Variable Reluctance Pressure Transducer

The magnitude of useful electrical output signal is proportional to the pressure induced change in flux magnitude. This can be expressed as

$$\Delta\Phi = \Phi_1 - \Phi_1' = \frac{F}{R_{T_1}} - \frac{F}{R_{T_1} + \Delta R_{\ell_1}} = \frac{F}{R_{T_1}} \left(\frac{\Delta R_{\ell_1}}{R_{T_1} + \Delta R_{\ell_1}}\right)$$

Also, at the same time

$$\Delta\Phi = \Phi_2' - \Phi_2' = \frac{F}{R_{T_1}} - \frac{F}{R_{T_1} - \Delta R_{\ell_1}} = \frac{-F}{R_{T_1}} \left(\frac{\Delta R_{\ell_1}}{R_{T_1} - \Delta R_{\ell_1}}\right)$$

The output is symmetrically bi-directional with respect to the neutral position, which corresponds to the zero-voltage reference point determined by the "bridge" circuit of Figure 4. Thus, the analog circuit of Figure 15A is useful in determining the form of the relationship between input pressure and electrical output, V_o, resulting from the connections shown in Figure 4 when the constants of proportionality between excitation voltage and the resulting MMF's, F_1 and F_2, are known. The assumptions concerning the effect of R_{DD}' are based on consideration of the Y-Δ transformation of the simplified circuit, shown in Figure 15B. Any changes in R_{DD}' are indirect effects due to changes in the magnetic field geometry in the center plate. They also slightly affect the local permeability of the affected areas and cannot be quantified. Therefore, the terms containing R_{DD}' are treated as constants. The sum of R_{ℓ_1} and R_{ℓ_2} is always constant and the terms are approximately equal. It can be shown that

$$R_{\ell_1} \times R_{\ell_2} = \left(\frac{R_{\ell_1} + R_{\ell_2}}{2}\right)^2$$

Then $R_{\ell_1} \times R_{\ell_2}$ is nearly constant. This causes a fixed component in Φ_1 and Φ_2, but does not affect the sensible output, $\Delta\Phi$. The additional fixed component, Φ_s, caused by straight-through flux penetration of the CP is shown as being caused by fixed reluctance, R_s. The magnitude of this component may become appreciable when thin center plates are used. This component appears in the electrical measurements of Section X as mutual inductance. The pressure-induced changes in R_c will not directly affect the sensible output, but will change the loading on the "power supplies," F_1 and F_2. This effect is discussed in Section X.

The expressions developed for the sensible output of a mechanically ideal VR transducer in response to a pressure input, which apply when ΔR_ℓ is small compared to R_ℓ, are of the basic form

$$y = c\left(\frac{x}{a + x}\right)$$

Therefore, the characteristic sensitivity function shown in Figure 16 is nonlinear. They also show that the signal output due to application of a pressure load is directly proportional to the input MMF (excitation) and inversely proportional to the total effective reluctance of the flux path consisting of the air gap and the center plate. As a result, the design of a VR transducer requires a compromise of sensitivity and linearity. The line $y = c\,\frac{x}{a_d}$ in Figure 16 results from selecting a given value of maximum rated or nameplate full scale (NFS) center plate deflection, a_d, as a fraction of a, the total unchanging equivalent path length. The equivalent path length takes into account the fact that the effective path length in air is μ_s times that in the CP material. The line $y = c\,\frac{x}{a_d}$ provides a reference from which the desired terminal linearity can be computed.

Changes in $R_{DD'}$ due to center plate deflection occur as a result of changes in the shape and magnitude of the flux entering and leaving the air gaps. Therefore, the total flux, flux density, and field shape within the CP will be affected by CP position. The average and microscopic local permeability of the portion of the CP adjacent to the pole pieces will also change. These complex second order effects will also contribute to nonlinearity of the output function, $\Delta\phi$, with respect to CP position.

There is reason to expect that both the fundamental and harmonic output will change with pressure input. This behavior will be affected greatly by the level of operating flux established by the applied electrical current (excitation). Shaping of the pole-piece face geometry is one possible way of modifying the magnetic circuit to improve overall nonlinearity. The effects of electrical loading of the transducer-input network combination upon the output signal are discussed in Section X.

External magnetic fields, if they are of sufficient strength and appropriate geometry, will add to the total instantaneous MMF of the magnetic circuit. This will change the effective permeability of the magnetic material and therefore the effective reluctance. AC fields and moving "DC" fields will therefore "modulate" the output of the transducer. Stationary magnetic fields will cause a change in output level. These effects are usually temporary and seldom cause a permanent change in the magnetic system.

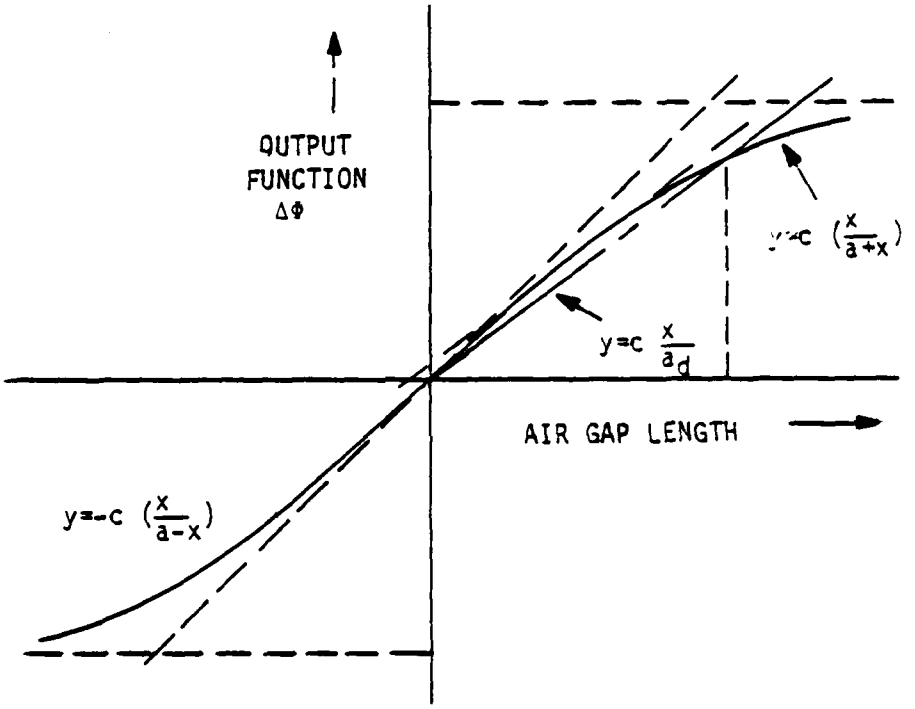

Figure 16. Characteristic Sensitivity Function - Variable Reluctance Pressure Transducer

SECTION VII

IN-CIRCUIT BEHAVIOR OF REAL IRON-CORE INDUCTORS

1. CURRENT-VOLTAGE RELATIONSHIPS

In practical cases such as VR pressure transducers, the input current to an inductor is often established by applying a voltage, e_T, across its two terminals. The resulting current is

$$i = \frac{e_T - N\frac{d\Phi}{dt}}{R_1}$$

N is the number of turns in the inductor coil and R_1 is a resistance composed of all internal loss elements. The counter-emf, $N\frac{d\Phi}{dt}$, can only be sensed in the external circuit indirectly by its effect on the current. The current is also related to the flux Φ through the magnetization curve *B-H* because *H* is proportional to Nxi and Φ is proportional to *B* for a given magnetic circuit geometry. Empirical simultaneous solutions of these two relationships are necessary to find the current-voltage characteristics of a real iron-core inductor in an electrical circuit. The current can be determined experimentally by the same method used in transformer design work to determine the "exciting current" (Reference 7). This is the current which a transformer draws at rated primary voltage with no current drawn from the secondary.[1] In Figure 17, e_g is a sinusoidally varying voltage having the value $e_g = E_{max}\sin\omega t$. It is applied across the inductor having a non-linear magnetic circuit and a resistance, R_1. The voltage, e_T, can be made nearly equal to e_g (that is, sinusoidal) by using a generator of very

1. The flux density in the transformer core under these conditions is abnormally small and the *B-H* characteristic curve is much different than at normal load conditions. Circuit inductor current waveform therefore resembles transformer operating current more than the pulse-like waveform usually shown in textbooks as transformer exciting current.

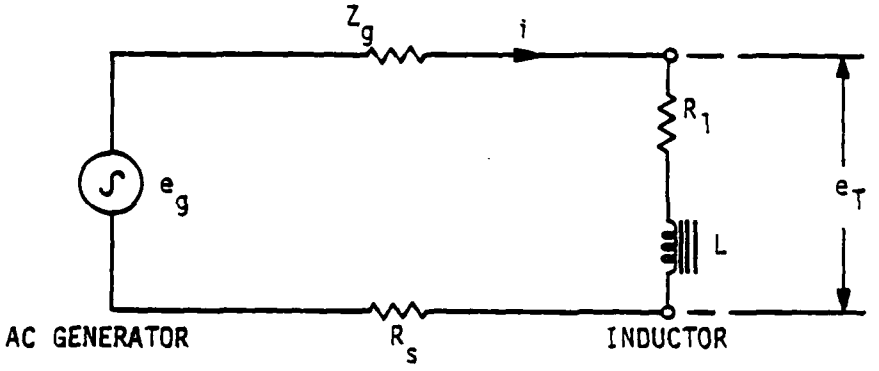

Figure 17. Inductor Test Model

low internal impedance, Z_g. In this situation, called "constant voltage" excitation, the current, i, will be forced to adjust to the simultaneous electrical relationships as shown in Figure 18. To determine the current from analysis, the B-H curve must be known and a waveform for Φ must be assumed and differentiated. Then, a trial current must be determined through use of the B-H curve. The iR product is then subtracted from the input voltage and the difference is compared with the original assumption for Φ. The process must be repeated until the assumed and derived waveforms of i are the same. In efficient inductors and transformers, R_1 will be small but not negligible. VR transducers and small household transformers have relatively high internal loss resistances. Where measurements of i are needed in practice, it can be sensed as a voltage drop across a resistor, R_s, which must be much smaller than R_1 or Z_g. If Z_g or any other series resistance in the series circuit is relatively large, the current will be determined by E_g and these resistances, becoming nearly sinusoidal. This condition is called "constant current," since changes in the coil inductance will have little effect on the current compared with these resistances. Then e_T, approaching equality with $N\frac{d\varphi}{dt}$, will adjust itself to meet the two simultaneous relationships, as shown in Figure 19.

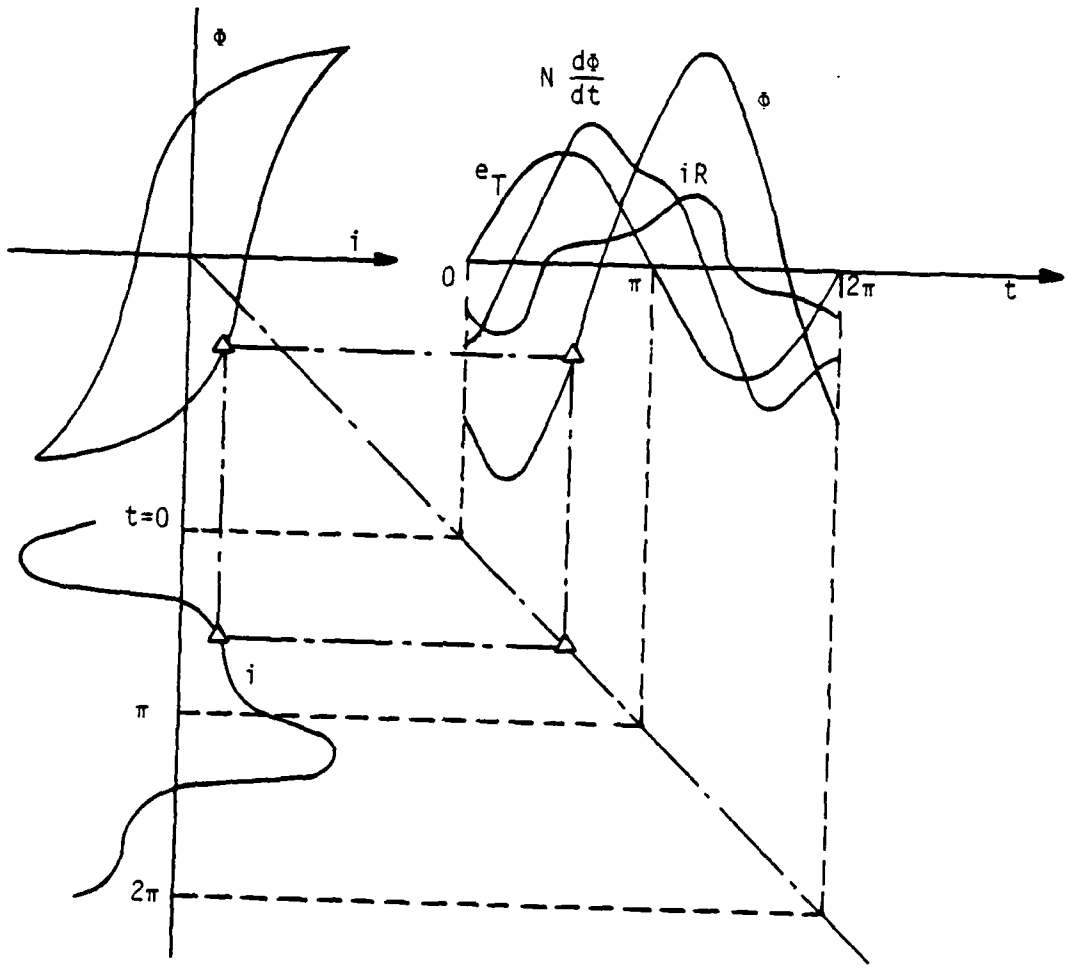

INDEPENDENT VARIABLE: $e_T = E_{T(max)} \sin\omega t$ (INEXORABLE APPLIED VOLTAGE)

DEPENDENT VARIABLE: i (COIL CURRENT)

GIVEN: $e_T + iR = N \frac{d\Phi}{dt}$

Figure 18. Flux-Current Determination of Inductor "Exciting Current"- Constant Voltage Excitation

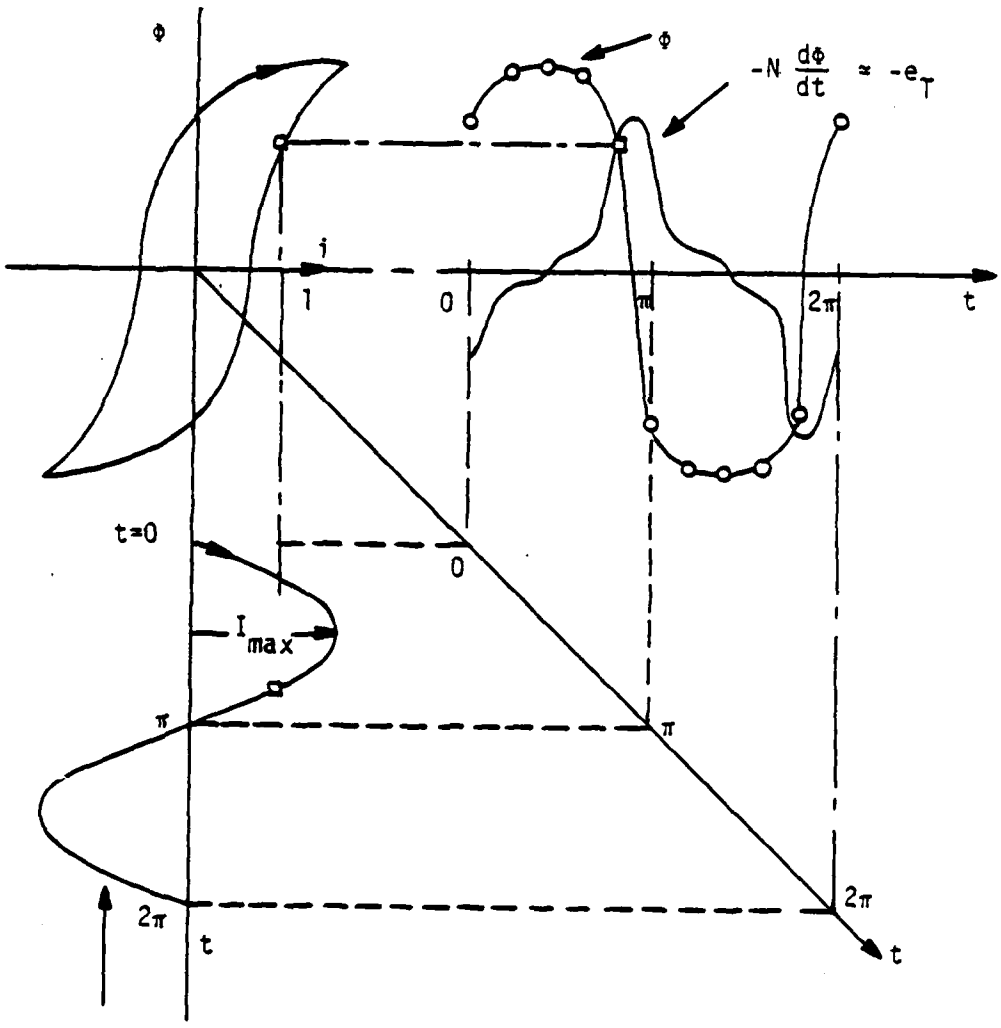

INDEPENDENT VARIABLE: $i = I_{max} \sin\omega t$ (APPLIED CURRENT)

DEPENDENT VARIABLE: e_T (TERMINAL VOLTAGE)

Figure 19. Flux-Current Relationships in Inductor - Constant Current Excitation

The functional relationship of flux versus current used in Figures 18 and 19 is obtained directly from the *B-H* curve of the magnetic material when a given magnetic circuit geometry and coil design is specified, since $\phi = B \times$ area and $H = N \times i$. The non-linear electrical behavior of magnetic circuits containing non-linear elements such as iron creates voltages having significant harmonic content. The effects of the harmonics in the output of a VR transducer on a signal conditioner must eventually be taken into account using the analysis of Section IV. The internal impedance of the source of excitation to the transducer and the AC resistance of its coils and interconnecting leads are therefore important circuit variables in a VR transducer-signal conditioner system. Due to the symmetry of the *B-H* relationship about the origin, the application of any periodic waveform, f(t), having half-wave symmetry (meaning $f(t) = -f[t \pm T/2]$), such as a sine wave, with respect to the *H* axis results in an output waveform B(t) which also has half-wave symmetry (Reference 25.) The Fourier coefficients, a_n, and b_n, for such a waveform are given by

$$a_n = \frac{2}{T} \int_{-T/2}^{+T/2} B(t)\cos n\omega t \, dt \text{ and}$$

$$b_n = \frac{2}{T} \int_{-T/2}^{+T/2} B(t)\sin n\omega t \, dt.$$

Both coefficients are zero for n even, which means that only odd harmonics are generated. The principle is illustrated graphically in Figure 20. The symmetry of the *B-H* curve would be destroyed by applying a DC or nonsymmetrical periodic external magnetic field to the magnetic circuit, changing the magnitude of the odd harmonics and adding even harmonics.

At relatively high values of input MMF, the B-H characteristics approach the horizontal straight line characteristic of air and free space. This condition, referred to as saturation, results in a flux wave form which is flat over almost all of the half-cycle. Thus, the waveform of the voltage, $N\frac{d\phi}{dt}$, becomes a very low duty cycle pulse in which high-order harmonics are dominant.

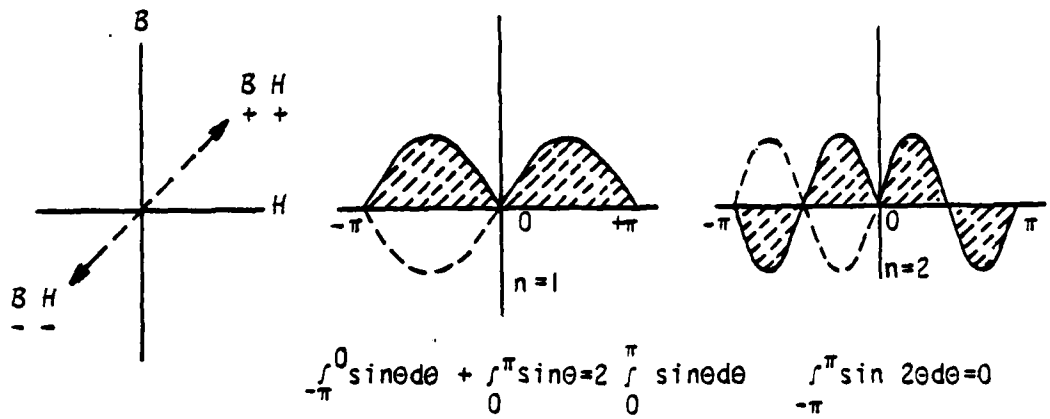

Figure 20. Half-Wave Symmetry Harmonic Cancellation

The effect of adding a relatively small air gap of length, ℓ_g, to an otherwise fixed geometry "iron" magnetic circuit is to increase its effective length by the factor $(1+\ell_g\frac{\mu_s}{\mu_o})$. In the constant voltage case, the current must increase to provide the necessary additional MMF(F = N·i), and the total flux will remain the same. This increase in current will be large, since $\frac{\mu_s}{\mu_o}$ can range from several hundred to several thousand. In the air gap, the flux-current relationship is linear, since μ_o is a universal constant. Therefore, the waveform of this component of current will be the same as the applied voltage. When this voltage is sinusoidal, the current will be a co-sinusoid (in quadrature). The addition of this large sinusoidal component to the total input current reduces its relative harmonic content. In a practical circuit having a finite coil resistance and generator impedance, there will be a significant reduction of that part of the circuit current available to create flux, due to voltage drops in these loss elements. At the iron-air interface, the flux lines will undergo a significant change in geometry, since the flux densities in the two media are different. For design purposes, these effects can be evaluated only by mapping the flux field to provide values of local flux density needed for circuit calculations.

Where electrical circuits contain harmonics generated in this manner by "iron" electromagnetic components, the analysis of these circuits can be done without error only if instantaneous values of voltage and current are used throughout. Since this is impractical, it is customary to deal with such circuits as though they contained separate generators of frequencies ω (the excitation frequency), 2ω, 3ω, ---$n\omega$, and treat the circuit in terms of steady state sinusoidal currents and voltages of each frequency separately. If this is done, the relative phase of each component must be preserved to avoid serious errors in some applications. The VR pressure transducer and the input network in combination may be represented as a two terminal output device containing n generators each having a voltage amplitude and relative phase angle corresponding to each value of steady state input pressure

load, holding all other circuit parameters constant. This concept is illustrated in Figure 21. The results in a total voltage "calibration" of the general form shown in Table 3. The phase reference, or time zero, can be incorporated in these "data" by setting A_0' to zero. The effects of these harmonics on the signal processor are evaluated in Section VIII. Some practical problems with harmonics encountered in attempts in the early phases of this study to measure transducer characteristics using standard inductance measurement techniques are described in Section X.

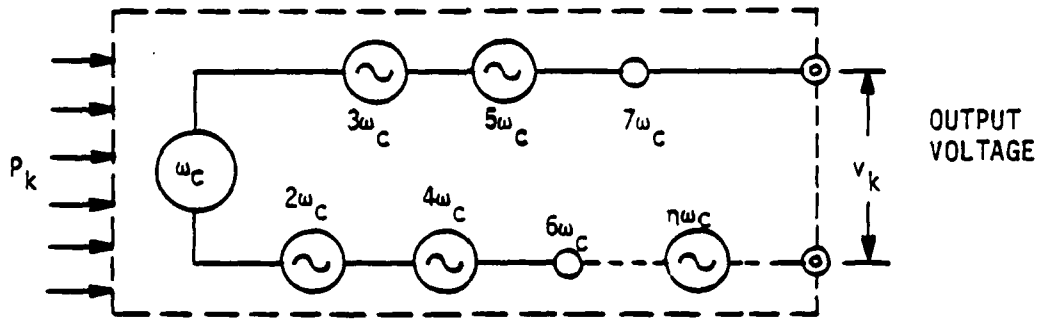

Figure 21. Total Output Transducer Equivalent

2. EDDY CURRENTS

A second result of establishing an alternating flux in the "iron" is the establishment of electrical currents within the magnetic material. These currents, called eddy currents, are created as a result of the time-varying MMF applied. The flow of these currents in the electrical resistance of the material causes power losses. They can be set up in any electrical conductor, whether magnetic or not. By use of the Faraday induction law relating AC flux density, the induced current, I, and the path geometry, the current and voltage-relationships in the external electrical circuit due to internal currents can be determined. The sequence of processes in the magnetic system which are detectable as electrical effects at the terminals of the inductor is shown in Figure 22. Each transition from magnetic to electrical form results in a time differentiation and therefore a multiplication of the amplitude by ω_c, accompanied by a phase shift of 90 degrees. The result

TABLE 3

STEADY-STATE CALIBRATION OUTPUT COMPONENTS
VARIABLE RELUCTANCE PRESSURE TRANSDUCER

Pressure Input % NFS	v_k, ELECTRICAL OUTPUT -- INSTANTANEOUS VOLTS
0	$v_o = A_o\cos\omega_c t + B_o\cos 2\omega_c t + C_o\cos 3\omega_c t + D_o\cos 4\omega_c t + E_o\cos 5\omega_c t + \ldots$
	$+ A_o'\sin\omega_c t + B_o'\sin 2\omega_c t + C_o'\sin 3\omega_c t + D_o'\sin 4\omega_c t + E_o'\sin 5\omega_c t + \ldots$
40	$v_1 = A_1\cos\omega_c t + B_1\cos 2\omega_c t + C_1\cos 3\omega_c t + D_1\cos 4\omega_c t + E_1\cos 5\omega_c t + \ldots$
	$+ A_1'\sin\omega_c t + B_1'\sin 2\omega_c t + C_1'\sin 3\omega_c t + D_1'\sin 4\omega_c t + E_1'\sin 5\omega_c t + \ldots$
80	$v_2 = A_2\cos\omega_c t + B_2\cos 2\omega_c t + C_2\cos 3\omega_c t + D_2\cos 4\omega_c t + E_2\cos 5\omega_c t + \ldots$
	$+ A_2'\sin\omega_c t + B_2'\sin 2\omega_c t + C_2'\sin 3\omega_c t + D_2'\sin 4\omega_c t + E_2'\sin 5\omega_c t + \ldots$
120	$v_3 = A_3\cos\omega_c t + B_3\cos 2\omega_c t + C_3\cos 3\omega_c t + D_3\cos 4\omega_c t + E_3\cos 5\omega_c t + \ldots$
	$+ A_3'\sin\omega_c t + B_3'\sin 2\omega_c t + C_3'\sin 3\omega_c t + D_3'\sin 4\omega_c t + E_3'\sin 5\omega_c t + \ldots$
80	$v_4 = A_4\cos\omega_c t + B_4\cos 2\omega_c t + C_4\cos 3\omega_c t + D_4\cos 4\omega_c t + E_4\cos 5\omega_c t + \ldots$
	$+ A_4'\sin\omega_c t + B_4'\sin 2\omega_c t + C_4'\sin 3\omega_c t + D_4'\sin 4\omega_c t + E_4'\sin 5\omega_c t + \ldots$
40	$v_5 = A_5\cos\omega_c t + B_5\cos 2\omega_c t + C_5\cos 3\omega_c t + D_5\cos 4\omega_c t + E_5\cos 5\omega_c t + \ldots$
	$+ A_5'\sin\omega_c t + B_5'\sin 2\omega_c t + C_5'\sin 3\omega_c t + D_5'\sin 4\omega_c t + E_5'\sin 5\omega_c t + \ldots$
0	$v_6 = A_6\cos\omega_c t + B_6\cos 2\omega_c t + C_6\cos 3\omega_c t + D_6\cos 4\omega_c t + E_6\cos 5\omega_c t + \ldots$
	$+ A_6'\sin\omega_c t + B_6'\sin 2\omega_c t + C_6'\sin 3\omega_c t + D_6'\sin 4\omega_c t + E_6'\sin 5\omega_c t + \ldots$
-40	$v_7 = A_7\cos\omega_c t + B_7\cos 2\omega_c t + C_7\cos 3\omega_c t + D_7\cos 4\omega_c t + E_7\cos 5\omega_c t + \ldots$
	$+ A_7'\sin\omega_c t + B_7'\sin 2\omega_c t + C_7'\sin 3\omega_c t + D_7'\sin 4\omega_c t + E_7'\sin 5\omega_c t + \ldots$
-80	$v_8 = A_8\cos\omega_c t + B_8\cos 2\omega_c t + C_8\cos 3\omega_c t + D_8\cos 4\omega_c t + E_8\cos 5\omega_c t + \ldots$
	$+ A_8'\sin\omega_c t + B_8'\sin 2\omega_c t + C_8'\sin 3\omega_c t + D_8'\sin 4\omega_c t + E_8'\sin 5\omega_c t + \ldots$
	⋮
0	$v_{12} = A_{12}\cos\omega_c t + B_{12}\cos 2\omega_c t + C_{12}\cos 3\omega_c t + D_{12}\cos 4\omega_c t + E_{12}\cos 5\omega_c t + \ldots$
	$+ A_{12}'\sin\omega_c t + B_{12}'\sin 2\omega_c t + C_{12}'\sin 3\omega_c t + D_{12}'\sin 4\omega_c t + E_{12}'\sin 5\omega_c t + \ldots$

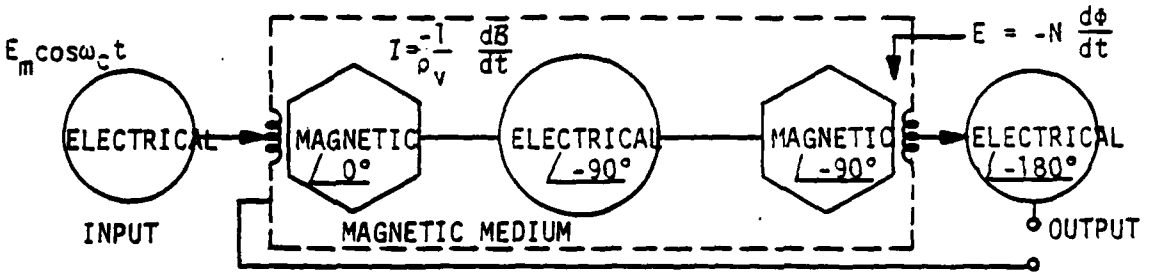

Figure 22. Eddy Current Model

is an effective overall phase shift of zero (-180 degrees) making the process a resistive or power dissipative one which is proportional in magnitude to ω_c^2. In the design of electrical machinery and power system components, these currents and voltages are of concern due to the operating inefficiency and equipment heating they cause. The power loss, W_{EC}, in a volume, V, of conducting material subjected to a sinusoidally varying flux having a value $B(t) = B_{max} \sin\omega_c t$ is given in Reference 7.

$$W_{EC} = \frac{\omega_c^2 \tau^2 B_{max}^2}{24\rho_v} \times V \text{ (watts)}.$$

In this expression, B is in gauss, ρ_v is the volume electrical resistivity of the conducting material, and τ is the thickness of an element of the volume in the direction shown in Figure 23. The volume is considered fixed and made up of a variable number of slabs, each having a thickness, τ, and length, h, which are electrically insulated from each other causing the path of the current I, to be long and thin. This increases the ratio of shunt-to-series resistance within the loop, which is beneficial. The thickness of the insulating layers between slabs is assumed to be zero, making the total width of the volume equal to the product $n\tau$. The volume resistivity is derived from test data on material samples. It is expressed as the voltage drop across two

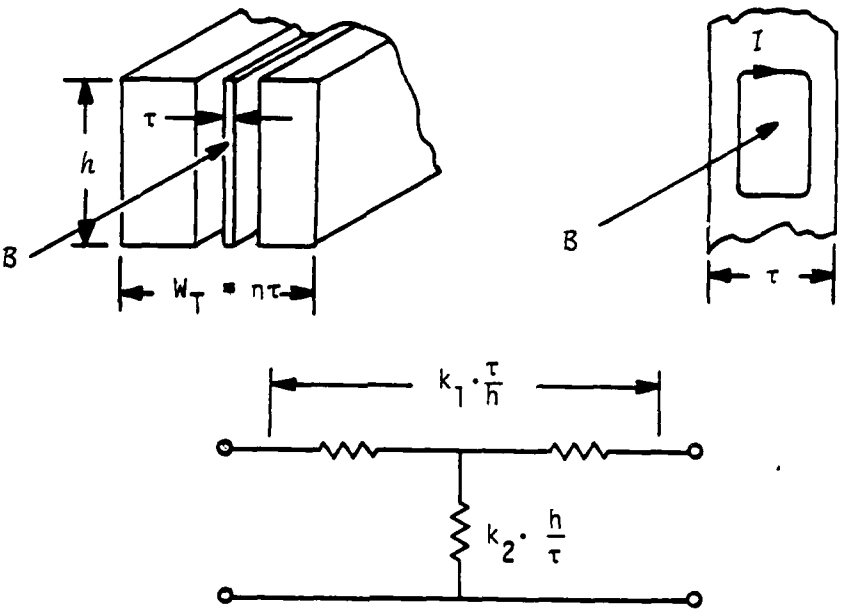

Figure 23. Eddy Current Geometry and Lumped Resistance Equivalent Circuit

opposite faces of a cube of unit dimension, caused by a uniformly distributed unit current flowing through (perpendicular to) those faces. The directional resistivity is defined by the relation

$$\frac{\vec{E}}{\vec{I}} = \vec{R} = \frac{\rho_v \ell}{A} \text{ (ohms)}$$

A is the cross sectional area of the face in the perpendicular plane. The units of length, having been derived in early work in materials physics, usually appear in data handbooks such as Reference 26 in centimeters, resulting in the dimension for ρ_v.

$$\rho_v = \frac{R(\text{ohms}) \times A(\text{cm}^2)}{\ell(\text{cm})} = \text{ohm-centimeters}$$

The derivation of eddy current power loss, W_{EC}, appearing in Reference 7, page 132, is in meters length, requiring that ρ_v be in ohm-meters or "ohms-per-meter-cube." Thus, most available handbook data, such as are found in Reference 26, must be multiplied by 10^{-2} $(\frac{\text{meter}}{\text{cm}})$ to be used in this expression. The derivation assumes geometric uniformity of flux

density in the medium, which may not be exactly true in practice for alternating flux. In the design of AC electrical equipment there are practical limits on the extent to which slab ("lamination") thickness can be reduced to reduce eddy current effects. The thickness of the insulation between laminations is finite rather than zero. Data from electrical steel manufacturers are available which show the manner in which test samples depart from the theoretical relationship. The eddy current losses as shown in this data do not extrapolate to zero as τ approaches zero.

Table 4 is a composite of data from several sources pertinent to the study of eddy current effects in various magnetic materials. The effect of temperature upon ρ_v is significant. Handbook data are based on the resistivity at 20 degrees Celsius. Temperature coefficients, α_T, given are applicable over a range of ±30 degrees Celsius from the value at 20 degrees. The corrected expression for ρ_v is then

$$\rho_v(T) = \rho_{v(20)}[1 + \alpha_T(T-20)]$$

Reference 8 gives an empirical expression for the total alternating current power losses in a closed path magnetic circuit from all sources in the form of a loss resistance, R_p.

$$\frac{R_p}{f_c L} = \mu(g + hB_{max}) + \mu k f_c.$$

Empirical coefficients are as follows:

g = residual coefficient
h = hysteresis coefficient
k = eddy current coefficient

In Table 4, the value k_6 is for core laminations of .006 inch thickness (τ = .006), and k_{14} is for.014 inch thickness laminations. This expression is useful in relating the contributions of each type magnetic process to the degradation of the quality factor or energy storage efficiency, "Q," of the inductor. By definition,

$$Q = \frac{X_L}{R_p} = \frac{2\pi f_c L}{R_p}. \quad \text{Then } \frac{R_p}{f_c L} = \frac{2\pi}{Q}$$

TABLE 4. HANDBOOK DATA -- MAGNETIC ALLOY RESISTIVITY

NAME OR COMPOSITION[1] [2]	%Fe	%Ni	ρ_v[3]	α T	k_6[4]	k_{14}
1. Pure Iron	100	0	9.78	.0064	--	--
2. High Strength Conductor Iron	100	0	--	.0035	--	--
3. Transformer Sheet	96	0[5]	60	--	--	--
4. "NILVAR"	64	36	80.5	.00135	--	--
5. "NICALOY"	52[6]	48	45	.0045	284	1550
6. "HYTEMCO"	30	70	20	.0045	--	--
7. Molybdenum "Permaloy" Dust	17	79[7]	$>10^6$	--	10	10

NOTES ( )

1. Names and composition of Alloys 4-7 are proprietary. Data from References 7 & 26.
2. Magnetic properties are strongly influenced by heat treatment and other processing variables.
3. All handbook data for resistivity values were in microhm-centimeters.
4. "k" values are eddy current loss coefficients; sub-scripts are sheet thickness in mils, where 1 mil = .001 inch.
5. 4 percent silicon.
6. Data for a similar alloy, Allegheny Steel 53-47, is available as a plot of core loss in watts per pound versus sheet thickness, Reference 7, p. 152..
7. 4 percent Molybdenum, compressed into shapes with binder

The frequency and lamination thickness have a strong effect on eddy current losses, which is evident from both forms of the loss relationship. The selection by the authors of References 10 and 23 of a 58 percent iron and 42 percent nickel alloy for VR transducer construction seems to have been based on the expected benefits of a minimum temperature coefficient, α_T, accompanied by a high value of ρ_v, such as is listed for "NILVAR" and other iron-nickel alloys of approximately 60-40 composition.

The one ohm-centimeter resistivity and low k coefficient of the alloy particle core material ("ferrite") is necessary for efficiency at high frequencies. The highest value of ρ_v for a solid magnetic material found in reference sources was 90 microhm-centimeters (90×10^{-8} ohm-meters). Since VR transducers are usually manufactured of materials chosen for corrosion resistance and structural qualities rather than their magnetic properties, commonly available handbook data are more of value to illustrate principles rather than to aid in design.

Due to the real power dissipative nature of the eddy current effect, the DC analog in Figures 11 and 15 is of little value in showing its influence on the electrical output of the VR transducer. In Figure 24, the AC analog is shown with both real and reactive elements. The eddy current effects appear as the lumped resistances R_p, R_s', and R_s, which have been shown to be sensitive to geometry, temperature and frequency. The AC resistance of the coils, R_c, is also shown. This representation brings out the weakening effect the eddy currents have on the coupling between the pressure stimulus, applied at L_1 and L_2, and the useful electrical output appearing at I_1 and I_2. A literal representation of the output voltage generation mechanism has also been added in Figure 24-b. The ammeters, I_1 and I_2, have been replaced by the current transformers, CT-1 and CT-2, which convert the currents to voltages. These voltage outputs are connected differentially to yield an output E_o which is proportional to $I_1 - I_2$.

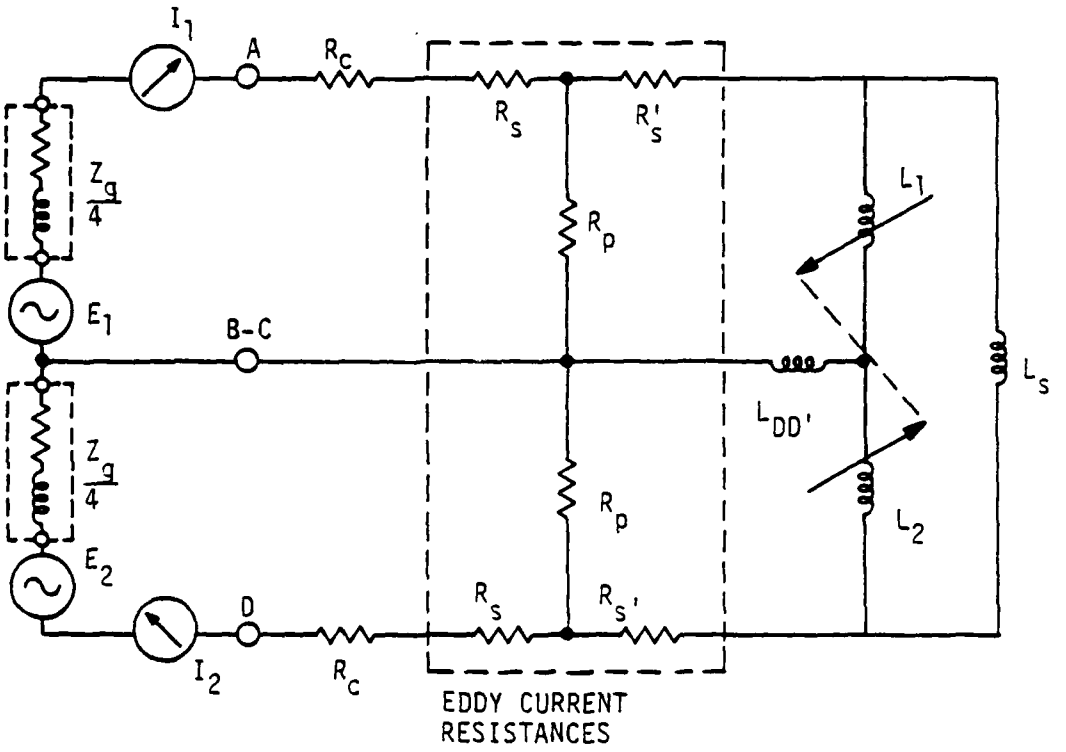

a) COMPLEX IMPEDANCE MODEL

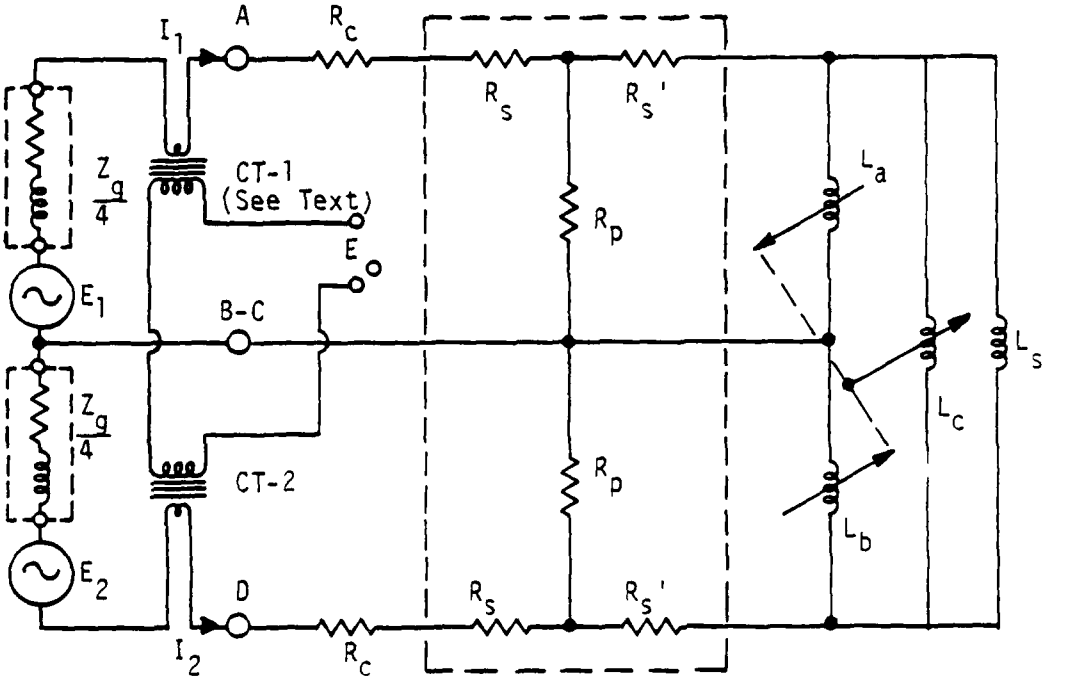

b) AFTER Y-Δ TRANSFORMATION OF INDUCTANCES

Figure 24. Complete Electrical Model - Variable Reluctance Pressure Transducer

The results of experiments performed to measure overall transduction characteristics of the transducers also served to verify the accuracy and completeness of this electrical model. Those results are presented in Section X.

The effect of temperature on the resistance of eddy current systems has been put to use in the design of electrical temperature and heat flux sensors.

SECTION VIII

EFFECTS OF THE SIGNAL PROCESSOR ON THE COMPLETE TRANSDUCER OUTPUT

In Section IV, time functions were used to develop the various discrete terms of the electrical output signal, r(t), resulting from multiplication processing of the signal from a VR transducer responding to a generalized input pressure, p(t). The form of this pressure signal, $p(t)\cos\omega_c t$, has a frequency domain counterpart (Fourier transform) given by $P(\omega) * [\delta(\omega-\omega_c) + \delta(\omega+\omega_c)]$, where the symbol * represents the convolution operation and δ is the Dirac impulse function. (Reference 14, page 73) In contrast with the piece-meal results obtained with time functions in Section IV, the frequency domain output function shown as $R(\omega)$ in Figure 8 concisely presents all sum and difference frequency components in the output. This is given in Reference 14, page 163, as

$$R(\omega) = F\{p(t)\cos\omega_c t \cdot f_2(t)\} = \pi[P(\omega-\omega_c) + P(\omega+\omega_c)] * F\{f_2(t)\}$$

$$= \pi \sum_{m=-\infty}^{+\infty} F_2(m)\{P[\omega-(m+1)\omega_c] + P[\omega-(m-1)\omega_c]\}$$

$F_2(m)$ is the discrete term series form of the transformed periodic multiplying function $f_2(t)$.

The context in which this expression appears in the cited reference is the definition of the spectrum of a demodulated double-sideband suppressed carrier (DSSC) amplitude modulated radio signal. It has the advantage of being concise and philosophically complete. It contains all phase and amplitude information and shows clearly the sum and difference nature of the frequency components. It would be particularly useful in cases where the pressure contains fluctuating components definable only in statistical terms.

Where stationary measurements and adjustments on real equipment must be dealt with, time functions are more accessible. They proved to be more useful because the critical part of the test work was concerned with measurements at or near the $\omega = 0$ axis. The "harmonic" components which contribute little to the translated output function, r, can readily be identified by inspection. The array of products contributing to the output is shown in Figure 25. Thus, an end-to-end channel calibration in the conventional meaning of volts output per unit applied pressure is obtained. It can be seen that the simplified sensitivity factor, n, of the ideal VR pressure transducer considered in Section II has no precise meaning when standing alone.

Those products averaging to zero, shown as the shaded area in Figure 25, constitute the nondata signal energy ϵ_p which is normally discarded by means of output filters or lost in the readout or data recording device due to its finite bandwidth. Another source of undesirable processor output is quadrature components of transducer output identified by the amplitude coefficients A', B', C', and so on. All processor outputs due to these components also average to zero since they are of the form $\sin u \cdot \cos u = \frac{\sin 2u}{2}$. Thus, they do not contribute to the desired signal, r. They do, however, contribute to the total scalar signal amplitude $[X^2 + (X')^2]^{1/2}$ within the signal conditioner. This quantity is the length or amplitude of the signal phasor which will be identified as $\Lambda_{A(X)}$. It can easily be measured using commonplace electrical instruments. Since signal amplitudes are often maintained within proper equipment operating limits by observations of r, the possibility exists that these quadrature signals could reach excessively high amplitudes due to improper equipment adjustments or malfunction without being detected. The signal amplifier portion of the signal conditioner could be driven into a nonlinear mode, causing amplitude errors and spurious modulation products. If the amplifier has sufficient operating range to handle these overloads, the processed signal still could be in error in the event that the signal amplitude approaches or exceeds that of the multiplier function $f_2(t)$.

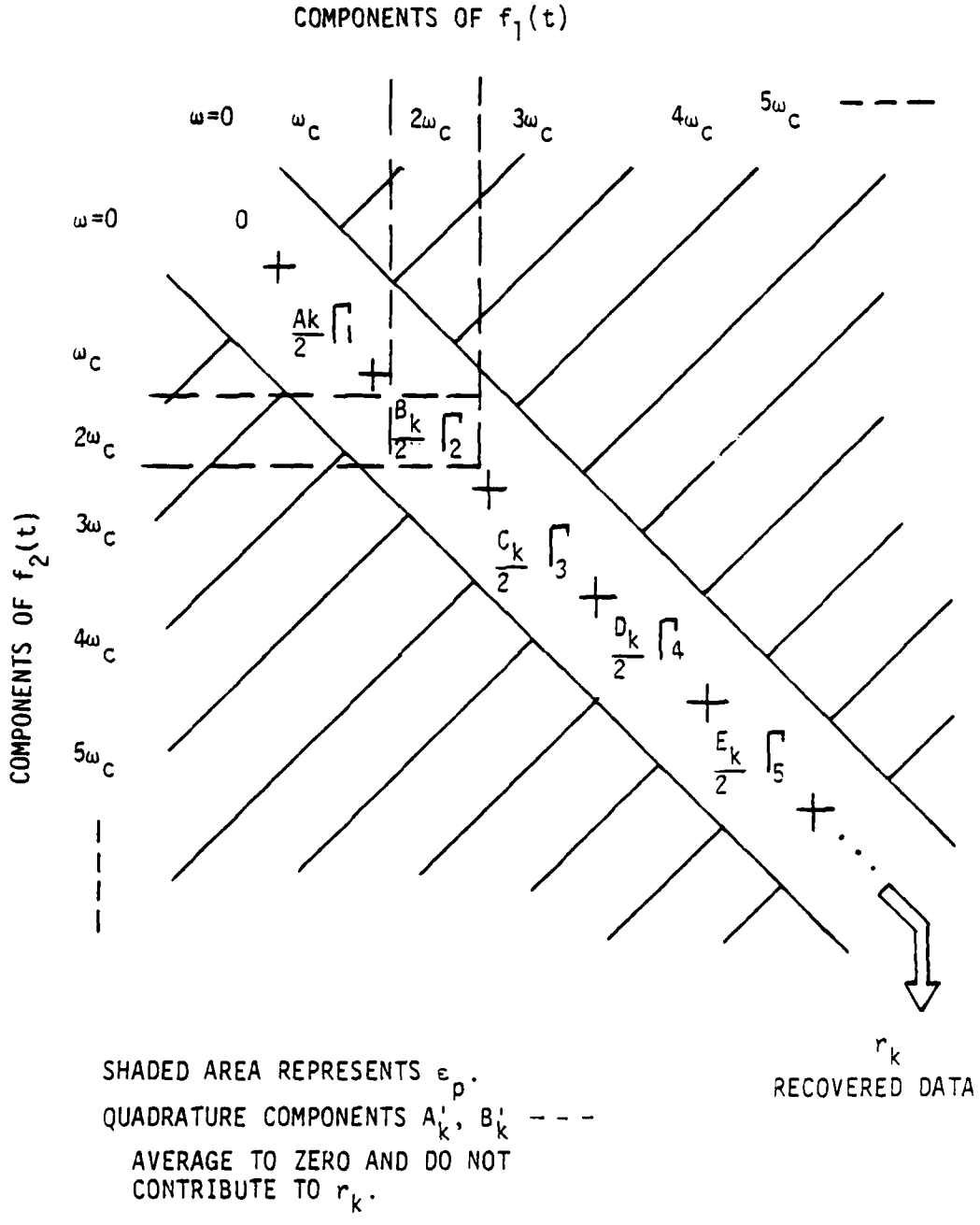

Figure 25. Data Output Products at One Steady State Pressure P_k-VR Pressure Transducer and Multiplier Processor

Large steady state quadrature signals may be detected and removed by providing a signal level indicator which indicates the average, peak or other value characteristic of the total signal amplitude. Such an indicator is often provided in equipment to simplify the adjustment of the transducer input circuitry, although they are used mainly for fine adjustments about zero. Standard practice is to establish zero measurand conditions on the transducer and adjust the electrical circuit to give an indication of zero signal. The indication given by a half-wave rectifier type voltmeter is the running average value of the sum of the fundamental and harmonics. This value at a given pressure input P_k is given by

$$V_{ind} = \frac{n_2}{\pi} \left[A_k + \frac{C_k}{3} + \frac{E_k}{5} + \frac{G_k}{7} + \ldots\right] \text{ volts}$$

The indication will be twice this value for a full wave rectifier. Normal equipment design practice is to provide nulling adjustments for the fundamental frequency only. These circuits add fundamental frequency voltages of magnitude U and U'. Since the harmonic content of the transducer is not zero, as would be the case with resistive or capacitive transducers, a zero indication will be obtained when

$$A_o = -\left[\frac{C_o}{3} + \frac{E_o}{5} + \frac{G_o}{7} + \ldots\right]$$

Only in the case where the harmonic coefficients are zero can a true null be obtained. A "null" condition requires that $A_o = U$ and $A'_o = U'$.

Signal amplitude indicators such as neon lamps or light-emitting diodes (LED) may be used instead of a meter, but these devices will respond to low duty cycle noise pulses as well as the instantaneous sum of the signal components.

The frequency translated signal processor output in response to a given steady state pressure load condition, P_k, is

$$r_k = \frac{2n_2}{\pi} \left[A_k - \frac{C_k}{3} + \frac{E_k}{5} - \frac{G_k}{7} + \ldots\right]$$

If U and U' have been adjusted with $P_k = 0$ to yield $V_{ind} = 0$, $A_o \neq 0$ and $[\frac{C_o}{3} + \frac{E_o}{5} + \frac{G_o}{7}] \neq 0$. Then r_o is not zero, and the signal conditioner will produce an output which is undesirable. This output is mainly due to the term $\frac{-2C_k}{3\pi}$. For convenience, and in the interest of simulating as nearly as possible the "bridge balancing" operation in DC resistive strain gage data channels, some FTSC equipment is designed with an integral, highly selective notch filter which reduces C_k and C_k' to nearly zero. This expedient introduces a number of complications in equipment design and operation. The most serious of these is the requirement for frequency stability of both the notch frequency and the frequency of the excitation oscillator, or for precise tracking of the two. Other complications are the effects of the non-ideal phase and amplitude transfer characteristics of the filter at the fundamental frequency. These practical equipment design problems are discussed in Section X.

The discussion of the output signals in a transducer and signal processor in Section IV was based on the use of the transducer output fundamental component as the phase reference. This is equivalent to equating to zero the coefficient for the quadrature component, A_o', in Table 3 and adjusting all the other amplitudes accordingly. Since there is no assurance that the output of a real VR transducer will be in phase with the excitation voltage, V_x, or that it will remain constant in phase at all pressure load values, the phase reference when real equipment is being considered will be taken as V_x. The phase relationships of the signal with respect to the modulating signal, $f_2(t)$ from Section IV, must also be considered. For simplification, only the fundamental of the signal will be considered. The vector relationships are illustrated in Figure 26. The phasor, $\bar{V}_o$, represents the undesirable output of the transducer and input network at zero pressure applied, having a magnitude $[A_o^2 + A_o')^2]^{1/2}$ and a phase angle $\tan^{-1} \frac{A_o'}{A_o}$. The initial settings of α_N and θ_N shown in Figure 26a are incorrect. In Figure 26b, they are shown after adjustment to be equal and opposite to $\bar{V}_o$. It is now necessary to impose a trial pressure load on the

transducer, causing the output signal $\overline{V}_S$. The value of processor output, r, will be maximum when the phase of either $\overline{V}_S$ or $\overline{V}_M$ is adjusted until the phasors for $\overline{V}_S$ and $\overline{V}_M$ coincide as shown in Figure 26b. This is the condition for which $\cos(\theta_S - \theta_M) = \frac{A_o}{[A_o^2 + (A_o')^2]^{1/2}} = 1$. This operation is commonly referred to as adjusting the "reference phase." Once it is accomplished, the trial load is removed and the indication of r_o will return to some value which differs from zero to the extent that harmonic products are present. It is then customary to "trim up" the adjustments of α_N and θ_N to achieve a presentable approximation to zero output. The equipment is then ready for taking data. Figure 26b shows the phase angle, θ_M, of the modulation function, $\overline{V}_M$, as the adjusted variable, rather than that of the signal, $\overline{V}_S$. This is preferable in practice because the exact amplitude of $\overline{V}_M$, α_M, corresponding to V_R in Figure 10, is not critical, and a simple phase shift circuit which could not maintain a constant value of H_2 would require extensive trial resettings of gain and phase adjustments to achieve the desired channel calibration. This approach would also introduce more components in the signal channel which could cause drift of n_2 or increase cost and complexity.

The foregoing analysis of the signals and adjustments affecting the processed signal output, r, shows that all components in the output of a mechanically ideal transducer and FTSC comprise a true, repeatable form of pressure analog. The signal processing operation on all these components is consistent and predictable given a few simple constraints on equipment design.

The LVDT is a device with a predominantly air magnetic circuit. The magnetic core only serves to control the geometry of the flux lines connecting the primary, which is supplied with the excitation voltage, with the secondary (output) windings. As a result, the excitation frequency phase shifts and harmonic output in the LVDT are much smaller and more predictable than those of a VR pressure transducer. Signal conditioners for use with LVDTs do not usually include the relatively elaborate phase shift and harmonic reduction circuits provided in signal conditioners intended for use with VR transducers. A more detailed discussion of the LVDT and signal conditioners designed expressly for them is contained in Reference 27.

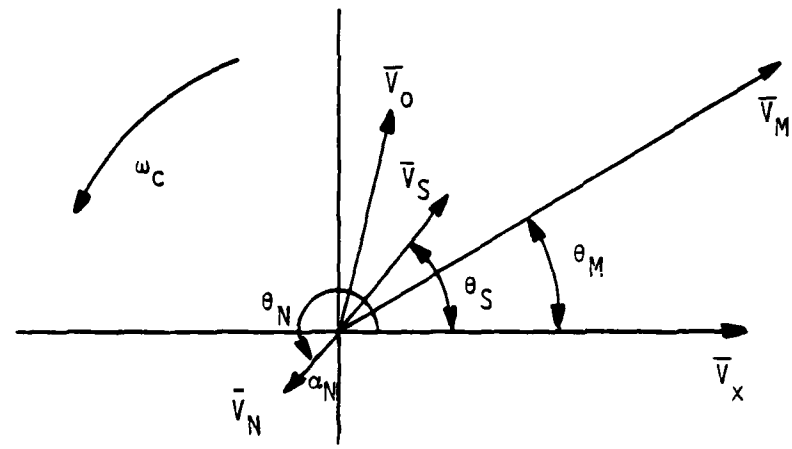

A) BEFORE ADJUSTMENT

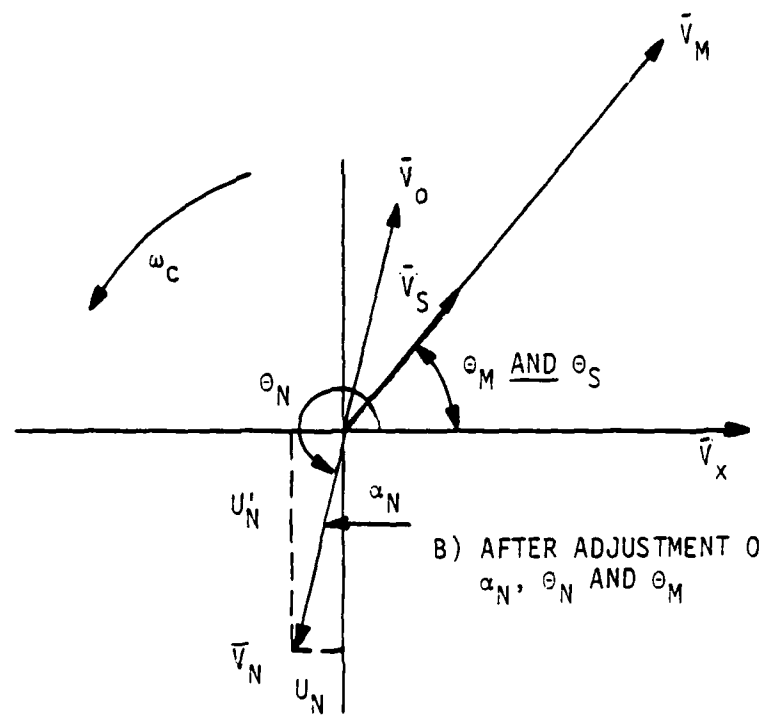

Figure 26. Fundamental Frequency Signal Voltage Phasors - Signals Conditioner Input Circuit

SECTION IX

EQUIPMENT DESIGN CONSIDERATIONS - SIGNAL CONDITIONERS

The two necessary functional elements of a frequency translating signal conditioner (FTSC) are

- Excitation Voltage Generator
- Two-Input AC Voltage Multiplier (Figure 9) or its equivalent.

Practical considerations often result in provisions for these additional functions:

- Signal Voltage Scaling - Variable gain AC amplification. Transformer ratios and variable voltage dividers in forward signal paths or feedback paths also implement this function.

- Offset Correction Adjustments - Amplitude and phase adjustments and means to sum the voltages U and U' with the signal X_o and X_o'. These are normally provided to cause the FTO to be zero when applied pressure is zero. They could conceivably be used to provide controllable zero offset instead.

- Phasor Control - Phase shifters to adjust the relative phases of $\bar{V}_X$ and $\bar{V}_M$. ("Reference Phase")

Depending upon the particular application, the following design options or convenience features may be added:

- Transformer isolation of the input circuit from electronics common (ground) and/or power line; and/or,
- Transformer isolation of the FTO circuit,
- Scalar signal amplitude indicator,

- Scalar signal amplitude limiter,

- Selection of input circuit configuration for 1-, 2-, or 4-arm transducers,

- Harmonic rejection networks,

- Excitation power distribution schemes to operate more than one transducer/conditioner set from a common source of V_x,

- Isolation/distribution schemes to provide a number of separate, independent output signals ("fan-out") from one transducer.

The precision of the FTSC standing alone is determined by the stability of

- Excitation voltage amplitude, V_x

- Multiplier "transfer function," η_3

- Amplification or scaling factor $H_2 = Re(\eta_2)$

- Input/output phase relationships, ϕ_N, in the gain electronics at the frequencies ω_c, $2\omega_c$, $3\omega_c$ - . . $n\omega_c$, as shown in Figure 4.

In terms of critical components required for construction, the precision of a signal conditioner is dependent on the stability of:

- Signal amplifier gain and phase relationships

- Resistors and capacitors in the phase shifting and coupling networks

- The transfer function of the multiplier functional block, η_3. In the case of the transformer coupled diode ring of Figure 10, this usually reduces to stability of resistors and of the current/voltage relationships in the diodes.

The addition of circuits providing design options and operating refinements does not introduce any other type of component stability problem. Only the parts count is increased.

The additional performance uncertainties introduced when combining the signal conditioner and VR transducer are:

- Effects of changes in the transducer as a load upon the excitation source. These effects can be minimized or eliminated by keeping the excitation source impedance low.

- Loading effects of the input circuit of the FTSC on the transducer. These can be minimized by keeping the impedance of the input circuit high.

- Effects of cable capacitances upon the transducer and input network. These can be minimized by keeping the transducer impedance low.

- Factors which affect the overall frequency response of the transduction-processing chain in the original or untranslated ("baseband") frequency regime, often referred to in the vernacular as the "dynamic" response of the system. These effects are not readily evident from the analysis of steady state performance.

Contributing factors to the overall data frequency response, aside from the transducer mechanical and pneumatic response, are the gain-frequency and phase-frequency relationships of the transducer input network and signal amplifier and, if used, the amplitude and phase characteristic of the output filter following the multiplier processor ("demodulator"). Since the transducer input network and amplifier operate in the translated frequency (ω_c) domain, their effects on frequency response in the data frequency (ω_f) domain may be overlooked. Since they arise mainly out of practical circuit considerations, they will be discussed with the experimental work described in Section X.

One system packaging approach results in the assumption of responsibility for all of these system response considerations by the equipment manufacturer. This approach is to enclose the transducer and signal conditioner (mainly electronic circuitry) in a single package. The result is a product described as a "DC In - DC Out" transducer.

These transducers provide the range sensitivity and other advantages of the VR transducer without the application complexity. The output signal level is high enough to feed most data acquisition system inputs (high level multiplexers) directly. The data frequency response capability of these units is usually confined to the quasi-steady state range, hence the name "DC Out." These units are not entirely free of "twiddlepot" adjustments. Several models inspected had recessed screw adjustments for "span" and "zero." Application problems likely to be encountered with these transducers are limited to those resulting from location of the electronics in hostile environments normally encountered by the transducer alone, and from system complications which may arise from operating more than one transducer from the same power supply (usually 28 volts DC) or with common grounds on the transducer or data system input circuit.

The equipment configuration which can provide optimum performance and allows the system designer the greatest amount of freedom also requires of the user a comprehension of the underlying principles of the "carrier" technique. The open channel or "knob job" equipment configuration consists of an interchangeable transducer, a connecting cable of arbitrary length, and an FTSC having an elaborate set of circuit adjustments and indicators to accommodate midstream changes in the transducer system. (Reference 28) This approach is often used in test instrumentation equipment intended for use in ground test facilities. It provides great operating flexibility and avoids imposing a requirement for ruggedness on anything but the transducerand pneumatic system. The pneumatic system often includes selector valves for applying zero pressure differential and various calibration pressures, tubing disconnects for changing system configuration, and often transducer heaters or coolers. The transducers are often mounted as an integral mechanical part of the pneumatic system hardware. Many of the line switching functions are remotely and/or automatically operated by solenoids or pneumatic actuators. The signal conditioner may be located remotely in a benign environment, near a wide variety of signal monitoring and recording devices.

The internal architecture of an FTSC of this kind which can provide optimum measurement precision when used with a VR transducer, is shown in Figure 27. Many commercial equipment designs have been based on this scheme in the past. A common source (oscillator) supplies the excitation voltage and the multiplier signal, $V_M \cos\omega_c t$. In addition to providing the previously explained advantages of transformers, their use makes possible a marked decrease in the number of active electronic devices in the system. Unlike vacuum tubes and transformers, the control of operating parameters of semiconductor devices throughout their useful life is subject to many unpredictable variables, such as source selection and initial screening test procedures, which must be included in the first cost of the equipment. Thus, it is in the interest of reliability that the performance requirements for these devices be relaxed by simplifying the electronics to the greatest extent possible.

When using transformers, the effects of temperature on the magnetic properties of the core and on copper resistance must be considered. Transformers of conventional laminated core and coil design operate at peak efficiency from 400 to 20,000 Hertz. However, the core material must be high-permeability alloy specifically designed for low power operation at audio frequencies. Four percent silicon steel used in small 60 hertz power transformers is not efficient and causes power losses, phase shifts and poor voltage regulation when used in low power signal circuits. Should VR transducers be developed which will operate at higher frequencies, transformer design is simplified, since particle cores and torroidal shapes can be used.

To achieve a relatively high ($\pm$5 volts) FTO at low impedance, the high level demodulator of Figure 10 must dissipate considerable power. The low-level demodulator followed by a DC data amplifier power output stage is often used. It may appear more efficient if the DC power supply requirements are not considered at the same time. The requirements for isolation, regulation and current capacity in the DC power supply for a DC data amplifier are considerably more stringent

AD-A130 695 EVALUATION OF THE VARIABLE RELUCTANCE TRANSDUCER/CARRIER AMPLIFIER METHOD..(U) AIR FORCE WRIGHT AERONAUTICAL LABS WRIGHT-PATTERSON AFB OH 2/3

UNCLASSIFIED D L MCCORMICK FEB 83 AFWAL-TR-82-2100 F/G 14/2 NL

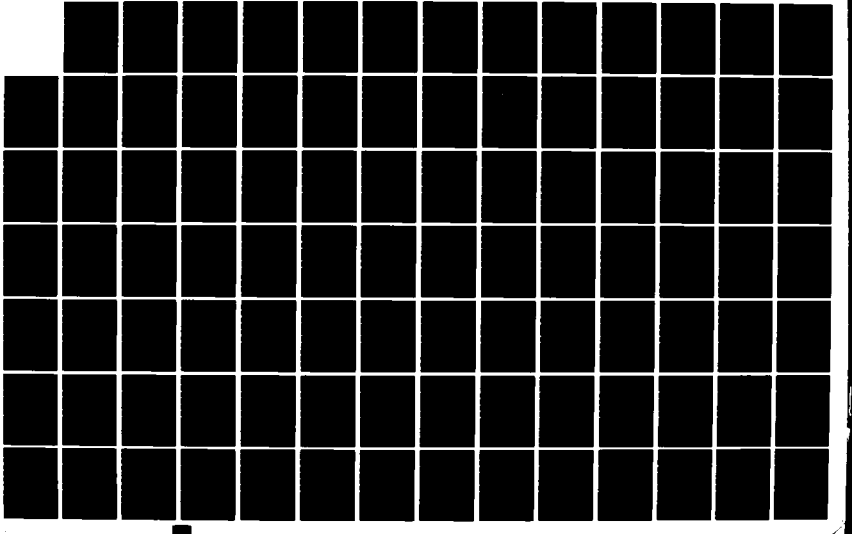

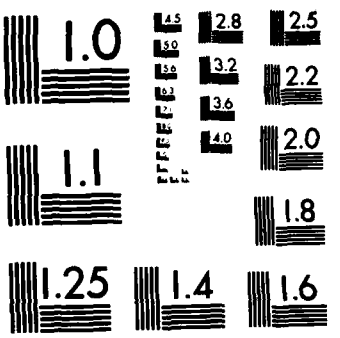

MICROCOPY RESOLUTION TEST CHART
NATIONAL BUREAU OF STANDARDS-1963-A

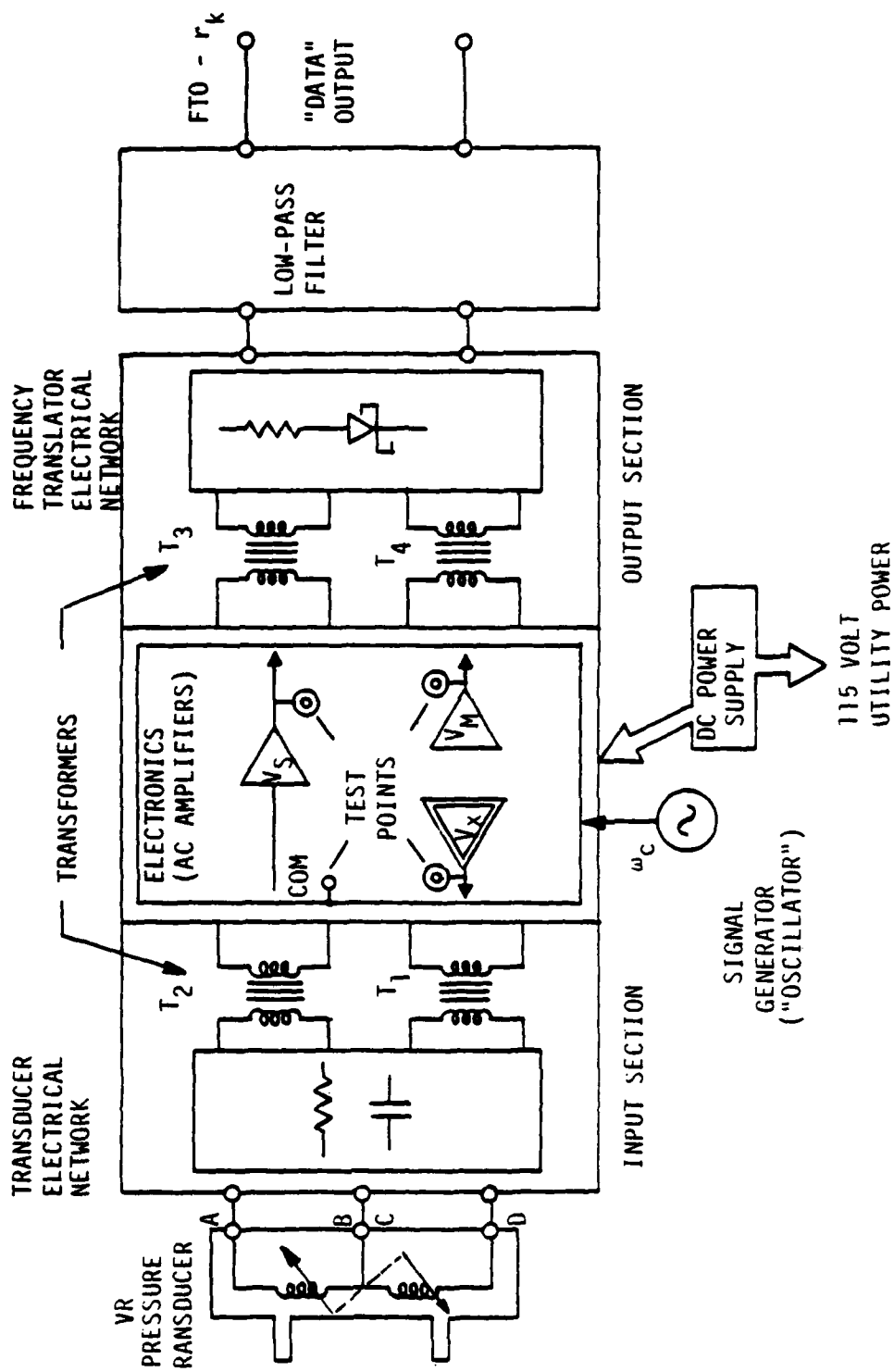

Figure 27. Internal Architecture - Frequency Translating Signal Conditioner

than those for an AC signal amplifier. Moreover, the isolation between channels and from power line is accomplished at a point involving a larger, less efficient 60 hertz power transformer connected to the 115 volt AC power distribution system. One transformer and regulator are required per channel for isolation, whereas all electronics for any number of high-level demodulation FTSC's may be fed from a common DC supply without affecting FTO isolation. In normal circumstances, regulation of the DC voltage will be much less critical.

If system requirements dictate a large voltage output signal at a very low impedance, the best design approach may be to obtain all the voltage gain in the AC circuits and use the DC amplifier only for current gain (impedance reduction). Zero and span drift and noise problems with such low gain DC amplifiers are minimal.

An interesting variation of the amplifier-multiplier FTSC is shown conceptually in Figure 28. It was used in an equipment design in the early history of electronic instrumentation and serves to illustrate the underlying communications system principles. A fixed carrier signal, $V_c = \alpha_c \cos\omega_c t$, which is large compared to the maximum transducer output, is summed in-phase with the transducer signal, V_s, creating a full AM signal like that shown in Figure 5(c). The signal in the transmission medium then becomes $[\alpha_c \eta_2 + \eta_1 \eta_2 (P_s + P_f \cos\omega_f t)]\cos\omega_c t$. The multiplication process then can be performed, after amplification, with a simple rectifier, since the sum signal never reverses phase. This "demodulation" process can therefore be thought of as "self-synchronous" and the second wire for the reference signal is not needed. The rectified form of the received carrier component, $V'_M \cos\omega_c t$ in Figure 5(c), is a large fixed DC offset component, $\eta_3 V'_M$. In order to shift the FTO at zero-measurand transducer output back down to zero volts, it is "bucked out" potentiometrically with a fixed D.C. supply, V_B[1].

1. In AM radio receivers, this steady state component is separated from the audio modulation with an R-C network. It can be used to adjust the gain (sensitivity), η_2, of the amplifier portion of the receiver inversely with received signal V'_M and sometimes to actuate a signal strength "S" meter.

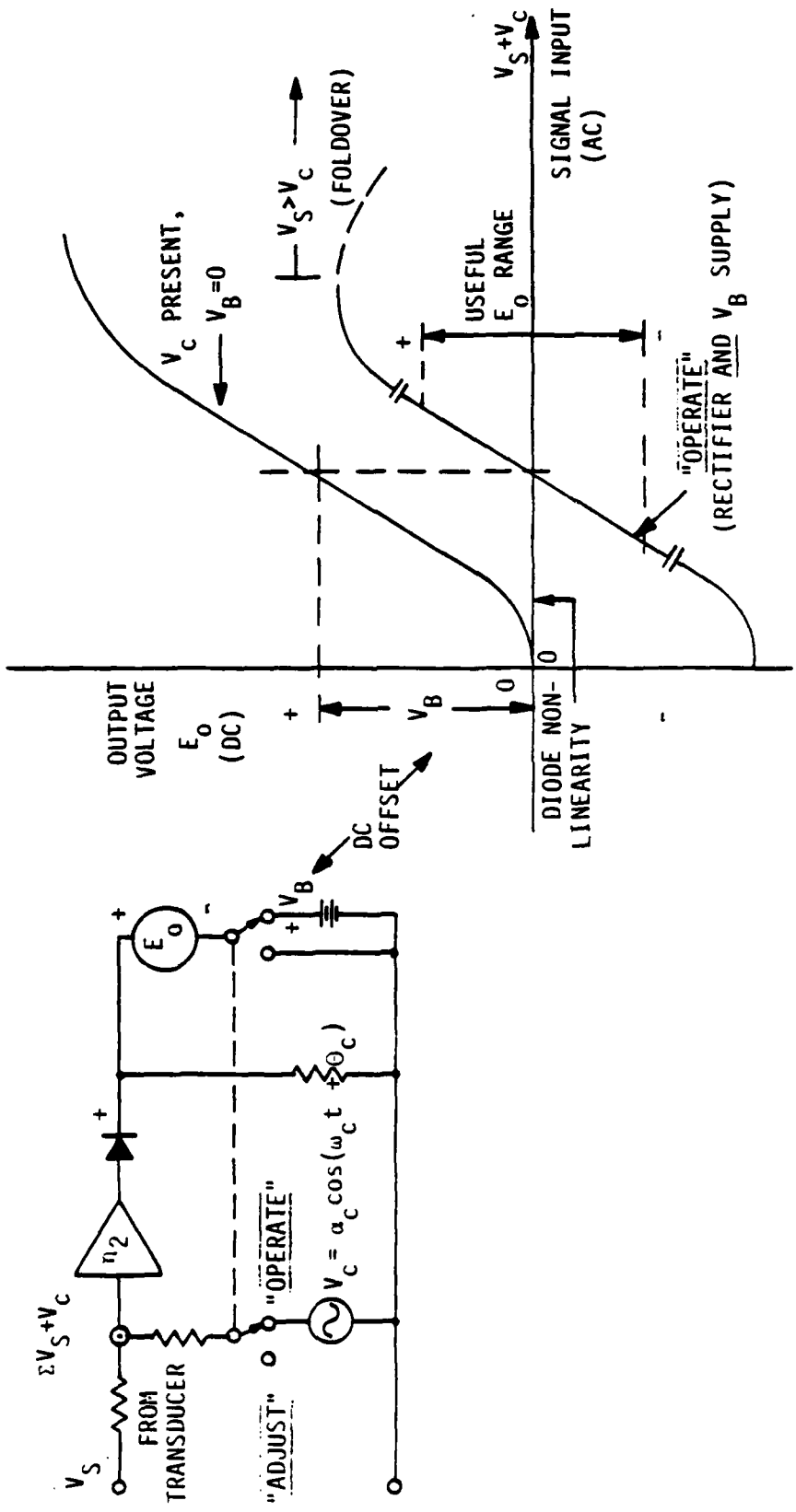

Figure 28. Full AM SIgnal Conditioner (Restored Carrier) - Variable Reluctance Pressure Transducer

This FTSC had some serious practical limitations. Circuitry used to develop the various AC and DC signals which affect the precision of the processing operation was not sufficiently stable. Bulky, inefficient vacuum tube amplifier and oscillator circuits were used. A four-channel package weighed over a hundred pounds. Rectifiers were unstable devices using sulfides and oxides of copper and magnesium (Reference 29) and the stability of the DC offset supply, V_B, was unsatisfactory. Operation of the system is illustrated by means of the input/output curve of Figure 28. The linear operating range of the signal amplifier must extend to include the combined amplitude of V_R and V_S of Figure 10. Due to the power-limited circuitry used in the equipment, signals of unexpectedly large amplitude sometimes caused a confusing output signal. The output in extreme cases would fold over and reverse polarity with increasing input signal without being detected. The equipment fell into disuse for these reasons. Using present day circuit technology, these performance inadequacies are easily correctable. The residual offset could be utilized in many applications requiring a suppressed zero. This approach does not suffer the power losses in current limiting resistors as does the ring modulator of Figure 10. A very low output impedance may be obtained at high output voltage levels. The rectifier diodes will be operating at a large signal level, insuring linearity. This approach to FTSC design is explained in more practical detail in Appendix D.

A characteristic of all forms of AC signal conditioners is the loss of the individual identities of the various internal signal voltages and their phase relationships. Once they are summed, they cannot easily be resolved into their original components. This complicates the work of troubleshooting installed data channels. One procedure which was helpful in speeding up pre-test channel adjustments and diagnostics is described in Section X. It consists of examining both the phase and amplitude of various signal voltages within the signal conditioner at specially selected test points with a phase coherent voltmeter. Some of these test points are shown in Figure 27.

SECTION X

EXPERIMENTAL RESULTS

1. PRELIMINARY TESTS

This evaluation program was initiated mainly because considerable difficulty was experienced in developing definitive methods of testing VR transducers for materiel acceptance. Temporary criteria were adopted for processing a large quantity of incoming units purchased from various vendors for aerodynamic test programs. These acceptance tests were limited to obtaining reasonably consistent measurements of inductance and "Q" for all units of a given make and model, holding the accessible control parameters, excitation voltage and frequency, constant at some purely arbitrary value. A standard impedance bridge was used. The test apparatus is shown in Figure 29, and some typical test data are contained in Table 5. A large increase in null signal was obtained with the band-pass filter switched out of the detector-amplifier unit, indicating a very poor definition of balance in the bridge due to harmonics in the test circuit. This condition was interpreted as being a basic inadequacy of the method, and its use was continued only as a temporary expedient. After testing some 150 VR transducers of various makes and models, all units purchased were determined to be free of open, shorted or grounded coil windings, seriously kinked center plates, pneumatic leaks, and other obvious defects. This was taken as an indication that no exceptional manufacturing problems are involved in producing inexpensive transducers which perform acceptably when used with certain "carrier amplifier" signal conditioners. As a management expedient, more detailed tests and calibrations were left to be performed as a part of the aerodynamic test programs. Successful application of the equipment was made possible in part by the availability of experienced circuit technicians for pretest channel rigging and troubleshooting. It was determined that the effects of transducer harmonics, lead capacities, and signal phase relationships upon signal conditioner output were the cause of some peculiar system behavior, making the circuit adjustment operation technique-sensitive. Establishing confidence in this equipment for more widespread use required resolution of all such uncertainties in performance.

EXCITATION: 1.4 VOLTS RMS, 1 KILO HERTZ
FILTER: BAND PASS - 1 KILOHERTZ

RECORD FOR	L_1	L_2
NULL VOLTAGE-FILTER IN	____	____
NULL VOLTAGE-FILTER OUT	____	____
"L" (MILLIHENRIES)	____	____
"Q" = $\frac{XL}{R}$	____	____

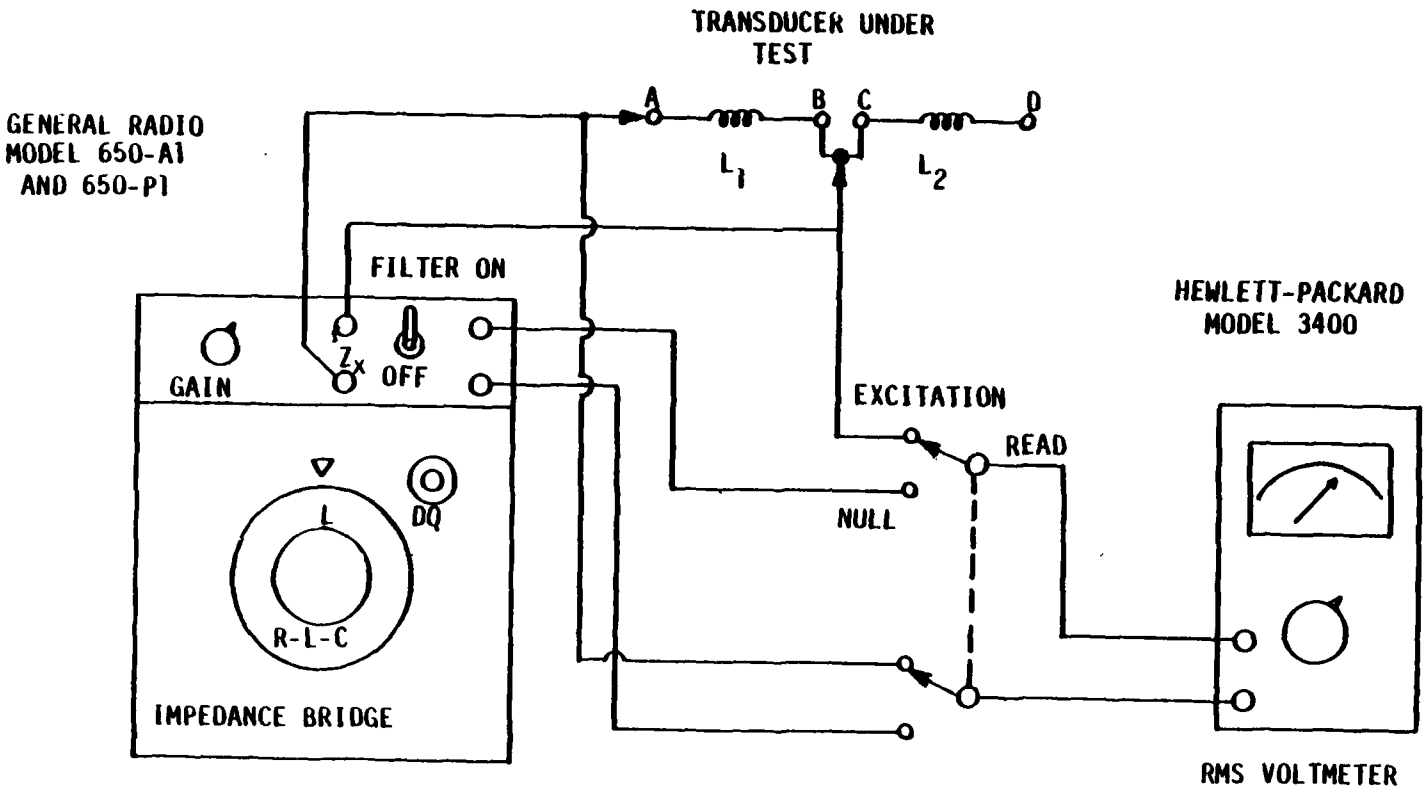

Figure 29. Equipment Arrangement - Electrical Inspection-Variable Reluctance Pressure Transducer

TABLE 5

TEST DATA - ELECTRICAL INSPECTION, IMPEDANCE BRIDGE METHOD

VARIABLE RELUCTANCE PRESSURE TRANSDUCER (Ref: Figure 29)

TRANSDUCER IDENTITY	NO LOAD		+FULL LOAD		-FULL LOAD		ZERO RETURN	
	L_1/Q_1	L_2/Q_2	L_1	L_2	L_1	L_2	L_1	L_2
A-01	23.5/2.05	23.4/2.08	25.0	22.4	22.3	24.9	23.6	23.4
A-02	22.7/1.95	24.2/1.9	24.0	22.6	21.2	25.5	22.4	23.9
A-11	19.5/1.73	19.6/1.72	20.0	19.3	19.1	20.2	19.5	19.6
A-12	19.4/1.90	19.6/1.89	20.0	19.4	19.2	20.1	19.6	19.6
A-13	22.4/1.88	22.4/1.89	23.6	21.5	21.5	23.4	22.4	22.4
A-14	18.5/1.77	19.0/1.75	19.0	18.7	18.3	19.5	18.6	19.0
B-02	23.2/3.7	23.5/3.7	22.3	24.9	24.5	22.5	23.2	23.5
B-03	23.2/3.7	23.6/3.7	22.4	24.8	24.3	22.7	23.2	23.6
B-04	22.0/3.6	21.9/3.6	21.2	23.5	23.3	21.0	22.0	21.9
C-01	23.0/3.5	22.8/3.55	22.5	23.7	23.9	22.1	23.0	22.8
C-02	24.2/3.6	23.9/3.75	23.6	24.5	25.0	23.3	24.3	23.9
C-04	23.6/3.75	23.6/3.8	23.0	24.5	24.5	23.0	23.6	23.6

L_1 = Inductance Reading, Coil A-B, Millihenries $Q = \frac{X_L}{R}$ Dial Reading Test Voltage 1.4 Volts RMS, 1 KHZ.

L_2 = Inductance Reading, Coil C-D, Millihenries Best Null: 4.5 Volts with 1 KHZ Filter.

32 Volts - No Filter

The hardware functional blocks necessary for implementing the signal processsing method of Figure 5(b) are shown in Figure 30. Definitive measurements of transducer output, v_k, at any steady state pressure, P_k, were desired. The many variables introduced by use of the frequency translating signal conditioner block were avoided by making voltage measurements directly upon v_k.

The various input circuits which can be used to develop the output voltage, v_k, from the passive transducer are shown in simplified form in Figure 31. The circuit shown as Case V is a mutually coupled bridge described in References 10 and 30. This circuit is current sensitive. According to the author of Reference 10, it was used with good results with a capacitive transducer at a carrier frequency of 400 kilohertz. The excitation voltage drop across the medium impedance windings of the VR transducers available for test proved to be a serious disadvantage. The circuit could be used with VR transducers if they were rewound with low impedance coils; that is, fewer turns of larger wire. It would then be less affected by shunt cable capacitances than the voltage-mode circuits. For commonly available transducers, such as those tested, the arrangement shown as Case II proved most desirable. It is the same as that shown in Figures 1 and 4. The only disadvantage of this circuit is the need for a center-tapped supply transformer, T_1

Manufacturers' recommendations for operating frequency, ω_c, and voltage, V_x, are often not explicit. Some exploratory measurements were made in an attempt to locate an optimum operating point. These measurements were made on the assumption that the electro-magnetic and electrical process efficiency would be bounded on the low frequency end by magnetization (hysteresis) losses and at the high frequencies by increasing eddy current losses. The equipment arrangement and plot of the results of this crude test are shown in Figure 32. Since the generation of harmonics is also a factor in the choice of excitation frequency and voltage, some trial measurements were made, as illustrated in Figure 33. The effects of excitation frequency, voltage and applied pressure are shown plotted in various ways in Figures 34, 35, and 36.

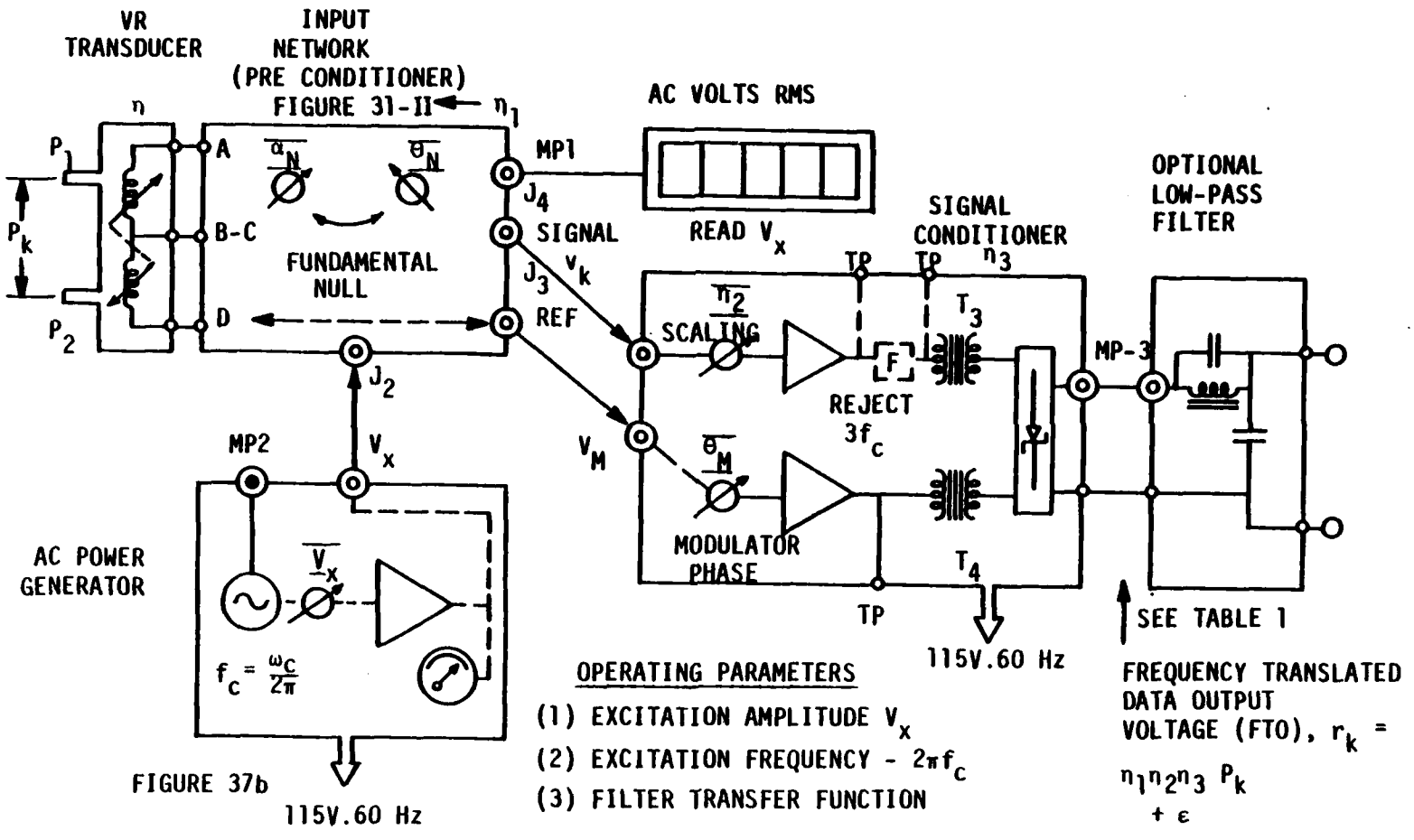

REFERENCE: FIGURE 5-b

TP = BENCH TEST POINT
MP = PARAMETER MEASURING POINT
___ = CIRCUIT ADJUSTMENT

Figure 30. Bench Test Apparatus - Variable Reluctance Pressure Transducer and Signal Conditioner

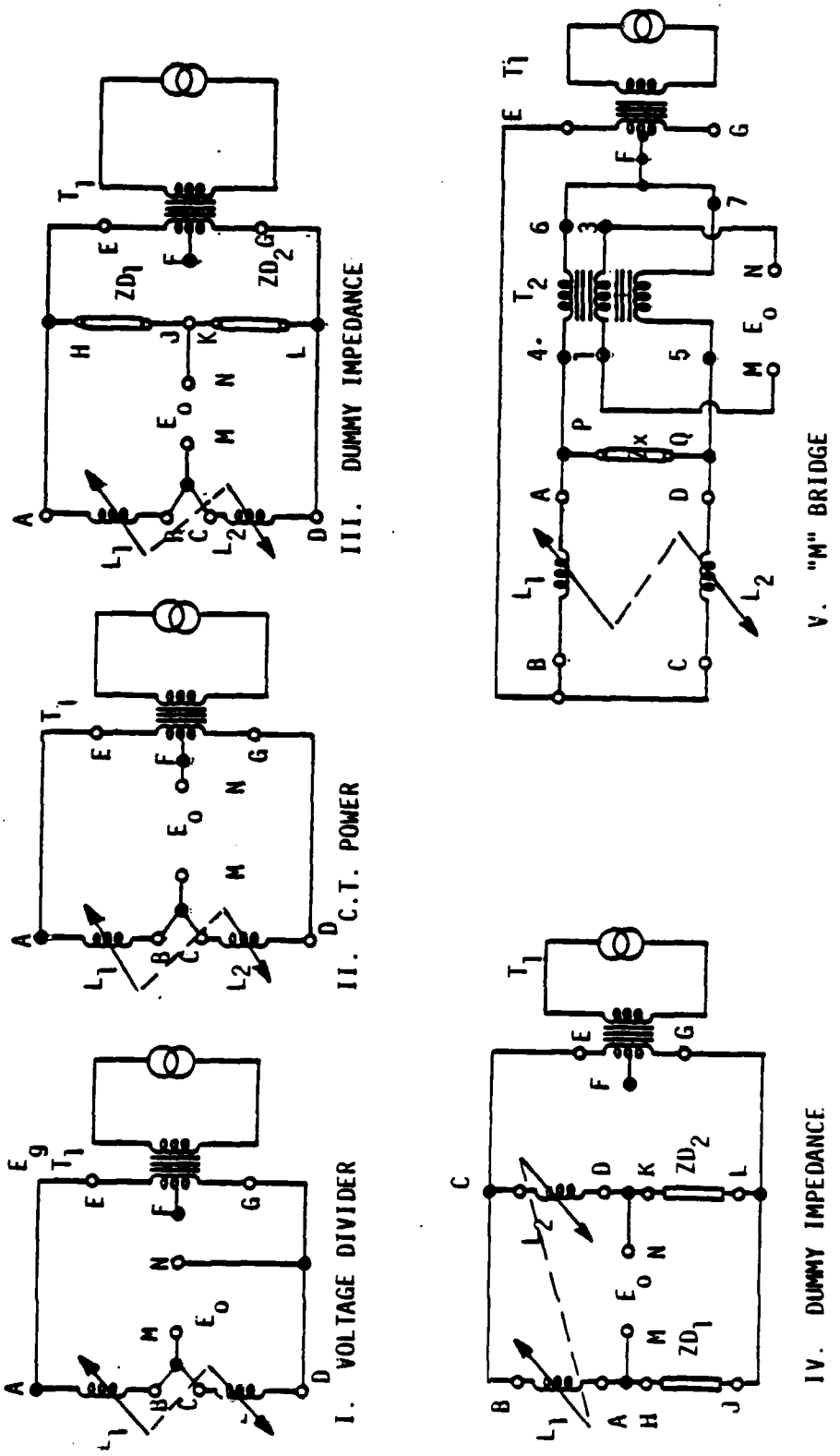

Figure 31. Transducer Test Input Circuits

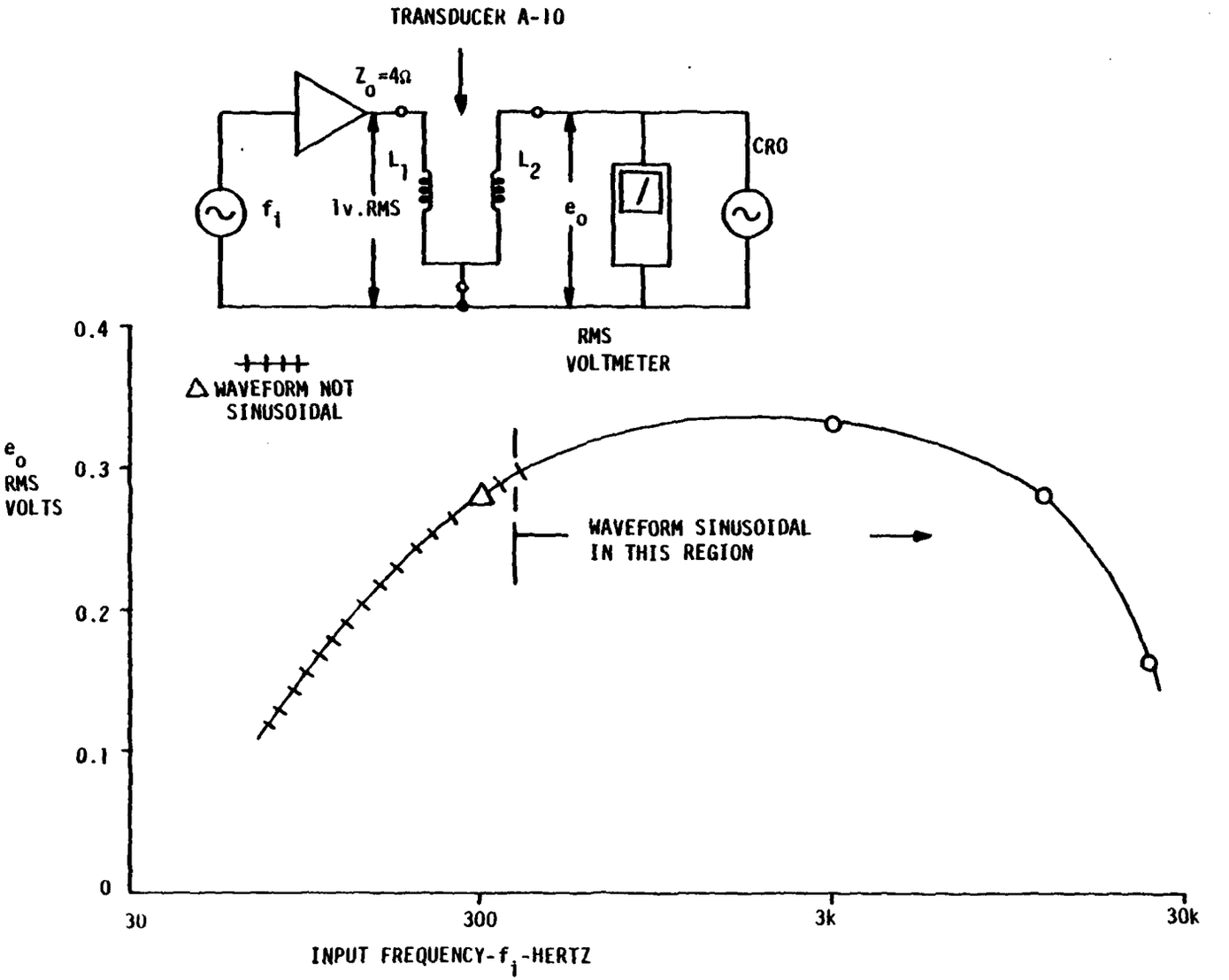

Figure 32. Mutual Inductance Test - Variable Reluctance Pressure Transducer

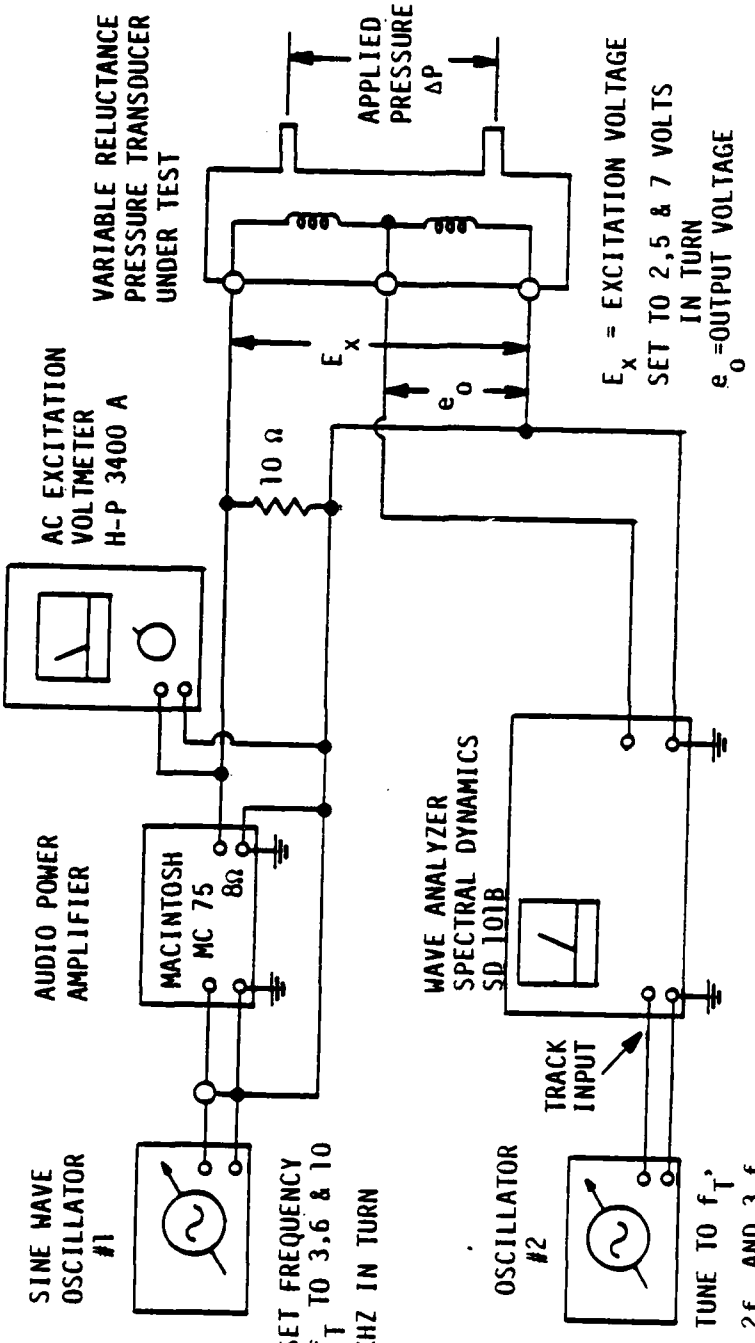

Figure 33. Test Equipment Connections - Preliminary Harmonic Output Tests - Variable Reluctance Pressure Transducer

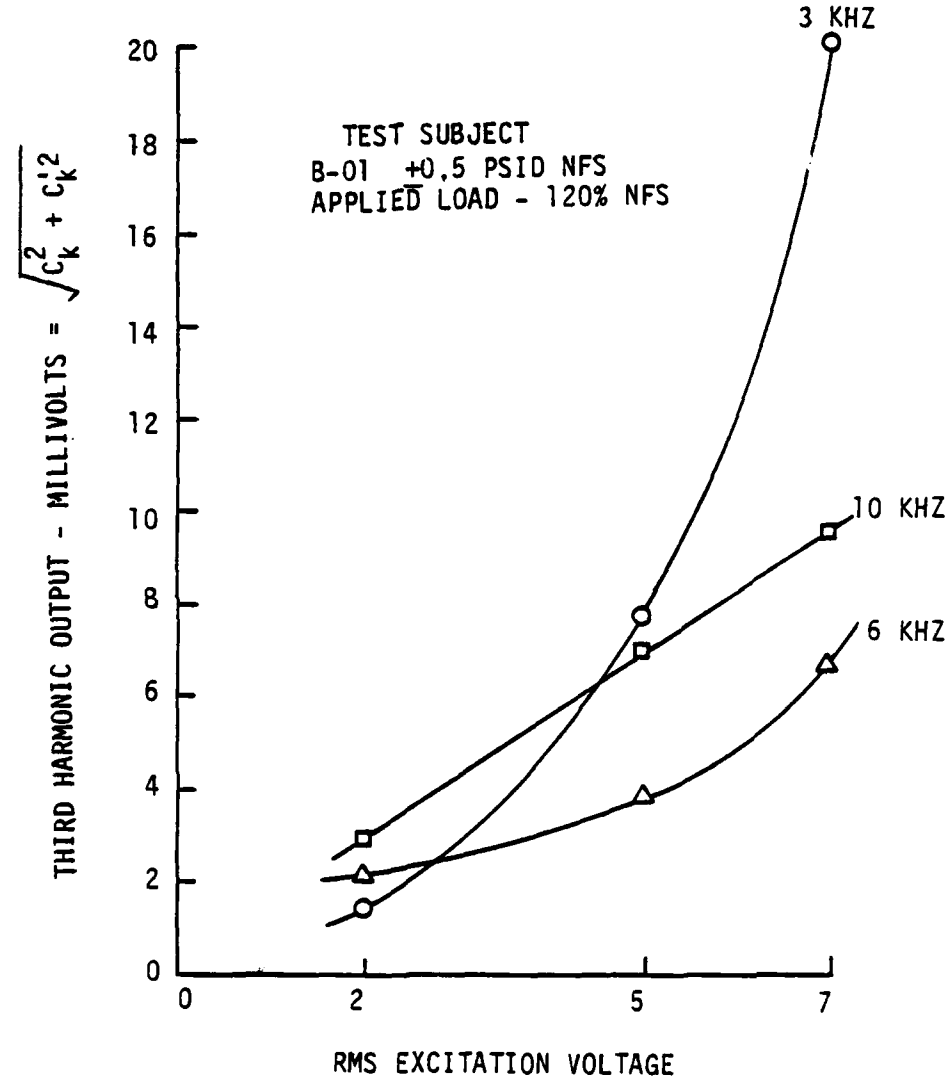

Figure 34. Third Harmonic Output - Transducer B-01

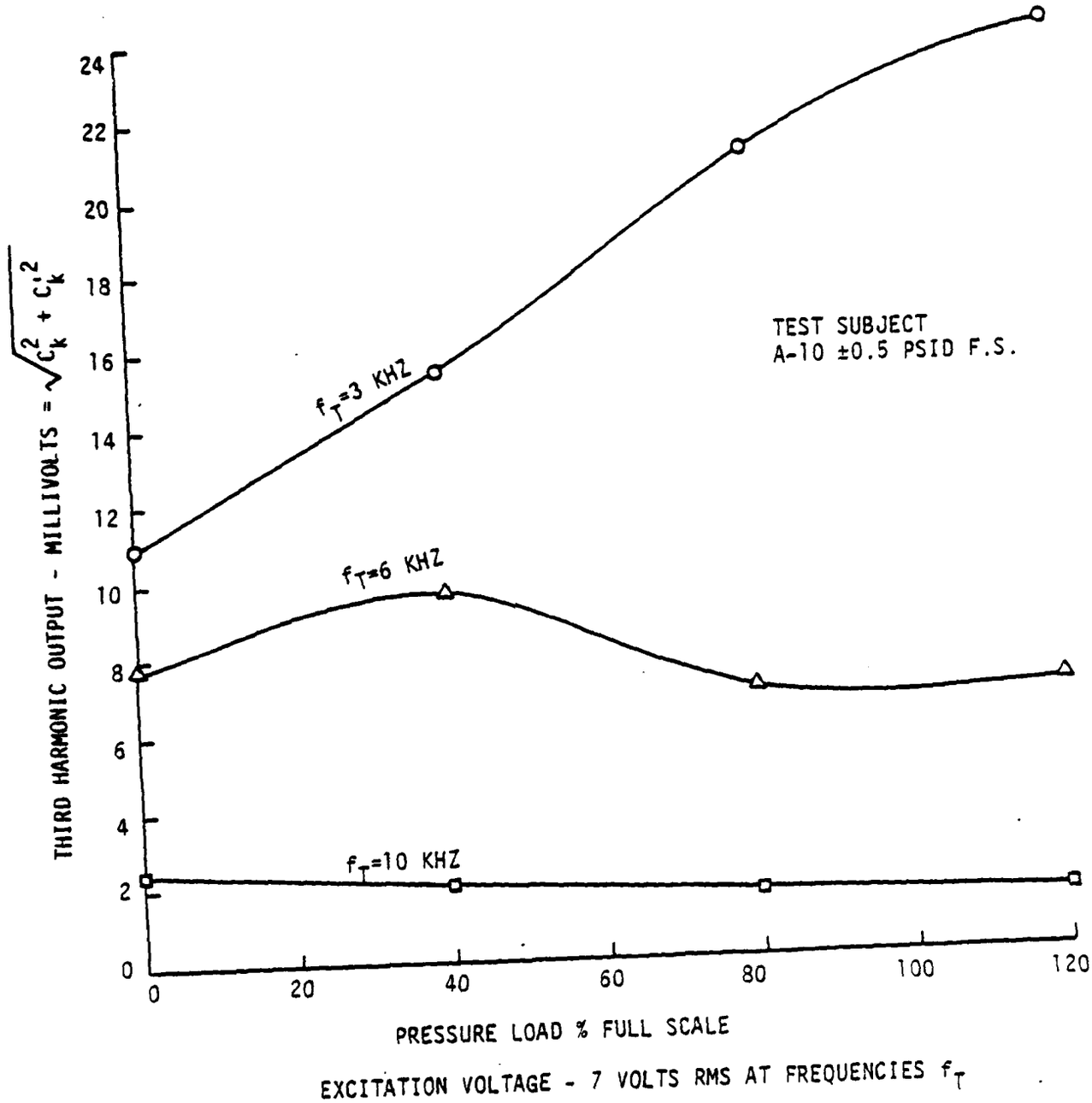

Figure 35. Third Harmonic Output - Transducer A-10

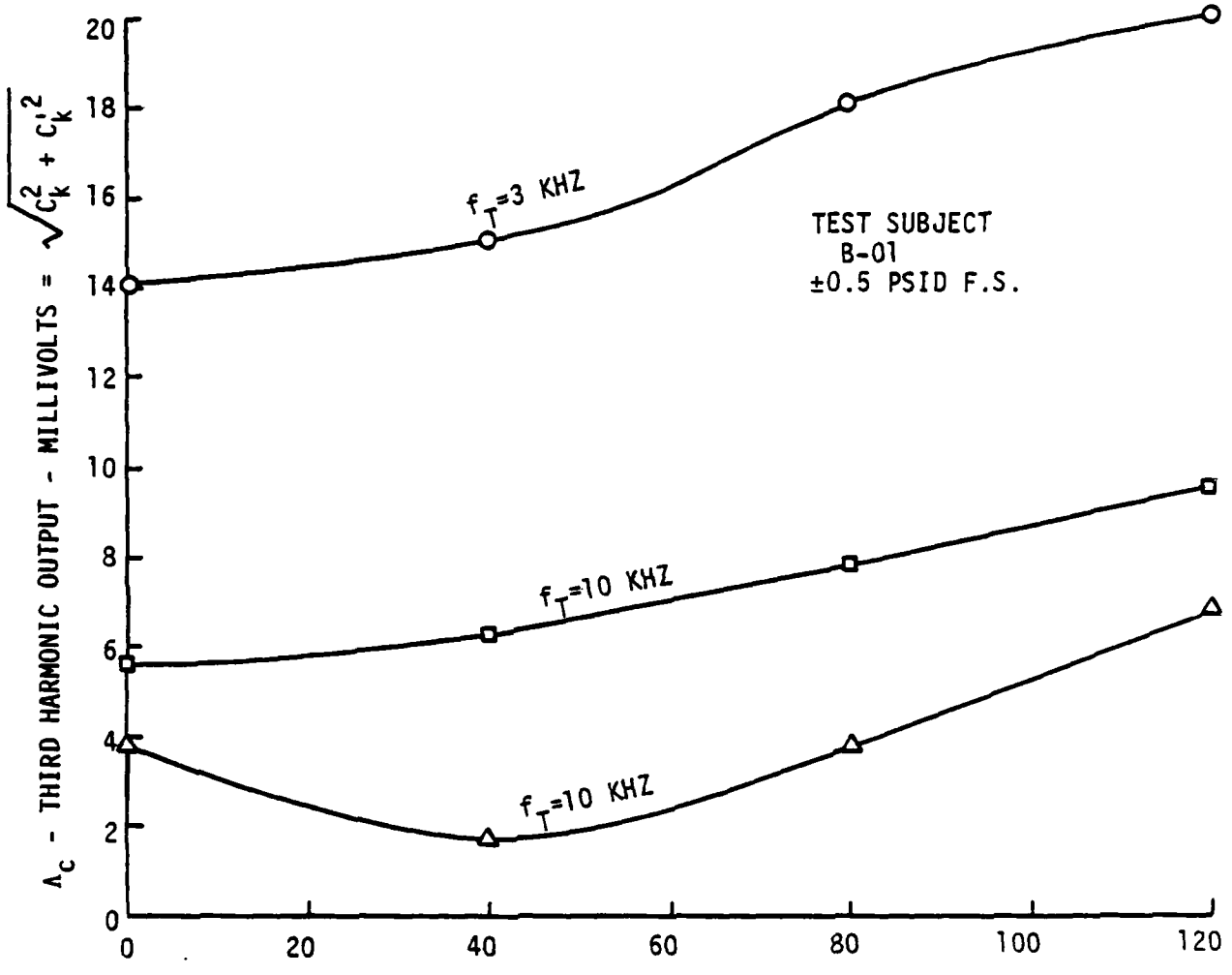

P_k - PRESSURE LOAD % NAMEPLATE FULL SCALE

EXCITATION VOLTAGE - 7 VOLTS RMS AT FREQUENCY f_T

Figure 36. Third Harmonic Output - Transducer B-01

These simple tests showed that a more detailed study of the transducer as a four-terminal electrical "black box" would be necessary before definite conclusions as to the best operating point, if any, could be drawn.

2. ELECTRO-MAGNETIC PERFORMANCE

Subsequent tests of this kind were conducted using the equipment arrangement of Figure 37. A typical set of curves of "secondary" output voltage versus input frequency is presented in Figure 38. Curves for three of the six values of "primary" input voltage are shown. The data in Figure 39 for transducer A-01 resulted from plotting the output-to-input voltage ratio against frequency at six values of input voltage. The data points to the left of the mid-frequency "humps" are of limited quantitative value because the coil is being fed constant voltage while its exact volt-ampere characteristics are uncertain. The shape of these curves in this region approximates the NMC to the degree that the current in the excited coil is frequency dependent. The nature of this relationship is illustrated by means of the low frequency model in Figure 40(a).

The curves such as are shown in Figure 39, therefore, are useful in determining the minimum desirable operating frequency and also the effects of the choice of excitation voltage at that frequency. Operation of the transducer at points to the left of the "hump" will result in high harmonic content in the output. Therefore, an operating point to the right of the peak is desirable. For this reason, standard VR transducers cannot be used as error sensors in AC servos operating at common ground power frequencies, although such use becomes increasingly practical at 400 and 800 Hertz. Difficulties experienced earlier in making inductance measurements were evidently the result of too high a choice of "volts-per-cycle" in the measurement circuit. These curves also show that changes in excitation frequency will cause changes in electrical output over and above those which can be accounted for by analysis of the transducer circuit as a linear network of R, L, and C elements.

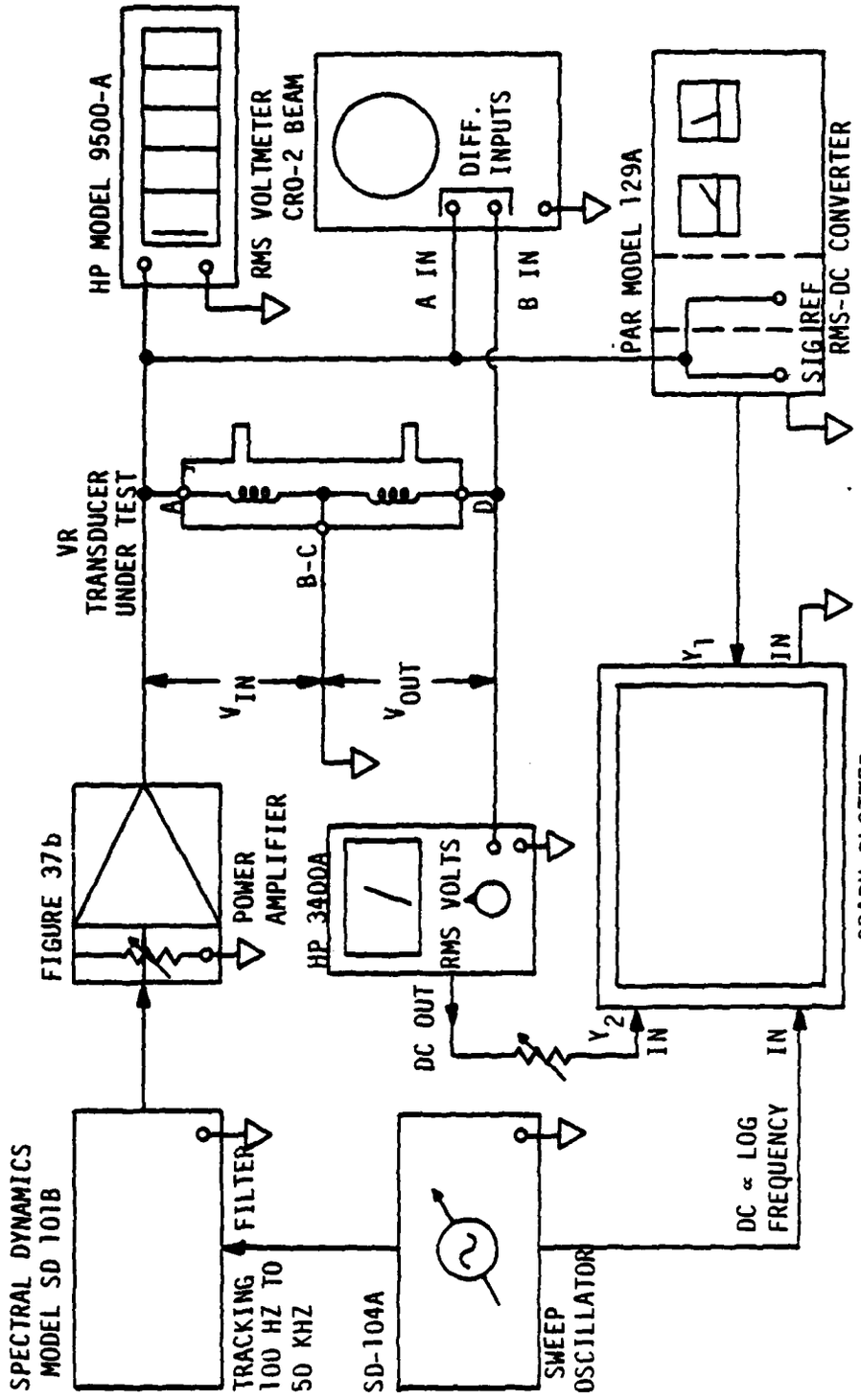

Figure 37a. Test Apparatus - Optimum Operating Point, Variable Reluctance Pressure Transducer

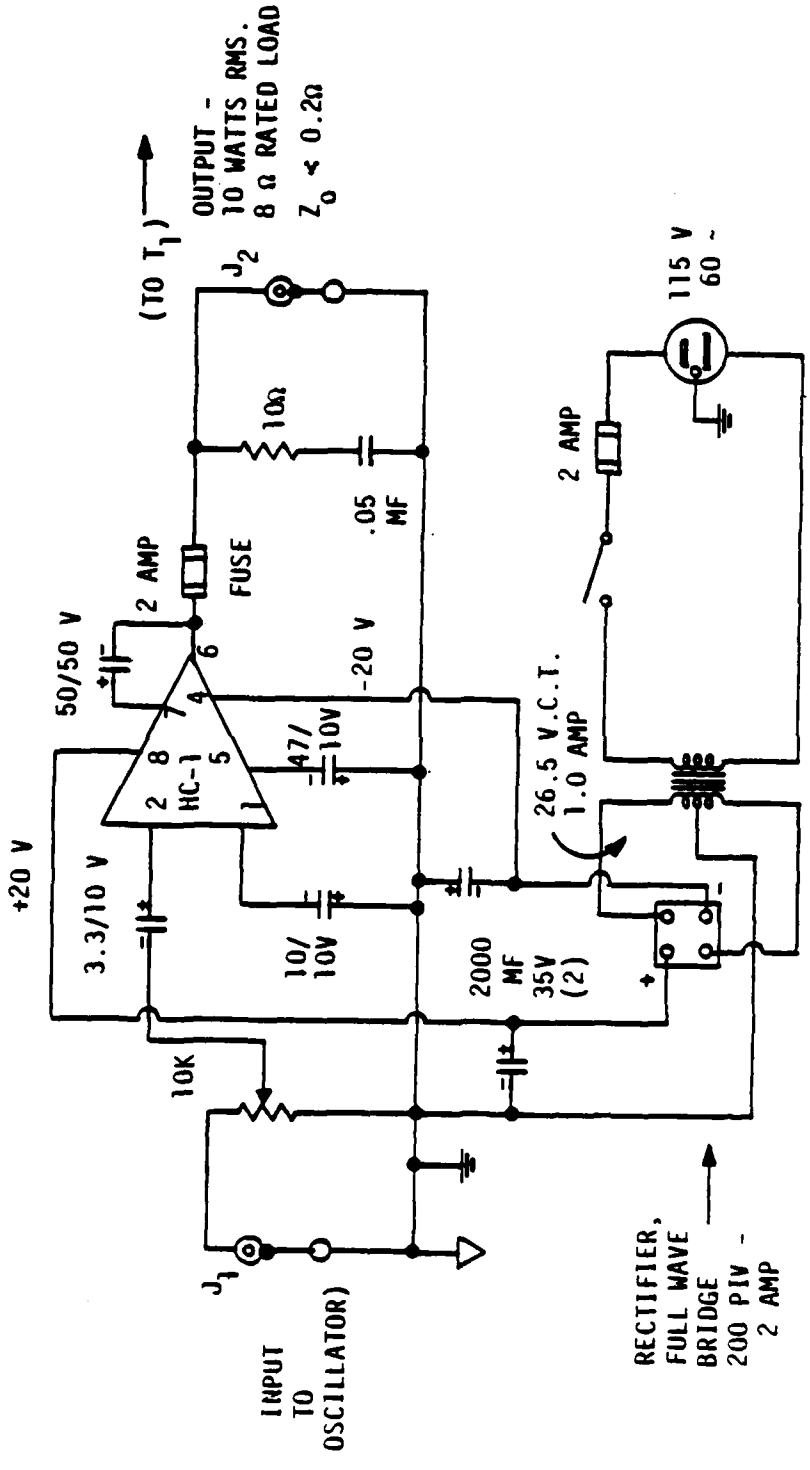

HC-1 = SANKEN HYBRID AUDIO POWER MODULE - SERIES SI-1010G

Figure 37b. Schematic - Power Amplifier, Transducer Excitation

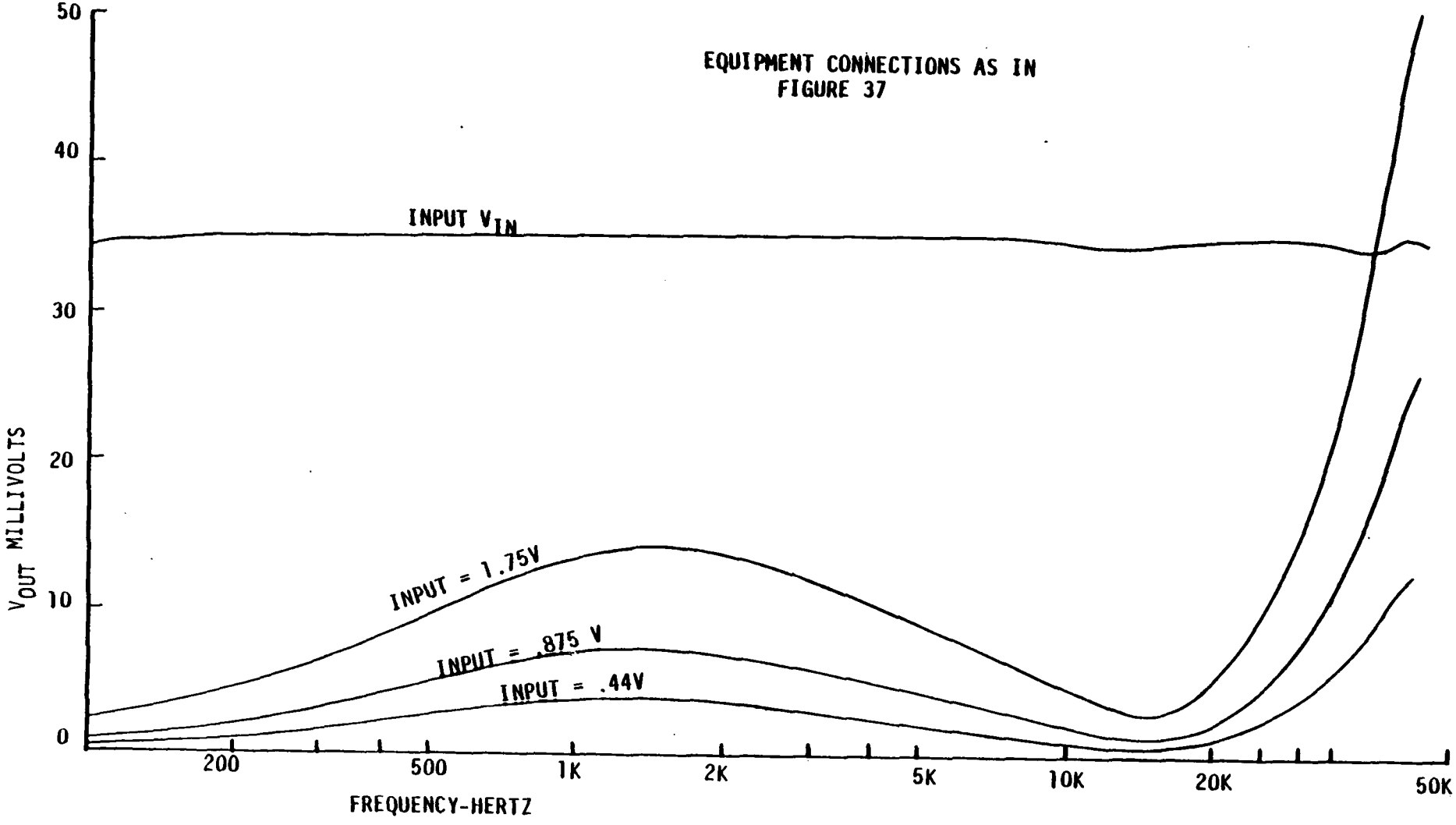

Figure 38. Electro-Magnetic Performance - Transducer D-01 (Typical) - Optimum Operating Point Test

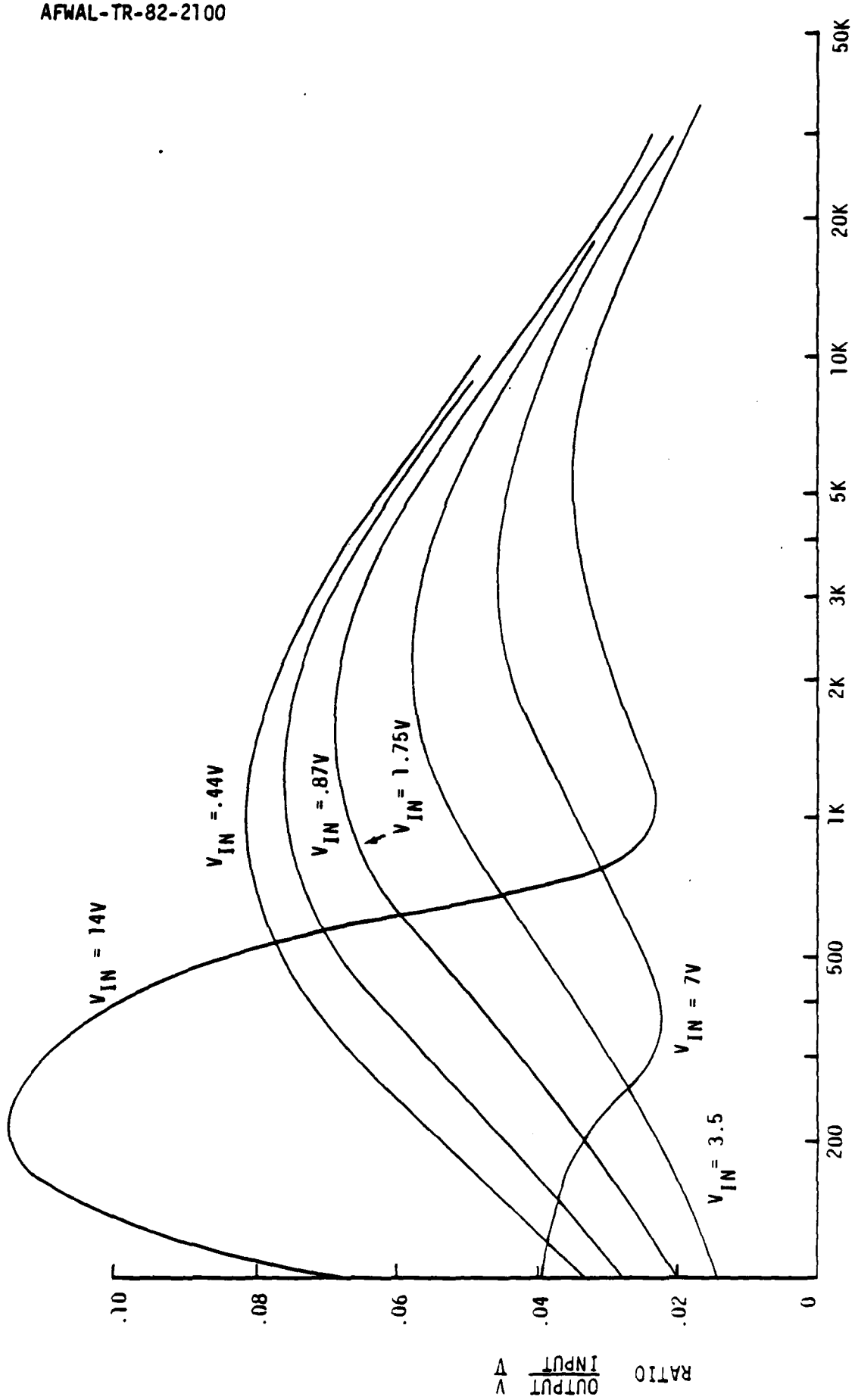

Figure 39. Electro-Magnetic Performance - Transducer A-01

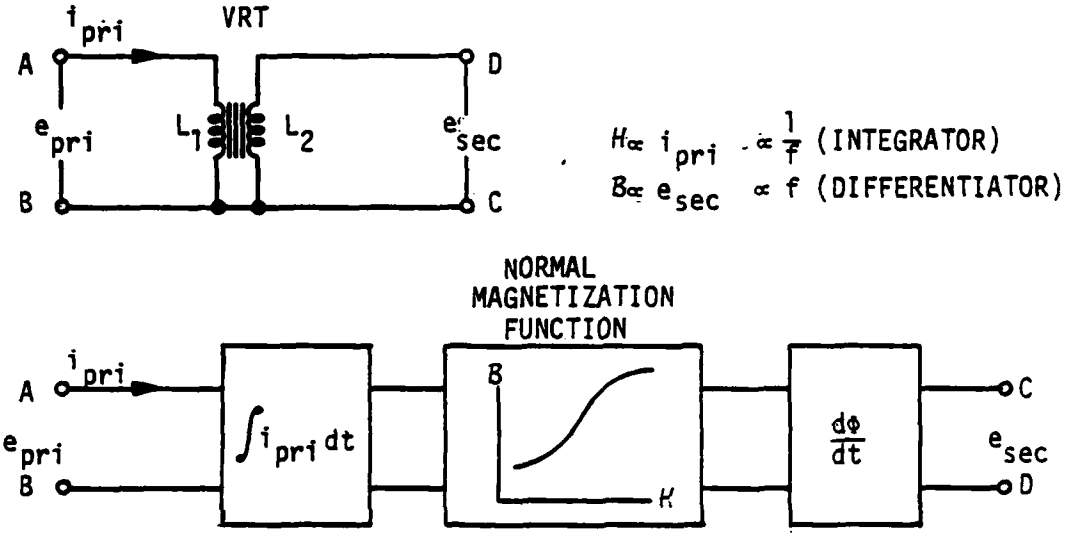

a) LOW FREQENCY MAGNETIZATION MODEL

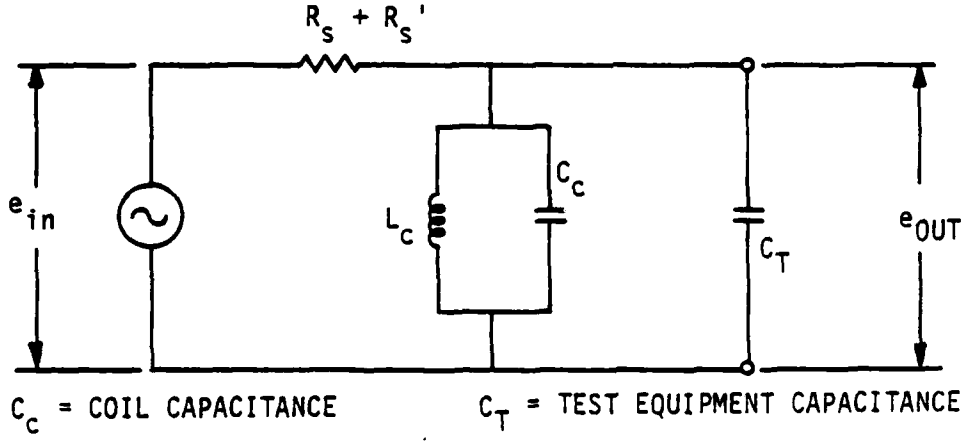

b) VERY HIGH FREQUENCY EDDY CURRENT EQUIVALENT CIRCUIT

Figure 40. Electrical Models of Magnetic Effects - Variable Reluctance Pressure Transducer

The voltage output-input relationships of all transducers at frequencies to the right of the hump are dominated by eddy current phenomena. The drop in output as frequency is increased appears less steep than might be inferred from the frequency-squared eddy current loss relationship. This is because the eddy current resistance network affecting the input-output ratio, shown in Figure 24, has a shunt component, R_p, as well as the series component, R_s. The sharp peak in output at the high frequency end in the curve of Figure 38 is due to the parallel resonance of the total circuit which is shown in simplified form in Figure 40(b). As the frequency is increased, both the shunt and series components of eddy current resistance rise rapidly until, at the frequency of resonance, the circuit becomes an undamped parallel combination of circuit and lead capacitances and the coil inductance, loosely coupled to the signal generator by the very high resistance $(R_s + R'_s)$.

At intermediate frequencies, the exact shape of the curves is due to the geometry of the magnetic circuit, particularly the ratio of length to area of the metal in the flux path. Curves for three types of transducers rated at 0.5 PSID nameplate full scale (NFS) are shown in Figures 41, 42, and 43. The complex interaction of main path flux and that penetrating the center plate is most evident in the curves for transducers 8-01 and C-05 which have relatively thin CPs. They show an output which does not drop nearly as rapidly with frequency as do the units with center plates of "normal" thickness. The eddy current losses in the CP volume bounded by r_e and t in Figure 13 are evidently reduced greatly because the relatively thin CP restricts the size of the current in the loops shown as *I* in Figure 23.

The curves of Figures 44 and 45 are for a very small transducer rated at 5 PSID NFS. All four coil terminals were accessible, making possible either coil connection polarity. The connections used in the test of Figure 44 are those which cause flux subtraction in the CP. The eddy current density in the CP is therefore much less than in the flux addition case of Figure 45. This reduces the eddy current losses and

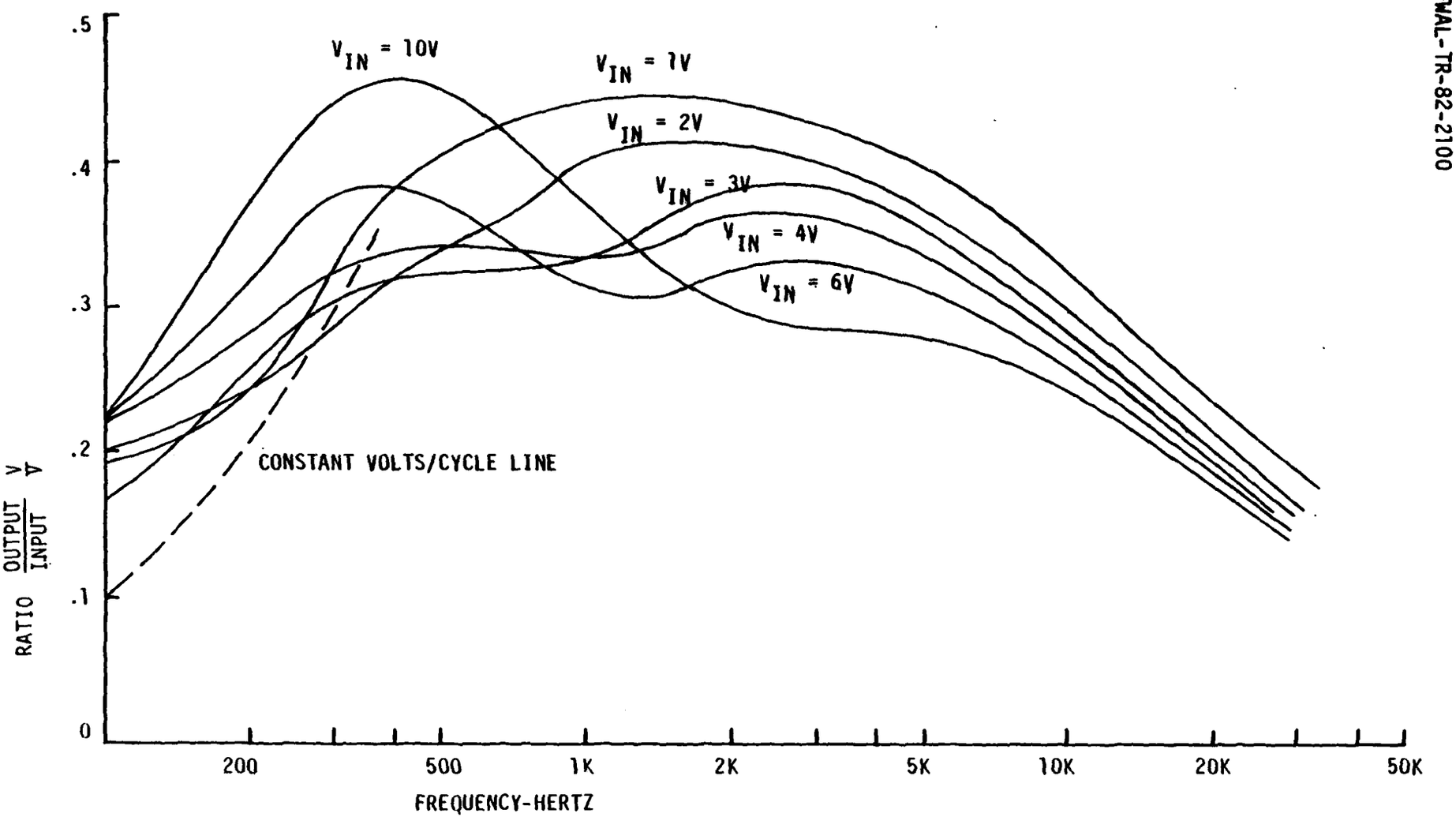

Figure 41. Electro-Magnetic Performance - Transducer A-10

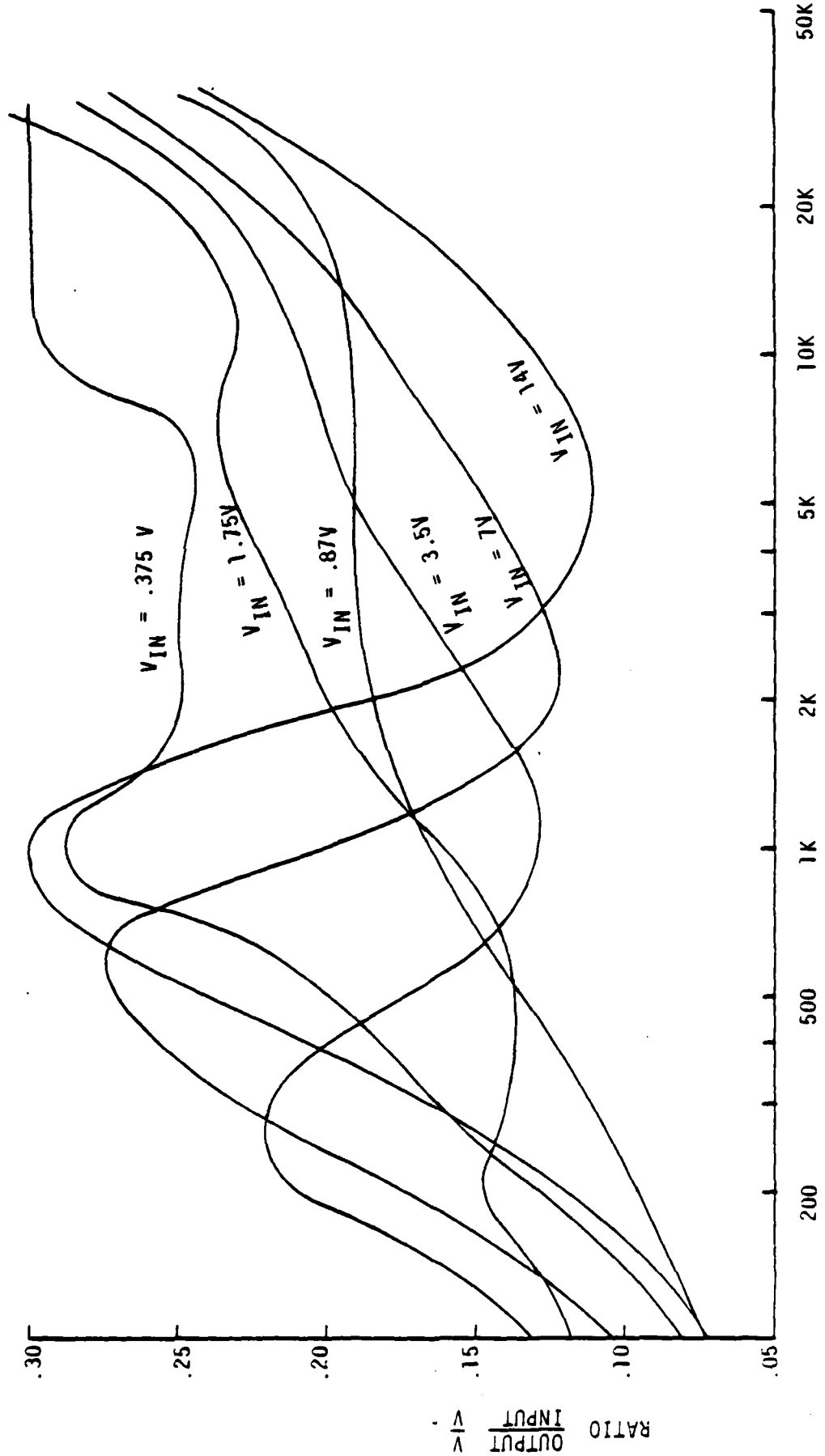

Figure 42. Electro-Magnetic Performance - Transducer B-01

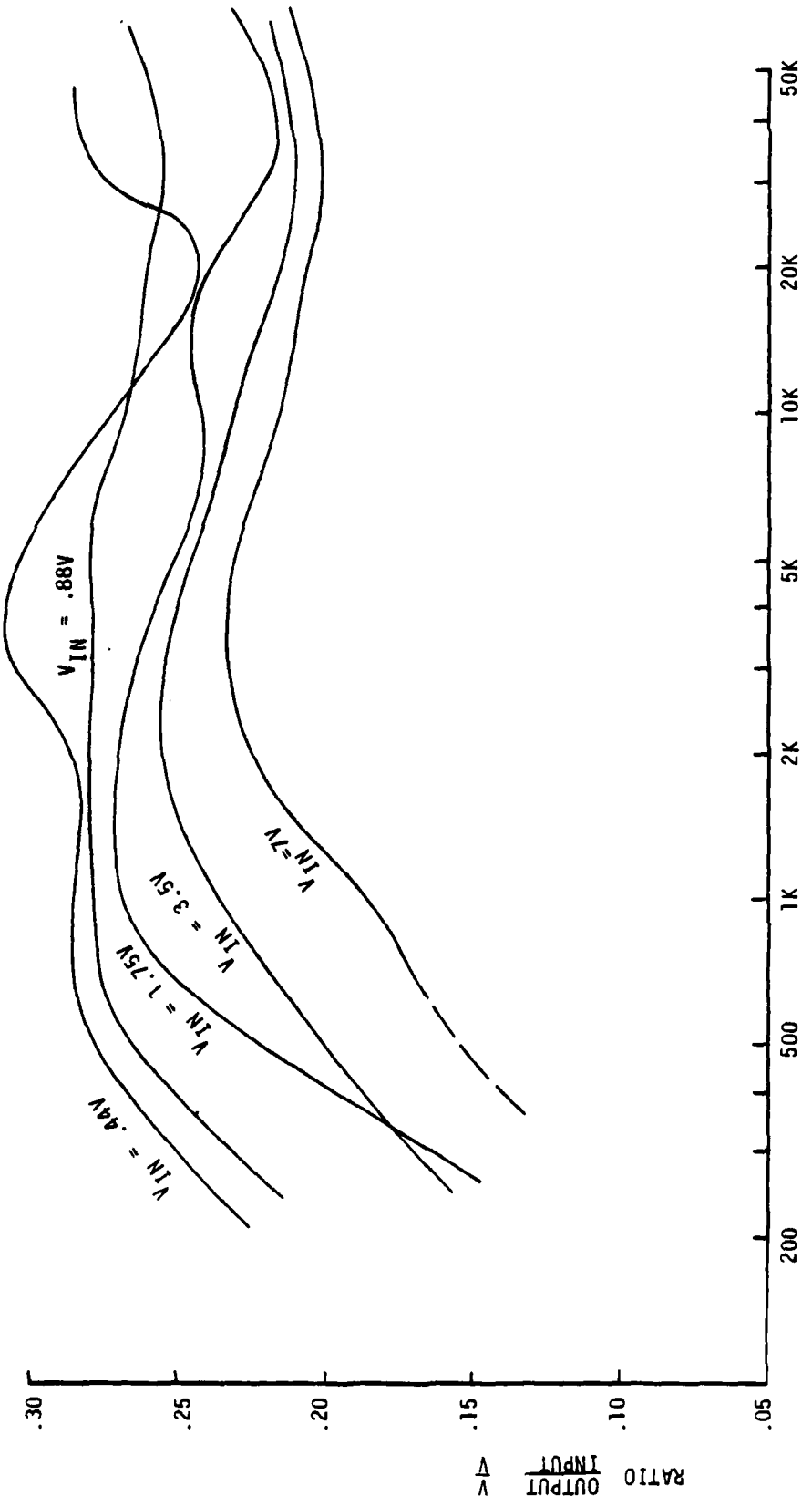

Figure 43. Electro-Magnetic Performance - Transducer C-05

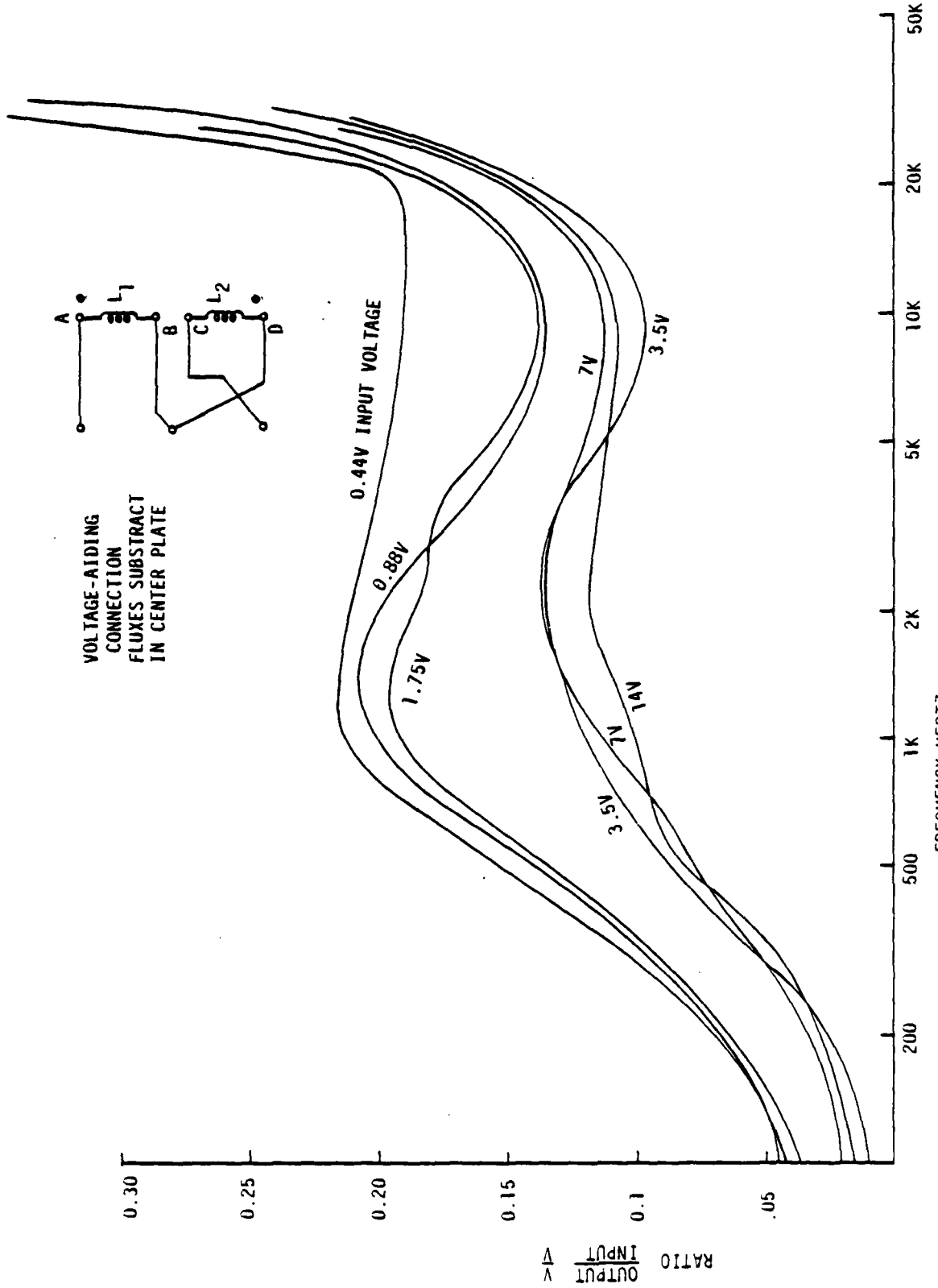

Figure 44. Electro-Magnetic Performance - Transducer D-01, Voltage Aiding Connection

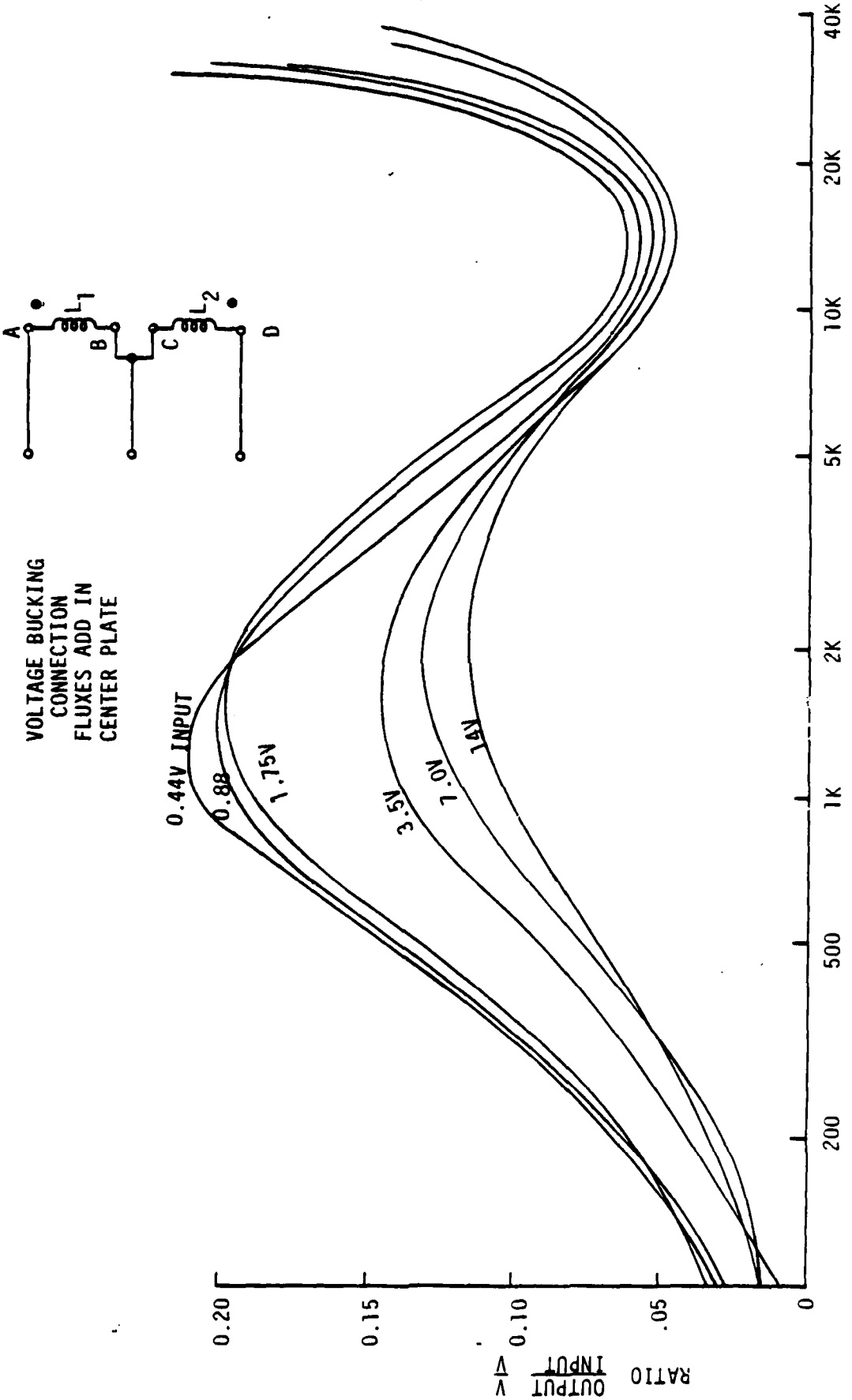

Figure 45. Electro-Magnetic Performance - Transducer D-01, Voltage Bucking Connection

causes the output/input voltage ratio to maintain its relatively high value up to the 10 kilohertz region, particularly at low values of excitation voltage. This result indicates that the most influential contributor to eddy current effects is the center plate, since the flux density in the body material is relatively low in either case.

The importance of controlling eddy current losses derives from the environmental effects upon the individual resistances shown in Figure 24. These problems increase rapidly with frequency. Attempting to maintain output by increasing the excitation voltage will aggravate this condition. The condition often referred to as zero drift is actually a change in output when the zero measurand output of the transducer is not zero. This is a natural condition which is often overlooked when guided by the prevalent concept of an inherently balanced "bridge."

Operating a transducer in the region where the output-input curves are most regular and evenly spaced will minimize the effects upon output of shifts in frequency and voltage in the excitation supply. Using this criterion, operating points chosen for all transducers fell in the 2 to 5 kilohertz region at 1 to 3 volts per coil (not total). These frequency values are close to those used in commonly available equipment. Excitation voltage values selected are somewhat lower than those in common use, since reduction of harmonics seems more desirable than the additional voltage output. These curves indicate that ouput sensitivity is not necessarily linear with excitation voltage, and a calibration at one value should not be used at another voltage by making a simple ratio correction. Curves in Figures 46 and 47 are for large transducers weighing almost two pounds and having center plates of normal thickness. The frequency location of the "humps" in these curves is very little different from that for the 19 gram transducer D-01, shown in Figure 44 and 45. This is consistent with previous evidence that magnetic path cross-section shape (aspect ratio) is the controlling factor in eddy current effects rather than total volume or mass. Figure 48 shows the output-input behavior of transducer F-01, which is not a classical type of transducer. The sensing element is a laminated E-core

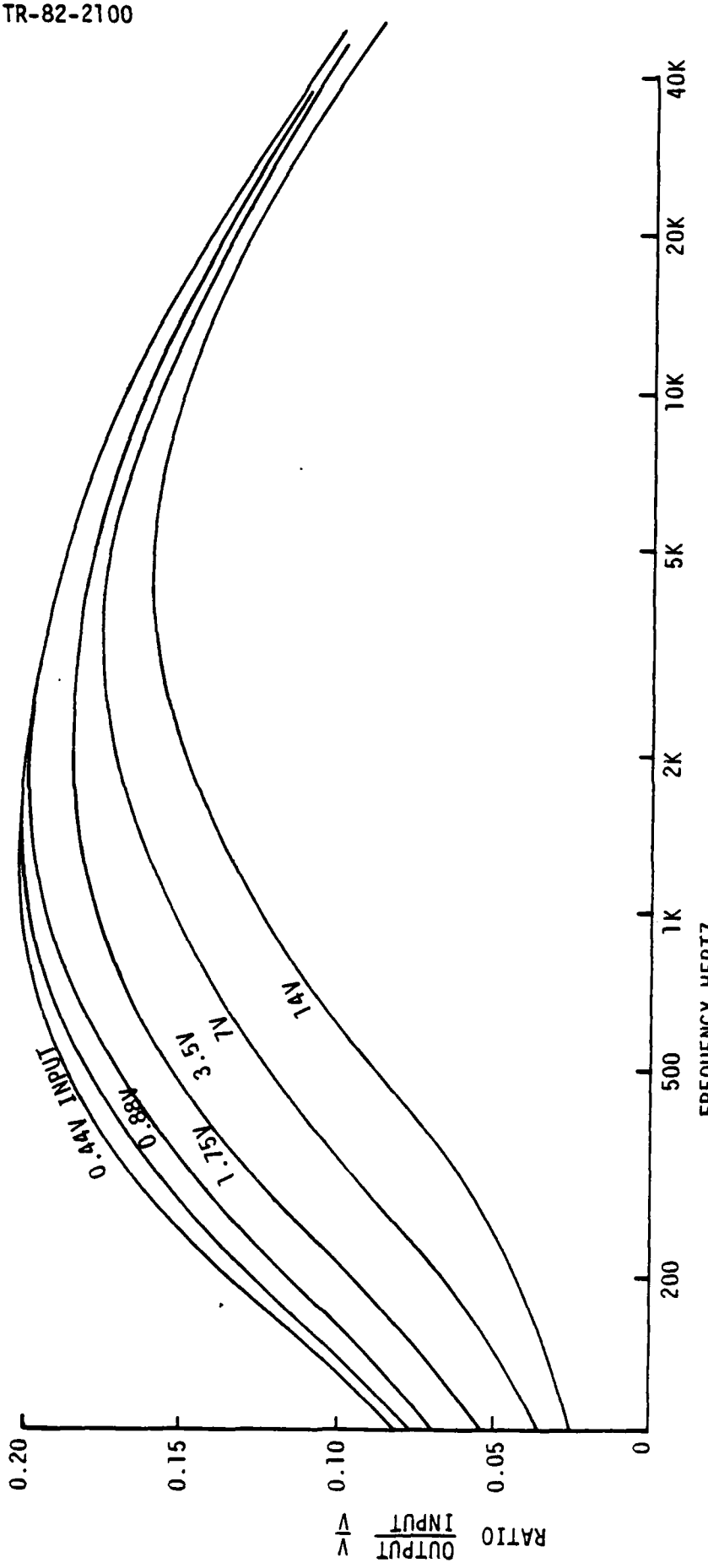

Figure 46. Electro-Magnetic Performance - Transducer C-10

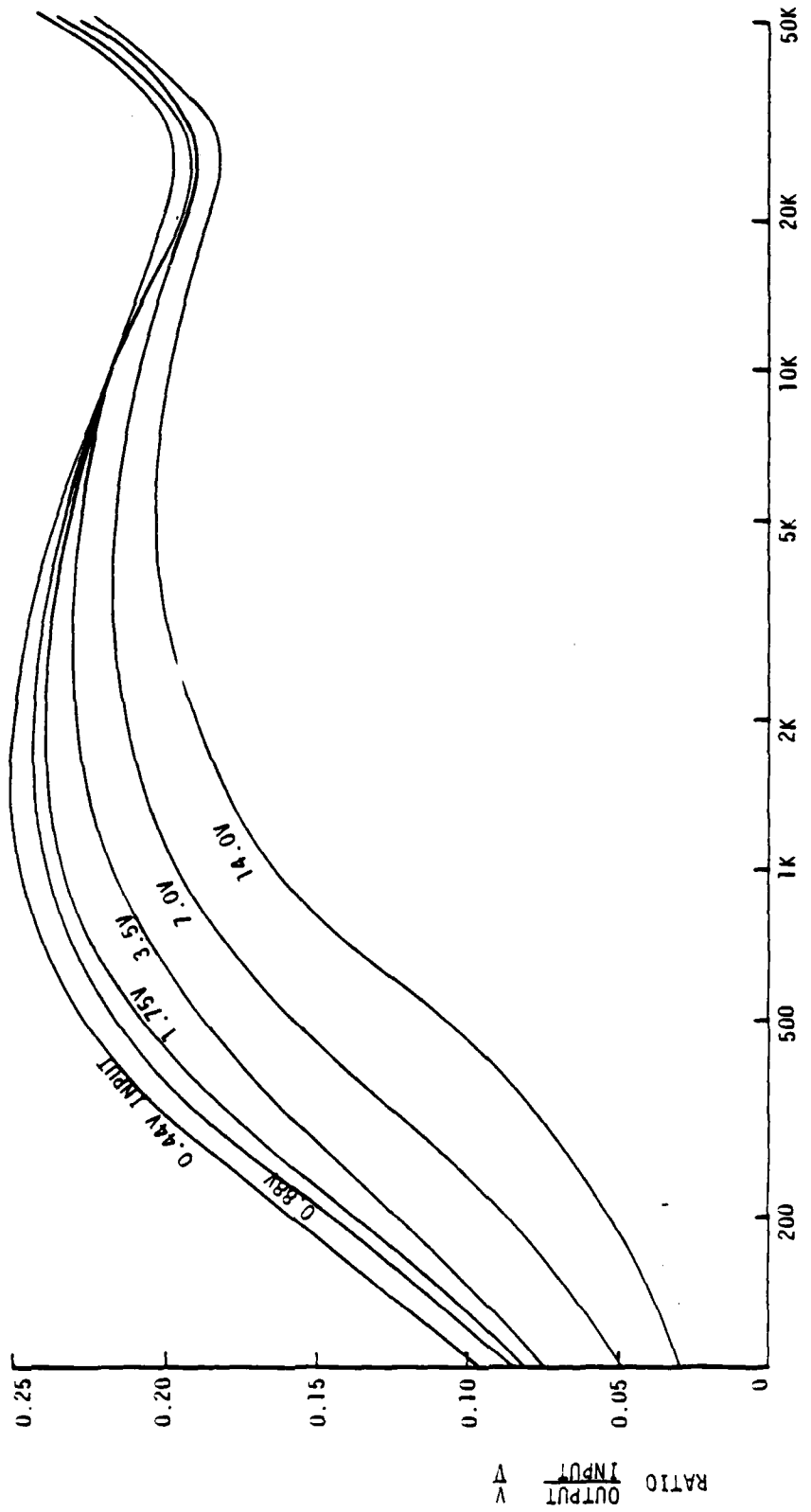

Figure 47. Electro-Magnetic Performance - Transducer E-01

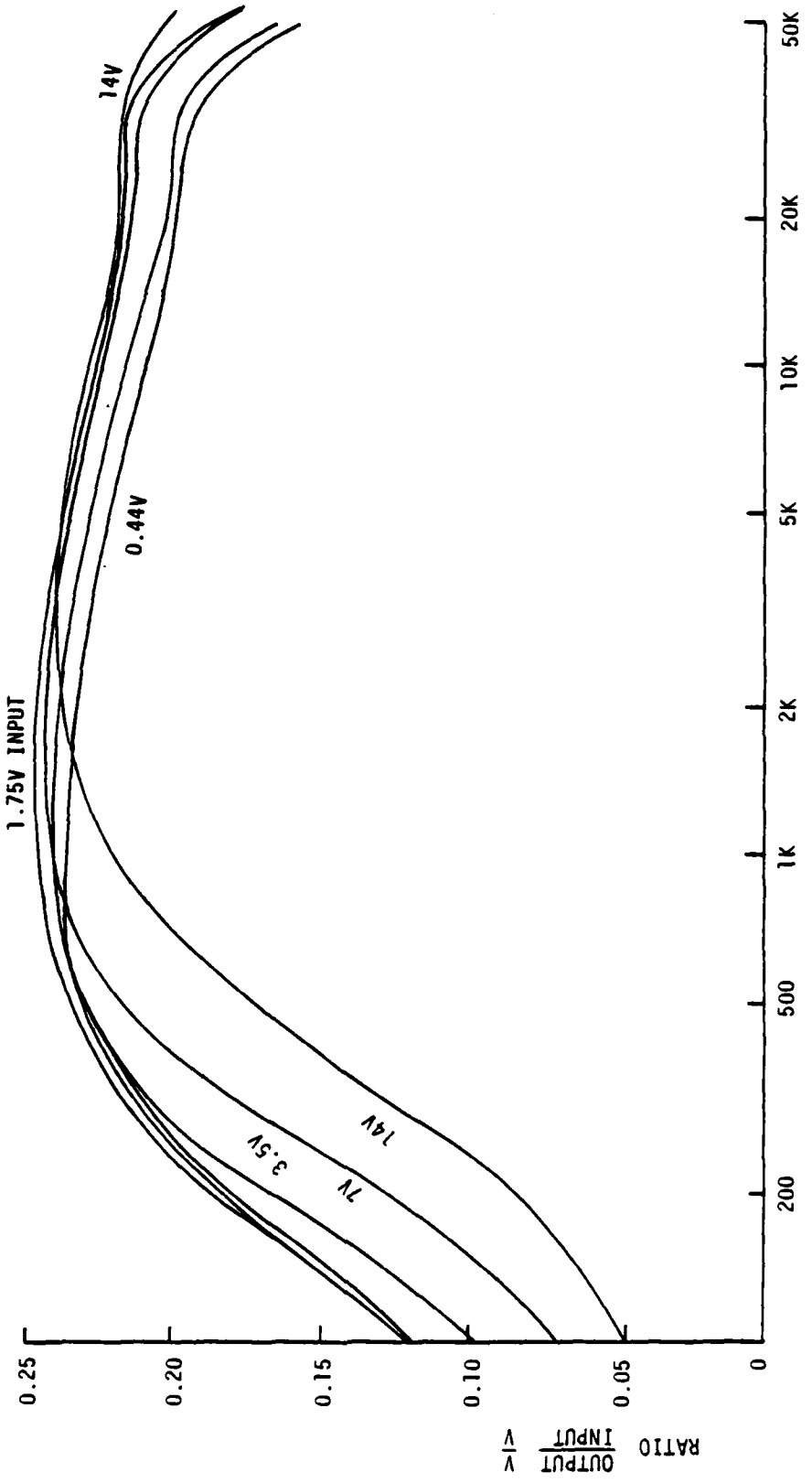

Figure 48. Electro-Magnetic Performance - Transducer F-01

such as is described in References 5 and 6. As a result, its electrical performance is much like that of an audio transformer of comparable size.

3. COIL IMPEDANCE MEASUREMENTS

The electrical impedance of the coils of the VR transducer affects its performance when connected to a signal conditioner. The following factors must be considered:

- The volt-ampere load imposed on the excitation power supply
- The signal source impedance represented by the transducer and the input network
- The relative magnitude of the various resistive components; namely, eddy current, skin effect, DC coil resistance and hysteresis loss
- The relative magnitude of reactive and resistive components of impedance and their effect on the magnitude and phase angle of the electrical output signal

Single-coil values of test voltage, V_T, and frequency, ω_T, for making impedance measurements were chosen based on the results of previous tests. In some cases, measurements at higher frequencies or voltages were made for comparison. In all cases, operation at values likely to result in high harmonic output were avoided. The equipment arrangement and method of calculation are shown in Figures 49 and 50, respectively. The resulting impedance data are summarized in Table 6. Coil connection "polarity" was determined by measuring the impedance of one coil alone, Z_c, and then the series combination, Z_T. The result is presented in the form of calculated mutual inductance, M. For a given value of applied excitation voltage, the transducer will present a lower impedance if the coils are connected in opposing polarity, or negative mutual inductance. A larger value of flux will exist in the CP, avoiding operation of the magnetic material in the extremely nonlinear portion of the B-H curve about the origin. This connection was used

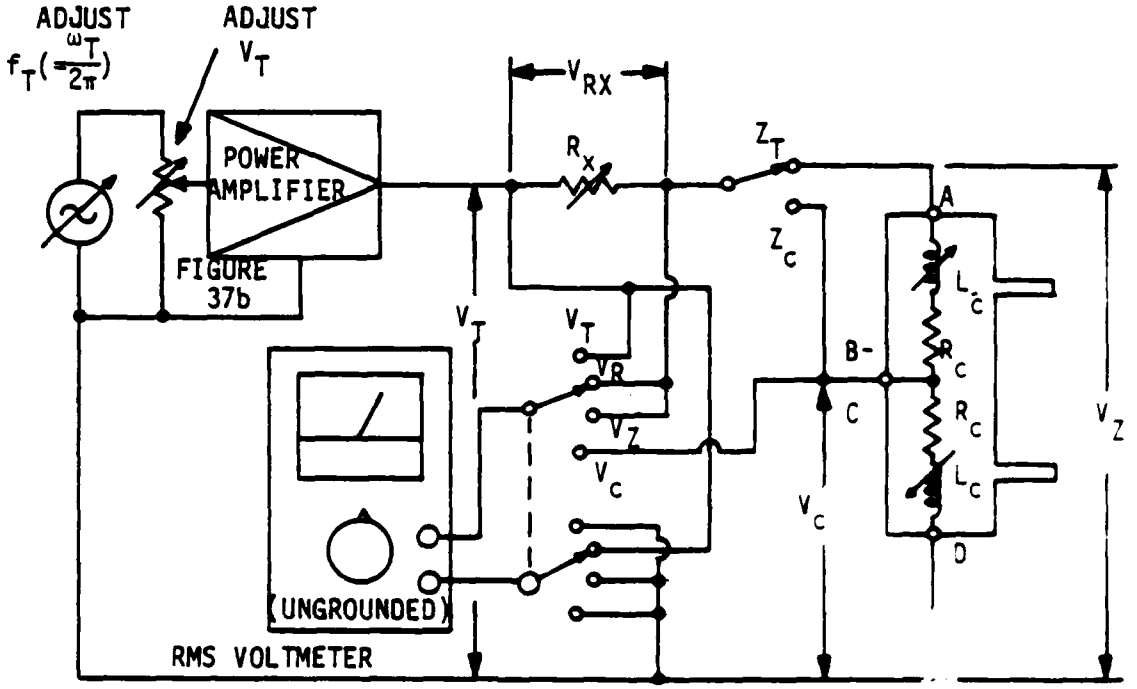

Figure 49. Voltage Vector Measurements for Impedance Calculations - Variable Reluctance Pressure Transducer

A. TOTAL IMPEDANCE (Z_T) MEASUREMENT

1. Set test frequency (f_T) as specified, f_T = _____ Hertz.
2. With switch in Z_T position, adjust R_x and V_T to give the following conditions simultaneously:

   a) V_C to be specified value = _____ RMS Volts.
   b) $V_{RX} = V_Z$.

3. Record: R_x = _____Ω; V_T = _____; $V_Z = V_R$ = _____(Volts)

B. SINGLE COIL IMPEDANCE (Z_C) MEASUREMENT

1. With switch in Z_C position, adjust R_x and V_T to give the following conditions simultaneously:

   a) V_C to be specified value as before.
   b) $V_{RX} = V_C$.

2. Record: R_x = _____Ω; V_T = _____; $V_R = V_C$ = _____(Volts).

C. CALCULATE VOLTAGE AND IMPEDANCE VECTORS AND MUTUAL INDUCTANCE, M, PER FIGURE 50.

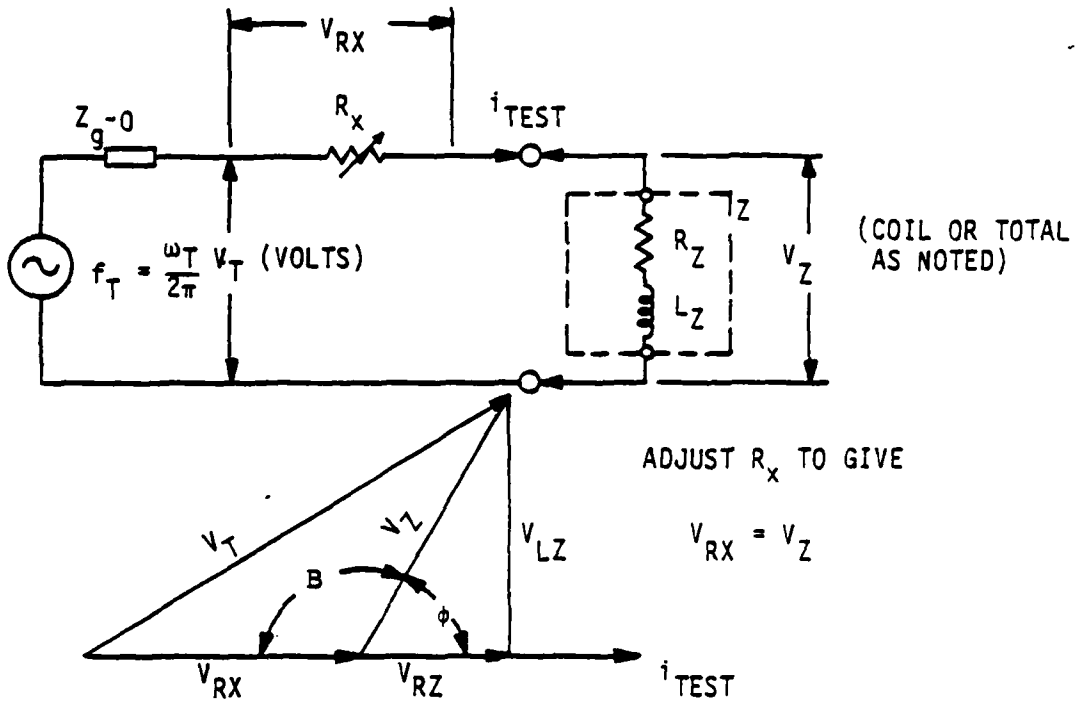

Figure 50. Calculation Method - Electrical Impedance Measurement - Variable Reluctance Pressure Transducer

$$\cos B = \cos (180-\phi) = \frac{V_{RX}^2 + V_Z^2 - V_T^2}{2 \cdot V_{RX} \cdot V_Z}$$

$$Z = R_x(\cos\phi + j\sin\phi) = R_Z + j\omega_T L_Z \text{ (OHMS)}$$

$$i_{TEST} = \frac{V_T}{[(R_x+R_Z)^2 + L_Z^2]^{1/2}} \times 10^3 \text{ (MILLIAMPERES)}$$

$$\text{COIL "Q"} = \frac{\omega_T L_Z}{R_Z} = \tan\phi$$

$$\text{MUTUAL INDUCTANCE } M = \frac{1}{2} [L_{TOTAL} - (L_1+L_2)] = \frac{1}{2} [L_{TOTAL} - 2L_c] \text{ (MILLIHENRIES)}$$

TABLE 6

IMPEDANCE MEASUREMENT DATA SUMMARY
VARIABLE RELUCTANCE PRESSURE TRANSDUCERS
MEASUREMENTS PER FIGURES 49 AND 50

f_{TEST} kHERTZ	Z/ϕ OHMS/DEGREES	$R_Z + j\omega L_Z$ OHMS	L MH.	Q	M MH.	R_{DC} PER COIL Ω
	Transducer A-01 V_C (TEST) = 1 Volt RMS					
2	$Z_T = 556/60.7$	272.1 + j484.9	38.6	1.78	-0.5	42
2	$Z_C = 297/56.7$	163.1 + j248.2	19.8	1.52		
6	$Z_T = 1257/54.7$	726.4 + j1026	27.2	1.41	+1.0	
6	$Z_C = 652/44.7$	463.4 + j458.6	12.6	0.98		
	Transducer A-10 V_C(TEST) = 2 Volts RMS					
2	$Z_T = 392/53.8$	231.2 + j316.5	25.2	1.4	-6.1	43
2	$Z_C = 282/56.5$	155.6 + j235.2	18.7	1.5		
6	$Z_T = 839/66.2$	338.8 + j767.5	20.4	2.26	+1.2	
6	$Z_C = 549/51.7$	340.4 + j338	9.0	1.26		
	Transducer B-01 V_C(TEST) = 0.5 Volt RMS					
3	$Z_T = 670/74.8$	175.7 + j646.6	34.3	3.7	-3.95	31
3	$Z_C = 420/71.8$	131.2 + j399.0	21.1	3.0		
9	$Z_T = 1780/74.8$	466.7 + j1717.7	30.3	3.7		
9	$Z_C = 1130/71.8$	352.9 + j1073.5	19.0	3.0	-3.85	
	Transducer C-05 V_C (TEST) = 2 Volts RMS					
3	$Z_T = 714/79.5$	130 + j702	37.2	5.4		33
3	$Z_C = 469/76.1$	112.6 + j455.3	24.2	4.0	-5.6	
9	$Z_T = 1950/83.9$	207.3 + j1939	34.3	9.36		
9	$Z_C = 1223/76.1$	302.7 + j1223	21.6	4.0	-4.5	
	Transducer C-10* V_C(TEST) = 1 Volt RMS					
2	$Z_T = 209/76.7$	48.1 +j203.4	16.2	4.23		16.7
2	$Z_C = 130/69.8$	44.9 +j114.5	9.1	2.72	-1.0	
6	$Z_T = 602/79.4$	110.7 + j591.7	15.7	5.34		
6	$Z_C = 365/69.8$	126.0 + j342.5	6.1	2.72	+1.75	

TABLE 6 (Concluded)

IMPEDANCE MEASUREMENT DATA SUMMARY
VARIABLE RELUCTANCE PRESSURE TRANSDUCERS
MEASUREMENTS PER FIGURES 49 AND 50

f_{TEST} kHERTZ	Z/ϕ OHM/DEGREES	$R_Z + j\omega L_Z$ OHM	L MH.	Q -	M MH.	R_{DC} PER COIL Ω
	Transducer D-01 V_c(TEST) = 1 Volt RMS					
2	Z_T = 1400/34.5	1154 + j793	63.1	0.7	-	465
	Transducer E-01* V_c(TEST) = 1 Volt RMS					
3	Z_T = 660/78.2	135.0 + j646.1	34.3	4.79	-4.35	
3	Z_c = 424/72.8	125.4 + j405.0	21.5	3.23		
9	Z_T = 1870/82.2	254 + j1853	32.8	7.3	-3.3	39.2
9	Z_c = 1150/74.8	301 + j1110	19.6	3.7		
	Transducer F-01 V_c(TEST) = 3.2 Volts RMS					
3	Z_T = 580/82.5	75.7 + j575	30.5	7.6	-4.83	24
3	Z_c = 382/80.9	60.7 + j377.2	20.1	6.2		

*Factory Installed Thermal Resistors Removed.

consistently by manufacturers in the assembly of transducers supplied with only three customer connection terminals. The reversal of sign of M with a change of frequency in some cases is a result of using constant voltage excitation, rather than constant ampere-turns input.

The very high resistive component of impedance in transducer D-01 is due mainly to the high AC resistance of the coil windings. Reactance changes causing useful output in this transducer are relatively small and are almost swamped by coil resistance and leakage reactance losses. This behavior illustrates the unavoidable trade-offs in electrical and magnetic performance and limitations encountered due to losses in attempting to maximize inductance for a given body design. No pressure calibrations were performed on this transducer for this reason.

Transducers C-10 and E-01 were constructed with temperature-dependent resistor networks embedded in the transducer body and electrically connected to the coils. These networks were designed to compensate for effects of temperature on the various resistive components of transducer impedance.[1] They were disconnected for all tests. Effects of temperature on complex impedance were evaluated by heating the transducers to 60 degrees Celsius. These data, along with normal room temperature values, are given in Table 7. The single parameter most indicative of change of sensitivity is the reactance angle found in the Z_T columns.

The impedance of the transducer as an electrical load on the excitation power source in the circuit of Figure 31 is that appearing across terminals E and G. It is equal to Z_T as measured. The output impedance of the transducer is obtained from the Thevenin equivalent circuit shown in Figure 51. Since the leakage inductance, Z_ℓ, of each

1. The resulting circuit configuration causes the input impedance of the signal conditioner to become part of the compensation network. Therefore, this method provides optimum results only when the transducer and readout equipment are matched.

TABLE 7

TEMPERATURE EFFECTS ON IMPEDANCE—
VARIABLE RELUCTANCE PRESSURE TRANSDUCER

TRANSDUCER IDENTITY	T_A = 27 Degrees C.		T_A = 60 Degrees C.	
	Z_T Ohms / Degrees	R_{DC} Ohms	Z_T Ohms / Degrees	R_{DC} Ohms
A-01	556 / 60.7	83.5	569 / 60.0	92.6
A-10	392 / 53.8	85.6	403 / 53	92.6
B-01	670 / 75	61.8	682 / 74	68.0
C-10*	209 / 76.7*	33.3	210 / 76.7*	36.5
D-01	1400 / 34.5	930	1510 / 31.7	1040
E-01	660 / 78.2	78.4	667 / 78.0	87.9
F-01	575 / 82.5	46.9	568 / 81.6	52.6

* C-10 Specifically designed for high temperature use.

All measurements at coil frequency and voltage given in Table 6.

half of the supply transformer T_1 is made low by design, the circuit output impedance across terminals M-N will be $\frac{Z_T}{4}$.

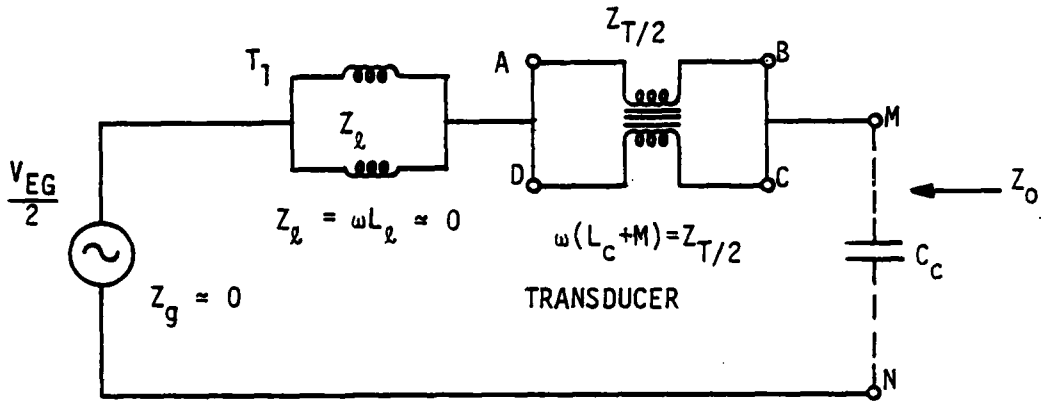

Figure 51. Output Impedance Equivalent Circuit

Since the effects of circuit and cable capacitances between point N and either E or G are equal, they can be evaluated by considering point N as the voltage node or "ground" point. This is true whether or not leads A-E and D-G are enclosed by the shield containing lead (B-C)-M. Cable capacitance can then be represented as a single capacitor, C_c, across points M and N. Where cable lengths are appreciable, fundamental and low order harmonic amplitude and phase will be affected. Parallel resonance may also occur at or near a frequency of a high order harmonic, even with short leads. Transducer impedance values from actual measurements at the frequency of interest must be used in evaluating these effects, rather than by calculation using a single frequency test value. Excitation voltage drops caused by series cable reactance may be kept low by using parallel or twisted pair conductors for leads A-E and D-G.

The low Q of these transducers makes them unsuitable for use as the pressure-dependent inductor in a pressure-to-frequency transduction device.

4. TRANSDUCER CIRCUIT OUTPUT MEASUREMENTS

Definitive measurements of the output, v_k, of the transducer and input network in response to steady state applied pressure, P_k, were made using the test apparatus shown in Figure 52. A uniform phase reference for the fundamental and all harmonics up to the seventh is provided by deriving the six harmonic reference frequencies and the excitation signal from the same oscillator. The frequency divider output waveform at the fundamental or excitation frequency is shaped by means of a narrow band-pass filter, and is applied as a reasonably pure sine wave to the input of the power amplifier supplying the transducer excitation. The filter sections were tuned to maintain a fundamental frequency phase shift of less than ± 0.2 degrees as read on the phase meter. The transducer input circuit Configuration II of Figure 31 was used for all tests. Although this excitation circuit undoubtedly generates a small amount of harmonics, these will contribute pressure-related (useful) components to the output, whereas transducer-generated harmonics may vary nonsystematically with pressure input. The effect of each may be readily evaluated by inspection of the data.

In-phase components (X) and quadrature components (X') of the fundamental (A+jA') and harmonics up to and including the seventh (G+jG') were measured with the Princeton Applied Research Model 129-A Two Phase/Vector Lock-In Voltmeter. (Reference 31.) Harmonic voltages were measured with most or all of the fundmental "nulled out" to avoid overloading the input circuit of the voltmeter. This was done by means of the circuit and controls marked α_N and θ_N in Figure 53. For practical reasons, raw data were taken in vector form, $A_x \angle \psi_x^{\circ}$ where A_x is the general phasor having a length $[X^2+(X')^2]^{1/2}$ and ψ_x is the phase angle, given by $\tan \frac{-1\ X'}{X}$. They were converted to two-phase form to simplify the evaluation of calibration curve shapes. Measurements were made at the test values of frequency, ω_T, and voltage, V_T, determined to be optimum in the foregoing tests and also at higher voltage values more typical of common practice. All data were taken with the CP in the vertical plane and the pressure load cycles were carried to 120 percent of NFS.

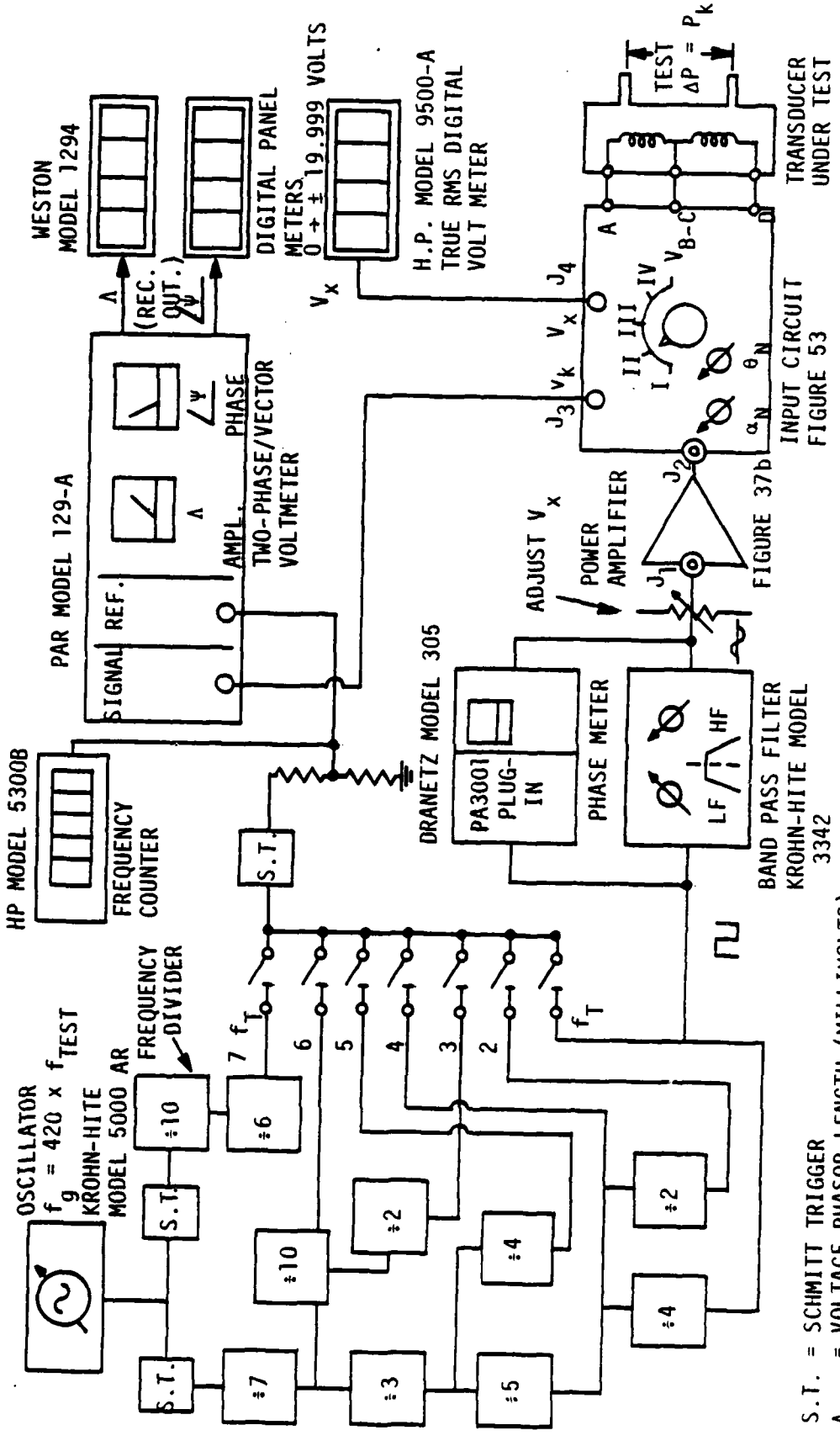

S.T. = SCHMITT TRIGGER
Λ = VOLTAGE PHASOR LENGTH (MILLIVOLTS)
Ψ = PHASE ANGLE (DEGREES)

Figure 52. Bench Test Apparatus - Phase-Coherent Transducer Output Measurement

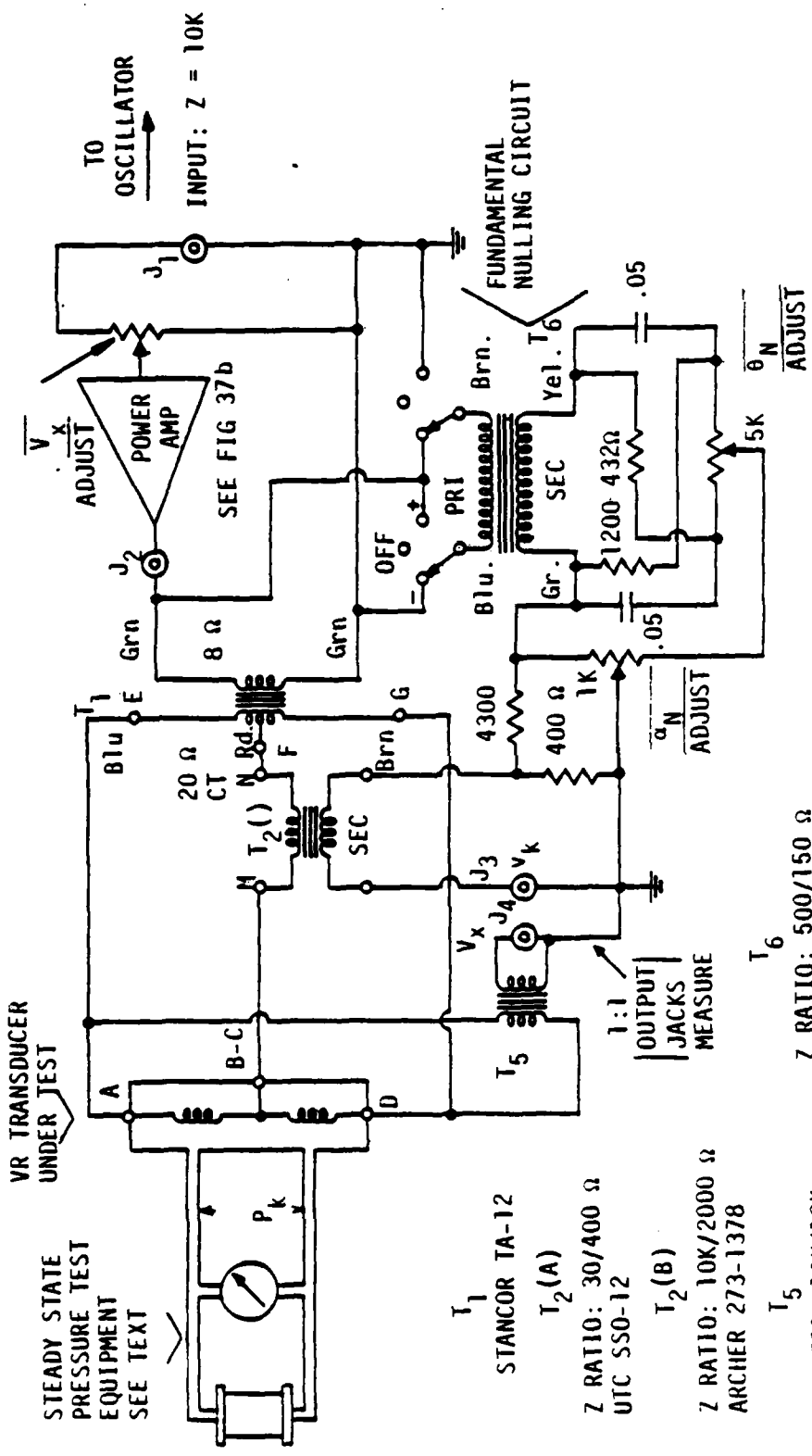

Figure 53. Input Circuit-Transducer Test - Configuration II

5. PRESSURE CALIBRATION EQUIPMENT

Conventional pneumatic and hydraulic techniques were used in this work. Such procedures are described in Reference 32.

The test pressures for transducers rated at 5 PSID NFS or higher were supplied from a fluid-filled tubulation system and generated by a piston type dead weight tester. The lower range transducers were pressurized pneumatically by means of a manostat, Penwalt Wallace and Tiernan Model FA149201. Pressures, P_k, were measured with a Penwalt Wallace and Tiernan precision gage, Model FA145, having a full scale range of zero to 4.5 PSID and a calibrated scale length of about 40 inches. Much of the frequency translated data used to evaluate performance of the low range transducers were derived from the work done in direct support of the aerodynamic study program reported upon in Reference 11. The equipment arrangement used in that work is shown in Figure 54. The FTSC shown operates the transducer at 5 volts, 6 kilohertz excitation. These calibrations were performed at room ambient temperatures and were carried to no higher than 100 percent of NFS.

6. STEADY STATE ELECTRICAL OUTPUT CHARACTERISTICS

The raw data for a 25 point steady state calibration of transducer C-05 are shown in Table 8.[2] Interpretation of these data would be facilitated by a review of the various methods of simplifying the instantaneous value of the voltage output of the VR transducer and input network. This information is presented in Table 9. The output of a nonideal FTSC is also given. In that expression, V_o is the amplitude of a zero and even order unbalance due to circuit asymmetry contributed by semiconductors, resistors or transformer taps in the demodulator circuit as shown in Figure 10. It is easily detected and measured by reducing

2. The term "calibration" is used throughout this section for convenience only. The original, non-routine approach to examining the output characteristics of the transducers and the unpredictable nature of the initial results places this work in the realm of "experiments."

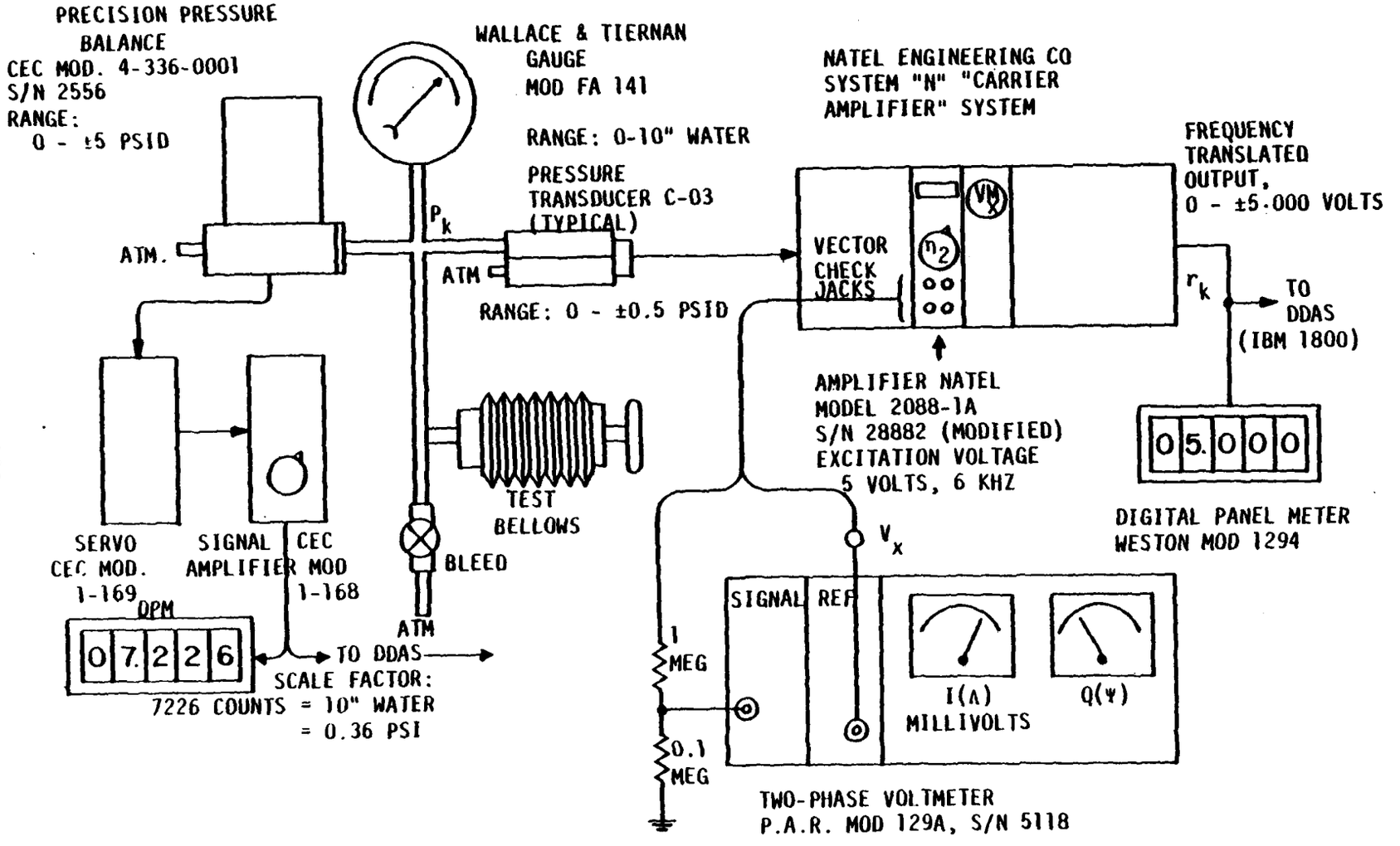

Figure 54. Pre-Test Calibration Scheme - Variable Reluctance Pressure Transducer and "Carrier Amplifier" (FTSC)

TABLE 8

CALIBRATION DATA - TRANSDUCER C-05 (REF: FIGURE 52)

OUTPUT MILLIVOLTS /DEGREES

APPLIED PRESSURE P_k % NFS (CP IN VERT. PLANE)	FUNDAMENTAL Λ_A MV	FUNDAMENTAL Ψ_A DEG	2nd HARMONIC Λ_B MV	2nd HARMONIC Ψ_B DEG	3rd HARMONIC Λ_C MV	3rd HARMONIC Ψ_C DEG	4th HARMONIC Λ_D MV	4th HARMONIC Ψ_D DEG	5th HARMONIC Λ_E MV	5th HARMONIC Ψ_E DEG	6th HARMONIC Λ_F MV	6th HARMONIC Ψ_F DEG	7th HARMONIC Λ_G MV	7th HARMONIC Ψ_G DEG
						- DATE 9/25 -								
0	13.7	/77	.06	/134	1.18	/128	.02	/151	.16	/173	.003	/182	.05	/64
+20	15.5	/108	.12	/111	1.34	/115	.02	/143	.19	/172	.003	/178	.06	/61
+40	20.1	/129	.08	/91	1.32	/108	--	--	.22	/165	.003	/181	.04	/82
+60	25.8	/141	.10	/100	1.45	/106	--	--	.25	/165	--	--	.05	/81
+80	32.3	/149	.09	/94	1.51	/101	--	--	.28	/168	.007	/180	.06	/78
+100	38.9	/153	.08	/92	1.59	/97	--	--	.30	/168	.008	/177	.09	/5
+120	45.9	/156	.07	/91	1.69	/94	--	--	.33	/169	--	--	.11	/8
+100	38.7	/154	.07	/90	1.57	/95	--	--	.31	/170	--	--	.10	/10
+80	31.9	/149	.07	/84	1.44	/95	--	--	.28	/167	.003	/184	.08	/3
+60	25.4	/142	.09	/96	1.45	/105	--	--	.25	/166	.01	/178	.05	/359
+40	19.7	/130	.07	/90	1.33	/107	--	--	.23	/165	.03	/170	.05	/354
+20	15.1	/107	.11	/99	1.34	/116	--	--	.19	/163	.003	/192	--	--
0	13.2	/76	.08	/91	1.24	/118	--	--	.17	/159	--	--	--	--

V_x = 4.002 ±0.006 Volts
Angles ±0.2°

$\frac{\omega T}{2\pi}$ = 2997 ±3 Hertz

- Low or Unreliable Reading

TABLE 8 (Continued)

CALIBRATION DATA - TRANSDUCER C-05 (REF: FIGURE 52)

OUTPUT MILLIVOLTS /DEGREES

APPLIED PRESSURE P_k % NFS (CP IN VERT. PLANE)	FUNDAMENTAL A_A MV	FUNDAMENTAL Ψ_A DEG	2nd HARMONIC A_B MV	2nd HARMONIC Ψ_B DEG	3rd HARMONIC A_C MV	3rd HARMONIC Ψ_C DEG	4th HARMONIC A_D MV	4th HARMONIC Ψ_D DEG	5th HARMONIC A_E MV	5th HARMONIC Ψ_E DEG	6th HARMONIC A_F MV	6th HARMONIC Ψ_F DEG	7th HARMONIC A_G MV	7th HARMONIC Ψ_G DEG
						- DATE 9/26 -								
0	13.8	/76	.04	/89	1.17	/112	--	--	.20	/172	.002	/194	.04	/196
-20	15.8	/50	.03	/109	1.09	/122	--	--	.17	/172	.002	/194	.03	/197
-40	21.4	/33	.03	/104	1.08	/131	--	--	.15	/173	.001	/192	.02	/199
-60	28.3	/23	.03	/98	1.14	/136	--	--	.13	/172	--	--	.01	/200
-80	35.2	/17	.03	/91	1.19	/142	--	--	.1'	/168	--	--	.002	/200
-100	42.3	/12	.03	/91	1.25	/148	--	--	.11	/157	--	--	--	--
-120	49.7	/9	.02	/91	1.31	/153	--	--	.06	/141	--	--	--	--
-100	42.6	/12	.03	/91	1.25	/147	--	--	.11	/158	--	--	--	--
-80	35.2	/16	.03	/92	1.19	/142	--	--	.05	/167	--	--	--	--
-60	28.4	/23	.03	/93	1.16	/135	--	--	.13	/171	.001	/196	.01	/198
-40	21.6	/33	.03	/98	1.13	/130	--	--	.16	/172	.002	/196	--	--
-20	16.0	/49	.03	/99	1.12	/122	--	--	.18	/173	.001	/197	.03	/194
0	13.0	/74	.04	/91	1.21	/110	--	--	.21	/172	--	--	.04	/192

TABLE 9

DEFINITIONS

TRANSDUCER OUTPUT VOLTAGE SIGNALS

A_k The magnitude of the in-phase component of fundamental frequency transducer circuit output voltage (in millivolts or volts as noted) at a steady-state applied pressure P_k. The phase reference is the sinusoidal excitation voltage V_x applied to the transducer circuit.

A_k' The magnitude of the quadrature component of fundamental frequency transducer circuit output voltage at steady state applied pressure P_k.

U_o The in-phase component of fundamental frequency voltage subtracted from A_o to create a net circuit output voltage in-phase component of zero at zero applied pressure P_0 ("zero measurand").

U_o' Quadrature component of fundamental frequency voltage subtracted from A_o' to create a net circuit output voltage quadrature component of zero at zero applied pressure. These quantities are related to the equipment adjustments shown in Figure 53 as follows:

$$\alpha_n \approx c \cdot \sqrt{U_o^2 + (U_o')^2} \quad \text{("Amplitude Balance")}$$

and

$$\theta_n \approx \tan^{-1} \frac{U_o'}{U_o} \quad \text{("Phase Balance")}$$

TABLE 9
(Concluded)

$\Delta_{A(k)}$ Gross Phasor Length $= \sqrt{A_k^2 + (A_k')^2}$ (millivolts)

$\Psi_{A(k)}$ $\tan^{-1} \frac{A_k'}{A_k}$ (degrees)

$\Delta'_{A(k)}$ Net Phasor Length $= \sqrt{(A_k - U_o)^2 + (A_k' - U_o')^2}$ (millivolts)

$\Psi'_{A(k)}$ $\tan^{-1} \frac{(A_k' - U_o')}{(A_k - U_o)}$ (degrees)

Frequency Translated Output (FTO)

Ideal FTSC

$$r_k = \frac{2\eta_2}{\pi} \left[\Delta'_{A(k)} - \frac{C_k}{3} + \frac{E_k}{5} - \frac{G_k}{7} + \cdots \right] \quad \text{(volts)}$$

Real Equipment Case (See Text)

$$r_k = \frac{2Vo}{\pi} \left[\frac{1}{2} + \frac{\pi}{4} \cos\omega_c t + \sum_{p=1}^{\infty} \frac{(-1)^p}{(4p^2 - 1)} \cos 2p\omega_c t \right] +$$

$$\frac{2H_2}{\pi} \Delta'_{A(k)} (1 + \varepsilon_A)\cos\phi_A \left[1 + \frac{2\varepsilon_1}{\pi} \left(\frac{1}{2} + \frac{\pi}{4} \cos\omega_c t + \sum_{q=1}^{\infty} \frac{(-1)^q}{(4q^2 - 1)} \cos 2q\omega_c t \right) \right] +$$

$$\frac{2H_2}{\pi} \left[(1 + \varepsilon_c) \frac{(-C_k)}{3} \cos\phi_c + (1 + \varepsilon_E) \frac{E_k}{5} \cos \phi_E - \cdots \right] \quad \text{(volts)}$$

the signal voltage to zero and observing the change in the DC level in the FTO when power to the reference side (V_M in Figure 10) is switched on and off. These output components are independent of the input signal, V_s. e_1 is the amplitude coefficient of a complex of spurious signals which vary directly with input amplitude V_s. These output components are due to demodulator circuit asymmetry and take the form of a half-wave rectified sine wave superimposed on the output of the demodulator. The component having a frequency, ω_c, is called "carrier leak." The high frequency components having frequencies $2p\omega_c$ and $2q\omega_c$ are called demodulator "hash" in the vernacular. In actual circuits, stray reactances may be present which affect both the amplitudes and phases of these components. However, these terms are not itemized completely because they have little effect on r(t) and are mainly an annoyance.

The coefficients ε_A, ϕ_A, ε_B, ϕ_B, and so on, are errors in signal amplitude and phase as a function of frequency, where η_2 departs from the ideal or design value of $1.00\angle 0°$. With the corrections in this form, the scalar gain, H_2, is used. Actual values for these errors are obtained from the steady state AC amplitude and phase characteristics (transfer function) of the signal path, in the form shown in Figure 4. They are caused by active component inter-element capacities, lead and transformer reactance, and the third-harmonic rejection network, if one is used. As an example, an ideal third harmonic rejection network would reduce C_k and C_k' to zero and have no effect on the phase and amplitude of signal components of any other frequency. The actual amplitude and phase characteristics of a commonly used rejection network, a parallel-T "notch" filter, is shown in Figure 55(a) and the circuit is shown in Figure 55(b). The effect of this network on passed frequencies is a function of its sharpness. The ideal characteristic may more nearly be realized by adding active (power) gain using a voltage-follower amplifier as shown in Figure 55(c). A more detailed discussion of these circuits is contained in References 33 and 34. The fundamental frequency phase error, ϕ_A, can be compensated for by a setting of the "reference phase" adjustment (θ_M) and the amplitude reduction can be compensated for by increasing H_2. Thus, the only deleterious effect of these errors under

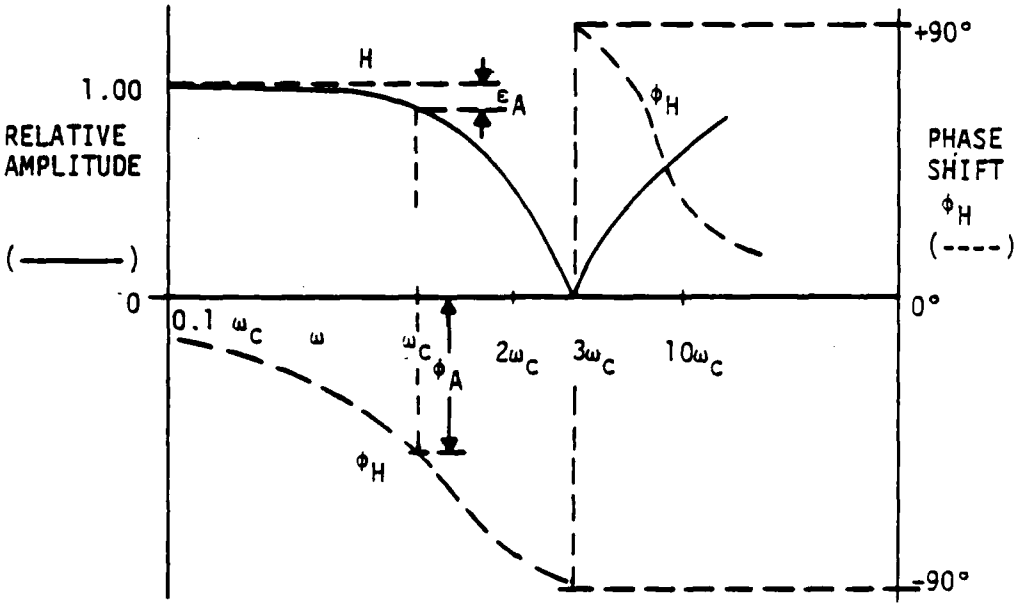

a) FREQUENCY CHARACTERISTICS

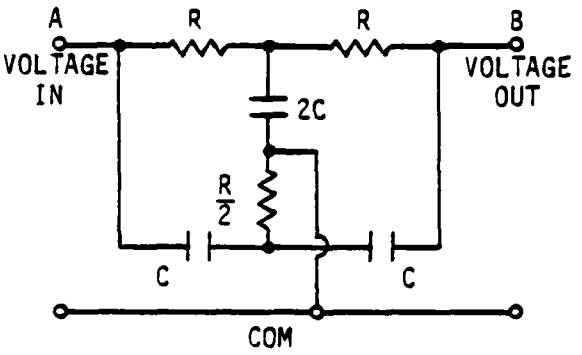

b) PARALLEL-T CIRCUIT

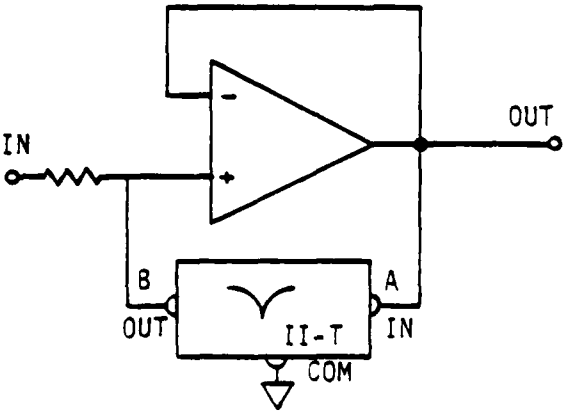

c) ACTIVE GAIN CIRCUIT

Figure 55. Circuit and Steady-State Electrical Characteristics - Parallel-T Third Harmonic Rejection Notch Filter

steady state conditions is from uncontrolled circuit changes due to environmental causes. Approximate measured values for ϵ_A and ϕ_A for the FTSC shown in Figure 54 are -0.1 (-10%) and -20 degrees respectively.

The phase and amplitude versus frequency characteristics of a VR transducer-FTSC combination are also affected by any loading of the transducer by the FTSC input circuit. This effect is further discussed as part of the test results on steady state calibration sensitivity.

Evaluation of the results of the steady state calibration tests was not unduly complicated by the multiplicity of ways of describing the transducer output signal. All significant trends were easily recognizable regardless of what form of output was used. However, the phase coherent voltmeter measurements gave evidence of some microscopic center plate behavior which might otherwide have been taken for random scatter caused by electrical or pneumatic system measurement uncertainties. Some significant CP behavior was detectable only by the persistent recurrence of certain values of phase and/or amplitude coefficients.

7. HARMONIC OUTPUT MEASUREMENTS

The harmonic content of transducer output as determined by the phase-coherent voltmeter method is in fair agreement with the preliminary measurements plotted in Figures 34, 35, and 36, which were made several years previously. The harmonic amplitudes at the selected test values of excitation voltage and frequency fall roughly into the ranges tabulated in Table 10. For convenience in deriving a single number, the magnitude of a given harmonic is arbitrarily defined as the phasor length measurement made at an applied pressure of +80 percent NFS expressed as a percentage of the measurement of the fundamental at that load point. That is,

$$\text{Nth Harmonic} = \frac{\Lambda_{N(+0.8)}}{\Lambda_{A(+0.8)}} \times 100 \ (\%)$$

TABLE 10

HARMONIC CONTENT IN OUTPUT - TYPICAL MEASURED VALUES,
VARIABLE RELUCTANCE PRESSURE TRANSDUCERS

HARMONIC ORDER -n	OUTPUT - PCT OF FUNDAMENTAL	SQUARE WAVE MULTIPLIER $\lvert\Gamma_n\rvert$	OUTPUT PRODUCT - PCT
2	0.5(%)	0	0(%)
3	5.0	$\frac{4}{3\pi} = 0.424$	2.1
4	0.1	0	0
5	1	$\frac{4}{5\pi} = 0.255$	0.26
6	0	0	0
7	0.5	$\frac{4}{7\pi} = 0.182$	0.1

Output - PCT, n-th Harmonic =

$$\frac{\Lambda_n(\pm 0.8)}{\Lambda_A(\pm 0.8)} \times 100\ (\%)$$

8. CALIBRATION CURVE SHAPE

Raw data such as that for transducer C-05, shown in Table 8, may be used directly for studying repeatability and hysteresis. Trends in calibration linearity and symmetry about the origin are not immediately evident from inspection of the fundamental frequency measurements. These were simplified by subtracting the zero measurand output ($A_o + jA'_o$) from all readings, as presented in Table 11. The phase angle, Ψ', of the useful electrical output with respect to excitation voltage then becomes apparent. Since the values for this transducer, 174 and 354 degrees respectively, are exactly 180 degrees apart, the net phasor lengths in the $\Lambda'_{A(k)}$ column may be compared directly when evaluating span and linearity characteristics. From Table 11, the average of the four values for $\Lambda'_{A(\pm 0.8)}$ is about 30.7 millivolts at the output of transformer T_{2B}. In this case, the actual transducer output is 30.7 $x\sqrt{5}$ because of the step-down transformer used. The deviations of actual measurements from the straight line $y = \frac{30.7}{0.8} x$ are plotted as in Figure 56. The curve $y = 945 \left(\frac{x}{24 + x}\right)$ was then used as a reference and deviations of test measurements from this curve were plotted as in Figure 57. In the positive load direction, the curve fit is improved. It could be further improved by discarding the final +20 percent NFS point. For negative measurand values the curve fit is poor and the higher values actually lie rather close to the straight line $y = 38.17x$.

Transducers C-03, C-04, and C-06 were part of a large lot purchased for an aerodynamics research test program. They were used in a pressure data system and calibrated with equipment similar to that shown in Figure 54. An eight-point calibration for transducer C-06 is shown in Figure 58. The characteristic S-shape is evident. The $\pm$ 0.2 percent deviation from linearity is typical of the calibration of all transducers in the lot. In most cases, departure from tne $y = c \frac{x}{a + x}$ shape could be reduced by using different values of c and a in the two load directions.

TABLE 11

FUNDAMENTAL FREQUENCY CALIBRATION DATA -
TRANSDUCER C-05
FIRST CALIBRATION - DATES: 9/25 and 9/26*

P_k %NFS	A_A/Ψ_A MILLIVOLTS/DEGREES	A MILLIVOLTS	A' MILLIVOLTS	A-U MILLIVOLTS	A'-U' MILLIVOLTS	A'_A/Ψ'_A MILLIVOLTS/DEGREES
0	13.7/77	+3.08	+13.3	(0)	(0)	0
+20	15.5/108	-4.79	+14.7	-7.9	+1.4	8.0 /170
+40	20.1/129	-12.6	+12.0	-15.7	-1.3	15.75 /184
+60	25.8/141	-20.1	+16.2	-23.2	+2.9	23.4 /173
+80	32.3/149	-27.7	+16.6	-30.8	+3.3	31.0 /174
+100	38.9/153	-34.7	+17.7	-37.8	+4.4	38.1-/173
+120	45.9/156	-41.9	+18.7	-45.0	+5.4	45.3+/173
+100	38.7/154	-34.8	+17.0	-37.9	+3.7	38.1-/174
+80	31.9/149	-27.3	+16.4	-30.4	+3.1	30.6-/174
+60	25.4/142	-20.0	+15.6	-23.1	+2.3	23.2+/174
+40	19.7/130	-12.7	+15.1	-15.8	+1.8	15.9 /173
+20	15.1/107	-4.4	+14.4	-7.5	+1.1	7.6 /172
0	13.2/76	+3.2	+12.8	+0.1	-0.5	0
*0	13.8/76	+3.3	+13.4	+0.2	+0.1	0
-20	15.8/50	+10.2	+12.1	+6.9	-1.3	7.0 /350
-40	21.4/33	+17.9	+11.6	+14.6	-1.8	14.7 /353
-60	28.3/23	+26.1	+11.1	+22.8	-2.3	22.9 /354
-80	35.2/17	+33.7	+10.3	+30.4	-3.1	30.6 /354
-100	42.3/12	+41.4	+8.8	+38.1	-4.6	38.4 /353
-120	49.7/9	+49.1	+7.8	+45.8	-5.6	46.1+/353
-100	42.6/12	+41.7	+8.9	+38.4	-4.5	38.7-/353
-80	35.2/16	+33.8	+9.7	+30.5	-3.7	30.7-/353
-60	28.4/23	+26.1	+11.1	+22.8	-2.3	22.9+/354
-40	21.6/33	+18.1	+11.7	+14.8	-1.7	14.9 /353
-20	16.0/49	+10.5	+12.1	+7.3	-1.3	7.4 /350
0	13.0/74	+3.58	+12.5	+0.5	-0.8	----

NFS = NAMEPLATE FULL SCALE

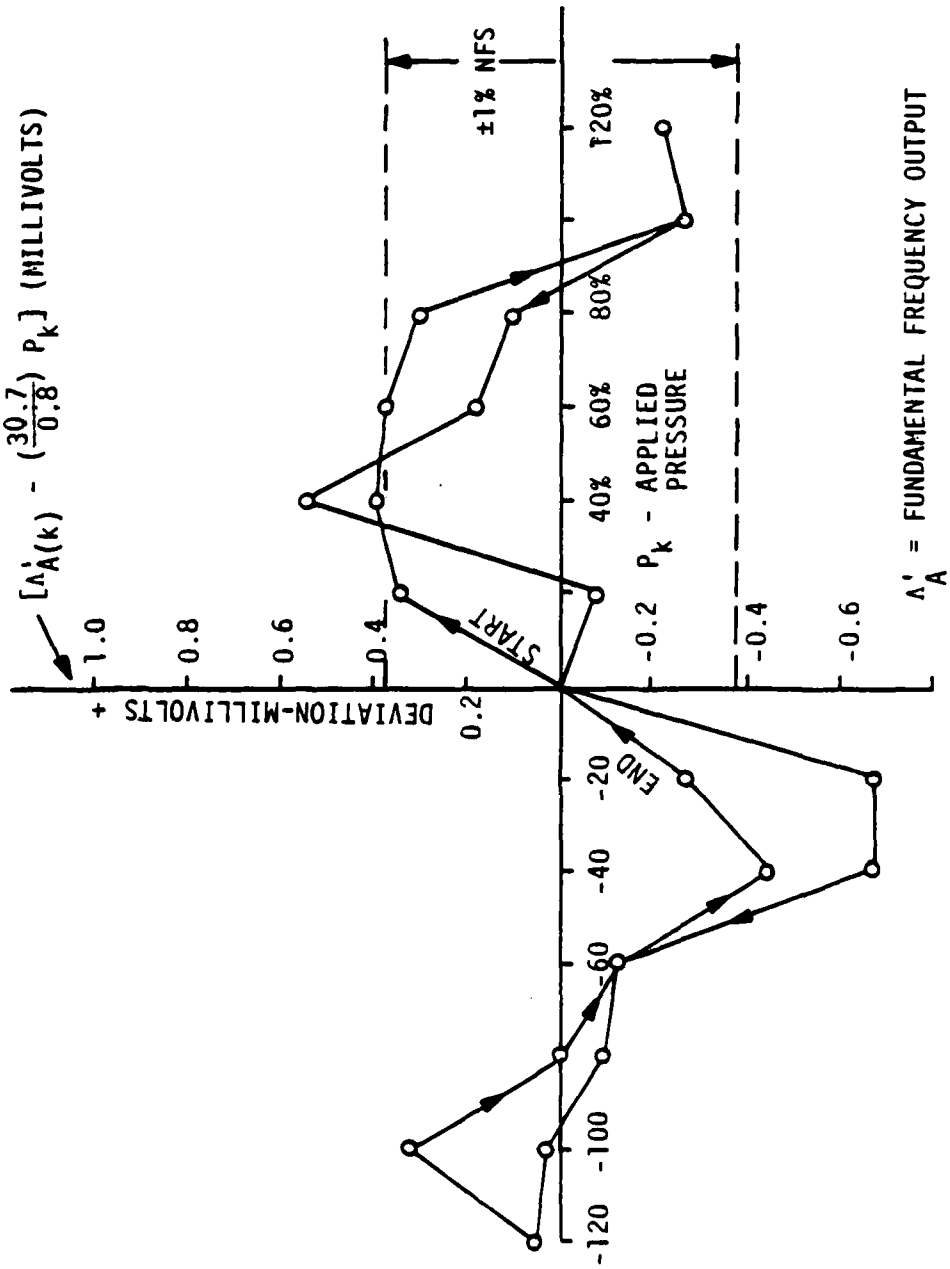

Figure 56. Calibration Data - Deviation from Selected Straight Line - Transducer C-05

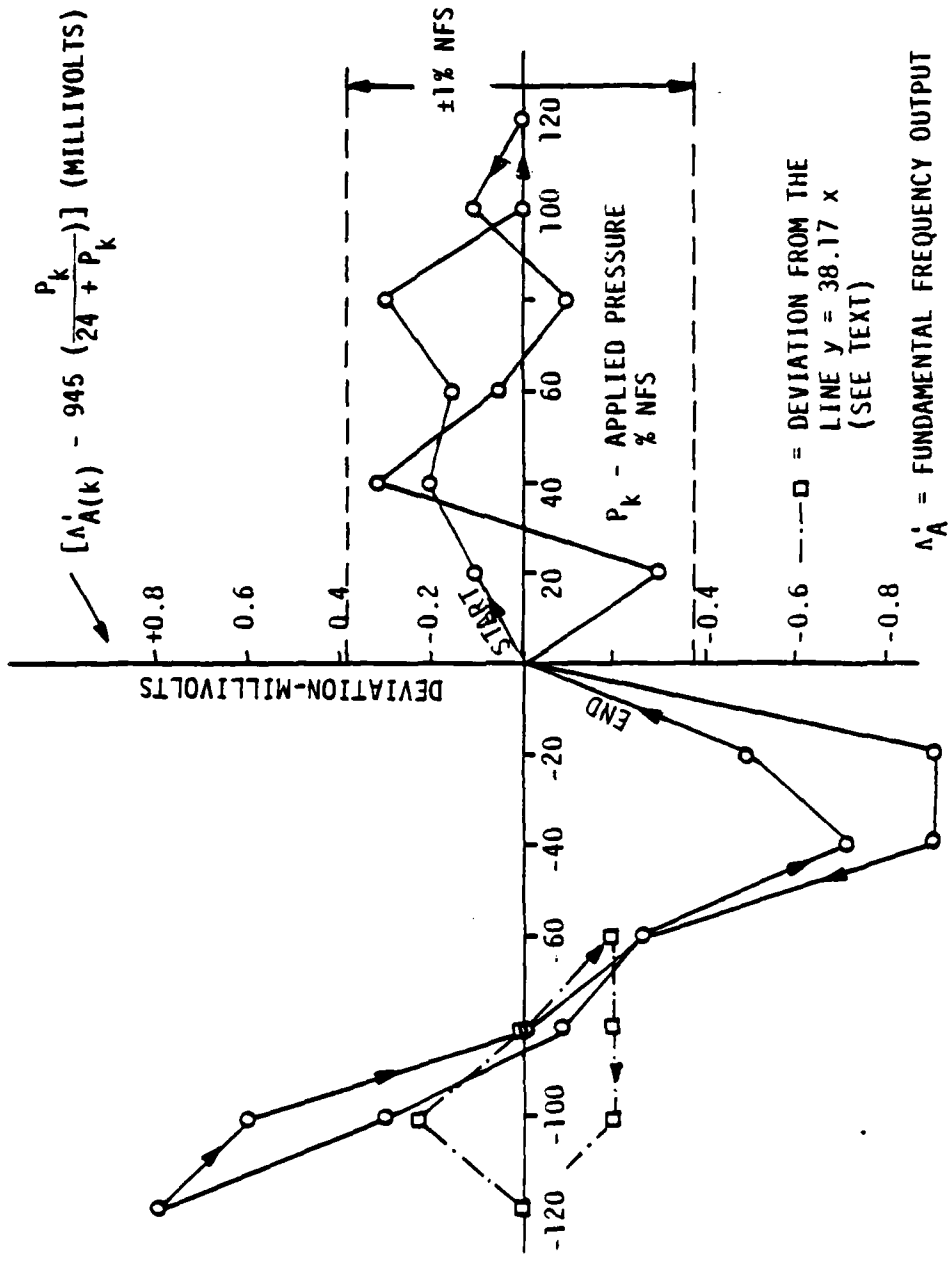

Figure 57. Calibration Data - Deviation from the Line $y = 945\ (\frac{x}{24 + x})$ Transducer C-05

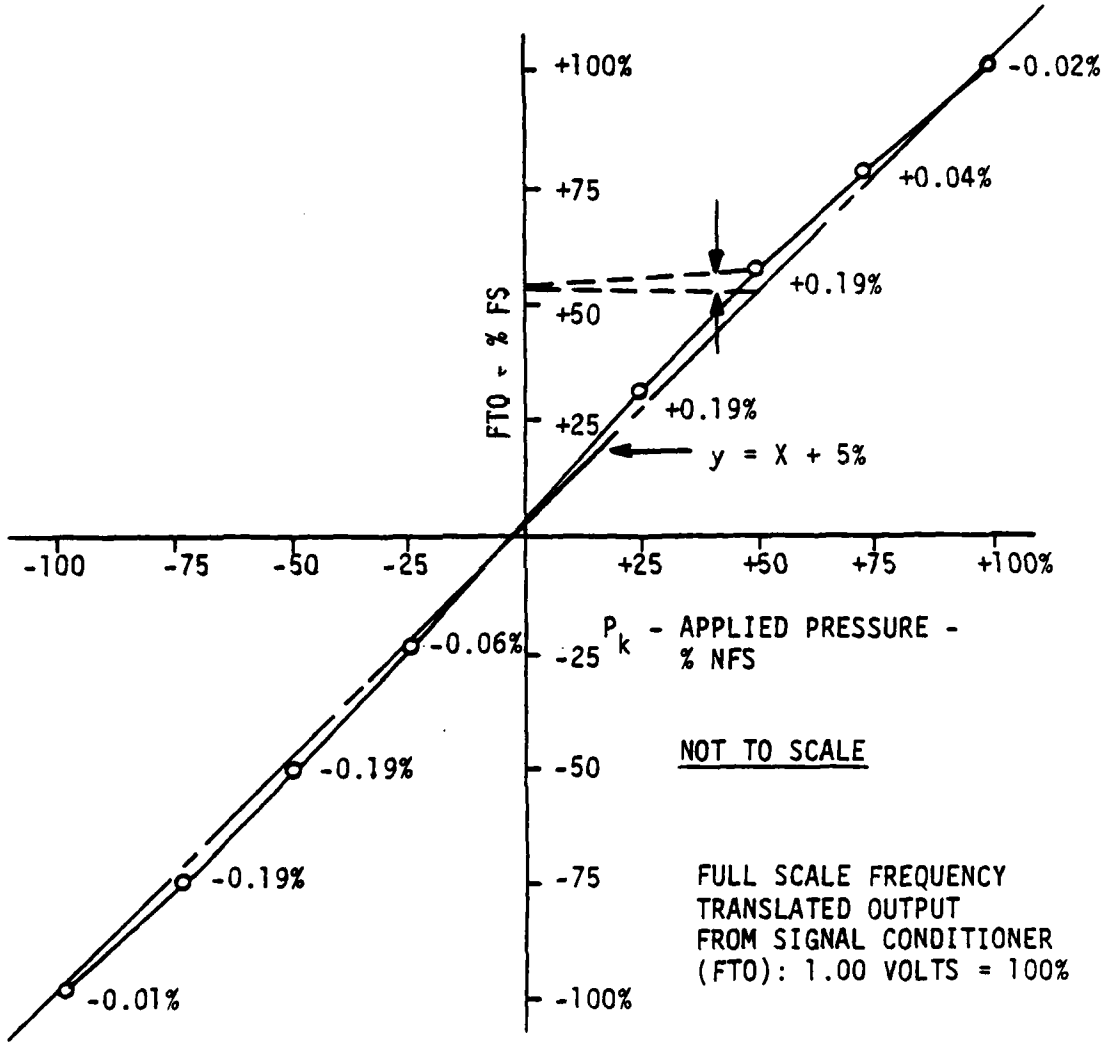

Figure 58. Installed System Pre-Test Calibration Data - Transducer C-06

Table 12 contains raw data from a 42-point calibration of transducer C-03 using the same equipment arrangement. The amplitude scaling factor, n_2, was arbitrarily set to give an FTO of approximately 4.6 volts for ten inches of water (0.36 PSID) applied pressure. In the aerodynamics research program using the equipment, these data were machined-reduced using a two-segment straight-line approximation. For the present study, the data were matched to the curve $Y_k = c \frac{P_k}{a + P_k}$ at 0, 70, and 100 percent of calibrated full scale (CFS). These values correspond to about 50 and 70 percent of NFS for the 0.5 PSID transducer. Separate curves were developed for the two load directions. The departures, $(r_k - Y_k)$, of the FTO readings from the calculated curve are also tabulated. The maximum departure was $\pm$ 0.022 volts which is 0.35 percent of NFS, or $\pm$ 0.0017 PSID. The average departure is considerably less, particularly at the higher load points. Hysteresis and scatter are clearly distinguishable as departures from the S-curve. No allowance has been made for measurement uncertainties in the pneumatic system.

The data from a different calibration of this transducer (C-03) were given a similar treatment. The quantity $(r_k - Y_k)$ is shown plotted against applied pressure in Figure 59. This plot illustrates the presence of errors from three sources: scatter, hysteresis, and an unfortunate selection of the r_k values from the measurements for use in the calculation of c and a. The "notches" in the curve going from +4 to +7 inches of water load points and from +8 to +5 inches of water are undoubtedly caused by "oil canning" of the CP. In the absence of such behavior, the curve would have taken the course indicated by the dashed lines. This behavior is also detectable in the negative pressure direction. The entire curve fit in the positive load direction was affected adversely because one of the +70 percent CFS output measurements was in the region of the occurrence of oil canning. The use of another value, such as the one at point X, to recalculate the curve would improve the overall curve fit noticeably.

TABLE 12

INSTALLED SYSTEM PRE-TEST CALIBRATION DATA
TRANSDUCER C-03 (REF: FIGURE 54)

$\lvert P_k \rvert$ Inches H_2O	$+P_k:Y_k = 135.5\left(\frac{P_k}{281.2+P_k}\right)$ FTO r_k(volts)	r_k-Y_k (volts)	$-P_k:Y_k = 232.2\left(\frac{P_k}{492.1+P_k}\right)$ FTO r_k(volts)	r_k-Y_k (volts)
0	+0.006	+0.006	+0.012	+0.012
1	+0.484	+0.005	-0.468	+0.003
2	+0.940	-0.015	-0.933	+0.007
3	+1.419	-0.009	-1.414	-0.007
4	+1.885	-0.012	-1.869	+0.003
5	+2.357	-0.006	-2.340	-0.004
6	+2.810	-0.016	-2.795	+0.002
7	+3.282	-0.004	-3.250	+0.007
8	+3.736	-0.006	-3.717	-0.002
9	+4.185	-0.011	-4.162	+0.009
10	+4.646	0	-4.625	0
9	+4.200	+0.004	-4.177	-0.006
8	+3.751	+0.009	-3.723	-0.008
7	+3.290	+0.004	-3.264	-0.007
6	+2.820	+0.006	-2.807	-0.010
5	+2.364	+0.005	-2.349	-0.013
4	+1.905	+0.008	-1.884	-0.012
3	+1.444	+0.016	+1.429	-0.022
2	+0.972	+0.017	-0.949	-0.009
1	+0.500	+0.021	-0.484	-0.013
0	+0.016	+0.016	+0.004	+0.004

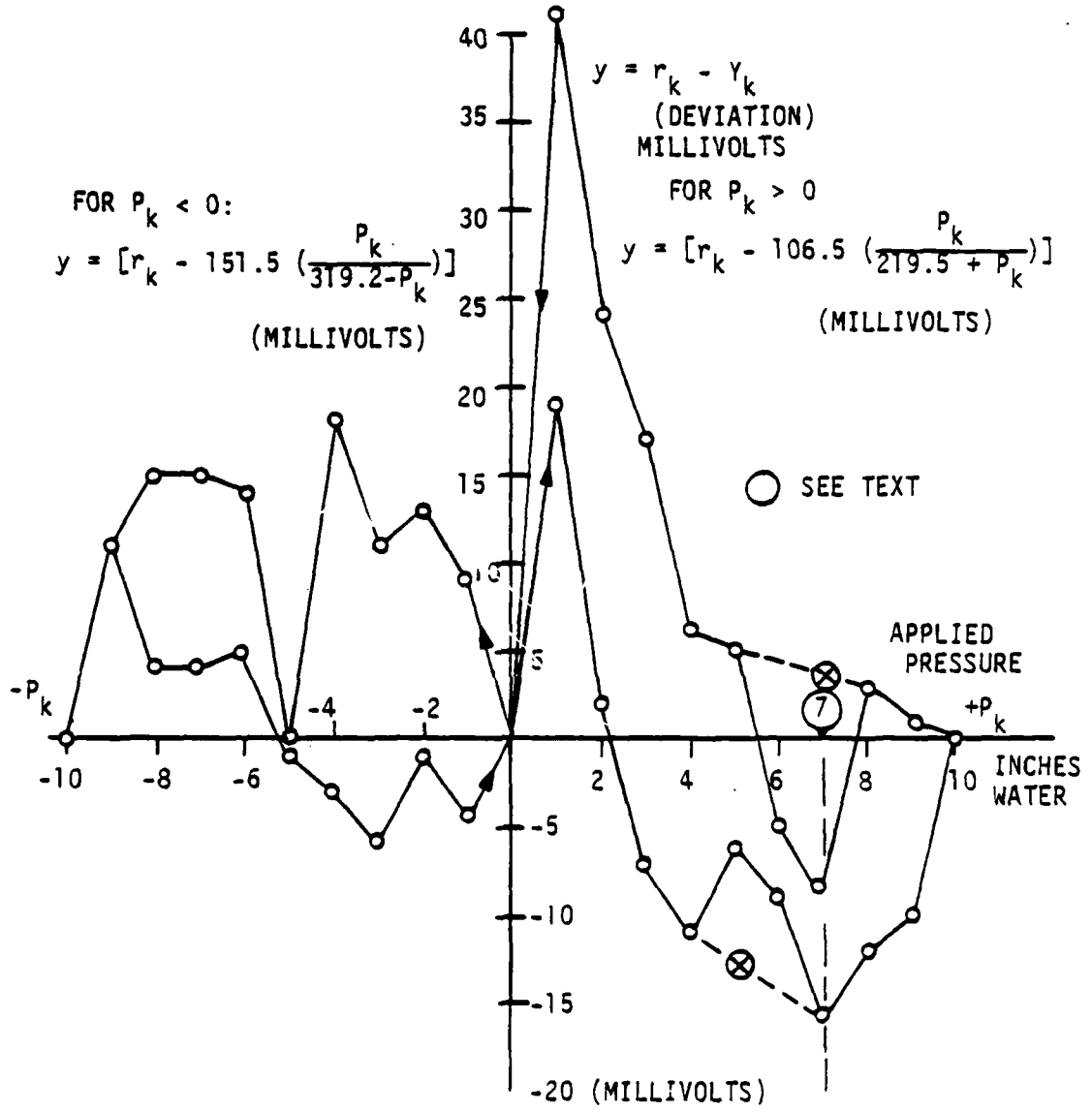

EQUIPMENT ARRANGEMENT
SHOWN IN FIGURE 54

Figure 59. Deviation of Measured Data from Calculated Curves - Second Pre-Test Calibration of Installed System - Transducer C-03

Figure 60 contains calibration data for three transducers having the same NFS ratings but two different designs and manufacturers. Points are plotted as deviations from straight lines through zero.

A comparison of typical calibration curve shapes for the three brands of 0.5 PSID NFS transducers shows the effect of design values of CP thickness, deflection, and air gap clearance. The curve in Figure 61 for transducer B-02 shows that the design value of full scale CP deflection is large relative to the air gap clearance due to use of a thin CP. The portion of this curve which conforms to the characteristic S-shape is confined to less than a third of the full scale range, and then the output rises rapidly as the CP approaches either pole piece. When this happens, differences in air gap clearances on the two sides become critical and asymmetries are much more pronounced. The measured output sensitivities of both B-01 and B-02 are about 50 percent higher than those of the C-01 group and almost double those of the A-10 group. The calibration curve for transducer A-18 in Figure 62 shows a pronounced negative curvature at the extremes of CP deflection. This is a result of the relatively thick CP. A lower ratio of gap clearance to maximum deflection was then required to maintain a desirable output level.

The calibration asymmetry of transducer B-01 was noteworthy. The fundamental frequency phasors for the $\pm$ 80 percent load points for this transducer are shown in Figure 63 as having lengths of 89.8 and 82.0 millivolts. If used with an FTSC, the choice of load direction during adjustment of the reference phase θ_M could obscure this discrepancy. The signal vector component resulting from an adjustment of θ_M of -28.4 degrees is 83.2 millivolts for negative 80 percent measurand and 82.0 millivolts for a positive 80 percent measurand. This apparent reduction in calibration asymmetry will appear in the FTO.

The possibility of damage or defects in the CP of this unit was checked by loading to $\pm$ 800 percent NFS. The results are shown in Figure 64. Similar data for transducer A-10 are shown in Figure 65. In both cases, the phase and amplitude discrepancies in terms of percent of reading diminished significantly, emphasizing the consequences of

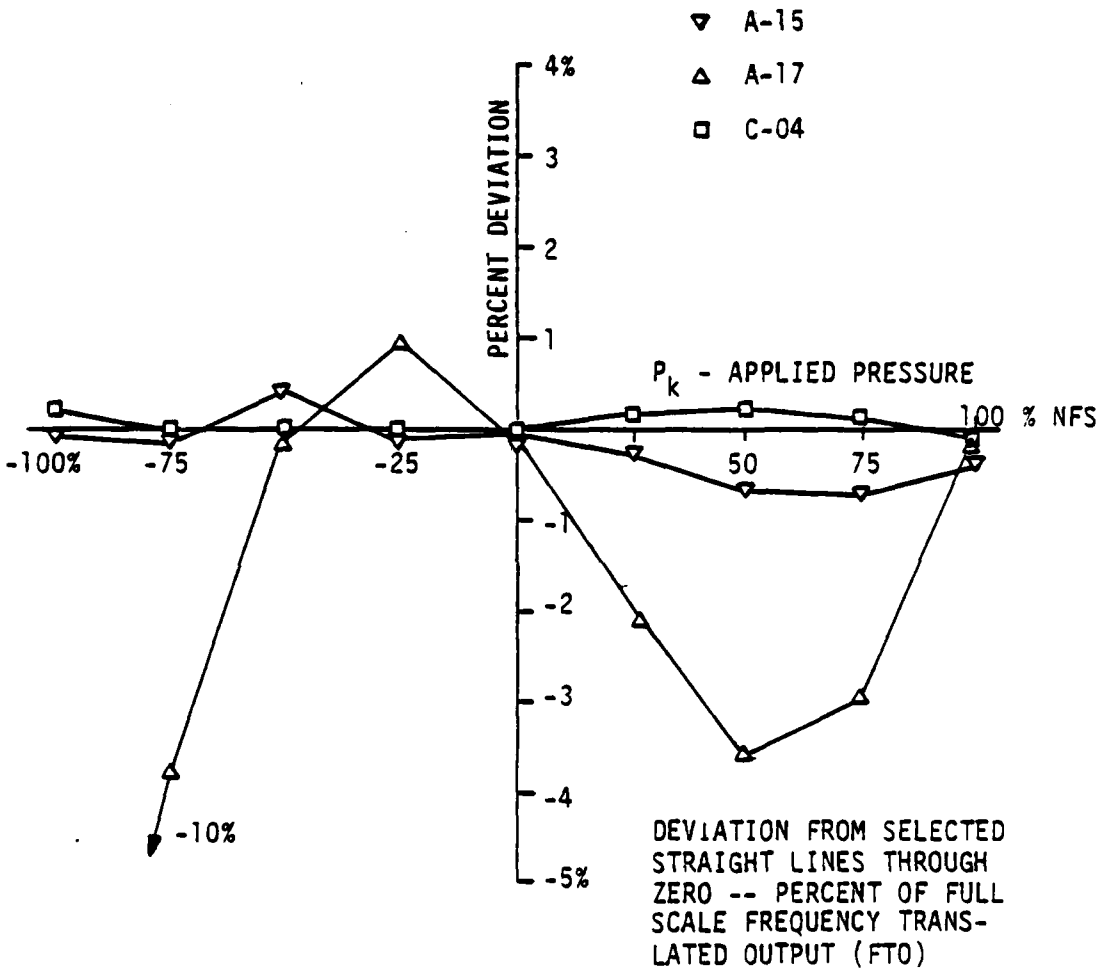

Figure 60. Installed System Pre-Test Calibration Data - Transducers A-15, A-17, and C-04

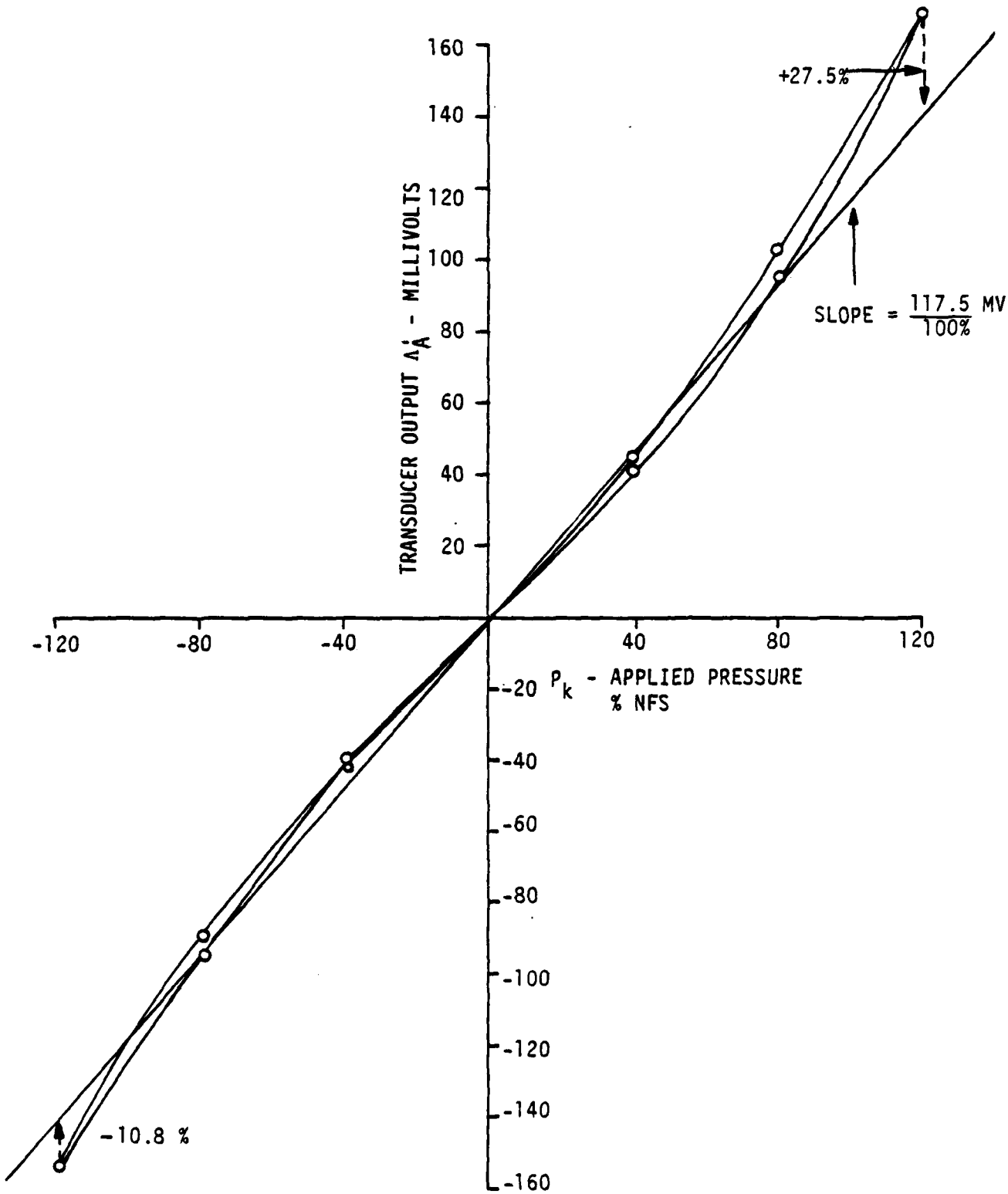

Figure 61. Calibration Data - Transducer B-02

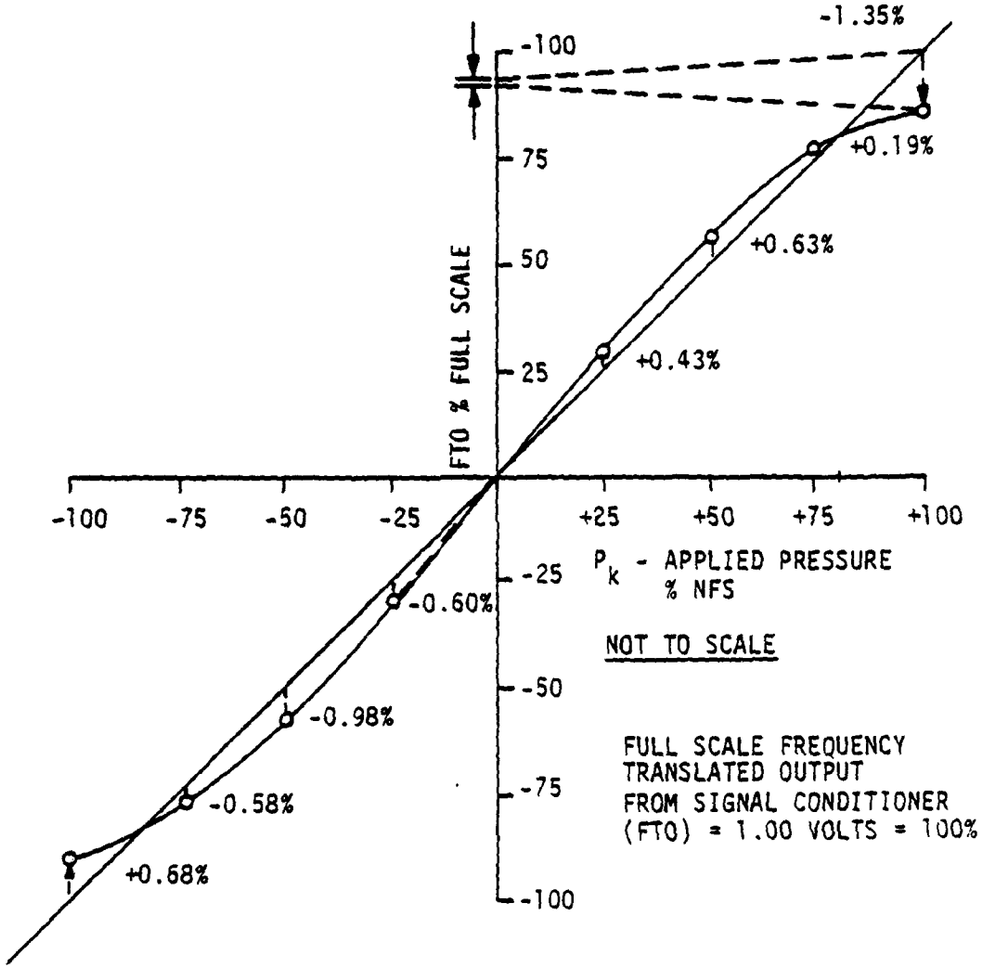

Figure 62. Installed System Pre-Test Calibration Data - Transducer A-18

P_k	Λ'_A	Ψ_A	Λ'_A	Ψ'_A	A-U	A'-U'
0	14.45	∠206°	0		0	
+80	91.2	∠159°	82.0	∠151.6°	-72.1	+39.0
-80	78.0	∠348°	89.8	∠353.7°	+89.3	-9.8
0	16.03	∠204°	1.6	∠190.6°	- 1.6	-0.2

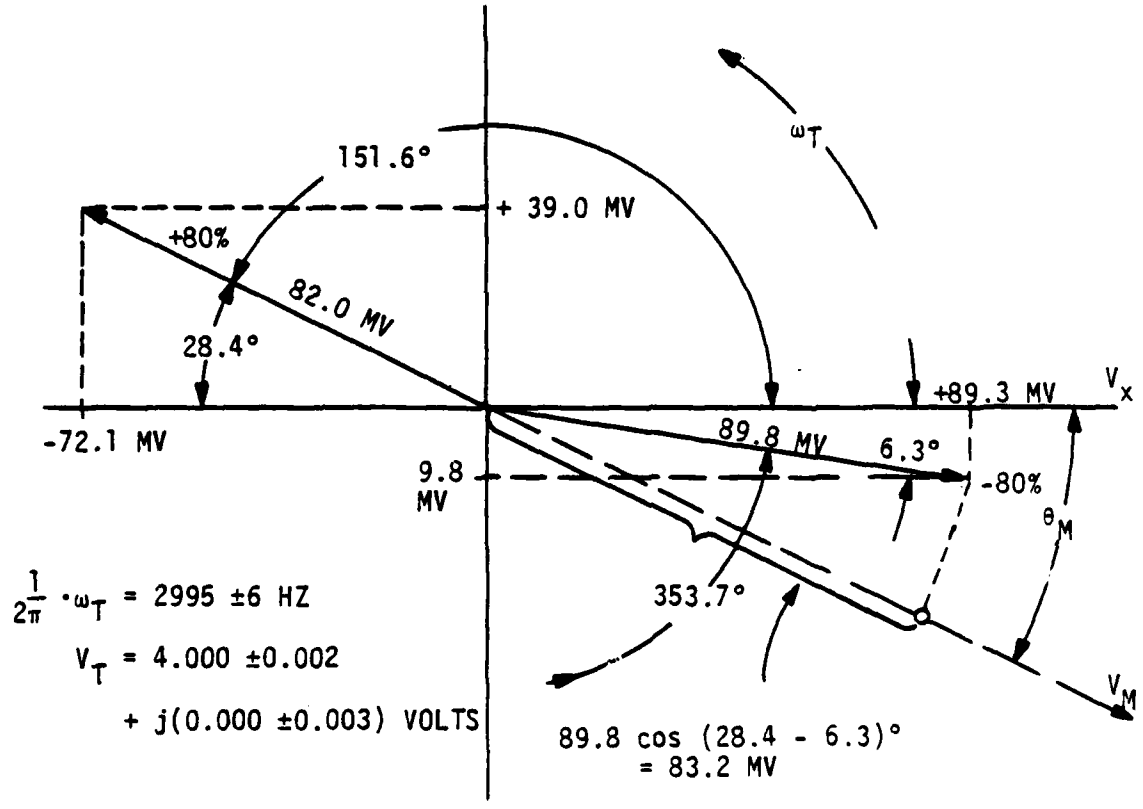

Figure 63. Fundamental Frequency Signal Phasors - Applied Pressure $P_k = \pm$ 80% NFS - Transducer B-01

P_k	Λ_A	$\angle\Psi_A$	Λ'_A	$\angle\Psi'_A$	A-U	A'-U'
0	12.23	$\angle 211°$	0		0	
+800	944.0	$\angle 159°$	936.5	$\angle 158.4°$	-870.8	+344.6
-800	974.0	$\angle 336°$	981.0	$\angle 336.6°$	+900.3	-389.6
0	13.0	$\angle 211°$	0.8	$\angle 211°$	- 0.7	- 0.4

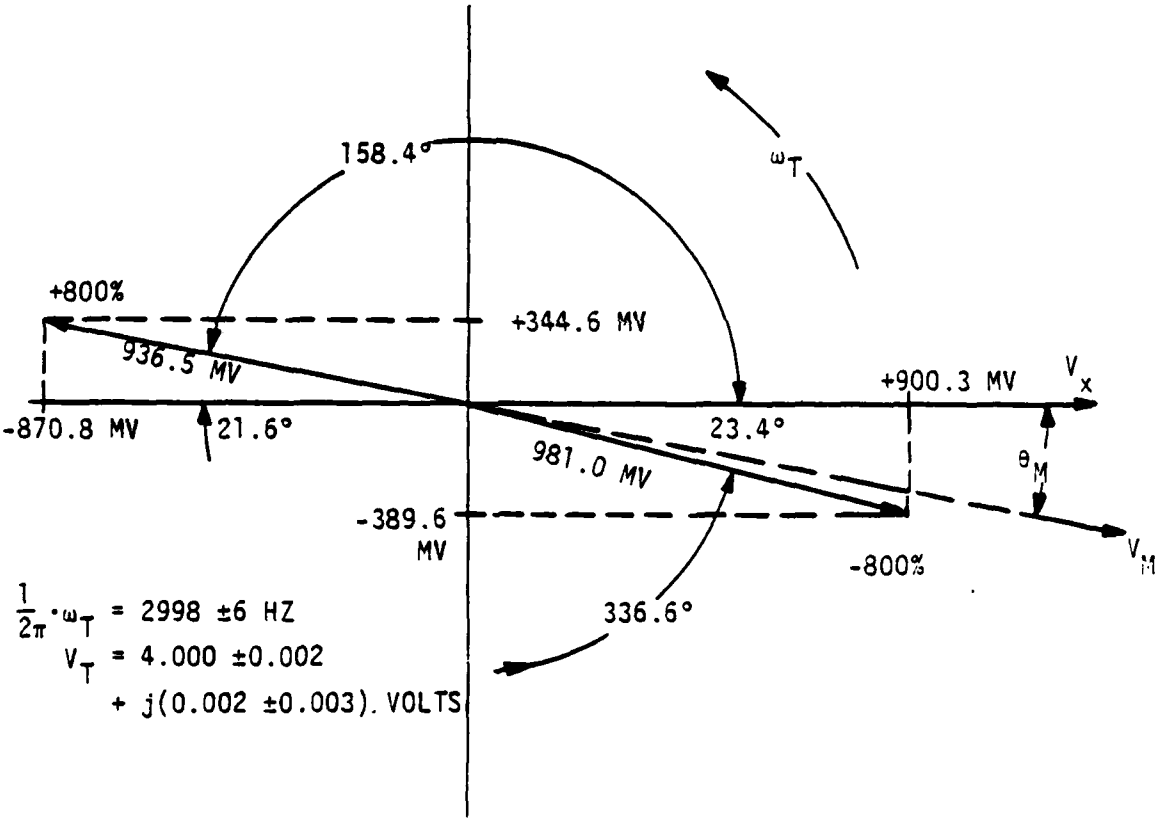

Figure 64. Fundamental Frequency Signal Phasors - Applied Pressure $P_k = \pm$ 800% NFS - Transducer B-01

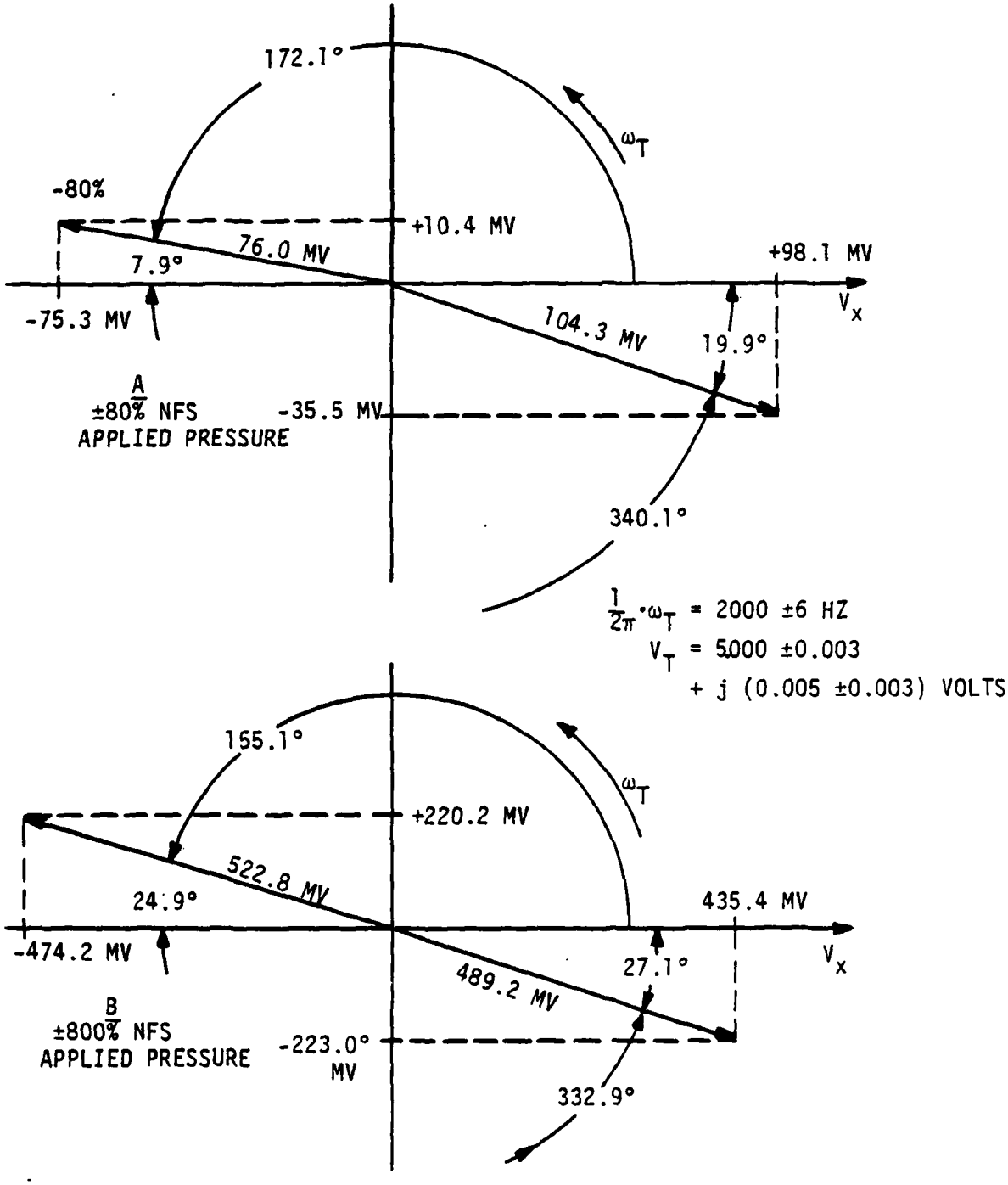

Figure 65. Fundamental Frequency Signal Phasors - Applied Pressure $P_k = \pm$ 80% and $\pm$ 800% NFS - Transducer A-10

assigning any given NFS rating to these units and the difficulty of determining what constitutes damage to or defects in the CP. Asymmetry of the same type was found in transducer C-10. This transducer is a large durable unit for use in adverse environments and has an NFS rating of zero to ± 50 PSID. The center plate is a machined section. Reversing the CP side-for-side had little effect on the span or zero, as shown in Figure 66, indicating that in this case, unequal air gap clearances were the sole cause of the asymmetry.

All data of this kind indicate that design choices of gap clearance, CP deflection, and production variables, as well as CP shape irregularities were the cause of all systematic nonideal calibration characteristics, except mechanical hysteresis, observed to this point. To test this conclusion, data taken on transducer F-01 were plotted in a similar manner. These are presented in Figure 67. This transducer does not use the center plate construction of the classical VR transducer. The pressure element and the electrical signal pick-off are articulated so that each may be designed for optimum performance. The "E-core" type of electrical pick-off used in this transducer has previously been described. It is constructed of electrical steel laminations, reducing eddy current effects to levels typical of those of audio transformers. As a result, it has a useful output about five times the typical values for classical type VR transducers and may be used with excitation levels up to about 25 volts RMS at three kilohertz.[3] (Figure 48) It was also built in a four arm bridge configuration by adding a second E-core and coils. The overall design results in a more linear, controllable pressure-output characteristic. The steady state precision and hysteresis characteristics of this transducer are wholly those of the pressure element, which is a hollow, twisted torsion tube fixed at the reference end. It is not as rugged, simple, and repairable as the classical VR type and was not manufactured in ranges lower than 5 PSID.

[3]The FTSC designed and manufactured by the same company for use with these units did not use electronic amplification. The transducer operated directly into a voltage demodulator.

P_k	Λ_A'	$\Lambda_A'^*$
+80%	282.5 ∠354.6°	(293.1 ∠354.2°)
-80%	212.4 ∠180.2°	(207.4 ∠181.3°)

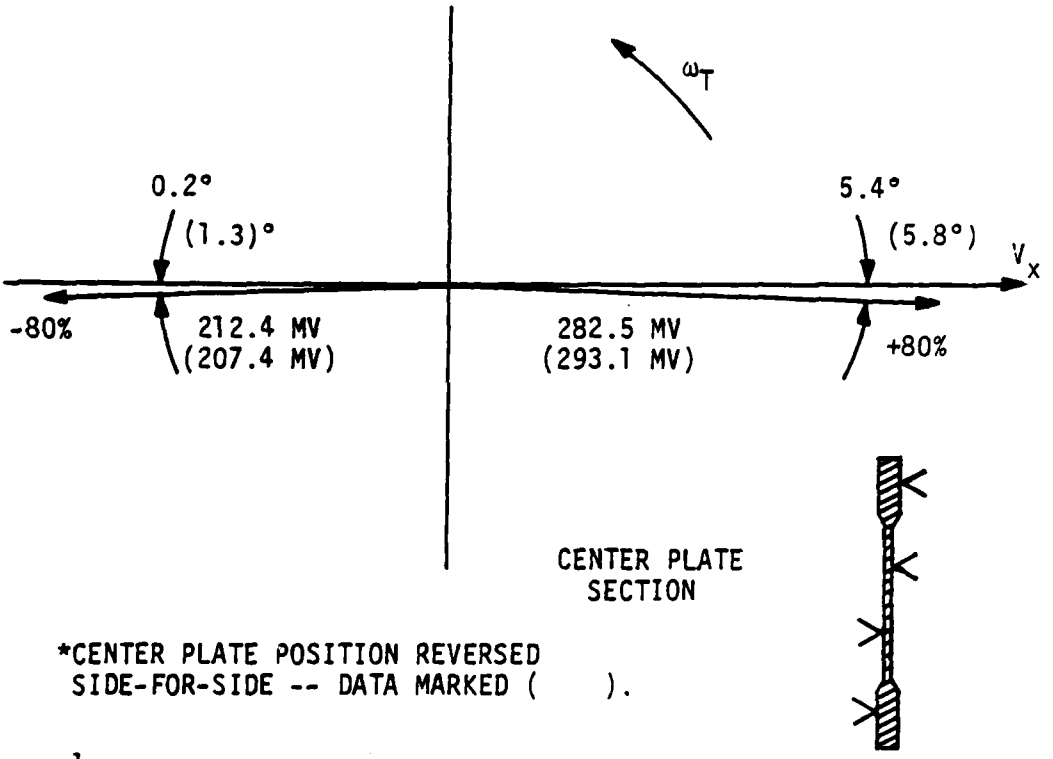

*CENTER PLATE POSITION REVERSED SIDE-FOR-SIDE -- DATA MARKED ( ).

$\frac{1}{2\pi} \cdot \omega_T$ = 2004 ±5 HZ

V_T = 5.008 ±0.005
+ j(0.008 ±0.005) VOLTS

Figure 66. Fundamental Frequency Signal Phasors - Applied Pressure $P_k = \pm$ 80% NFS - Transducer C-10

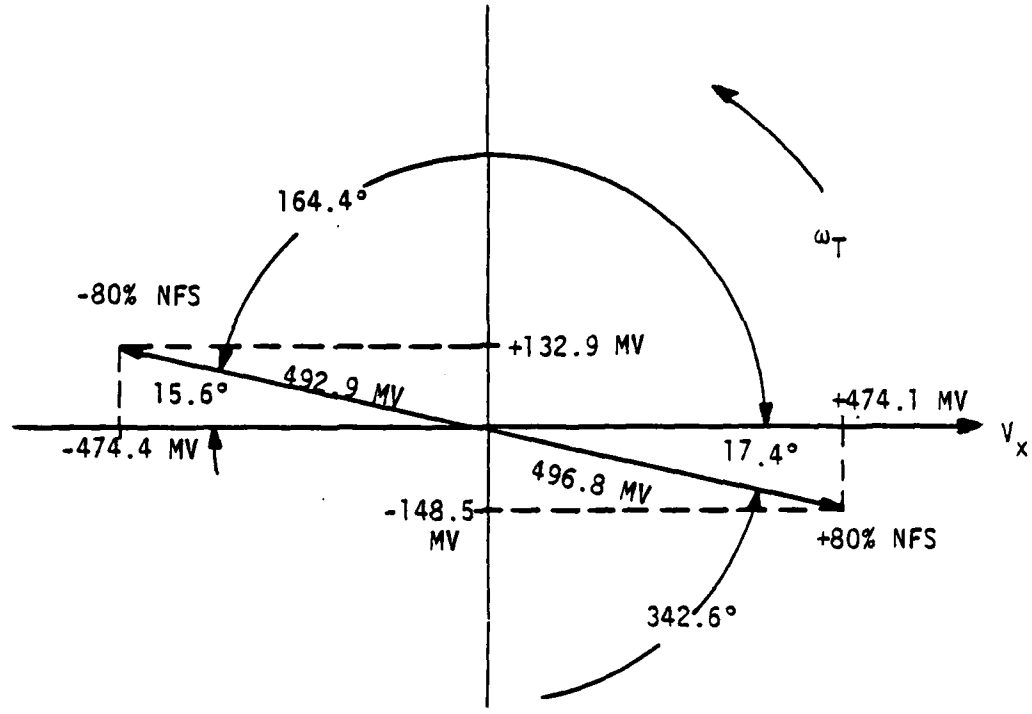

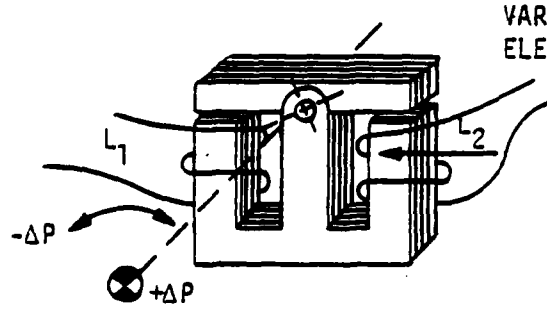

VARIABLE RELUCTANCE ELECTRICAL PICK-OFF

LAMINATED ELECTRICAL STEEL CORE AND ARMATURE

TO PRESSURE ELEMENT

$\frac{1}{2\pi}\omega_T$ = 2997 ±5 HERTZ

V_T = 5.003 ±0.002 + j(0.004 ±0.003) VOLTS

Figure 67. Fundamental Frequency Signal Phasors - Applied Pressure $P_k = \pm$ 80% NFS - Transducer F-01

The nameplate full scale rating of transducer F-01 was ± 5 PSID. The mechanical resonant frequency is about 500 Hertz as compared with several thousand Hertz for a classical VR transducer of the same range.

Wherever the asymmetry of fundamental signal output is very pronounced, it is accompanied by an even greater asymmetry in even order harmonic output. Figure 68 shows the second harmonic output, $\Lambda'_{B(k)}$, of transducer B-01, plotted against pressure load.

The curve shapes for some transducers tested were a composite of the various forms. Many showed entirely different shapes in the first and third quadrants. As examples, the curves of FTO for transducers A-15 and A-19 are shown in Figures 69 and 70 respectively. The curve of fundamental net phasor length, $\Lambda'_{A(k)}$, versus applied pressure, for transducer B-01 is shown in Figure 71. The center plate of each transducer in these groups seems to possess its own peculiar "personality." The calibration of Figure 71 was carried out to only ± 80 percent of NFS, resulting in greatly reduced hysteresis.

The results of these curve shape tests may be combined with those for optimum electrical operating point to strengthen some of the conclusions concerning the relative design approaches taken by the three manufacturers of the 0.5 PSID transducers. The high frequency eddy current losses indicated that A-10 has a relatively thick CP and the curve shape confirms this. It also suggests that the gap clearances were made small to maintain electrical output. Transducer B-01 has the thinnest CP, a rather large gap clearance and large design values of NFS deflection. The CP thickness and gap clearance for transducer C-05 appear to lie between these extremes as a result of design compromises in favor of curve shape at the expense of electrical output and zero measurand hysteresis ("zero return"). Performance of transducers B-01 and B-02, particularly with regard to hysteresis, suggests that these transducers should actually be rated at 0.3 or 0.4 PSID NFS, rather than 0.5 PSID.

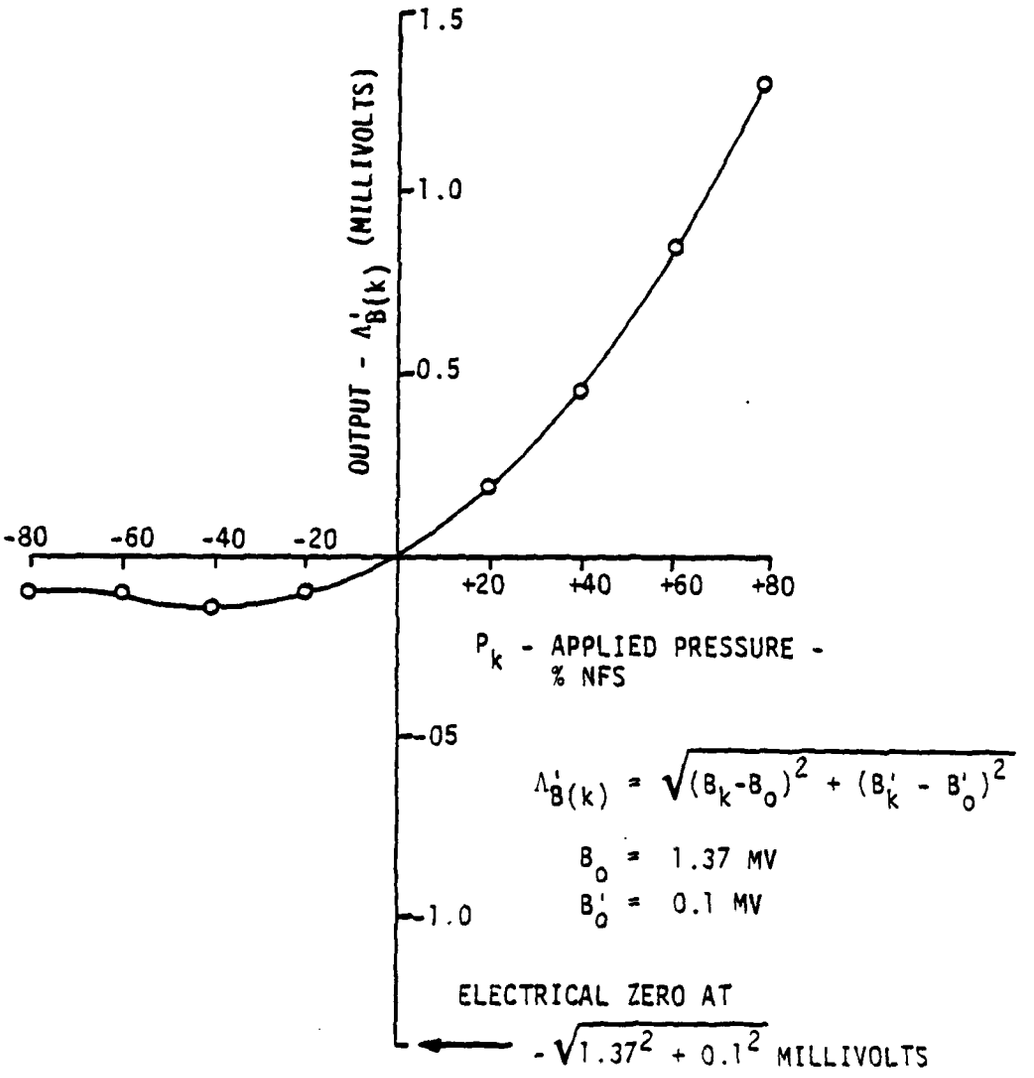

Figure 68. Calibration Data - Second Harmonic - Transducer B-01

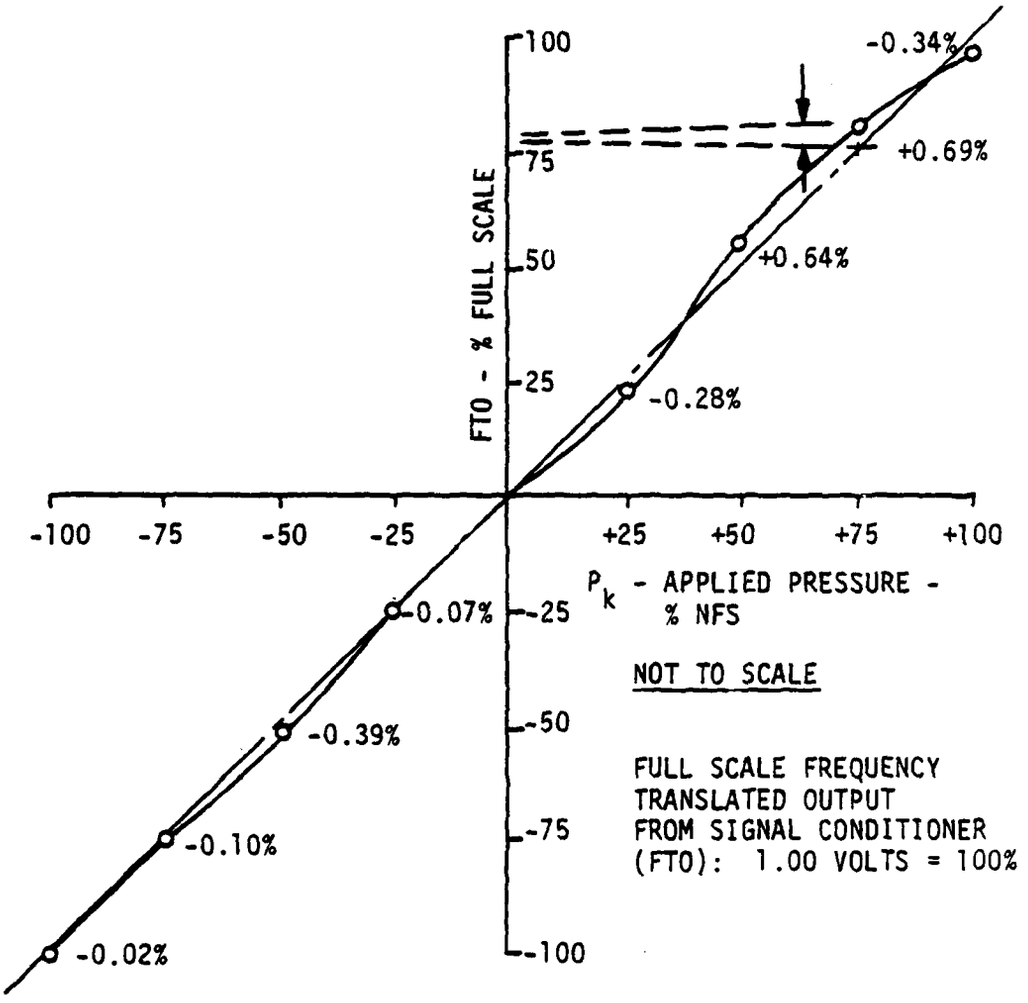

Figure 69. Installed System Pre-Test Calibration Data - Transducer A-15

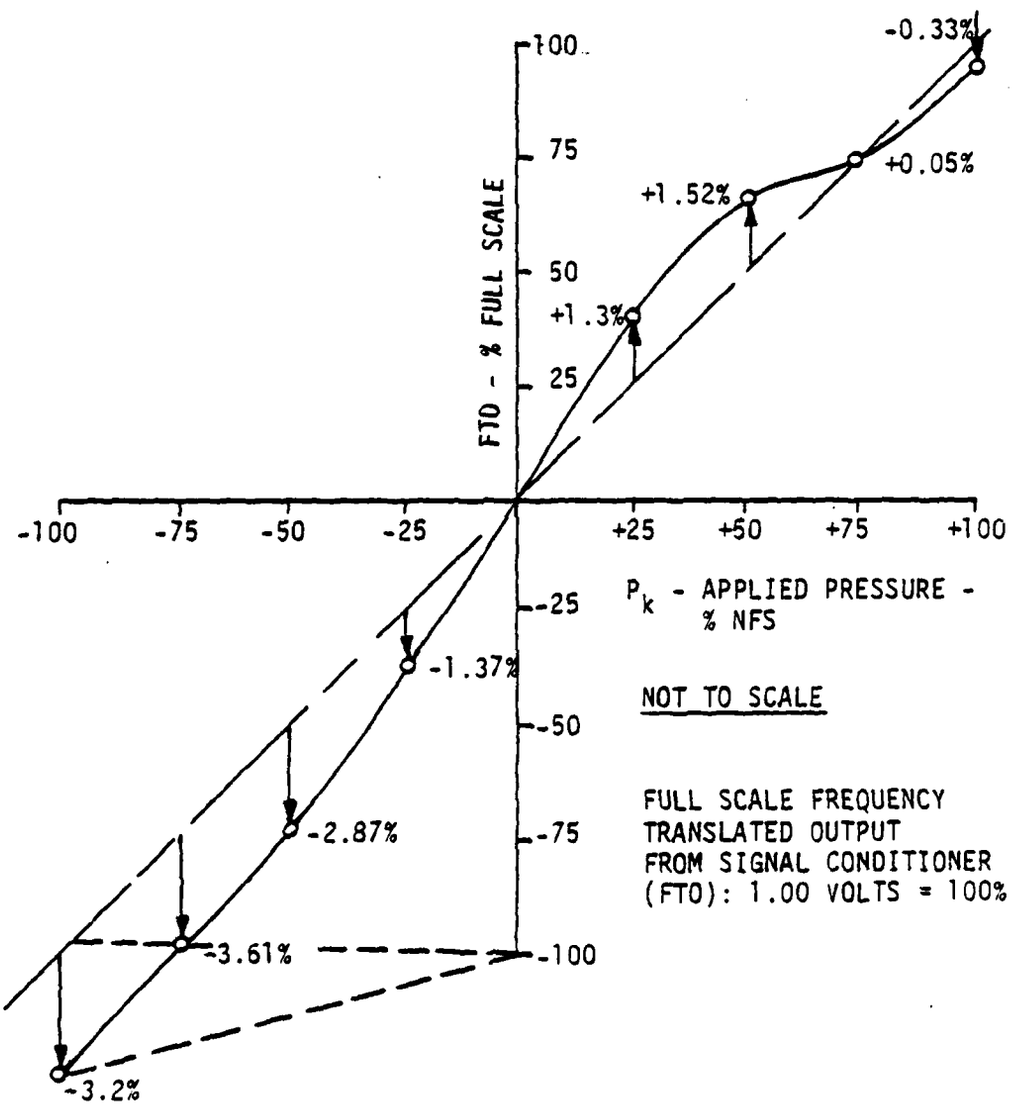

Figure 70. Installed System Pre-Test Calibration Data - Transducer A-19

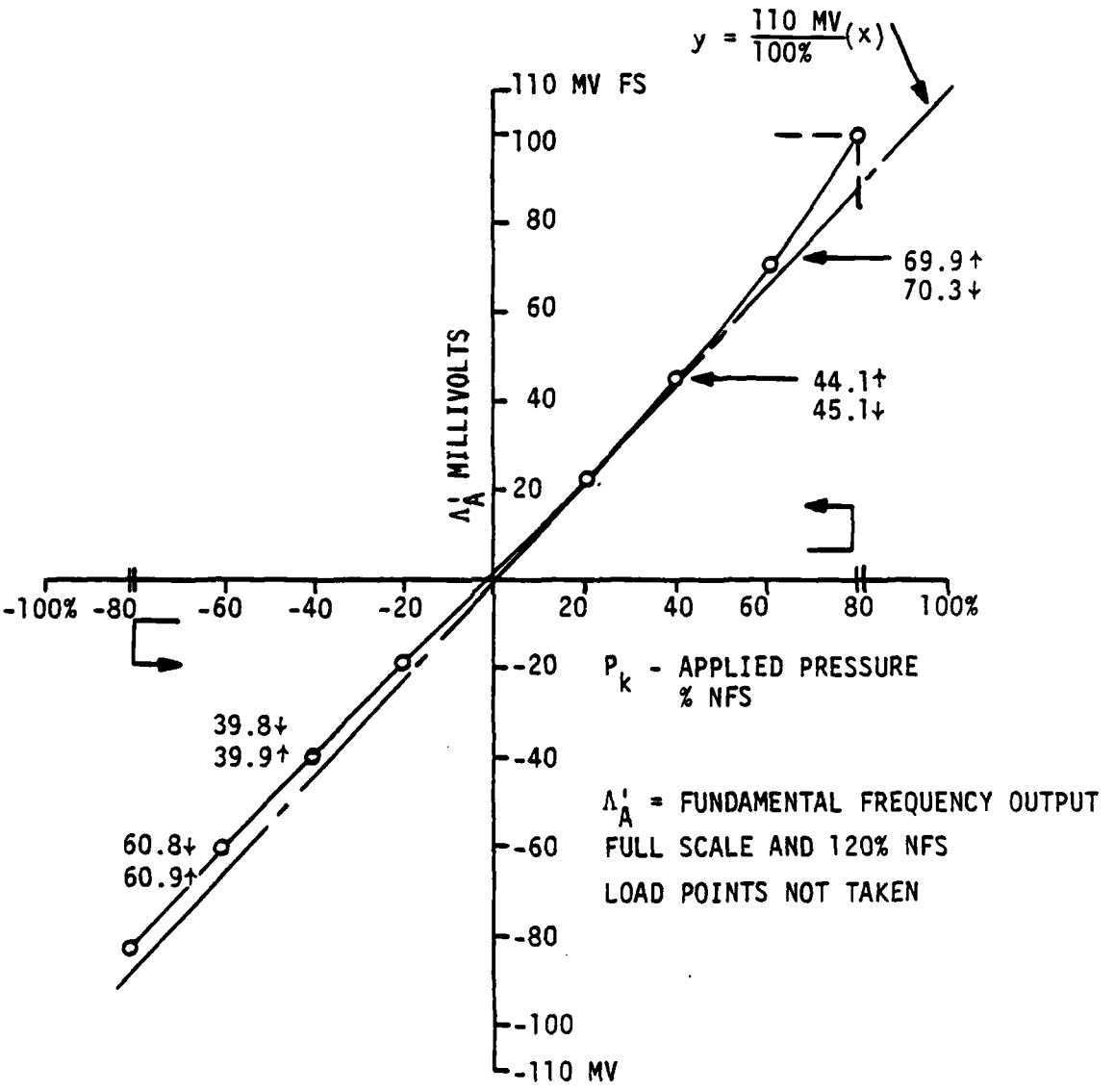

Figure 71. Calibration Data - Transducer B-01

9. CALIBRATION REPEATABILITY

Data at the ± 80 percent NFS load points for transducers A-10, B-01 and B-02 consistently adhered to the four-valued pattern shown conceptually in Figure 72. This complicates the problem of determining repeatability as such. In all cases, the zero returns were quite good, particularly after completion of the load cycle, shown as point Z. The differences in the slow cycle hysteretic behavior of the center plates at zero and at various load points is generally consistent with the findings reported upon in Reference 35, except for zero returns.

The hysteresis spread in the measured values at points A, B, C, and D for transducer C-05 and others of its class was sufficiently low to make it a logical choice for further testing specifically to determine long term calibration stability. This was done by taking zero and ± 80 percent NFS load points from day to day and concluding this sequence with a 13 point calibration. Table 13 is a summary of these test results, giving both fundamental frequency and third harmonic measurements. Normal procedure in all previous testing was to "exercise" the CP by applying pressures of random magnitude and direction before calibration. This procedure was purposely omitted in the tests which yielded the data in columns dated 9/27 and 9/28. The effect of applying a strong "DC" magnetic field was to decrease the effective permeability of the magnetic material in that side and therefore its inductance. This created a large temporary change in zero-measurand output, $\Lambda_{A(0)}$. The span sensitivity was also reduced by about 50 percent. There appears to be no permanent change in transducer output as a result of its exposure to DC or AC magnetic fields of any strength. This appears to be due to the fact that the CP annulus, which is most susceptible to these effects, is well protected by the body mass and also is being continuously "degaussed" by the excitation current. The dominant controllable factor in calibration repeatability appears to be the pretest mechanical stress cycling of the center plate.

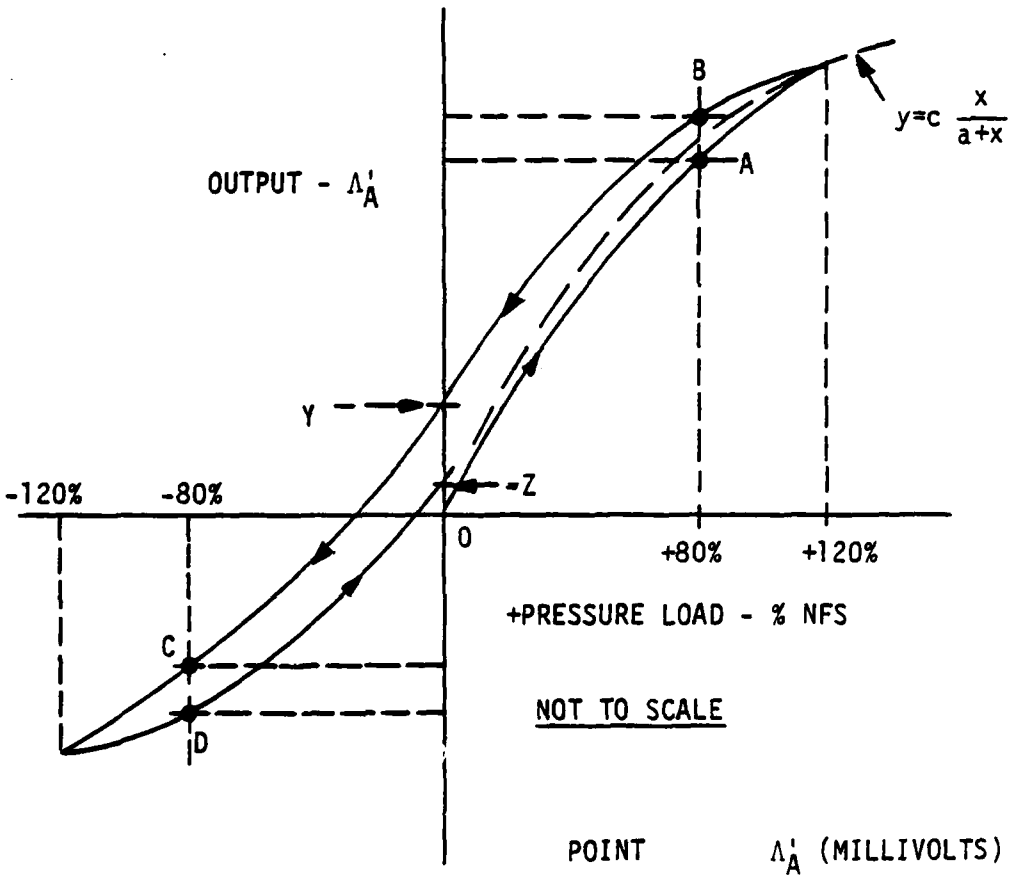

DATA FOR TRANSDUCER B-02

f_{TEST} = 3.0 KILOHERTZ

V_T = 4.0 VOLTS RMS

FUNDAMENTAL FREQUENCY OUTPUT - Λ'_A

POINT	Λ'_A (MILLIVOLTS)
0	0.0
A	+94.5
B	+103.5
Y	+ 0.45
C	-88.8
D	-93.5
Z	+ 0.22

Figure 72. Typical Calibration Characteristic - Variable Reluctance Transducer

TABLE 13

CALIBRATION REPEATABILITY - TRANSDUCER C-05

TRANSDUCER OUTPUT Λ(MILLIVOLTS) Ψ (DEGREES)

PRESSURE % NFS P_k	DATE: 9/25-26* FREQ.	Λ	Ψ	9/27 Λ	Ψ	9/28 Λ	Ψ	9/28+ Λ	Ψ	9/29 Λ	Ψ	10/2 Λ	Ψ
0	$\omega_T(\Lambda_A)$	13.7	∠77°	12.8	∠73	11.8	∠72	255	∠7	13.7	∠78	13.8	∠78
	$3\omega_T(\Lambda_C)$	1.18	∠128	1.12	∠150	1.17	∠146	3.93	∠48	1.18	∠93	1.22	∠127
+80 ↑	ω_T	32.3	∠149	31.4	∠160	32.1	∠150	233	∠9	32.7	∠148	32.4	∠148
	$3\omega_T$	1.51	∠101	1.49	∠122	1.50	∠122	4.18	∠50	1.51	∠67	1.53	∠100
+80 ↓	ω_T	31.9	∠149									32.7	∠148
	$3\omega_T$	1.44	∠95									1.54	∠78
0	ω_T	13.2	∠76									13.8	∠78
	$3\omega_T$	1.24	∠118									1.18	∠126
-80 ↓	ω_T	35.2	∠17	35.2	∠15	35.0	∠14	277	∠6	34.6	∠17	34.2	∠17
	$3\omega_T$	1.19	∠142	1.19	∠178	1.21	∠177	3.66	∠46	1.17	∠125	1.22	∠159
-80 ↑	ω_T	35.2	∠16									34.3	∠17
	$3\omega_T$	1.19	∠142									1.25	∠160
0	ω_T	13.0	∠74	11.5	∠71	13.1	∠74	255	∠8	13.7	∠77	13.8	∠78
	$3\omega_T$	1.21	∠110	1.18	∠148	1.19	∠145	3.93	∠49	1.20	∠88	1.21	∠128°

V_x = 4.002 ±0.006 VOLTS, $\frac{\omega_T}{2\pi}$ = 3005 ±6 HERTZ, ANGLES ∠0 ±0.2°, LOAD = T_{2B}

*NEGATIVE PRESSURE DATA TAKEN ON 9/26. +PERMANENANT MAGNET ATTACHED-ONE SIDE.

Complete data from the final calibration of transducer C-03 dated 10/2 are presented in Table 14 and 15. These may be compared with earlier calibration data on the same transducer in Tables 8 and 11. Data from two calibrations of transducer B-01 taken one week apart are presented in Table 16. Partial data from two calibrations of transducer C-03 using the FTSC and equipment arrangement of Figure 54 are given in Table 17. The signal for the two-phase voltmeter was taken from a point within the FTSC just after the third harmonic filter and before the demodulator. The in-phase and quadrature voltage readings (I and Q) so obtained were intended only for evaluating the usefulness of this instrument as a circuit diagnostic tool, but they nevertheless yielded some interesting repeatability data as well.

10. CALIBRATION SENSITIVITY RATINGS

Single number sensitivity ratings of the transducers were derived for classification purposes from the fundamental frequency test data previously discussed. Measurements at + 80 percent NFS were selected which appeared to be typical or non-remarkable. They are presented in Table 18. Some tests were made with a step-up transformer, $T_{2(A)}$ in Figure 53, which loaded the transducer. Others were made with another transformer, $T_{2(B)}$, which provided a voltage step-down and virtually infinite load impedance. To provide a valid comparison, all data were normalized to equivalent open circuit values as they would have appeared at the transducer output terminals; that is, at terminals M and N in Figure 53. Data taken with the high impedance load, transformer $T_{2(B)}$, may be normalized by multiplying measurements by $\sqrt{5}$. The normalization of data made with transformer $T_{2(A)}$, which loads the transducer, requires that the reflected load impedance be determined, as well as the voltage step-up ratio. The impedance at the primary of this particular transformer in the 2-5 kilohertz range with the secondary open-circuited was determined to be $50\Omega\angle 75^{\circ}$. This is due to leakage reactance in windings and magnetization losses in the core. (Reference 8) It matches closely the fundamental frequency phase angle of the transducer for this reason, and simplifies the load correction process to the calculation of a simple voltage divider. This is shown

TABLE 14

CALIBRATION DATA - TRANSDUCER C-05 (REF: FIGURE 52)

OUTPUT: Λ(AMPLITUDE) MILLIVOLTS /Ψ (ANGLES) DEGREES

APPLIED PRESSURE P_k % NFS	FUNDAMENTAL Λ_A	$/\Psi_A$	2nd HARMONIC Λ_B	$/\Psi_B$	3rd HARMONIC Λ_C	$/\Psi_C$	4th HARMONIC Λ_D	$/\Psi_D$	5th HARMONIC Λ_E	$/\Psi_E$	6th HARMONIC Λ_F	$/\Psi_F$	7th HARMONIC Λ_G	$/\Psi_G$
						DATE: 10/2 --								
0	13.8	/78	.15	/155	1.22	/127	--	--	.14	/168	.002	/191	.21	/192
+40	20.4	/130	.15	/151	1.39	/109	--	--	.20	/168	--	--	.07	/197
+80	32.4	/148	.15	/154	1.53	/100	--	--	.25	/169	--	--	.09	/200
+120	46.4	/156	.30	/154	1.91	/107	--	--	.31	/169	--	--	.11	/202
+80	32.7	/148	.16	/155	1.54	/78	--	--	.25	/169	--	--	.09	/201
+40	20.4	/130	.18	/166	1.38	/110	--	--	.24	/172	--	--	.04	/76
0	13.8	/78	.13	/164	1.18	/126	--	--	.19	/172	.002	/189	.02	/80
-40	21.1	/35	.10	/176	1.11	/148	--	--	.13	/174	.005	/188	.01	/86
-80	34.2	/17	.02	/178	1.22	/159	--	--	.08	/174	.007	/190	--	--
-120	48.4	/9	.08	/175	1.34	/171	--	--	--	--	.009	/190	.03	/201
-80	34.3	/17	.10	/180	1.25	/160	--	--	.08	/175	.008	/189	--	--
-40	21.2	/34	.11	/179	1.13	/146	--	--	.13	/173	.004	/180	.01	/87
0	13.8	/78	.13	/157	1.21	/128	--	--	.18	/173	--	--	.02	/220

V_x = 4.002 ±0.006 VOLTS $\quad \frac{\omega_T}{2\pi}$ = 3005 ±6 HERTZ ANGLES TO ±0.2 DEGREES

- LOW OR UNRELIABLE READING LOAD IMPEDANCE (T_{2B}) ≃ ∞

TABLE 15

FUNDAMENTAL FREQUENCY CALIBRATION DATA

TRANSDUCER C-05

SECOND CALIBRATION DATE: 10/2

% NFS	OUTPUT - MILLIVOLTS /DEGREES					
P_k	Λ_A /Ψ_A	A	A'	A-U	A'-U'	Λ'_A /$\Psi_{A'}$
0	13.8 / 78	+ 2.9	+13.5	(0)	(0)	(0)
+40	20.4 /130	-13.1	+15.6	-16.0	+2.1	16.1 / 172.5
+80	32.4 /148	-27.5	+17.2	-30.4	+3.7	30.6 / 173.1
+120	46.4 /156	-42.4	+18.9	-45.3	+5.4	45.6 / 173.2
+80	32.7 /148	-27.7	+17.3	-30.6	+3.8	30.8 / 172.9
+40	20.4 /130	-13.1	+15.6	-16.0	+2.1	16.1 / 172.5
0	13.8 / 78	+ 2.9	+13.5	0	0	0
-40	21.1 / 35	+17.3	+12.1	+14.4	-1.4	14.5 / 354.5
-80	34.2 / 17	+32.7	+10.0	+29.8	-3.5	30.0 / 353.3
-120	48.4 / 9	+47.8	+ 7.6	+44.9	-5.9	45.3 / 352.5
-80	34.3 / 17	+32.8	+10.0	+29.9	-3.5	30.1 / 353.3
-40	21.2 / 34	+17.6	+11.9	+14.7	-1.65	14.8 / 353.6
0	13.8 / 78	+ 2.9	+13.5	0	0	0

TABLE 16

CALIBRATION REPEATABILITY

VARIABLE RELUCTANCE PRESSURE TRANSDUCER B-01

APPLIED PRESSURE P_k % NFS	DATE	OUTPUT - MILLIVOLTS ∠DEGREES						
		$\Lambda_A \angle\Psi_A$	$\Lambda_B \angle\Psi_B$	$\Lambda_C \angle\Psi_C$	$\Lambda_D \angle\Psi_D$	$\Lambda_E \angle\Psi_E$	$\Lambda_F \angle\Psi_F$	$\Lambda_G \angle\Psi_G$
0	20 June	14.5 ∠206	0.23 ∠167	0.53 ∠292	.06 ∠303	0.06 ∠351	0.02 ∠186	0.1 ∠102
	27 June	14.8 ∠205	1.37 ∠356	0.45 ∠278	.09 ∠193	0.1 ∠27	0.03 ∠268	0.09 ∠110
+80	20 June	91.2 ∠159	2.5 ∠317	4.4 ∠235	0.13 ∠323	0.57 ∠301	0.13 ∠46	0.2 ∠27
	27 June	112 ∠177	2.59 ∠343	4.23 ∠238	0.09 ∠345	0.9 ∠343	0.02 ∠255	0.45 ∠79
-80	20 June	78 ∠348	0.53 ∠187	3.4 ∠52	0.03 ∠194	0.78 ∠173	0.04 ∠247	0.25 ∠200
	27 June	71.3 ∠350	1.4 ∠348	3.1 ∠69	0.1 ∠165	0.73 ∠163	0.03 ∠27	0.26 ∠230
0	20 June	16.0 ∠204	0.25 ∠168	0.58 ∠288	0.07 ∠300	0.05 ∠2	0.02 ∠245	0.1 ∠92
	27 June	14.9 ∠205	1.26 ∠356	0.41 ∠282	0.08 ∠202	0.06 ∠30	0.04 ∠268	0.1 ∠104

V_T = 4.004 ± 0.003 Volts

Angles to ± 0.2 Degrees

$\frac{\omega_T}{2\pi}$ = 3000 ± 2 Hertz

Output Loaded with Transformer T_{2A}.

TABLE 17

CALIBRATION REPEATABILITY - INSTALLED SYSTEM
VR TRANSDUCER AND SIGNAL CONDITIONER
(REF: FIGURE 54)

TRANSDUCER C-03

PRESSURE - P_k INCHES WATER	FIRST CALIBRATION OUTPUTS MILLIVOLTS I*	Q*	VOLTS FTO	SECOND CALIBRATION OUTPUTS MILLIVOLTS I*	Q*	VOLTS FTO
0	0.00	-0.18	+0.012	-0.02	-0.09	+0.012
-1	-0.82	-0.08	-0.468	-0.82	-0.08	-0.464
-2	-1.62	+0.02	-0.933	-1.62	+0.06	-0.930
-3	-2.47	+0.14	-1.414	-2.43	+0.15	-1.400
-4	-3.30	+0.30	-1.869	-3.30	+0.20	-1.857
-5	-4.10	+0.30	-2.340	-4.15	+0.30	-2.337
-6	-4.90	+0.40	-2.795	-4.90	+0.40	-2.782
-7	-5.70	+0.55	-3.250	-5.70	+0.55	-3.237
-8	-6.50	+0.65	-3.717	-6.45	+0.65	-3.690
-9	-7.20	+0.80	-4.162	-7.20	+0.80	-4.146
-10	-8.05	+0.85	-4.625	-8.00	+0.85	-4.603
-9	-7.25	+0.80	-4.177	-7.20	+0.80	-4.146
-8	-6.54	+0.70	-3.723	-6.50	+0.65	-3.701
-7	-5.70	+0.50	-3.264	-5.70	+0.55	-3.248
-6	-4.90	+0.40	-2.807	-4.90	+0.40	-2.791
-5	-4.15	+0.30	-2.349	-4.15	+0.30	-2.338
-4	-3.30	+0.30	-1.884	-3.30	+0.30	-1.878
-3	-2.50	+0.08	-1.429	-2.49	+0.17	-1.417
-2	-1.67	+0.02	-0.949	-1.67	+0.08	-0.944
-1	-0.86	-0.02	-0.484	-0.85	-0.06	-0.477
0	-0.02	-0.18	+0.004	-0.02	-0.18	+0.008

*6 Kilohertz Signals - RMS Values

TABLE 18

MEASURED CALIBRATION SENSITIVITY VALUES - FUNDAMENTAL FREQUENCY

VARIABLE RELUCTANCE PRESSURE TRANSDUCERS

$$\text{Sensitivity } S = \Lambda'_{A\ (+0.8)} \times \frac{1}{0.8} \div V_x$$

TRANSDUCER IDENT.	EXCITATION VOLTS V_T	$\frac{\omega_T}{2\pi}$(KHz)	S $\frac{MV}{V}$ Full Scale	S' $\frac{MV}{V}$/PSI
A-01	2	2	29.4	5.9
A-10	5	2	17.2	34.5
B-01	4	3	31.8	63.6
B-02	4	3	34.0	68.0
C-05	4	3	21.4	42.7
C-10	5	2	33.5	0.67
F-01	5	3	131.9	26.4

schematically in Figure 73. The effective source impedance, Zg, has been previously determined to be $Z_{T/4}$, where Z_T values are available from Table 6. Since the transformer T_{2A} has a voltage step-up ratio of $\sqrt{\frac{400}{30}}$, the actual open circuit fundamental frequency output of the transducer across terminals M-N is 0.274 times that obtained from the voltage divider calculation. Therefore

$$V_{oc} = V_{meas} \times 0.274 \left(\frac{Z_G + Z_L}{Z_L}\right)$$

In the case of transducer B-02, $\Lambda'_{A(+0.8)}$ was measured at 94.5 millivolts

$$V_{oc} = 94.5 \times 0.274 \times \frac{167 + 50}{50} = 112.4 \text{ millivolts}$$

This may be compared with the actual measurement at open circuit conditions of 113.3 millivolts. This current mode of operation might be desirable where effects of lead shunt capacities, such as C_c in Figure 51, or electrostatic noise pickup are objectionable. This loading changes the relative amplitude and phase of the various harmonics disproportionately. Data for transducer B-02 in Table 19 illustrate this point.

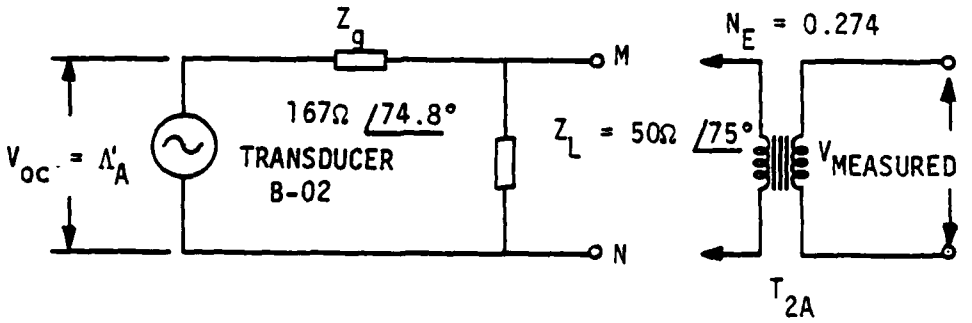

Figure 73. Transducer Output Load Circuit

TABLE 19

ELECTRICAL OUTPUT LOADING EFFECTS -

VARIABLE RELUCTANCE PRESSURE TRANSDUCER B-02

CALCULATED OUTPUT AT TRANSDUCER TERMINALS M&N (FIGURE 53)

APPLIED PRESSURE P_k % NFS	ELECTRICAL LOAD	OUTPUT - MILLIVOLTS ∠DEGREES						
		$A'_A \angle \Psi'_A$	$A_B \angle \Psi_B$	$A_C \angle \Psi_C$	$A_D \angle \Psi_D$	$A_E \angle \Psi_E$	$A_F \angle \Psi_F$	$A_G \angle \Psi_G$
0	T_{2A}*	0	.02 ∠238	0.6 ∠0	.01 ∠46	.08 ∠178	.01 ∠76	.04 ∠173
	T_{2B}**	0	.38 ∠354	4.3 ∠216	.11 ∠108	.38 ∠344	.04 ∠291	.38 ∠220
+80	T_{2A}	25.9 ∠353	.13 ∠334	1.48 ∠255	.04 ∠49	.32 ∠166	.03 ∠58	.14 ∠176
	T_{2B}	113.3 ∠351.5	.18 ∠145	3.24 ∠335	.13 ∠131	.83 ∠177	.02 ∠79	.22 ∠91
-80	T_{2A}	24.3 ∠177	.1 ∠170	.63 ∠32	.01 ∠150	.14 ∠351	.01 ∠68	.06 ∠303
	T_{2B}	104.6 ∠173	.85 ∠345	9.8 ∠202	.16 ∠85	1.56 ∠348	.16 ∠227	.92 ∠231
0	T_{2A}	0	.02 ∠231	.25 ∠270	0	.08 ∠177	.01 ∠75	.04 ∠120
	T_{2B}	0	.3 ∠355	4.4 ∠290	.11 ∠95	.4 ∠344	.09 ∠292	.03 ∠274

* T_{2A}: $Z_L = 50 \angle 75^\circ$ (Ω). All measurements of A were multiplied by $\sqrt{\frac{30}{400}}$.

** T_{2B}: $Z_L = \infty$ (Ω). All measurements of A were multiplied by $\sqrt{5}$.

$V_T = 4.000 \pm .005$ Volts

$\frac{\omega_T}{2\pi} = 3002 \pm 4$ Hertz

Angles to ± 0.3 Degrees

11. OTHER OBSERVATIONS

A small but measurable droop in excitation supply voltage, V_X, was observed as loads were applied during calibrations made with the FTSC equipment arrangement similar to that shown in Figure 54. This droop, measured to be about 50 millivolts (or 1%) at a pressure load of $\pm$ 100 percent NFS, is caused by the change in loading on the excitation power supply from the pressure-dependent inductance L_c in Figure 24. Voltage droop was not present in tests using the equipment of Figure 52. This was due to the very low output impedance of the amplifier and transformer T_1, shown in Figure 53, as measured at terminals E and G. This supply actually represents a "brute force" approach which would be neither practical nor necessary outside the laboratory. The remarkable zero returns exhibited by transducers which otherwise show poor or undesirable calibration characteristics are probably due to the continuous dithering of the CP by the excitation power. Proof of this assertion would be difficult and was not attempted. The calibration of transducer B-02 under open-circuit conditions was made several months after the calibration with the 50 ohm load of transformer T_{2A}. The open-circuit output calculated from the earlier measurements at calibration point "A", Figure 72, was 112.4 millivolts at 353 degrees. The actual open-circuit measurement at the same calibration point several months later was 113.3 millivolts at 352 degrees. The long-term stability of this model is undoubtedly much better than indicated by the data for unit B-01 in Table 16. The center plate of that transducer was probably damaged or defective before any calibration were made.

SECTION XI

PERFORMANCE WITH NON-STATIONARY PRESSURES

1. FACTORS LIMITING FREQUENCY RESPONSE

The inherent response mechanism of a VR transducer - FTSC channel has been defined sufficiently to consider the upper frequency limitations of the method. It will be assumed temporarily that pressures of any frequency may reach the transducer CP, thereby eliminating tubing lag time uncertainties. Values for maximum allowable phase and amplitude errors associated with a desired maximum data frequency $\omega_{f(max)}$ must then be specified. There are a number of system characteristic frequencies which limit $\omega_{f(max)}$.

ω_M is the frequency of predominant mechanical resonance of the transducer center plate, usually the first circular bending mode. If the damping characteristics are known, the response errors may be corrected reliably up to about 80 percent of ω_M. Normally, however, damping characteristics are not sufficiently predictable or controllable to give reliable results at such high frequencies. A commonly used rule of thumb sets a maximum useful limit on $\omega_{f(max)}$ due to the cause at $\omega_M/5$.

ω_a is the practical upper frequency limit of pressure data, p(t), which will "survive" the frequency translation ("demodulation") operation and appear at the output of the FTSC as r(t). This frequency is dependent on ω_c, and can be expressed as ω_c/N. The value of N is constrained on the low end by the possibility of creating spurious DC and low frequency components in r(t) due to frequency folding (Reference 36) In theory, N may approach a minimum value of 2, but in practice, higher values are necessary, with a value of 5 commonly being used. This conflicts with the desirability of keeping N as low as possible to minimize ϵ_p, the lost high frequency information. If very sharp cut-off low pass filters are available, N values of 3 or 4 might be allowable. (Table 1). Note that in AM radio broadcasting, this problem does not become evident, since a useful maximum audio (data) frequency, ω_a, of 10 kilohertz and a typical carrier frequency, ω_c, of 1 megahertz constitute an N value of 100, which

is easy to realize. This is also true of many capacitive transducers, since they usually require a high excitation frequency to produce a useful output signal amplitude.

ω_b is the frequency of forced vibration of the center plate due to unequal forces of magnetic pull toward the pole pieces set up by the alternating current excitation in the coils. An imbalance in the two opposing forces could be created by minute differences in coil or airgap geometry, asymmetry of spring rates in the CP on either side of the neutral position, or a deflection of the CP due to applied pressure. Asuming the waveform of the applied excitation ampere-turns causes a sinusoidal flux density, the unbalance in the flux density, $\beta'(t)$, will be $\beta'_{max}\sin\omega_c t$. A current will be induced in the CP which is proportional to $\frac{d\beta'}{dt}$, or $\omega_c\beta'_{max}\cos\omega_c t$. This current will react with the original differential flux density to cause a force which is proportional to $\beta' xi$, or $(\beta'_{max}\sin\omega_c t)\cdot(\omega_c\beta'_{max}\cos\omega_c t)$. Since this reduces to $1/2\omega_c(\beta'_{max})^2\sin 2\omega_c t$, the force and deflection fundamental frequency, ω_b, will be equal to $2\omega_c$.

ω_v is the frequency of acoustic resonance of the internal cavity of the transducer. Most VR transducers, such as A-10, B-01, and C-05 are constructed with external extension pipes for attaching pneumatic tubing. Information on acoustic resonance of these transducers standing alone is of limited usefulness. It does, however, provide an indication of the upper response limit of any pneumatic system which includes the transducer. ω_v will be affected by gas composition because of specific heat effects. All of the sample VR transducers except D-01 and F-01 have complex internal pneumatic paths which include branches for bleeding hydraulic fluid. This makes it virtually impossible to determine the acoustic behavior of these transducers by mean of analysis.

Simultaneous consideration of the above frequency-dependent effects and stimulus-response relationships shows the complex nature of the practical upper limit of $\omega_{f(max)}$. An additional constraint will result from any non-linearity of the mechanical force-deflection relationship in the CP. Unless ω_M differs greatly from ω_b, "beats", or sum and difference frequencies, may be created mechanically in the CP and appear in the FTO. Since both excitation frequency and CP resonance often fall in the range from 2 to 20 kilohertz, creation of beats is a distinct possibility. Spurious signals of several thousand Hertz observed by the author of Reference 10 in the FTO of his capacitive transducer were attributed to the presence of electrostatic attraction forces. Fluctuating pressures containing frequency components in the same range might also cause additional beats unless they are removed in the connecting tubulation.

The concept of ω_a, the maximum pressure data frequency which will "survive" the frequency translation or "demodulation" process, was discussed in Section IV using well-known theory from amplitude modulation communication systems. This theory also defines the effects of other elements in the path of the signal in the ω_c regime through the FTSC upon signals corresponding to non-stationary pressures in the original frequency regime, ω_f. This regime is called the "baseband" in communications work. The other elements or devices in the ω_c signal path may include active gain devices, circuit stray reactances, notch networks and transformers. Both the amplitude and phase characteristics, of the kind shown in Figures 4 and 55, will affect the amplitude and phase relation between the original pressure, p(t), and the processed signal, r(t).

2. CENTER PLATE VIBRATIONAL CHARACTERISTICS

Center plate resonant frequency values for commercially available VR transducers are frequently stated with the qualification "nominal", implying that the values are estimations or approximations based on physical dimensions. The electrical arrangement of Figure 74 was devised in an attempt to detect and possibly measure mechanical resonance of the CP in-place in the transducer. The three types of low range (0.5 PSID)

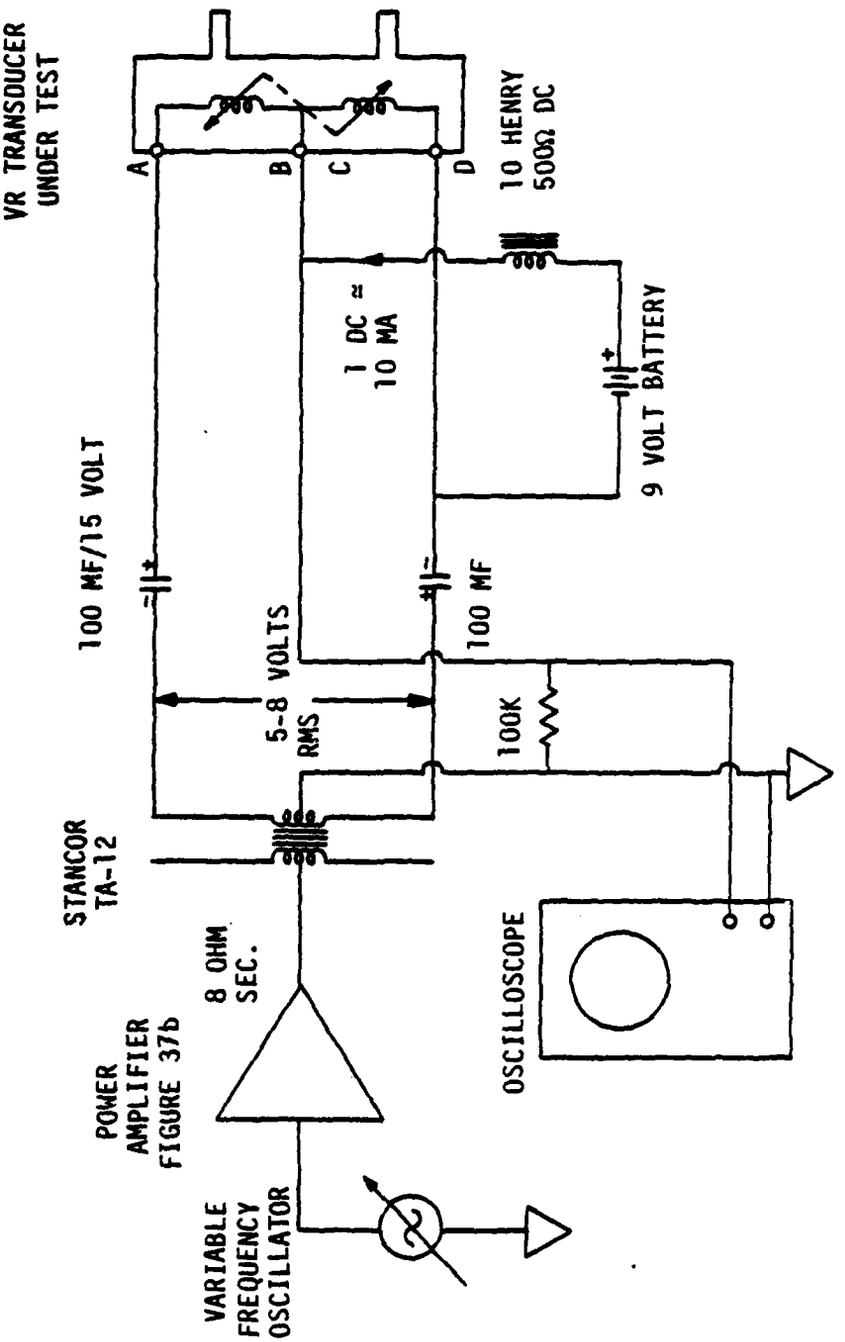

Figure 74. Center Plate Mechanical Resonance Test Scheme - Variable Reluctance Pressure Transducer

transducers emitted double-frequency sound under normal operating conditions, particularly units B-01 and B-02. The addition of the DC component of current in coil (B-C)-D increased the audible vibration at the fundamental forcing frequency. The character of the sound changed somewhat with pressures applied. Measurements of ω_M were tried only at atmospheric pressure.

The test on C-05 produced audible output from several hundred to about 12,000 Hertz. There were noticeable peaks in electrical output induced in coil A-(B-C) due to motion of the CP. These peaks were located at 600, 3400, and 9900 Hertz. The peak at 600 Hertz was rather broad and the increase in audible output was not pronounced. The peak in electrical output virtually disappeared when one or both pressure ports were partially or fully stopped off, but the sound became very prominent. This rise in sound emission is due to acoustical resonance within the CP chamber, internal air passages and the external connection pipes, which extend one-half inch out of the body. There was a moderately broad peak in electrical signal at 3400 Hertz. With one or both ports stopped off, this peak shifted to 3800 Hertz. There was a very sharp electrical peak of predominately sinusoidal character at 9900 Hertz, accompanied by a sharp rise in sound emission. The electrical peak was not affected by covering the ports.

The disparity in resonance sharpness at the 3400 and 9900 Hertz peaks suggests that these are the locations of two different shape modes and not a harmonic relationship. They both seem to be genuine mechanical resonances. However, the frequency ratio 9900/3400 does not corespond to any of the mode shapes given in Reference 22 for circular plates clamped at the circumference. This response is probably due to shape or stress irregularities in the CP induced in manufacturing similar to those exhibited by unit C-03 under steady state conditions (Figure 59). The moderate shift in frequency of the mechanical resonance at 3400 Hertz caused by changes in air compression damping is typical of low "Q" resonant systems.

Similar results were obtained in tests on transducers A-10 and B-01. The results are summarized in Table 20.

TABLE 20

VIBRATIONAL CHARACTERISTICS OF CENTER PLATE SUSPENSIONS
LOW RANGE VARIABLE RELUCTANCE PRESSURE TRANSDUCERS

Transducer Identity	Acoustical Resonance ω_V(Hertz)	Principal Open/Closed ω_M(Hertz)	Higher Modes (Hertz)
A-10	700	6700/6250	None
B-01	570	4800/5000 and 6900/6900	15K
C-05	600	3400/3800	9900

The overall construction of the other classical type VR transducers was different from the low range types and no acoustical resonances were detectable. This is a shortcoming of the test method. These transducers were higher pressure range types and vibrations were not evident with the limited excitation forces available. One exception was unit C-11, which is a large, bulky unit rated at $\pm$ 10 PSID NFS. It exhibited a mechanical resonance at 5800 Hertz.

3. RESPONSE MEASUREMENT TECHNIQUES

Attention was then directed toward the possibility of making end-to-end response calibrations using a periodic pressure function as the test measurand. The two items of special test equipment needed are a variable-frequency generator of pneumatic or hydraulic pressures and an FTSC having known phase and amplitude throughput characteristics. Actual electrical measurements should be made on the FTSC to define these characteristics. The amplitude (gain) and phase characteristics of AC servo systems are important because they affect system stability and response under closed loop conditions. Methods and test equipment for bench-testing AC servomechanisms can be used to test the response of FTSC's provided they will operate at the higher center frequencies used in VR transducer work. Any electrical signal generator which will

generate a "carrier" frequency, ω_c, amplitude modulated with a baseband frequency, ω_f, which can be varied from near zero to ω_c/N can be used to measure directly the ω_f response of an FTSC. This method is illustrated in Figure 75. The impedance, Z_D, is a simulation of the VR transducer which should be included in cases where loading by the FTSC input circuit might be significant. This test method will eliminate all unknowns in the electrical response of the FTSC and pave the way for making end-to-end pressure response tests.

If the potential upper frequency capability of any VR transducer design is to be realized in practice, the commonly used method of introducing the pressure medium into the CP chamber must be changed. The awkward external tubulation made necessary by the radial connecting pipes, shown in Figure 1, can be eliminated by drilling one or both access ports axially through the center of the body and pole piece. This method of construction was used in the case of transducer D-01, which was available with an internal opening in each body half, or with external threaded nipples. The internal opening geometry is more compatible with the close coupling arrangements needed with high-frequency pressure calibrators, and would reduce or eliminate the application problems at medium frequencies caused by internal acoustical resonances exhibited by transducers A-10, B-01 and C-05.

The "dynamic" pressure generator for calibrating transducers described in Reference 37 has a useful upper limit, $\omega_{f(max)}$, of over 2000 Hertz. It is a hydraulic device, thereby eliminating calibration uncertainties caused by gas compressibility. Much useful information about frequency-dependent effects can be obtained using methods which provide only a relative indication of output as frequency is varied, rather than one which is highly accurate in the absolute sense. The method described in Reference 37 is to compare the output of the transducer under test with that of a "reference" transducer which behaves in a known manner with respect to frequency. A flush-mounted piezoelectric transducer is used as a reference in this and many other calibration schemes because of its very high resonant frequency and because its signal output, although very low, is exceptionally uniform in

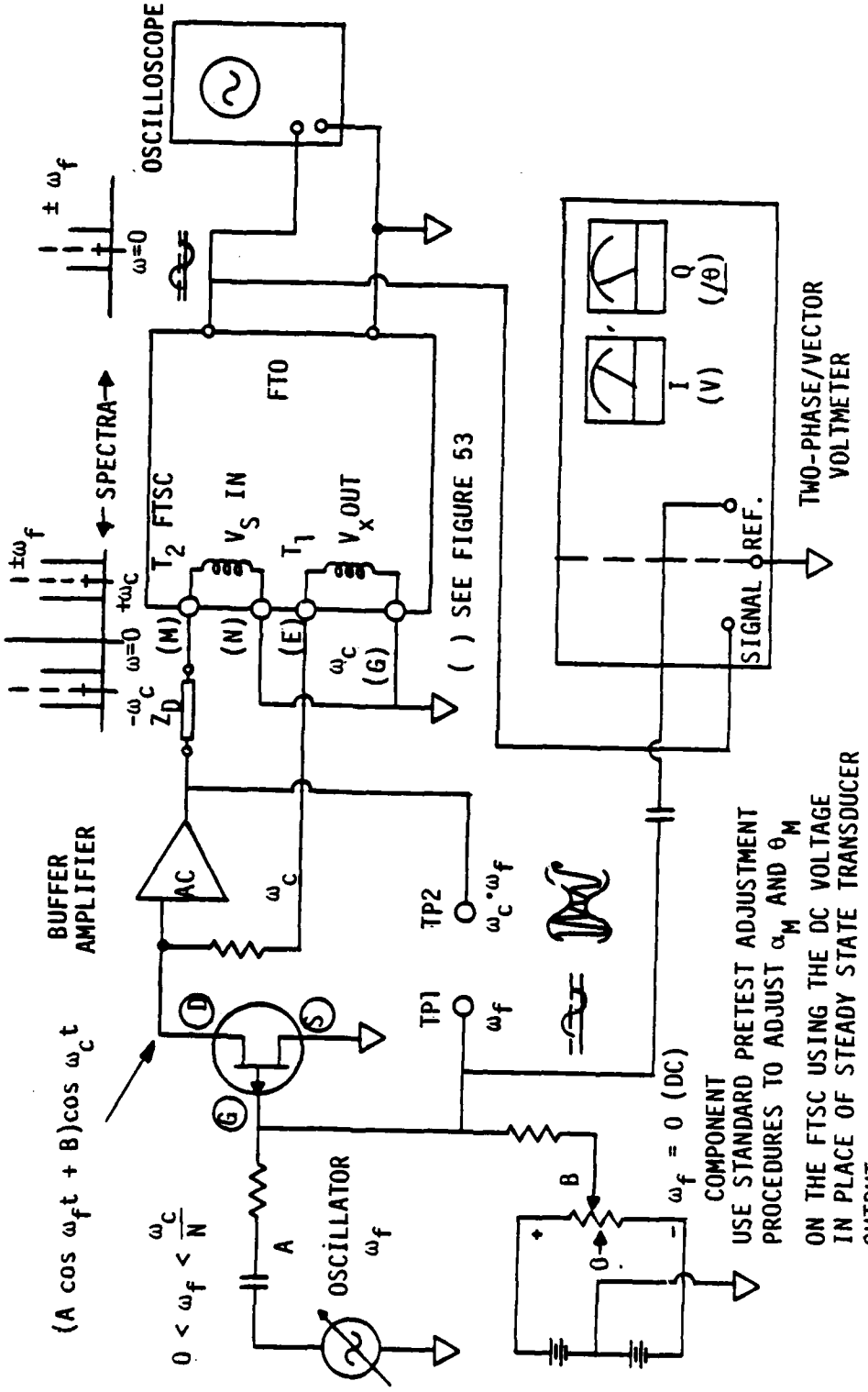

Figure 75. Experimental Frequency Response Test Scheme - Frequency Translating Signal Conditioner

amplitude and phase with respect to frequency above several Hertz. Research tests on the response of a VRT/FTSC channel would consist of comparisons of both phase and amplitude of the FTO with the output of the piezo-electric transducer channel. To eliminate electrical uncertainties at the high frequencies, a special high-frequency FTSC would be required, and the temperature of the transducer must be closely controlled. The total calibration error in the system described in Reference 37 is stated as $\pm$ 4 percent in the frequency range from 35 to 2000 Hertz. The void in the spectrum from zero to 35 Hertz could be filled by a positive volumetric displacement pneumatic device; that is, one which generates the function $\Delta V/V$. Such a device can be constructed with an eccentric-operated bellows driven by a variable speed motor. A steady-state component can be superimposed on the fluctuating pressure. Continuity with respect to frequency is assured when there is a substantial overlap region of frequencies in which the phase and amplitude response of the high-frequency-limited transducer (such as "diaphragm" types) and the low-frequency limited piezo-electric reference transducer are identical. This continuity, combined with the high accuracy of steady-state (zero-frequency) test methods would give a very reliable account of the channel response over the entire range from zero to at least 1000 Hertz. The upper frequency limit would be set by the electrical parameter, ω_c/N, and by the volumetric change $\Delta V/V$ in the VR transducer due to center plate compliance[1].

Reference 37 and three other papers describing periodic pressure generators of different kinds have been synopsized for the reader's convenience in Appendix C.

Due to the complexity and scope of the effort necessary, no actual response tests were performed in this program.

---

[1] For example the manufacturer of transducers B-01 and B-02 quotes the volumetric change under NFS pressure as 1.2×10^{-4} cubic inch out of a total of 2.6×10^{-3} cubic inch.

AD-A130 695 EVALUATION OF THE VARIABLE RELUCTANCE TRANSDUCER/CARRIER AMPLIFIER METHOD. (U) AIR FORCE WRIGHT AERONAUTICAL LABS WRIGHT-PATTERSON AFB OH

3/3

UNCLASSIFIED D L MCCORMICK FEB 83 AFWAL-TR-82-2100 F/G 14/2 NL

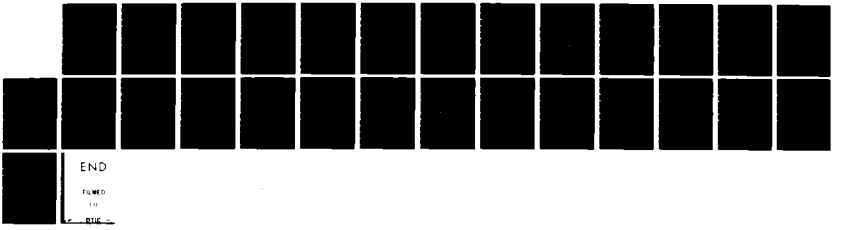

END

FILMED

DTIC

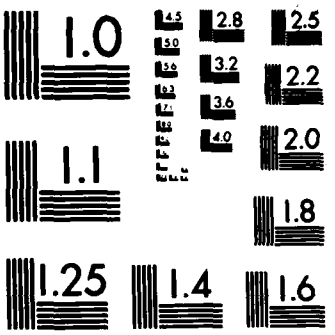

4. OUTPUT FILTERS

By convention, output filters are included as an integral part of most FTSC's. The need for these filters was discussed in Section IV. By including these filters in his equipment, the vendor of FTSC's of necessity makes some assumptions as to the type of output device which the customer will use. Since these filters operate directly in the baseband or ω_f frequency regime, their effects on the data may be determined by straightforward electrical circuit analysis. The use of active ouptut filters has become common. In many cases, the same circuits are used to provide post-demodulation voltage or power gain. Since they must pass the steady-state component, r_s, the DC stability and common mode performance requirements for FTSC output filters are the same as for any other signal conditioner. This puts the burden of isolation from grounds and other signal lines on the DC power supplies for the filter circuitry rather than on the "demodulator" transformers, shown as T3 and T4 in Figure 27. The stability of these DC supplies directly affects the zero-level and span (calibration) of the entire channel, so they must possess very good voltage regulation. The signal conditioner used in the work described in Reference 11 used active low-pass output filters at the $\pm$ 5 volt level, with one output terminal of each channel connected to equipment ground ("single-ended"). Although the ouput data lines were several hundred feet long, the differential isolated input amplifiers in the data acquisition system were very effective in eliminating ground loops and other noise problems.

SECTION XII

DESIGN IMPROVEMENTS AND APPLICATION TECHNIQUES FOR VARIABLE RELUCTANCE PRESSURE TRANSDUCERS

Possible improvements which might increase the precision of measurements made with VR pressure transducers range from minor changes in circuit and mechanical installation details to major changes in structural design and materials. Table 21 summarizes some of the more obvious changes and gives some specific examples. It appears that incorporating such improvements might also result in some loss of the inherent simplicity of the basic design. When considering changes to improve performance, it is desirable to retain as much as possible the present qualities of corrosion resistance, electrical feed-through integrity, low internal volume, CP replaceability, and ruggedness.

Center plate manufacture is a critical factor in the performance of these transducers. The center plates of both the capacitance and VR transducers constructed by the author of Reference 10 were made by machine turning, as illustrated in Figure 12(e). The deflection characteristics and stability were reported to be quite satisfactory, but the author first found it necessary to reduce instability due to high local assembly stresses by cutting notches in the edges of the thick outer section. This method seems preferable to manufacturing CP's from flat stock. It also allows for the possibility of contouring the cross section in the region of the pole pieces to improve linearity. The response to thermal shock of a transducer having a CP of this kind should be quite good.

Whenever the application will allow, a number of performance improvements could be obtained by using the tandem arrangement of identical transducers shown in Figure 76 instead of a single transducer. When arranged as shown, the deflections of the center plates of both transducers VRT-1 and VRT-2 in response to acceleration will cause a net electrical output of zero across terminals (B-C) and (B'-C'). By cross-connecting pressure ports, a positive pressure applied to P_1 and P_2' will

TABLE 21

POSSIBLE DESIGN IMPROVEMENTS

VARIABLE RELUCTANCE PRESSURE TRANSDUCERS

IMPROVEMENT	BENEFIT
1. GEOMETRIC CHANGES	
a. Pole Piece Shapes	A, F
b. Cross Sectional Shape of Center Plate (CP)	A, C
c. Body Metal Removal	A, B
2. CONSTRUCTION DETAILS	
a. Machined, Slotted CP	B, C, F
b. Dual Tandem Integration (One Piece)	B, D
c. Cable Attachment Details	E
d. Axial Pressure Entrances	A, G
3. NEW MATERIALS - Body and/or CP	A, B, C
4. ELECTRICAL CIRCUIT CHANGES	
a. Low Z Coils (Current Mode) - Less Turns - Larger Wire	A, D, G
b. Temperature Compensating Wire	B
c. Reduce AC resistance (Wire Material, Shape Factor)	A, D
d. β-Sense Coil Feedback - See Figure 78	B

BENEFITS

A. Higher Frequency Operation
B. Stability
C. Precision and Mechanical Hysteresis
D. Increased Output Signal
E. Durability
F. Linearity
G. Miniaturization

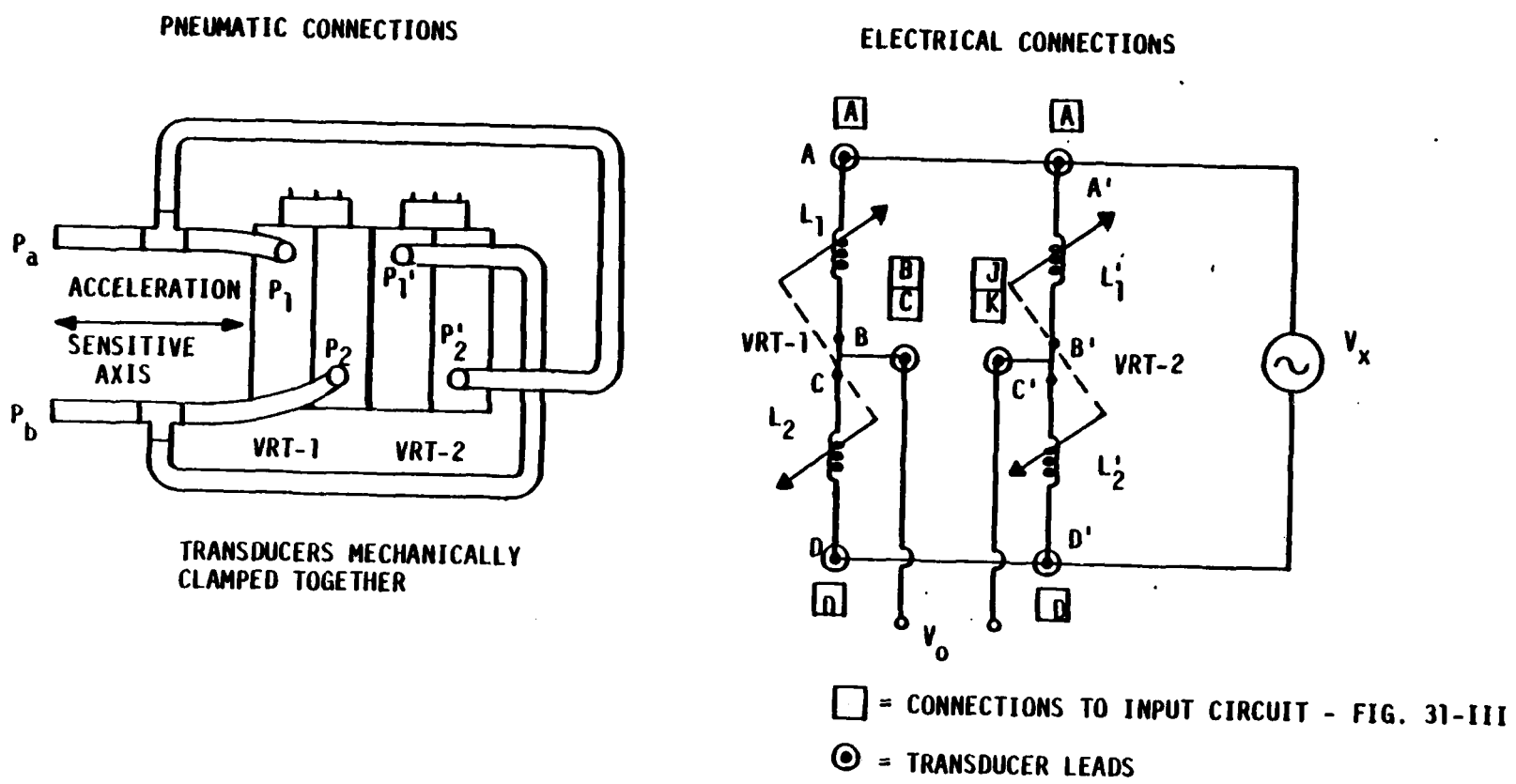

Figure 76. Tandem Installation - Variable Reluctance Pressure Transducer

increase both L_1 and L_2' and decrease L_2 and L_1', causing an electrical output twice that of a single transducer. Moreover, the currents in leg $(L_1 + L_2)$ and leg $(L_1' + L_2')$ will have the same harmonic content giving a better null of all harmonics at zero input pressure, as well as the fundamental. Asymmetry of calibration slopes about the origin may be reduced by proper pairing of transducers. In the case of a new design, a single case half might be machined so as to include two pole-piece recesses side-by-side, giving a one-piece dual element assembly.

This tandem arrangement has the following disadvantages:

- It complicates the pneumatic inlet geometry.[1]

- The load on the power supply is doubled, and its impedance as a signal source is doubled.

- It requires an additional lead wire per channel.

- For a given design of the active elements, the bulk and materials cost will be doubled.

A conceptual design of a CP incorporating both the notched machined structure and a side-by-side dual element is shown in Figure 77a. Another possibility for improving electrical performance at high frequencies would be a CP constructed of high-resistivity or non-conductive material having a thin deposited or bonded layer of magnetic material of optimum shape for the flux return paths. This concept is illustrated in Figure 77b. The return flux paths for each side of the transducer are separated, reducing the mutual coupling between the coils. The relatively small magnetic cross section would require the use of relatively low excitation flux densities, but the signal output level would still be adequate because of the reduction in eddy current losses.

---

[1] If the second transducer is used only as an anti-acceleration dummy, no pneumatic connections are needed and an internal pneumatic bleed between the two sides of the CP would be provided. The electrical circuit would then become a two-active arm bridge with dummy impedances like that of Figure 31-III.

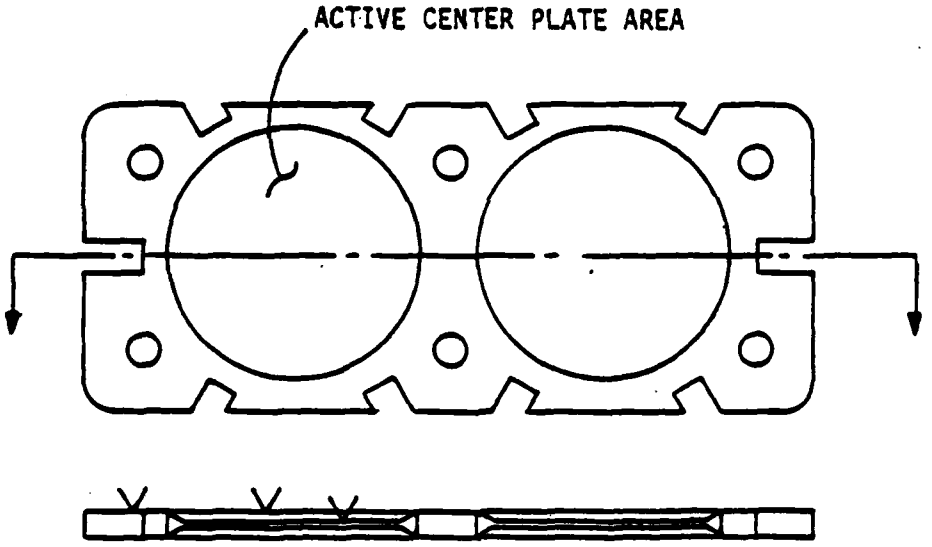

A. MACHINED DUAL ELEMENT

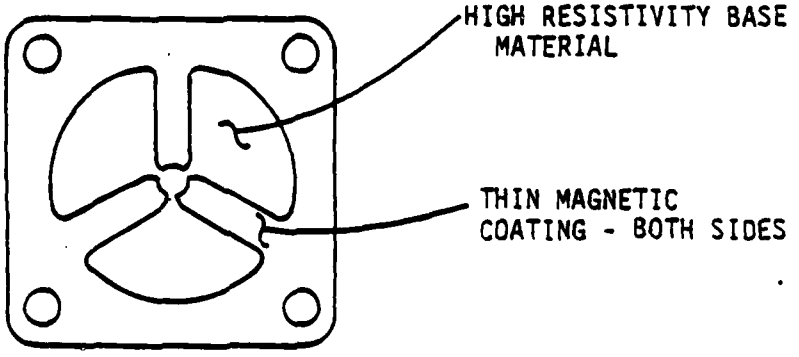

B. HIGH RESTIVITY CENTER PLATE

Figure 77. Center Plate Design Concepts

Some external circuit techniques are available which can reduce drift in output and zero due to changes in transducer temperature. The temperature-sensitive resistances which comprise the eddy current system affect the input current to the transducer when it is fed constant voltage. There will also be a variable drop in signal output voltage in this network if the signal conditioner input circuit places a current load on the transducer. These effects can be minimized without resorting to temperature-dependent resistors by the following methods:

- Provide a second coil for sensing flux density in one or both pole pieces and use the voltage generated to control the input current to the transducer.

- Keep the input impedance of the signal conditioner very high.

- Use a potentiometric circuit such as in Figure 53 to null the zero-measurand fundamental frequency output. Circuits such as shunt resistance and capacitances which force current through the transducer coils should be avoided.

The first method (a) is illustrated in Figure 78. The control parameter is the average output of the two coils (E-F) and (G-H). This instantaneous-value feedback loop may present some loop stability problems. Since the drift of concern is slow, a frequency-translated control loop incorporating a voltage-controlled amplifier might be used, as illustrated in Figure 78(b).

A major obstacle to manufacturing miniature versions of the VR transducer is the difficulty of winding and installing the coils. This can be remedied by using fewer turns. Output signal level can be maintained by proper choices of impedance (turns) ratios for transformers T_1 and T_2 in Figures 31 and 35. Other circuit techniques which can be applied to the practical problem of measuring pressures with VR transducers are described in Appendix E. They are of less general interest from the standpoint of product improvement.

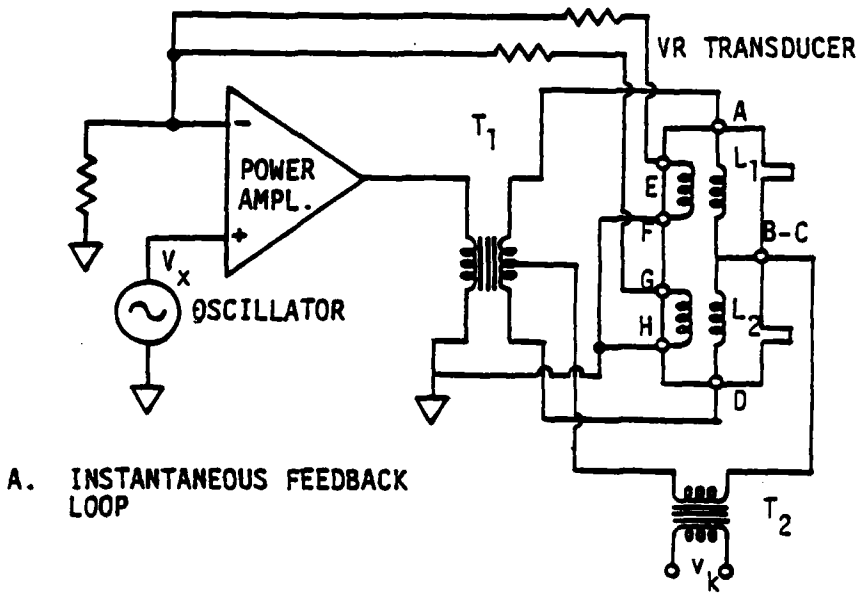

A. INSTANTANEOUS FEEDBACK LOOP

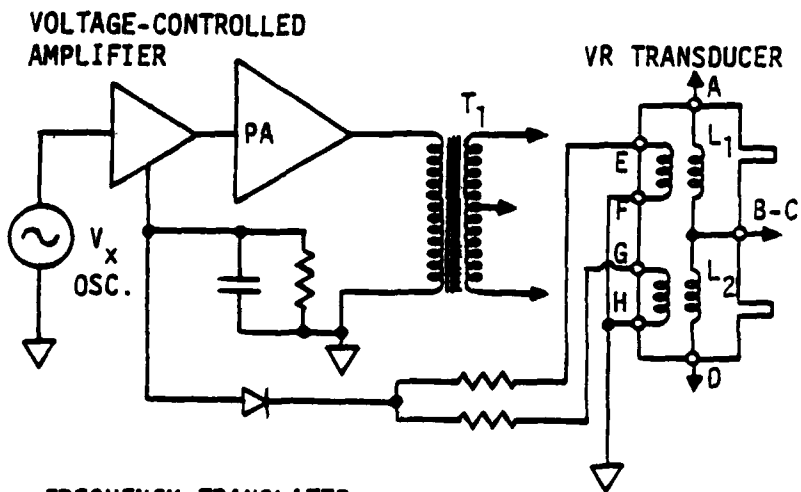

B. FREQUENCY-TRANSLATED CONTROL LOOP

Figure 78. β-Sense Coil Constant-Current Excitation Scheme - Variable Reluctance Pressure Transducer

A design modification which permits direct axial pneumatic entrance to the CP is illustrated in Figure 79. Case halves could be manufactured in either the radial or axial configuration and still be electrically identical. They could then be combined as required for a given installation, such as the aerodynamic surface shown.

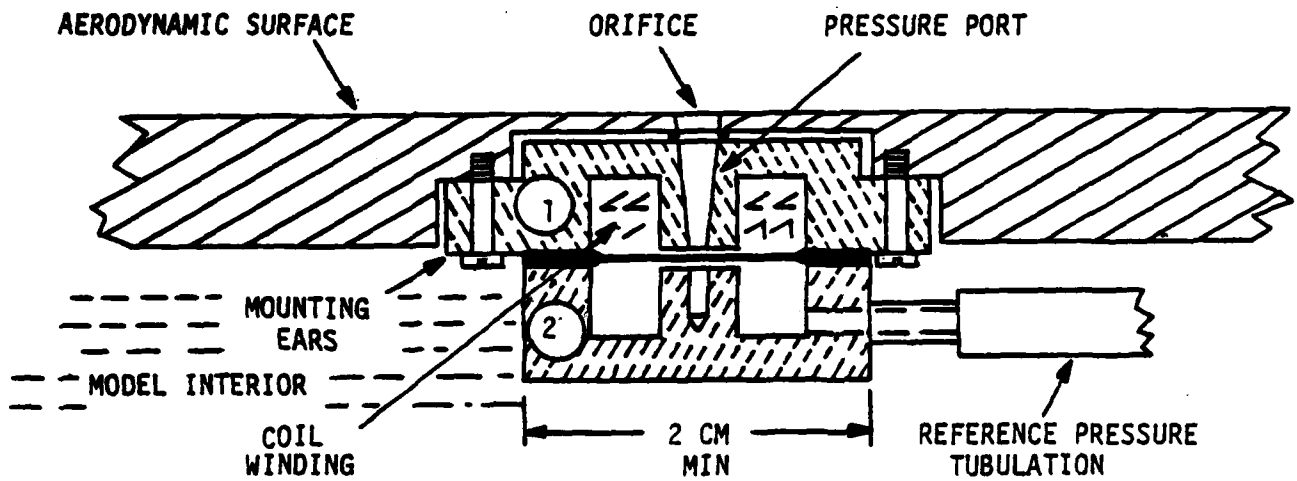

(1) NEW AXIAL PORT CASE HALF.

(2) CONVENTIONAL RADIAL PORT CASE HALF WITH FLUX BALANCER HOLE ADDED.

Figure 79. Case-Half Modification for Specific Application - Variable Reluctance Pressure Transducer

SECTION XIII

CONCLUSIONS

1. MEASUREMENT PRECISION

If manufacturing consistency can be achieved, present designs of VR transducers can provide steady-state calibration characteristics at least as good as those obtained from transducer C-03. This kind of transducer would be of considerable value in low speed aerodynamics testing of the type described. Application problems would consist of reconciling desired and achievable high-frequency response and designing the physical installation. The custom of providing only radial pneumatic ports severely restricts the useable frequency response. Removal of this limitation by providing axial openings would increase the usefulness of the transducer by allowing more flexibility in tubulation system design.

In the present state of development, individual selection of transducers and avoidance of severe temperature environments are virtual necessities. With individual end-to-end steady state and response pressure calibrations, reasonable values for maximum measurement imprecision due to all causes except large ambient temperature changes may be stated for classification purposes as follows:

$\pm$ 0.3 Percent of Nameplate Full Scale steady state amplitude

$\pm$ 3.0 Percent of Nameplate Full Scale up to a frequency of $\omega_M/5$ or $\omega_c/5$, whichever is lower

$\pm$ 20 degrees at maximum baseband (ω_f) frequency if ω_c is no greater than 6 kilohertz

With minor product improvements, mainly control of centerplate deflection characteristics, these same specifications could be applied to a given make and model of transducer as a class without resorting to selection and rejection procedures. Then it may become practical to create and apply standards and practices covering calibration and operation of VR transducers with both steady-state and fluctuating

pressures. Statement of standard test conditions and electrical parameters of the kind used in the tests described in Section X would be part of the standards. The specifications for curve shape in lieu of linearity might be stated in the form of central values and tolerance limits for the constants a and c in the characteristic curve $y = c\ (\frac{x}{a + x})$. With the same minor manufacturing improvements as before and individual selection of transducers, the following measurement precision may be achievable:

$\pm$ 0.10 Percent of Nameplate Full Scale steady state amplitude

$\pm$ 2.0 Percent of Nameplate Full Scale up to $\omega_M/3$ or $\omega_c/3$, whichever is lower, with appropriate filter in the FTSC

$\pm$ 5 degrees at maximum baseband (ω_f) frequency if ω_c is no greater than 6 kilohertz

2. FREQUENCY RESPONSE TESTING

Because of the inherent characteristics of both the VR transducers and the available periodic test pressure "generators", a natural barrier seems to exist at about 2-3 kilohertz, limiting the reliability of response test data above those frequencies. At present, response tests can be performed at all frequencies below this limit with sufficient accuracy to be considered "calibrations". At higher frequencies, available techniques can be used to expose significant performance deficiencies, but the accuracy of transduction can only be inferred, using knowledge of the physical structure and geometry of the transducer. However, this capability should suffice for testing VR transducers in their present state of development and for the immediate future.

3. FUTURE PRODUCT DEVELOPMENT AND IMPROVEMENT

The more venturesome VR transducer product improvements which appear feasible in the near future have been discussed in Section XII.

4. SIGNAL CONDITIONERS

Frequency-translating signal conditioners for VR transducers do not represent a serious design or manufacturing problem. The field of automotive and consumer electronics can be sources of technology for manufacturing reliable FTSC's for aerospace use. The two-phase voltmeter is a very useful tool in studying electrical circuit operation in the entire range of work from equipment design to troubleshooting installed systems.

5. CHARACTERISTIC CURVE SHAPE

In applications where a specific calibration curve shape is required, the transduction characteristic of Figure 15 can be modified point-by-point by means of a very small scale digital sub-system. These microprocessors possess sufficient speed that both quasi-steady state and fluctuating FTO signals can be accommodated. They could be included as an integral part of the FTSC. These microsystems could also be used to remove specific, unwanted transducer responses to pressure fluctuations or mechanical vibration. There appears to be little advantage in using the digital sampling approach to frequency translation, as shown in Figure 9b(4), unless it is planned as an integral part of the total data acquisition scheme.

6. PERFORMANCE OF EQUIPMENT USED IN TESTING

All equipment used in the testing phase which has been identified by make and model performed satisfactorily for the use at hand. Treatment of data was arranged so as to avoid conclusions as to its performance with respect to the manufacturer's specifications and comparisons with similar equipment from other manufacturers.

APPENDIX A

DEFINITIONS FOR AERODYNAMIC MEASUREMENTS IN COMPRESSOR TESTING

Steady-State (Or Stationary) - Variables measured while the test process is being held at a given operating point for a time period which is very long compared to the period of the least rapidly varying significant aerodynamic process.

Transient - A shaped forcing function, or the compressor response thereto, usually from one commanded steady-state operating point to another.

Static - A pressure measured with the vector velocity, u, of the gas at zero.

Dynamic - This word should only be used for subsonic aerodynamic velocity head, "q", given by $q = 1/2\ \rho u^2$. It should not be used to refer to fluctuating or oscillating variables or the instrumentation used to measure and record them.

Fluctuating (Or Non-Stationary) - Varying randomly; or, varying rapidly in response to some undefined or spurious forcing function.

Oscillating - Varying in a periodic manner.

Quasi Steady-State - Variables or measurements which change at a sufficiently slow rate that their measurement, recording, and analysis can be simplified with little or no error by assuming that it is actually steady-state.

Average - The value of a variable or measurement which originally contained fluctuations at a high frequency after being processed to remove all components above some lower frequency. An assumption is made, based on an analysis of the experiment, that all frequencies above a

certain value are of no significance in the particular data interpretation problem at hand and must be removed or averaged to simplify this interpretation or analysis.

APPENDIX B

TYPICAL TUBULATION SYSTEM FREQUENCY CHARACTERISTIC

CONDITIONS ASSUMED

Tubing Length: 7 feet

Tubing Diameter: 1/8" O.D., 0.08" I.D.

Steady State Pressure Level: $P_s = 20 \times P_f$

Temperature: $610^{\circ}R$

$\frac{\omega_f}{2\pi}$(Hz)	AMPLITUDE REDUCTION - %	SECOND HARMONIC DISTORTION - %
0.1	2	0
1.0	6	0.7
3.0	10	---
10.0	20	6.3
100.0	--	70

SOURCE:

Fisher, J., Shaffernocker, W., Stanforth, C., and Williams, J., "Instrumentation Design Study for Testing a Hypersonic Ramjet Engine on the X-15 A-2," 1965. NASA Contractor Report CR-62148.

APPENDIX C

SYNOPSIS OF FOUR SELECTED REFERENCES ON GENERATION OF PERIODIC PRESSURES

1. Development and Testing of Techniques for Oscillating Pressure Measurements Especially Suitable for Experimental Work in Turbomachinery," H. Weyer and R. Schodl. Paper no. 71-FE-28, ASME Fluids Engineering Conference, Pittsburgh, PA., May 9-12, 1971.

This paper describes a siren-type generator having a frequency range from below 100 Hertz to over 4000 Hertz. It consists of a rotating wheel with a complex arrangement of circumferential and axially-oriented slots on the outer rim and air supply and pressure take-off ports on the inner face of a stator. The pressure supply used was about 1.6 times atmospheric discharge. The device generates a rectangular-shaped wave. It was not intended for transducer calibration. The authors' abstract is as follows:

> "Strong pressure oscillations of high frequencies and high amplitudes occur in the region of turbomachine rotors. The measurement of the average pressures resulting from these oscillations is one of the most important measuring problems in turbomachinery, because the pneumatic measuring systems usually used in such tests yield average pressures which normally do not agree with true time-integrated values. This paper deals with an investigation aimed at the development of techniques which permit the measurement of well-defined average values of oscillating pressures. Three different methods developed and tested at DFVLR are described. Two of them - a hydraulic and mechanical one - are able to measure the true time-averaged pressures with an accuracy better than 0.5 percent of acting pressure amplitude. The third procedure is based on an evaluation method by means of which the average pressures indicated by special pneumatic measuring systems can be correlated to the true time-weighted values. Experimental and computed results are presented showing a very good agreement."

2. "An Experimental Evaluation of Unsteady Flow Effects On An Axial Compressor," G. Reynolds, W. Vier, and T. Collins, AF Technical Report, AFWAL-TR-73-43, July 1973.

This report includes a description of a large (44 inch diameter) "siren" type device consisting of several fixed and rotating perforated discs which "chop" the air flowing into the atmospheric inlet of the fan type compressor. The result is a uniform planar wave front of periodically varying pressure ranging in frequency from 42 to 800 Hertz. The device was not intended to be used for calibrating transducers. The author's abstract is as follows:

> "A test program has been successfully completed to obtain fundamental information concerning the behavior of a fan compressor unit when subjected to planar pressure and flow pulses. Testing was conducted at two corrected fan speeds over a range of input pressure amplitudes and frequencies. A total of 24 fan surges and approximately 57 "steady-state" data points was obtained. The General Electric- developed Planar Pressure Pulse Generator (P^3G) was used to produce a sinusoidal-type pressure disturbance to a current technology two-stage fan inlet. A thorough complement of dynamic instrumentation, consisting of approximately 45 transducers, was utilized throughout the testing. Data reduction is complete and several fundamental results have been obtained."

3. "Improvement of a Large-Amplitude Sinusoidal Pressure Generator for Dynamic Calibration of Pressure Transducers," R. Robinson. NASA Contractors Report CR-120874, February 1972.

> Author's Abstract
>
> "Results of research on the improvement of a sinusoidal pressure generator are presented. The generator is an inlet-area-modulated, gas-flow-through device (siren type) which has been developed to dynamically calibrate pressure transducers and pressure probes. Tests were performed over a frequency range of 100 Hz to 20 kHz at

average chamber pressures (bias pressure) between 30 and 50 psia (21 and 25 N/cm^2-abs) and between 150 and 300 psia (104 and 207 N/cm^2-abs). Significant improvements in oscillation pressure waveform were obtained but with reduction in available generator oscillation pressure amplitude range. Oscillation pressure amplitude, waveform, and waveform spectral content are given as functions of frequency for the two bias pressure conditions. The generator and instrumentation for frequency, amplitude, and spectrum measurements are described."

4. "A New Dynamic Pressure Source for the Calibration of Pressure Transducers," C. Vezzetti, J. Hilten, J. Mayo-Wells, P. Lederer. NBS Technical Note 914, June 1976. (Also listed as Reference 37).

Author's Abstract:

"A dynamic pressure source is described for producing sinusoidally varying pressures of up to 34 kPa zero-to-peak, over the frequency range of approximately 50 Hz to 2 kHz. The source is intended for the dynamic calibration of pressure transducers and consists of a liquid-filled cylindrical vessel, 11 cm in height, mounted upright on the armature of a vibration exciter which is driven by an amplified sinusoidally varying voltage. The transducer to be calibrated is mounted near the base of the thick-walled aluminum tube forming the vessel so that the pressure-sensitive element is in contact with the liquid in the tube. A section of the tube is filled with small steel balls to damp the motion of the 10-St dimethyl siloxane working fluid in order to extend the useful frequency range to higher frequencies than would be provided by an undamped system.

The dynamic response of six transducers provided by the sponsor was evaluated using the pressure sources; the results of these calibrations are given."

APPENDIX D

OPERATING PRINCIPLE-RESTORED CARRIER FREQUENCY TRANSLATING SIGNAL CONDITIONER

The functioning of this equipment can best be illustrated by referring to a more detailed functional block diagram, Figure D-1, and the following step-by-step adjustment procedure.

1. Establish zero measurand on the transducer.

2. With zero injected carrier (switch in "Balance" position), adjust α_N and θ_N to give minimum output as indicated on the "Balance Indicator."

3. Put a trial pressure load of 1/2 to 3/4 of the desired full scale value in the positive direction on the transducer.

4. Add injected carrier by setting the switch to "Operate." Adjust θ_C for a DC voltage maximum at the FTO terminals (E_o).

5. Test the system polarity by increasing the pressure slightly. If the output indication decreases, reverse transducer connections A and D and repeat steps 1 through 4.

6. Remove the pressure load and adjust α_C for zero output at the FTO terminals.

7. Adjust "Gain" for desired calibration with test pressure applied.

8. Fine-trim the adjustments by repeating steps 3, 4, and 6.

The voltage phase relationships shown in Figure 26 apply to this equipment when V_M is replaced by V_C. The amplitude of the output from transformer, T_3, would then be represented by the sum of phasors $\bar{V}_C$ and $\bar{V}_S$. Therefore, the output is directly affected by the magnitude of $\bar{V}_C$.

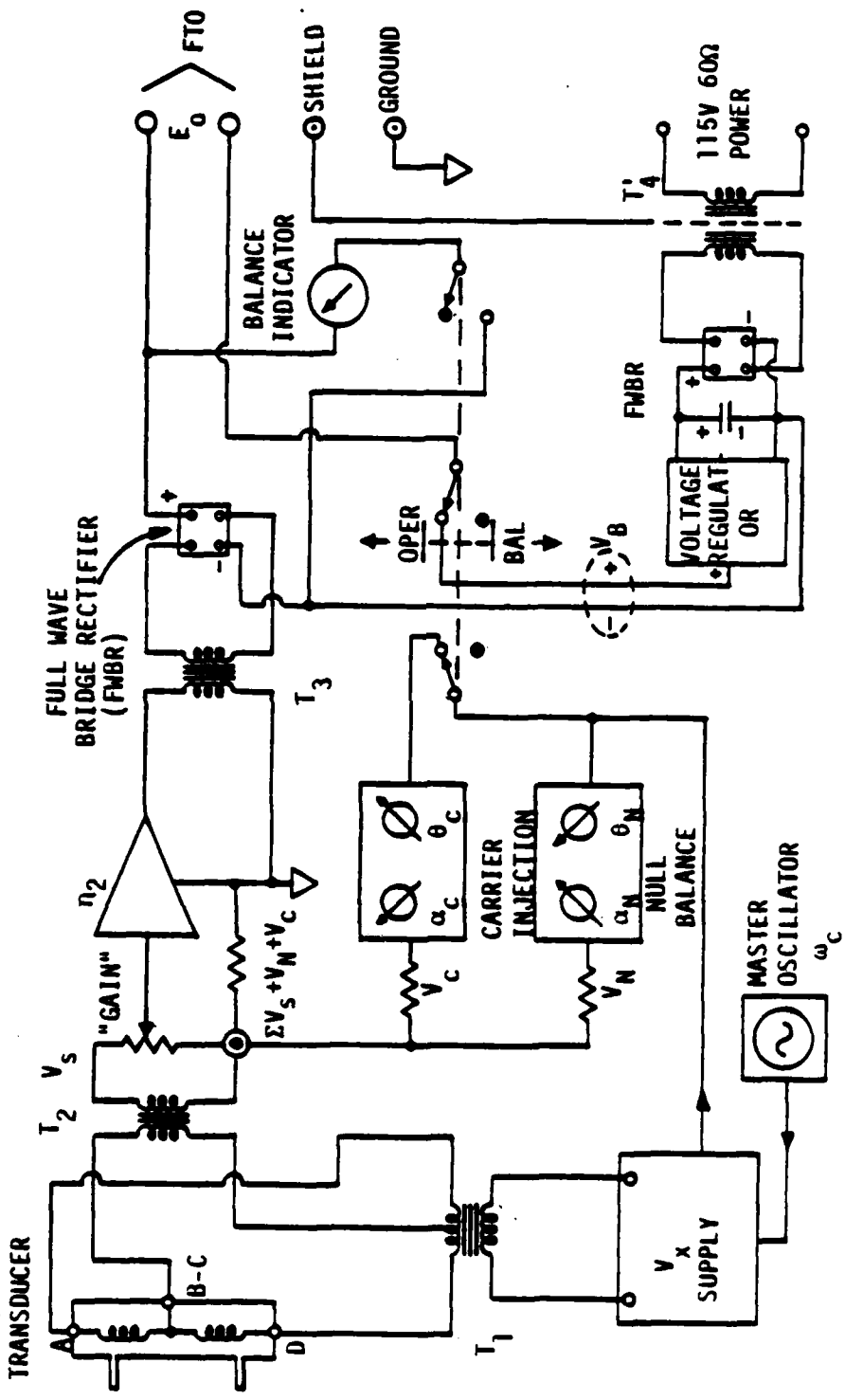

Figure D-1. Functional Schematic - Restored Carrier (Full AM) Frequency Translating Signal Conditioner

APPENDIX E

CIRCUIT VARIATIONS FOR SPECIAL INSTALLATIONS VARIABLE RELUCTANCE PRESSURE TRANSDUCER

There are several simple rules governing the use of variable reluctance pressure transducers in typical ground test facility applications. These apply to both conventional and special electrical circuit arrangements, and are as follows:

a. Thermal effects on the electrical characteristics of the transducer are due to eddy current resistance, changes in the effective permeability of the case and centerplate material, and resistance in the coil windings and leads to the signal conditioner. These effects are temporary if temperatures do not exceed 250 degrees Celsius. To date, efforts in developing special high-temperature VR transducers, such as test unit C-10, have been limited.[1] The use of temperature-dependent resistors to compensate for the effects of eddy currents on span and zero is quite common.

b. Where long cables are necessary, a higher impedance excitation power feed is advantageous because voltage drop in the line can be reduced. An additional voltage sense line might also be provided. In severe cases, compensation of IR drop variations with temperature can be accomplished by means of temperature-dependent resistors.

c. Impedance levels and circuit "ground" configurations can easily be manipulated with transformers. The same temperature considerations in (a) above pertaining to the transducers apply to transformers.

d. Low impedance transducers are less susceptible to adverse loading effects from the FTSC input circuit and from line capacitances.

---

[1]Transducers C-10 and C-11 are certified by the manufacturer to operate within specifications at temperatures up to 600 degrees F.

e. Dielectric properties and electrostatic shielding efficiency of shielded cables are not critical.

f. The circuits are not sensitive to high frequency EMI, nor do they create same.

g. Connection points such as screw terminals and solder joints must be secure and corrosion free. Defects would probably appear first as calibration shift and zero drift due to resistive effects, although these are less serious than in DC and strain gage circuits in which useful signals are much smaller. However, these points may also behave as semiconductors, degrading the inherent immunity of the carrier system to normal mode noise. With these non-linear elements in the circuit, any electrical noise present will modulate the carrier and appear in the output of the FTSC together with the pressure data. High intensity low frequency magnetic fields impinging on the transducers and transformers will interfere with the signal, but their effect will be temporary.

Common audio equipment techniques may be used to provide a wide variety of circuit and installation configurations. Figure E-1 shows a multi-channel scheme which meets some particular installation requirements, among them cable bulk. It illustrates some of the general principles applicable to these circuits and the additional design and installation flexibility provided by transformers. The need for long cables from the power distribution transformer T_D to the signal conditioner room is reduced to one unshielded #18 lead ("bus"). One or more of the shields of the signal leads can be used as the return line. The current in this bus will be less than 0.6 milliampere per transducer. Only a single shielded wire of any common kind per transducer is required for each of the signals. T_D is an 8 watt, 70.7 volt line-to-voice-coil transformer with a 16/4 ohm secondary, located within 20 feet of the transducers. These transformers are intended for use in loudspeaker circuits of sound distribution systems and operate efficiently up to about 30 kilohertz. With low impedance transducers (Z_T = 200 Ohms), the individual power leads need not be shielded but should be a tightly twisted pair of #20 or larger wire. A centralized

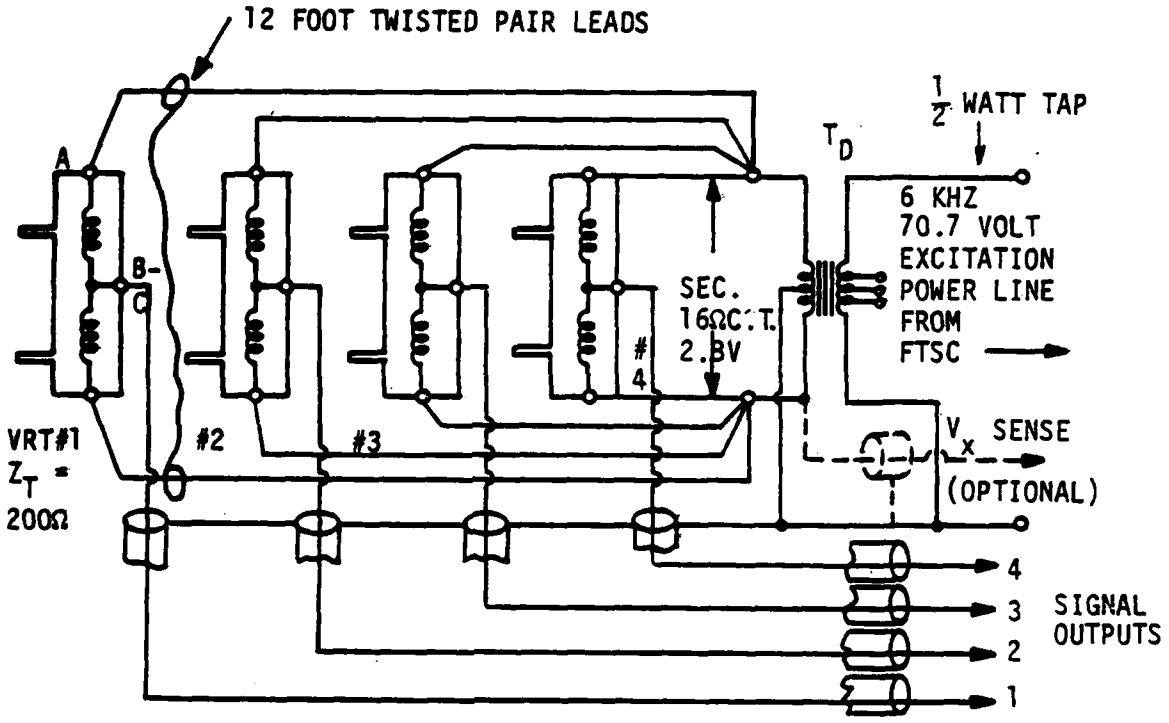

T_D = 8 WATT 70.7 VOLT LINE DISTRIBUTION TRANSFORMER -- SEC: 4Ω AND 16Ω OUTPUT TO SPEAKER, (2.8 VOLTS V_x).

A. MULTIPLE TRANSDUCER EXCITATION POWER FEED ("BUS")

B. TRANSFORMERLESS CIRCUIT

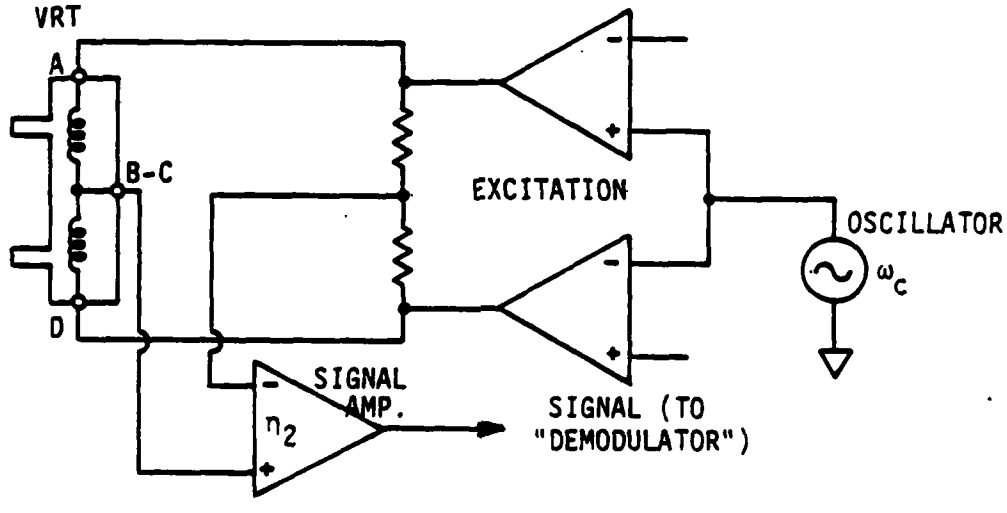

Figure E-1. Transducer Applications Circuitry

excitation power distribution ("bus") system for many transducer channels can be created by expanding this concept.

Transformerless circuits such as shown in Figure E-1(B) may be used when the FTSC electronics can be located very near or integral with the transducer. Long lengths of high impedance low-level signal leads must be avoided.

It is possible to provide several completely independent output signals from one transducer. The circuit common, scale factor (slope) and zero (intercept) for each output may be independent and a fault in one output will not affect the others. This is done by adding more "signal conditioner" blocks as shown in Figure 30 and operating all of them from the same signal and reference voltages and into a common input circuit.

REFERENCES

1. Editor, Reluctive, Inductive and Eddy Current Pressure Transducers, Measurements and Data, Vol. 8, No. 4, July-August 1974, pp 64-69.

2. C. P. Zicko, New Applications Open Up for the Versatile Isolation Amplifier, Electronics, March 27, 1972, pp 96-100.

3. Allen E. Fuhs and Marshall Kingery, Editors, Instrumentation for Airbreathing Propulsion (F. G. Pollack, Advances in Measuring Techniques for Turbine Cooling Test Rigs: Status Report, pp 371-386), MIT Press, Cambridge, Mass., 1974.

4. F. J. Walker, Variable Reluctance Type Pressure Transducers or Devices Using Magnetic Effects, Fundamentals of Aerospace Instrumentation, Vol. 1, pp 13-17, Fourteenth International ISA Aerospace Instrumentation Symposium, 1968, Instrument Society of America, Pittsburgh, PA.

5. S. F. Pickett and A. J. Smiel, Performance Evaluation of Velocity Measurement Systems, Air Force Weapons Laboratory, Kirtland Air Force Base, NM 87117, AFWL-TR-74-219, April, 1975.

6. Johansson, James, Variable Reluctance Sensors, Instrument and Control Systems, March 1967, p 107.

7. Staff, Department of Electrical Engineering, Massachusetts Institute of Technology, Magnetic Circuits and Transformers, John Wiley and Sons, New York, 1946.

8. International Telephone and Telegraph Corporation, Reference Data for Radio Engineers, Fourth Edition, American Book-Stratford Press, Inc., New York, 1956.

9. M. H. Aronson, "Low Level Measurements-7, Chopper Amplifiers," Measurements and Data, Vol. 11, No. 2, March-April 1977.

10. W. R. MacDonald and P. W. Cole, A Sub-Miniature Differential Pressure Transducer for Use in Wind Tunnel Models, Technical Note No. INSTN 169, Royal Aircraft Establishment (Farnborough), January 1961 (UK).

11. F. R. Ostdiek, A Cascade in Unsteady Flow, Air Force Aero Propulsion Laboratory, Wright-Patterson Air Force Base, Ohio 45433, AFAPL-TR-76-115, December 1976.

12. T. Asanuma, A. Takaku, A. Okajima and T. Tanikatsu, Measurements of Surface Pressure on an Eliptical Airfoil Oscillating in Uniform Flow, Institute of Space and Aeronautical Science, Tokyo University, Volume 9, April 1973, pp 323-341 (In Japanese).

REFERENCES (Cont'd)

13. Document 118, Compliment to RCC Document 106, Sec 75, Telemetry Group, Range Commanders Council, 8th Transducer Workship Edition, April 1974, Sec. 2-6b(2) (d).

14. B. P. Lathi, Communications Systems, John Wiley and Sons, New York, 1968.

15. User's Instruction Manual, Oscilloscope Plug-In "Q" Unit, Tektronix, Inc., Beaverton, Oregon.

16. D. Cooper, B. Bixby and L. Carver, "Power Schottky Diodes - A Smart Choice for Fast Rectifiers," Electronics, February 5, 1976, pp 85-89.

17. J. Millman and H. Taub, Pulse, Digital and Switching Waveforms, McGraw-Hill, Inc., New York, 1965.

18. R. O. Decker, Transistor Demodulator for Magnetic Amplifiers in A. C. Servo Applications," Transactions, AIEE, Part I, March 1955, pp 121-123.

19. R. L. Morrison, Grounding and Shielding Techniques in Instrumentation, Second Edition, John Wiley and Sons, Inc., New York, 1977.

20. M. B. Coffee, "Common-Mode Rejection Techniques for Low Level Data Acquisition," Instrumentation Technology, July 1977, pp 45-49.

21. R. J. Roark, Formulas for Stress and Strain, Fourth Edition, McGraw-Hill Book Company, Inc., New York, 1974.

22. H. F. Olson, Elements of Acoustical Engineering, Second Edition, D. VanNostrand Company, Inc., New York, 1947.

23. J. L. Patterson, A Miniature Electrical Pressure Gage Utilizing A Stretched Flat Diaphragm, NACA Technical Note 2659, 1952.

24. A. Heyser, "Development of Pressure Measuring Devices for a Blowdown Wind Tunnel at the DVL," NATO AGARD Report Number 165, March 1958.

25. M. E. VanValkenburg, Network Analysis, Second Edition, Prentice-Hall, Inc., Engelwood, New Jersey, 1964.

26. Pender and DelMar, Electrical Engineers Handbook, Electrical Power, Fourth Edition, John Wiley and Sons, New York, 1949.

27. E. E. Herceg, Handbook of Measurement and Control, Schaevitz Engineering, Pennsauken, New Jersey, 1972.

REFERENCES (Concluded)

28 W. Scharf, "Carrier Amplifiers for Low Level Measurement," Measurements and Data, Volume 8, Number 4, November-December, 1975, pp 99-101.

29. R. S. Caruthers, "Copper Oxide Modulators In Carrier Telephone Systems," The Bell System Technical Journal, Volume 18, 1939, pp 315-337.

30. H. A. M. Clark and P. B. Vanderlyn, "Double Ratio A. C. Bridges With Inductively Coupled Ratio Arms," Proccedings of the Institution of Electrical Engineers, Volume 96, Part III, Paper Number 972, January 1949, pp 189-202. (UK)

31. Product Catalog T-218B, Princeton Applied Research Corporation, Princeton, New Jersey, September 1973.

32. P. S. Lederer, Methods for Performance-Testing of Electromechanical Pressure Transducers, NBS Technical Note 411, February 1967.

33. R. C. Dobkin, Linear Applications Handbook 1, Linear Brief LB-5, High Q Notch Filter, National Semiconductor, Inc., Santa Clara, California, 1969.

34. J. R. Bainter, "Active Filter Has Stable Notch and Response Can be Regulated," Electronics, October 2, 1975, pp 115.

35. Engineering Bulletin 6626, "Capacitive Pressure Sensors," Rosemount Engineering Company, Minneapolis, Minnesota, Circa 1968.

36. R. Ramirez, "The Fast Fourier Transforms Errors Are Predictable, Therefore Manageable," Electronics, June 13, 1974, pp 96-102.

37. C. Vezzetti, J. Hilten, J. F. Mayo-Wells and P. Lederer, A New Dynamic Pressure Source for the Calibration of Pressure Transducers, NBS Technical Note 914, June 1976.

*USGPO: 1983-659-062-1008

END

FILMED

9-83

DTIC